

**Surface Treatment and Adhesive Bonding of Commercial  
PVC**

**Mojtaba Amini Dahaghi**

**A thesis submitted in partial fulfilment of the  
requirements of the School of Architecture, Computing  
and Engineering, University of East London for the degree  
of Doctor of Philosophy**

**June 2013**

## **Abstract**

The bonding of rigid PVC to a plasticised PVC film using a reactive hot melt polyurethane adhesive has been investigated in order to improve the stability and durability of the bonding between the PVC and the adhesive. (The primers used to modify the surface of rigid PVC are mainly solvent-based products, either methylene chloride based or methyl ethyl ketone based). With Adhesion Promoters, such concerns are environmental (High VOC emissions and clean-up costs), introductions of dirt, high maintenance costs, and safety. Chlorinated solvents, most commonly used in Adhesion Promoters, are highly flammable and toxic which in turn is dangerous to plant and personnel alike. These solvent-based products were band by European Union environment agency in2011. Alternative surface modification technique should replace the solvent prima to modify the surface of the commercial PVC.

Consequently the flame treatment technique was employed to modify the surface of the commercial PVC before bonding to a plasticised PVC film by using a reactive hot melt polyurethane adhesive.

Before surface modification of the PVCs, the PVC samples were investigated by employing surface analysis's techniques such as X-ray photoelectron spectroscopy (XPS), contact angle measurements (CAM), atomic force microscopy (AFM) and energy dispersive X-ray (EDX) and DMA. In order to avoid the damage of the PVC samples while they expose to X-ray irradiation. Initially, XPS and EDX were employed in a X-ray degradation study of PVC to determine the maximum time a PVC sample can be exposed to an X-ray source where X-ray has minimum effect on the surface of PVC. The samples used in the degradation study were pure PVC (drop cast in THF on to aluminium foil to produce a PVC film as reference) and three industrial PVC blends. EDX analysis of a pure PVC specimen exposed to an X-ray source showed 5% degradation after ten minutes X-ray exposure. Additionally, a further degradation study was undertaken in which a 1mm diameter gold disc was sputter coated on to PVC sample surfaces. This study revealed that the PVC concentration decreased due to X-ray degradation, however, the Au/C ratio remained constant suggesting there was no redistribution of C on to the PVC samples.

A liquid propane gas (LPG) based flame treatment was used to modify the surface of rigid PVC (Veka) to improve its wettability and its adhesive properties. The surface properties and chemistry of the modified surface were characterised by CAM, XPS and AFM. Results show that the LPG flame treatment of the PVC (Veka and Rehau) produces both morphological and compositional changes of the surface. LPG flame treatment of the PVC V and R resulted in an increase in the surface free energy of the PVC surface. CAM result for the LPG flame treated PVC showed increased wettability of the PVC sample. The ultra-low-angle microtomy (ULAM) technique was developed to impart a ultra-low  $\theta$ -angle taper through polymeric multilayers at ambient temperatures. Here the ULAM technique has been enhanced by in situ cooling of the samples using a cryo-stage (C-ULAM). XPS line scan analysis across a UV primer/PVC interface exposed using C-ULAM indicates penetration of UV primer in to the PVC formulation. XPS line scan analysis of C-ULAM exposed PU/PVC and PVC/PU/PVC interfaces shows penetration of PU in to PVC formulation. The UV primer shows greater penetration in to the PVC ( $\Delta Z = 8\text{nm}$ ) than reactive hot melt PU adhesive ( $\Delta Z = 5\text{nm}$ ) due to its application in the liquid phase at ambient temperature. The penetration of PU in to the PVC increased after LPG flame treatment of the PVC due to changing surface roughness of PVC by flame treatment.

Dynamic Mechanical Analysis (DMA) was employed to investigate effect of LPG flame treatment on the mechanical property of the PVC samples, nineteen months after surface modification of PVCs samples by LPG flame treatment. The DMA results indicate that when the PVC sample treated by flame while the release agent is on the surface of the PVC, the release agent and PVC promote a strong bond and therefore become one solid sample together. The result was indicated that, an increase of 10% in storage modulus, from 8083 MPa for samples without RA to 8822 MPa for samples with RA. These results are in agreement with the results from AFM analysis.

By comparing the result of the tan delta of PVC-V with release agent before and after flame treatment, it can be seen that the effect of flame treatment on tan delta profile is not significant. Also the temperature value at tan delta peak indicates the value of glass transition temperature. The fact that this has not significantly changed indicates that the nature of the material has not changed after the flame treatment.

In order to study the mechanical property of sandwich layer samples, made of (Rigid PVC/PU adhesive/ Plasticised PVC), with different curing system the Dynamic mechanical analysis (Three point bending/ DMA) of all sandwich layer samples were carried out nineteen months after they have bonded together. The result obtained from DMA results shows 10% increase on loss modules test of sandwich layers, which bonded while prima was applied on the surface of the PVC.

## Table of Contents

<b>Abstract</b> .....	I
List of Figures.....	1
List of Tables.....	6
Abbreviations .....	7
ACKNOELEDGMENTS .....	9
Chapter 1 .....	10
1 Introduction .....	10
1.1 Adhesive .....	10
1.2 Polyurethane .....	13
1.2.1 Polyurethane Consumption .....	15
1.2.2 Polyurethane Adhesive.....	16
1.2.3 Hot melt adhesive.....	17
1.2.4 Polyurethane hot melt adhesives .....	18
1.2.5 Application and industrial usage of polyurethane hot melt adhesives.....	18
1.3 Project aim .....	19
1.4 Project objectives .....	19
1.5 Research Gap and previous research methodologies.....	20
1.6 Thesis Structure .....	22
Chapter 2 .....	24
2 Literature Review .....	24

2.1	Introduction.....	<b>Error! Bookmark not defined.</b>
2.2	Polyvinylchloride.....	24
2.3	PVC Applications .....	25
2.4	Polyurethane .....	30
2.4.1	Introduction to polyurethane .....	30
2.4.2	Methylene diphenyl diisocyanate (MDI) adhesives .....	30
2.4.3	Polyurethane chemistry .....	32
2.4.4	Mechanical interlocking.....	33
2.4.5	Diffusion theory .....	34
2.4.6	Electronic theory .....	34
2.4.7	Adsorption theory.....	35
2.5	X-ray photoelectron spectroscopy .....	35
2.6	Process of photoemission.....	35
2.6.1	Depth of analysis.....	37
2.6.2	Instrumentation .....	38
2.6.3	Vacuum system .....	38
2.7	X-ray sources .....	38
2.7.1	Twin anodes .....	38
2.7.2	X-ray monochromators .....	39
2.8	Time of flight secondary ion mass spectrometry.....	40
2.8.1	Principle of the technique.....	40
2.8.2	Instrumentation .....	41
2.8.3	Primary ion beam sources .....	41
2.8.4	Electron bombardment.....	42
2.8.5	Time of flight mass analyser .....	42
2.9	AFM.....	43
2.10	Contact angle measurements.....	45

2.11	Flame treatment.....	47
2.12	Why Flame Treatment.....	48
2.12.1	Applications of Flame Treatment.....	48
2.12.2	Benefits .....	49
2.12.3	Main Applications.....	<b>Error! Bookmark not defined.</b>
2.12.4	Main Advantages .....	<b>Error! Bookmark not defined.</b>
2.12.5	Benefits of gas flame treatment.....	<b>Error! Bookmark not defined.</b>
2.13	Dynamic mechanical analysis (DMA) .....	50
2.13.1	Introduction.....	<b>Error! Bookmark not defined.</b>
2.13.2	Instrumentation .....	51
2.13.3	Features of the DMA.....	51
2.13.4	Three point bending .....	52
2.14	PVC and adhesives.....	53
2.14.1	PVC Degradation .....	53
2.15	PVC surface modification .....	58
2.16	Contact angle measurements.....	60
2.17	Production of jacket window profiles .....	60
2.18	PU Reactive hot melt adhesives and buried interfaces .....	61
Chapter 3	.....	64
3	Experimental details .....	64
3.1	PVC degradation study .....	64
3.1.1	Introduction to PVC .....	64
3.2	Experimental.....	66
3.2.1	Materials used .....	66
3.2.2	Sample preparation.....	66

3.3	XPS analysis .....	67
3.4	EDX analysis .....	68
3.5	Microtomy .....	69
3.6	XPS - line scans .....	72
3.7	ToF-SIMS analysis .....	73
3.8	Treatment and Modification .....	73
3.8.1	Introduction.....	73
3.9	Flame treatment .....	74
3.9.1	Materials.....	75
3.9.2	Sample preparation.....	75
3.10	Contact Angle Measurements .....	76
3.11	XPS Analysis .....	76
3.12	Water Break Test.....	77
3.13	Flame Treatment .....	78
3.14	AFM Analysis .....	80
3.15	Dynamic mechanical analysis of samples before and after surface modification.....	80
3.16	Polyurethane hot melt adhesives .....	81
3.16.1	Materials used .....	81
3.16.2	PU Sample preparations .....	82
3.16.3	Microtomy samples.....	83
3.17	XPS analysis of PU adhesives.....	84
3.18	Microtomy process.....	84

3.19	XPS linescan analysis of Interface .....	84
3.20	ToF SIMS analysis .....	85
3.20.1	Dynamic mechanical analysis of sandwich layered samples with different curing systems 85	
Chapter 4	.....	86
4	Results and Discussion .....	86
4.1	XPS analysis of pure PVC .....	86
4.2	EDX analysis of pure PVC .....	88
4.3	Line scans analysis of pure PVC .....	90
4.4	ToF-SIMS analysis of pure PVC .....	91
4.5	X-ray degradation study of PVC window profile .....	92
4.6	X-ray degradation study of plasticised PVC foil .....	99
4.7	X-ray degradation study of PVC with gold disc .....	100
4.8	XPS analysis before surface modification .....	104
4.9	XPS analysis after surface modification .....	112
4.10	Contact angle measurements .....	123
4.11	ToF-SIMS analyses .....	127
4.12	AFM analysis .....	134
4.13	Dynamic mechanical analysis .....	138
4.14	XPS analysis of PU hot melt adhesives .....	143
4.15	Microtomy of buried interface .....	146

4.16	XPS analysis of buried interface .....	147
4.17	DMA of sandwich layer .....	155
Chapter 5 .....		157
5	Conclusions .....	157
5.1	Review of literature .....	157
5.2	Degradation of PVC.....	157
5.3	Surface treatment .....	160
5.4	Analysis of PU .....	163
5.5	Line scan analysis .....	164
5.6	Future work.....	166
References .....		168
Appendix .....		175
6	Appendix .....	175
6.1	Appendix 1.....	175
6.2	Appendix 2.....	175
6.3	Appendix 3.....	177
6.4	Appendix 4.....	178
6.5	Appendix 5.....	180

# List of Figures

1-1 LIST OF THE COMMODITY THERMOPLASTICS .....	11
FIGURE 1. 1-2 SHOWS PVC WINDOW PROFILE PLAIN, AND ALSO WITH TWO DIFFERENT DECORATIVE JACKET .....	12
FIGURE 1-3 WORLD CONSUMPTION OF PU ELASTOMERS IN 2005.....	15
FIGURE 1-4 DIISOCYANATE REACTION WITH A POLYOL.....	16
2-1 FIGURE SALE OF DIFFERENT PRODUCTS OF PVC IN EUROPE IN 2007 .....	26
FIGURE 2-2 AMOUNT OF PVC WINDOW PROFILES USED IN WEST EUROPEAN IN 1998.....	28
FIGURE 2-3 SCHEMATIC DIAGRAM OF THE XPS PROCESS, SHOWING PHOTOIONIZATION OF AN ATOM BY THE EJECTION OF A 1S ELECTRON [ERROR! REFERENCE SOURCE NOT FOUND.].....	36
FIGURE 2-4 : RELAXATION OF THE IONIZED ATOM OF FIGURE 11 BY THE EMISSION OF A $KL_{2,3}L_{2,3}$ AUGER ELECTRON [ERROR! REFERENCE SOURCE NOT FOUND.].....	37
2-5 FIGURE : RELAXATION OF THE IONIZED ATOM OF FIGURE 11 BY THE EMISSION OF A $KL_{2,3}L_{2,3}$ AUGER ELECTRON [ERROR! REFERENCE SOURCE NOT FOUND.].....	38
FIGURE 2-6 PRINCIPLE OF X-RAY MONOCHROMATOR[ERROR! REFERENCE SOURCE NOT FOUND.] .....	40
FIGURE 2-7 SCHEMATIC DIAGRAM OF A MODERN HAS AND TRANSFER LENS[]. <b>ERROR! BOOKMARK NOT DEFINED.</b>	
FIGURE 2-8 SCHEMATIC DIAGRAM OF A MODERN HAS AND TRANSFER LENS[]. <b>ERROR! BOOKMARK NOT DEFINED.</b>	
FIGURE 2-9 SCHEMATIC DIAGRAM OF A MODERN HAS AND TRANSFER LENS[]. <b>ERROR! BOOKMARK NOT DEFINED.</b>	
FIGURE 2-10 SCHEMATIC DIAGRAM OF A MODERN HAS AND TRANSFER LENS[].....	41
2-11 FIGURE SCHEMATIC DIAGRAM OF REFLECTRON TOF-SIMS INSTRUMENT [ERROR! REFERENCE SOURCE NOT FOUND.].....	43
2-12 FIGURE SHOWS SCHEMATIC IMAGE ABOUT THE AFM PROCESSING .....	44
2-13 FIGURE SHOWS CONTACT ANGLE MEASUREMENT INSTRUMENTS.....	45
FIGURE 2-14 IMAGE OF LIQUID CONTACT THE SURFACE OF THE SAMPLE .....	46
FIGURE 2-15 SINGLE AEROGEN FLAME TREATMENT MACHINE.....	48
FIGURE 2-16 SHOWS SOME SAMPLE OF THE PRODUCTS TREATED WITH FLAME FOR LABELLING.....	49
FIGURE 2-17 : <i>THE DMA'S OSCILLATORY FORCE</i> .....	51
FIGURE 2-18 : DMA SCHEMATIC DIAGRAM.....	52
FIGURE 2-19 TENSION SAMPLE HOLDER .....	<b>ERROR! BOOKMARK NOT DEFINED.</b>
FIGURE 2-20 - PVC WINDOW PROFILE WITH AND WITHOUT JACKET WINDOW.....	61
FIGURE 3-1 - SAMPLE OF PVC PROFILE LEFT AND PLASTICIZED PVC RIGHT .....	67
FIGURE 3-2 SHOWS ESCALAB MKII (THERMO SCIENTIFIC, EAST GRINSTEAD, UK) INSTRUMENT .....	68

FIGURE 3-3 - SCHEMATIC OF THE COPPER BLOCK WITH AN ANGLE OF 0.4° .....	70
FIGURE 3-4 - MICROM USED- MOTORISED ROTARY MICROTOMY (HM355S), SETUP FOR C-ULAM.....	71
FIGURE 3-5 – SCHEMATIC DIAGRAM OF ASSEMBLED C-ULAM COMPONENTS.....	71
FIGURE 3-6 SHOWS SIGMA PROBE SPECTROMETER VGSCIENTIFIC .....	72
FIGURE 3-7 SHOWS IONTOF GMBH (MÜNSTER, GERMANY) TOF.SIMS 5 .....	73
FIGURE 3-8 DYNE INK KIT FOR MEASURING DYNE LEVEL OF SAMPLES.....	78
FIGURE 3-9 PICTURES OF FLAME TREATMENT MACHINE (AEROGEN FT SINGLE BURNER), WITH PARAMETERS POINTED OUT BY ARROWS .....	80
FIGURE 3-10 SHOWS DMA.Q800 V7.5 BUILD 127 MODEL IN LEFT AND DUAL CANTILEVER AT RIGHT.....	81
FIGURE 3-11 - (A) PICTURE OF THE RESIN TIN AND CUBE INSIDE OF THE OVEN, (B) MELTED RESIN WITH TAPERED CUBE, (C) COATING OF THE SUBSTRATE BY RESIN.....	83
FIGURE 3-12 - SHOWS IMAGE OF SANDWICH LAYER OF PVC 4 WITH RELEASE AGENT BONDED TO PVC PLASTICISED FILM BY PU 740-29-4 .....	83
FIGURE 4-1 -XPS SURVEY SPECTRUM NUMBER 1 AT THE TOP AND 40 BELOW OF PURE PVC FILM .....	86
FIGURE 4-2 - DEGRADATION INDEX OF PURE PVC, REFERENCE SAMPLE AS FUNCTION OF TIME .....	88
FIGURE 4-3 E EDX ANALYSIS OF A PURE PVC BEFORE THE SAMPLE WAS EXPOSED TO X-RAYS (AT TIME ZERO, $X_0$ ) .....	89
FIGURE 4-4 EDX ANALYSIS OF PURE PVC AFTER SEVENTY MINUTES X-RAY EXPOSURE .....	89
FIGURE 4-5 - DEGRADATION INDEX OF PURE PVC BY EDX AFTER 70 MINUTES X-RAY EXPOSURE (BY TWINE ANODE AL SOURCE).....	90
FIGURE 4-6 - COMPOSITIONAL DEPTH PROFILE OF PURE PVC, OBTAINED BY PERFORMING AN XPS LINE SCAN ANALYSIS ALONG A C-ULAM TAPER THROUGH THE PVC EXPOSED TO X-RAYS FOR 70 MINUTES. INSET IS AN OPTICAL MICROGRAPH OF THE DEGRADED PURE PVC .....	91
FIGURE 4-7 - SHOWS NEGATIVE TOF-SIMS SPECTRA FROM THE BULK REGION OF PURE PVC (UPPER SPECTRA)AND FROM A DEGRADED REGION ( LOWER SPECTRA). THE INSET IS AN OPTICAL MICROGRAPH OF THE SPECIMEN.....	92
FIGURE 4-8 - XPS SURVEY SPECTRUM OF PVC-V WITH AND WITHOUT RELEASE AGENT.....	93
FIGURE 4-9 – SHOWS THE DEGRADATION INDEX OF PVC-V WITH RELEASE AGENT .....	95
FIGURE 4-10– SHOWS THE DEGRADATION INDEX OF PVC-V WITHOUT RELEASE AGENT.....	96
FIGURE 4-11–SHOWS THE DEGRADATION INDEX OF PVC-R WITH RELEASE AGENT.....	97
FIGURE 4-12 SHOWS THE DEGRADATION INDEX OF PVC-R WITHOUT RELEASE AGENT.....	97
FIGURE 4-13 - OPTICAL MICROGRAPH OF A CROSS SECTION THROUGH PLASTICISED PVC FILM MOUNTED IN RESIN. ....	99
FIGURE 4-14 - SHOWS THE DEGRADATION INDEX OF PLASTICISED PVC.....	100
FIGURE 4-15 – SHOWS THE DEGRADATION INDEX OF PVC-V WITH GOLD DISC .....	101
FIGURE 4-16 – SHOWS THE DEGRADATION INDEX OF PVC-V WITH GOLD DISC .....	102
FIGURE 4-17 - SHOWS THE DEGRADATION INDEX OF PLASTICISED PVC WITH GOLD DISC .....	102

FIGURE 4-18 - SHOWS THE DEGRADATION INDEX OF THE PVC-V, PVC-R AND PLASTICISED PVC SAMPLES .....	104
FIGURE 4-19 - SHOWS THE SURVEY SPECTRA OF PVC V 1 WITH AND WITHOUT RA BEFORE FT .....	105
FIGURE 4-20 SHOWS THE HIGH RESOLUTION SPECTRUM OF C1S OF PVC V 1 WITH AND WITHOUT RA BEFORE FT.....	106
FIGURE 4-21 - SHOWS THE SURVEY SPECTRUM OF PVC V 2 WITH AND WITHOUT RA BEFORE FT.....	106
FIGURE 4-22 - SHOWS THE HIGH RESOLUTION SPECTRA OF C1S OF PVC V2 WITH AND WITHOUT RA BEFORE FT.....	107
FIGURE 4-23 - SHOWS THE HIGH RESOLUTION SPECTRA OF C1S OF PVC V2 WITH AND WITHOUT RA BEFORE FT.....	107
FIGURE 4-24 SHOWS THE SURVEY SPECTRUM OF PVC R1 WITH AND WITHOUT RA BEFORE FT.....	109
FIGURE 4-25 -SHOWS THE HIGH RESOLUTION SPECTRUM OF C1S OF PVC R 1 WITH AND WITHOUT RA BEFORE FT.....	109
FIGURE 4-26 - SHOWS THE SURVEY SPECTRUM OF PVC R2 WITH AND WITHOUT RA BEFORE FT.....	110
FIGURE 4-27 SHOWS THE HIGH RESOLUTION SPECTRUM OF C1S OF PVC R2 WITH AND WITHOUT RA BEFORE FT.....	111
FIGURE 4-28 SHOWS THE SURVEY SPECTRA AND HIGH RESOLUTION SPECTRA OF PVC R2 PLAIN BEFORE FT .....	111
FIGURE 4-29 SHOWS THE SURVEY SPECTRUM OF PVC V1 JUST AFTER FT, 12 WEEKS AFTER FT AND 12 WEEKS AFTER WITH HEXANE.....	113
FIGURE 4-30 SHOWS THE HIGH RESOLUTION SPECTRUM OF C1S OF PVC V1 JUST AFTER FT AND 12 WEEKS AFTER FT WITH HEXANE .....	114
FIGURE 4-31 SHOWS THE SURVEY SPECTRUM OF PVC V2 JUST AFTER FT, 12 WEEKS AFTER FT AND 12 WEEKS AFTER FLAME FT WITH HEXANE .....	115
FIGURE 4-32 SHOWS THE HIGH RESOLUTION SPECTRUM OF C1S OF PVC V2 JUST AFTER FT AND 12 WEEKS AFTER FT WITH HEXANE .....	115
FIGURE 4-33 SHOWS THE SURVEY SPECTRUM OF PVC V2 PLAIN JUST AFTER FT, 12 WEEKS AFTER FT AND 12 WEEKS AFTER FT WITH HEXANE .....	116
FIGURE 4-34 SHOWS THE HIGH RESOLUTION SPECTRUM OF C1S OF PVC V2 PLAIN JUST AFTER FT AND 12 WEEKS AFTER FT WITH HEXANE .....	117
FIGURE 4-35 SHOWS THE SURVEY SPECTRUM OF PVC R1 JUST AFTER FT, 12 WEEKS AFTER FT AND 12 WEEKS AFTER FT WITH HEXANE .....	118
FIGURE 4-36 HIGH RESOLUTION SURVEY SPECTRUM OF C1S OF PVC R1 JUST AFTER FT AND 12 WEEKS AFTER FT WITH HEXANE .....	119
FIGURE 4-37 SURVEY SPECTRUM OF PVC R2 JUST AFTER FT, 12 WEEKS AFTER FT AND 12 WEEKS AFTER FT WITH HEXANE.....	120
FIGURE 4-38 HIGH RESOLUTION SPECTRUM OF C1S OF PVC R2 JUST AFTER FT AND 12 WEEKS AFTER FT WITH HEXANE.....	120

FIGURE 4-39 SURVEY SPECTRUM OF PVC R2 PLAIN JUST AFTER FT, 12 WEEKS AFTER FT AND 12 WEEKS AFTER FT WITH HEXANE .....	121
FIGURE 4-40 HIGH RESOLUTION SPECTRUM OF C1S OF PVC R2 PLAIN JUST AFTER FT AND 12 WEEKS AFTER FT WITH HEXANE .....	122
FIGURE 4-41 SHOWS IMAGE OF CONTACT ANGLE OF PVC R BEFORE AND AFTER FLAME TREATMENT.	124
FIGURE 4-42 POSITIVE TOF-SIMS SPECTRA OF PVC V1 IN TOP ROW, V2 MIDDLE ROW AND V2 PLAIN IN BOTTOM ROW AT MASSES 43, 55, 57 BEFORE AND AFTER FLAME TREATMENT. ....	127
FIGURE 4-43 RESULT OF THE POSITIVE TOF-SIMS ANALYSIS OF PVC V1 IN RED , V2 BLUE AND V2 PLAIN IN PURPLE RELATED TO ACRYLIC PEAKS NORMALISED BY TOTAL ION AT MASSES 59, 87, 101 AND 139 BEFORE AND AFTER FLAME TREATMENT .....	129
FIGURE 4-44 RESULT OF THE POSITIVE TOF-SIMS ANALYSIS OF PVC V1 IN RED , V2 BLUE AND V2 PLAIN IN PURPLE RELATED TO IRGANOX 1010 AT MASSES 203 AND 259 ALSO IRGAFOS 168 AT MASS 441 PEAKS NORMALISED BY TOTAL ION BEFORE AND AFTER FLAME TREATMENT .....	130
FIGURE 4-45 POSITIVE TOF-SIMS SPECTRA OF PVC R1 IN TOP ROW, R2 MIDDLE ROW AND R2 PLAIN IN BOTTOM ROW AT MASSES 43, 55, 57 BEFORE AND AFTER FLAME TREATMENT. ....	131
FIGURE 4-46 RESULT OF THE POSITIVE TOF-SIMS ANALYSIS OF PVC R1 IN RED , R2 BLUE AND R2 PLAIN IN PURPLE RELATED TO HYDROCARBONS PEAKS NORMALISED BY TOTAL ION AT MASSES 43, 55, AND 57 BEFORE AND AFTER FLAME TREATMENT .....	132
FIGURE 4-47 SHOWS RESULT OF THE POSITIVE TOF-SIMS ANALYSIS OF PVC R1 IN RED , R2 BLUE AND R2 PLAIN IN PURPLE RELATED TO ACRYLIC PEAKS NORMALISED BY TOTAL ION AT MASSES 59, 87, 101 AND 139 BEFORE AND AFTER FLAME TREATMENT .....	133
FIGURE 4-48 RESULT OF THE POSITIVE TOF-SIMS ANALYSIS OF PVC R1 IN RED , R2 BLUE AND R2 PLAIN IN PURPLE RELATED TO IRGANOX 1010 AT MASSES 203 AND 259 ALSO IRGAFOS 168 AT MASS 441 PEAKS NORMALISED BY TOTAL ION BEFORE AND AFTER FLAME TREATMENT .....	134
FIGURE 4-49 AFM HEIGHT IMAGES AND AFM SPECTRUM OF PVC V SAMPLES BEFORE AND AFTER FT..	136
FIGURE 4-50 AFM HEIGHT IMAGES AND AFM SPECTRUM OF PVC R SAMPLES BEFORE AND AFTER FT..	137
FIGURE 4-51 STORAGE MODULUS PLOTS OF PVC-V WITH RA BEFORE AND AFTER FT .....	139
FIGURE 4-52 TAN DELTA OF PVC V WITH RA BEFORE AND AFTER FT .....	140
FIGURE 4-53 COMPARING THE LOSS MODULUS OF PVC V WITH RA BEFORE AND AFTER FT .....	141
FIGURE 4-54 COMPARING THE STORAGE MODULUS OF PVC V 2 WITH AND WITHOUT RA AFTER FT ....	142
FIGURE 4-55 COMPARING THE LOSS MODULUS OF PVC V2 WITH AND WITHOUT RA AFTER FT .....	142
FIGURE 4-56 THE STUDY OF SURFACE CONCENTRATION (AT %) OF C, O AND N IN PU 740-29-4 AS FUNCTION OF TIME (TWO MONTHS) .....	144
FIGURE 4-57 SURVEY SPECTRUM OF PU 740-29-4 ACQUIRED AT THE SAME DAY WAS COATED ON TO ALUMINIUM FOIL AND AFTER 3 MONTHS .....	144
FIGURE 4-58 THE HIGH-RESOLUTION SIGNAL OF C1S HAS BEEN FITTED WITH THREE CURVES. THE CH/C-C/ C=C GROUP AT 284.94 EV AS REFERENCE, C-O/C-OH GROUP AT 286.55 EV AND O-C=O GROUP AT 289.14 EV .....	145

FIGURE 4-59 HIGH-RESOLUTION SPECTRA OF C1S FROM PU 740-29-4 TWO MONTHS AFTER IT WAS COATED ON TO ALUMINIUM FOIL.....	146
FIGURE 4-60 VARIATIONS IN CL AND SI ACROSS A C- ULAM ( -2°C ± 2) PRODUCED TAPER ACROSS A BURIED PVC/UV PRIMER INTERFACE REGION. EACH SUCCESSIVE ANALYSIS POINT INCREASES THE ANALYSED DEPTH BY 1.53µM. INSET IS A DIGITAL IMAGE OF THE SAMPLE AFTER C-ULAM SECTIONING .....	148
FIGURE 4-61 VARIATIONS IN CL AND SI CONCENTRATION ACROSS A ULAM PRODUCED TAPER THROUGH A BURIED PVC/UV PRIMER INTERFACE REGION AT ROOM TEMPERATURE. EACH SUCCESSIVE ANALYSIS POINT INCREASES THE ANALYSED DEPTH BY 1.53µM. INSET IS S DIGITAL IMAGE OF THE UV/PVC-V INTERFACE EXPOSED BY C-ULAM. ....	149
FIGURE 4-62 VARIATION IN CL AND O CONCENTRATIONS ACROSS A C-ULAM-2°C ± 2 PRODUCED TAPER THROUGH A BURIED PU 740-29-4/PVC INTERFACE REGION. EACH SUCCESSIVE ANALYSIS POINT INCREASED THE ANALYSED DEPTH BY 1.6µM. INSET IS A DIGITAL IMAGE OF C- ULAM PRODUCED TAPER OF PU 740-29-4/PVC. ....	150
FIGURE 4-63 VARIATION IN CL AND O CONCENTRATION ALONG A C-ULAM PRODUCED TAPER ACROSS A BURIED PU 740-29-4/PVC 4 + RELEASE AGENT INTERFACE REGION. EACH SUCCESSIVE ANALYSIS POINT INCREASED THE ANALYSED DEPTH BY 1.5µM. INSET IS A DIGITAL IMAGE OF A PVC-V SAMPLE. ....	151
FIGURE 4-64 VARIATION IN CL AND O CONCENTRATION CHANGE A C-ULAM (-2°C ± 2) PRODUCED TAPER ACROSS A BURIED PLASTICISED PVC /PU 740-29-4/PVC 4 + RA INTERFACE REGION. EACH SUCCESSIVE ANALYSIS POINT INCREASED THE ANALYSED DEPTH BY 1.5µM. INSET IS A DIGITAL IMAGE OF THE PVC-V SAMPLE.....	152
FIGURE 4-65 SHOWS TWO DIFFERENT SAMPLE THAT HAVE MICROTOMEED THAN ANALYSED BY XPS LINE SCAN ANALYSIS.....	153
FIGURE 4-66 VARIATION IN CL AND O CONCENTRATION CHANGE A C-ULAM (-2°C ± 2) PRODUCED TAPER ACROSS A BURIED PLASTICISED 3729 INTERFACE REGION. EACH SUCCESSIVE ANALYSIS POINT INCREASED THE ANALYSED DEPTH BY 1.5µM. INSET IS A DIGITAL IMAGE OF THE PVC-V SAMPLE. ....	154
FIGURE 4-67 VARIATION IN CL AND O CONCENTRATION CHANGE A C-ULAM (-2°C ± 2) PRODUCED TAPER ACROSS A BURIED PLASTICISED PVC 372970D4 + RA.....	154
FIGURE 4-68 VARIATION IN CL AND O CONCENTRATION CHANGE A C-ULAM (-2°C ± 2) PRODUCED TAPER ACROSS A BURIED PLASTICISED 3728 70 D.....	155
FIGURE 4-69 COMPARING LOSS MODULUS OF 3728 AND 3729 .....	156
FIGURE 4-70 COMPARING STOTAGE MODULUS OF 3728 WITH 3729 .....	156

## List of Tables

1.1- COMMON USES OF HOT MELT ADHESIVES .....	19
TABLE 2.1 TYPES OF ADDITIVES USED IN PVC.....	27
TABLE 2.2 SHOWS THE LIST OF ADDITIVES USED IN UPVC PRODUCT-WINDOW FRAME PROFILE.....	29
TABLE 2.3 OPERATING PARAMETERS FOR COMMON SOURCES[ERROR! REFERENCE SOURCE NOT FOUND.] .....	42
3.1-PARAMETERS USED FOR FLAME TREATMENT OF PVC WINDOW PROFILE VEKA.....	79
4.1 XPS QUANTITATIVE SURFACE ANALYSES AND DEGRADATION STUDY OF PURE PVC.....	87
TABLE 4.2 QUANTITATIVE XPS SURFACE ANALYSES FROM THE DEGRADATION STUDY OF THE PVC-V SAMPLES.....	94
TABLE 4.3 XPS QUANTITATIVE SURFACE ANALYSES FROM THE DEGRADATION STUDY OF PVC- R SAMPLES .....	98
TABLE 4.4 XPS QUANTITATIVE SURFACE ANALYSES FROM THE DEGRADATION STUDY OF A PVC- PLASTICISED FOIL SAMPLE.....	100
TABLE 4.5 XPS QUANTITATIVE SURFACE ANALYSES FROM THE DEGRADATION STUDY OF PVC V, R AND PLASTICISED PVC AFTER A GOLD DISC WAS DEPOSITED ON THE SURFACE OF SAMPLES. ....	103
TABLE 4.6 QUANTITATIVE OF XPS SURFACE ANALYSES OF PVC (V) SAMPLES BEFORE FLAME TREATMENT .....	108
TABLE 4.7 RESULTS OF C1S PEAK FITTING OF PVC V SAMPLES BEFORE FT .....	108
TABLE 4.8 QUANTITATIVE OF XPS SURFACE ANALYSES OF PVC (R) SAMPLES BEFORE FLAME TREATMENT .....	111
TABLE 4.9 RESULTS OF C1S PEAK FITTING OF PVC R SAMPLES BEFORE FT.....	112
4.10- QUANTITATIVE SURFACE ANALYSES OF PU HOT MELT ADHESIVES AS FUNCTION OF TIME.....	143
TABLE 4.11- CHEMICAL BONDS IN THE PU 740-29-4 SAME DAY IT WAS COATED ON ALUMINIUM FOIL	145
TABLE 4.12- CHEMICAL BONDS FOUND IN THE PU 740-29-4 TWO MONTHS AFTER IT WAS COATED ON TO ALUMINIUM.....	146

## Abbreviations

AFM	Atomic force microscopy
ARXPS	Angle-Resolve XPS
ASA	Acrylic styrene acrylonitrile
BA	Butyl Acrylate
CAM	Contact angle measurements
C-ULAM	Cry – Ultra low angle microtomy
DMTA	Dynamic Mechanical Analysis
DSA	Drop shape analysis
EDX	Energy dispersive X-ray spectroscopy
FT	Flame treatment
HDT	Heat deflection temperature
IR	Infrared
LMIS	Liquid metal ion source
LPG	Liquid Propane gas
PE	Polyethylene
PP	Polypropylene
PPVC	Plasticised PVC
PTFE	Poly tetrafluoroethylene
PU	Poly urethane
PVC	Poly Vinyl chloride
PVDF	Polyvinylidene fluoride
PVDF	Polyvinylidene fluoride
RA	Release agent

SEM	Scanning electron microscopy
STM	Surface Tension Measurement
SWM	Surface Wettability measurement
THF	Tetrahydrofuran
TOF SIMS	Time of the flight mass spectroscopy
UHV	Ultra high vacuum
ULAM	Ultra low angle microtomy
UPVC	Unplasticised PVC
UV	Ultra violet
XPS	X-Ray photoelectron spectroscopy

## **ACKNOELEDGMENTS**

First and foremost, I would like to thank my Director of Studies Dr Hossein Saidpour at UEL for his valuable guidance and advice. He inspired me greatly to excel in this project and his willingness to motivate me contributed tremendously to my success in this project.

Also I would like to thank my second supervisor Dr Hossein Jahankhani who was also very encouraging in this project.

I would like to express my sincere gratitude to Professor John Watts and Dr Maria-lour Able, for their supervision at the University of Surry.

I am thankful for financial Support provided by EPSRC for my PhD sponsorship.

I would like to thank my Industrial supervisor Dr Andrew Slark and his company ICI (Henkel) for support and providing the material for my research.

I would like to thank Professor Jim Castel and Dr Steven Hender for all their help and encouragement during the work I carried out at the University of Surrey.

I would like to thank Aerogen company specially Mr Eddie Grant for allowing me to use their flame treatment equipment for surface modification of my samples in the factory.

Above all, my deepest gratitude and everlasting love goes to my wife, Noushin and my beautiful daughter Narges and my wonderful son Mohammad Ali, for their additional tolerance and endless patience particularly throughout the final stages of this project.

They were my encouragement and inspiration to complete this study.

Finally, I would like to thank all the members of my family specially my mother and my father (who passed away recently and are not here to see this moment) for they love, support and encouragement. Without their prayers and backing, I doubt if I would have been able to succeed in any stage of my studies and life ambitions.

# Chapter 1

## 1 Introduction

### 1.1 Adhesive

Adhesives are as old as civilization (Comyn, 1997). It is known that adhesives have been used to bond wood since at least the time of the ancient Egyptians. Animal glues were the adhesives used until the development of casein glues (for wood aircraft frames) during World War II. Synthetic resin adhesives, such as urea-formaldehyde (UF) and polyvinyl acetate (PVA), were developed subsequently and remain in common use (Gonzalez, A et al, 1989).

Adhesives are substances capable of adhering to other substances, creating bonds between them (Bruyne, N.A & Houwink, R, 1962). Adhesives, to meet customer needs, possess a wide range of properties derived from synthetic resins. Some synthetic adhesives, such as the epoxy resins, are strong enough to be used in construction in place of welding or riveting these are referred to as structural adhesives. Adhesive tapes have a coating of pressure-sensitive adhesive (Kinloch, 1987).

Adhesion and cohesion are the attractive forces between material bodies. A distinction is usually made between an adhesive force, which acts to hold two separate bodies together (or to stick one body to another) and a cohesive force, which acts to hold together the like or unlike atoms, ions, or molecules of a single body. A number of phenomena can be explained in terms of adhesion and cohesion. For example, surface tension in liquids results from cohesion, and capillarity results from a combination of adhesion and cohesion (Comyn, 1997).

In a similar manner to adhesives, polymers have a long history of use. Although most people believe that polymers are recently developed materials, this is not strictly true, except for synthetic polymers. Natural polymers have been used throughout the ages, chiefly wood, which itself is a complex polymer/polymer composite, and natural fibres,

notably cotton, wool and silk. Some natural polymers were used as thermoplastics in the 19<sup>th</sup> century, notably casein (from milk), shellac (from the lac insect) and horn (based on the natural polymer keratin) has been used as a plastic for much longer (Wang,Q and B.K, 2005). However, the plastics industry is often considered to have been founded in the 1860s with the discovery and use of a modified cellulose polymer, cellulose nitrate, by Parkes (1862) in England and Hyatt (1869) in the USA. A major boost to the infant plastics industry was given in 1906 with the discovery by Beakeland of the first synthetic polymer, known as polyoxybenzyl methylen glycol anhydride (Bakelite). Many other synthetic polymers were developed on an increasingly large scale in the late 1920s and 1930s, including polystyrene, polyvinyl chloride and several thermosetting polymers (Evans, 1999). Today plastic materials are dominated by four main group of polymers, which are the basis of the so-called commodity plastics (see Figure 1.1).

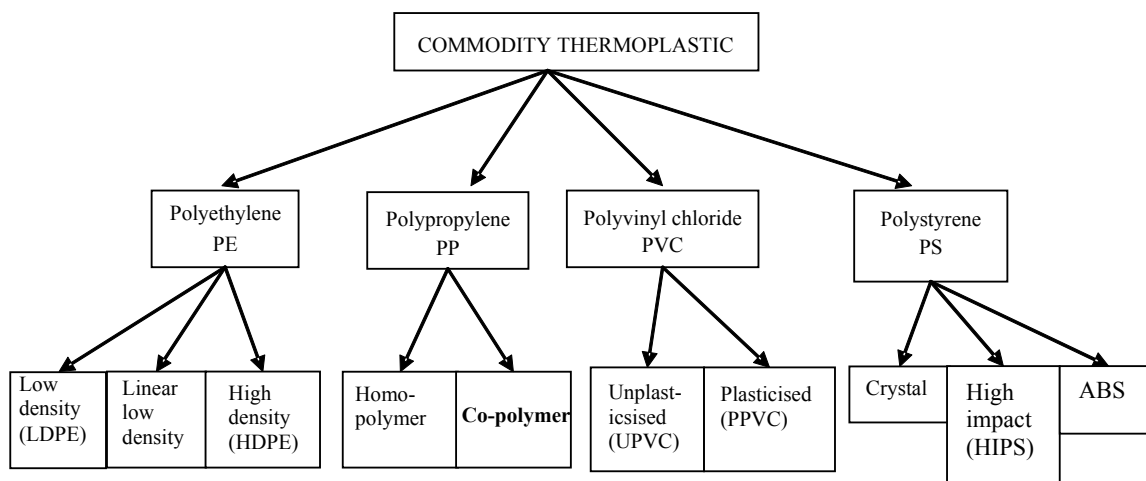


Figure 1-1 List of the commodity thermoplastics

Good adhesion between a polymer and an adhesive is required in a number of important technologies including adhesive bonding, printing, and painting. To achieve a satisfactory level of adhesion it is often necessary to pre-treat the polymer by one of a wide range of methods. Some polymers lack suitable functional groups to form good adhesive bonds; therefore the surface of the polymer needs to be modified to introduce such functional groups. Polymers with no active functional group include low and high-density polyethylene and polypropylene. A wide variety of methods and technique of surface modifications, Including (plasma treatment, corona discharge and flame

treatments) are available for introducing new functional groups to the surfaces of polymers. The effect of each treatments have different lifetime; some of them have short lifetime, and effect of surface modification of some methods last longer (Comyn, 1997). Flame treatment, to enhance adhesion to polymers, has been used since the early 1950s. One of the first applications of flame treatment was to enhance print adhesion to low density polyethylene. Flame treatment has a number of advantages over the other main methods including treating large areas of a polymer, no reverse-side treatment, no creation of pinholes, and no ozone production. Flame treatment involves the combustion of air and natural gas or a specific alkane (propane).

Polyvinyl chloride was discovered in the nineteenth century and ever since has been used in many different industries such as building and construction, packaging, wire and cable, transport etc. More than half of the PVC produced today goes to the construction industries for items such as windows and doors (Arki, Esen and Balkose, D, 2002). Trocal (Troisdorf, Germany) was the first company in the world to innovate with windows and doors made from PVC. The first steps of the work in this field dates back to 1954 (Tydenik, 2003). Figure 1.2 shows images of PVC window profile from left to right plain in white colour and two others with decorative jacketing cover respectively.



Figure 1-2 shows PVC window profile plain, and also with two different decorative jackets

An extrusion line with a twin-screw extruder, is used to produce PVC profiles for window frames, doorframes etc. The original colour of a PVC window profile is white but for aesthetic reasons the PVC window profile can be laminated with a decorative plasticised PVC foil. This process of decorating a window profile using a PU hot melt adhesive to bond a plasticised PVC foil to the window profile is known in the trade as jacketing. The jacketing of a PVC-window profile with a decorative film is a specialist field in profile

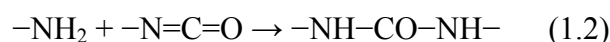
refinement. Approx. 15-20% of the PVC profiles used in the production of windows today are film-laminated. The decorative film is mostly imitation wood, however plain colour films are also available. The most commonly used jacketing film is weather resistant, acrylate-coated PVC film, and more recently, a polyvinylidene fluoride (PVDF) based film. Almost 90% of these jacketed profiles are bonded using PU-hot melts adhesives which are specially produced for this application. The adhesive are dispensed with rollers or slot nozzles. Before jacketing, the window profiles are primed inline to improve the adhesion of the PVC profile surface, which is strongly influenced by the production process, and then laminated with the adhesive-coated film via a roller system. The primers used are mainly solvent-based products, either methylene chloride or methyl ethyl ketone based. These primers are used to improve the adhesive bonding between the profile surface, and the PU hot melt adhesive. Methylene chlorides volatility and its ability to dissolve a wide range of organic compounds makes it a useful solvent for many chemical processes. Concerns about its effect on health have led to a search for alternatives in many of the areas in which these primers are used (Rossberg, M et al, 2006). Because these primers are based on very volatile solvent, they introduce a lot of organic molecules into the atmosphere and these are not friendly to the environment. Primers based on volatile organic solvents are banned by the European Union, for environmental reasons since 2011. An alternative treatment must be found to replace these primers so that PVC window profile jacketing can continue, one possible candidate for this role is flame treatment.

In this study flame treatment was carried out to modify the surface of the commercial PVC window profile and improve its wettability and adhesion properties because the effect of the flame treatment lasts much longer than that obtained with other surface modification techniques. The elapsed time between surface treatment and the bonding of PVC may be significant, and for this reason a surface treatment that is long-lived is required. Flame treatment introduces reactive, functional, oxygen bearing groups to the surface of the PVC and increases the surface free energy, and it make the surface of the PVC more wettable, ensuring good bonding between PVC and adhesive, paint, etc.

## **1.2 Polyurethane**

Since its first introduction to the market in the 1950s, polyurethanes have been widely used in adhesives and coatings applications. Polyurethane has excellent mechanical

properties such as high strength, toughness and durability due to the elasticity of the urethane network, and also has good chemical resistance to solvents and oil (Comyn, 1997). Polyurethane contains the urethane linkage (-NHCOO-) its backbone chain, and it is formed by reaction of an isocyanate with a polyol in the presence of a catalyst and additives. The isocyanate is generally referred to as the “A-side” and the polyol, catalyst and additives are referred to as the “B-side”. The isocyanate group reacts with compounds that contain active hydrogen groups such as hydroxyl, water, amines, urea and urethane, but also other isocyanates. In the reaction with water, carbamic acid is produced, and the carbamic acid breaks down into an amine and carbon dioxide. The amine then reacts with another isocyanate to form a substituted urea, as shown in equation 1:



Equation 1 shows the reaction of Isocyanate with Carbamic

Polyurethane, (PU) is a polymer consisting of a chain of organic units joined by urethane links. Polyurethane polymers are formed through step-growth polymerization by reacting a monomer containing at least two isocyanate functional groups with another monomer containing at least two hydroxyl (alcohol) groups in the presence of a catalyst. Polyurethanes are widely used in high resiliency flexible foam seating, rigid foam insulation panels, microcellular foam seals and gaskets, durable elastomeric wheels and tires, automotive suspension bushings, electrical potting compounds, high performance adhesives and sealants, Spandex fibres’, seals, gaskets, carpet underlay and hard plastic parts (Woods, 1990).

The pioneering work on polyurethane polymers was conducted by Otto Bayer and his coworkers in 1937 at the laboratories of I.G. Farben in Leverkusen, Germany (Farben, 1937). They recognized that using the polyaddition principle to produce polyurethanes from liquid diisocyanates and liquid polyether or polyester diols seemed to point to special opportunities, especially when compared to already existing plastics that were made by polymerizing olefins, or by poly condensation. The new monomer combination also circumvented existing patents obtained by Wallace Carothers on polyesters (Bert, 2004).

Polyurethane elastomers are noted for their toughness, flexibility, strength, abrasion resistance, shock absorbency and chemical resistance. Their physical properties can be tailored to a wide variety of end uses by adjusting the mix and nature of the raw materials. Because they are relatively expensive compared with most other elastomers, they are used primarily in demanding applications such as automotive bumper covers/fascias/trim, solid tires, industrial rollers, shoe soles, sport boots and various mechanical goods.

### 1.2.1 Polyurethane Consumption

The United States, Western Europe, China and other Asian countries are currently the major producing and consuming regions for polyurethane elastomers. In 2005, global consumption of PU was 1.6 million tons. Chinese consumption accounted for 26% of the world total and the next highest was Western Europe with 22%. The United States accounted for 15% of world consumption and the largest percentage of cast elastomers. Japanese consumption is dominated by thermoplastic polyurethane elastomers. Growth in consumption of polyurethane elastomers in the United States will average 3.1% per year through 2010; growth in Western Europe will average 2.2%, and growth in Japan will average 2.2% (Woods, 1990). Figure 1.3 is a pie chart showing the world consumption of PU elastomers in 2005.

**World Consumption of Polyurethane Elastomers—2005**

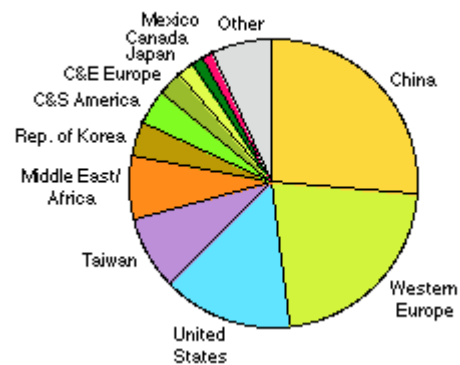


Figure 1-3 world consumption of PU elastomers in 2005

The first essential component of a polyurethane polymer is the isocyanate. Molecules that contain two isocyanate groups are called di-isocyanates. These molecules are also referred to as monomers or monomer units, since they themselves are used to produce polymeric isocyanates that contain three or more isocyanate functional groups. Isocyanates can be formed, such as diphenylmethane di-isocyanate (MDI) or toluene di-

isocyanate (TDI) (David,D.J & Staly, H.B, 1969). Figure 1.4 shows the reaction between the di-isocyanate and polyol to produce polyurethane.

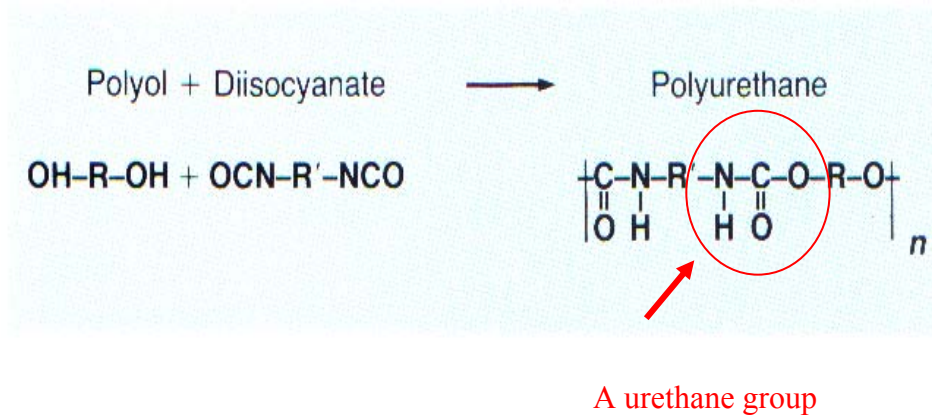


Figure 1-4 Diisocyanate reaction with a polyol

MDI and TDI are increasingly marketed as commodity aromatic chemicals, with worldwide consumption of approximately 4.0 million and 1.9 million tonnes respectively in 2007. Between years 2006-2007, global demand for MDI increased by an estimated 8.0% whilst TDI demand grew by 4.7%. Global demand for MDI is forecast to grow at 6-8% per year during 2008 and 2009.

Furniture and bedding is still the leading area of demand for polyurethane materials, but demand from the construction industry is catching up fast. Polyurethane materials are mainly used in the form of rigid foam as an insulation material, but also in coatings, adhesives and sealants (Eling, B & Phanopolous, C, n.d.).

### 1.2.2 Polyurethane Adhesive

Polyurethane chemistry has made valuable contributions to adhesive bonding technology making available many varied raw materials for the production of adhesives with a wide range of performance characteristics. Polyurethane adhesives vary widely in composition and are used in many different applications in various market segments. Polyurethane adhesives are normally defined as those adhesives that contain a number of urethane

groups in the molecular backbone or urethane group are formed during use. Polyurethane adhesives can be classified into the following product types:

1. Solvent born adhesives. Polyurethane solvent adhesives consist of a high molecular weight hydroxyl terminated polyurethane (MW approximately 100,000) dissolved in a solvent.
2. Hot melt adhesives. These adhesives also consist of high molecular weight hydroxyl-terminated polyurethane.

### **1.2.3 Hot melt adhesive**

Hot-melt adhesives are first introduced to industrial application in the 1950s. Recently, they have found applications in the assembly process, particularly in attaching the back panel to the top, bottom, and side panels of kitchen cabinets. The adhesive is applied as a "bead" at temperatures of at least 150°C and upon cooling develops maximum strength. Typical open time is about 8 to 10 seconds, for all practical purposes, assembly and curing times are eliminated. Information from the kitchen cabinet industry indicates that Ethylene vinyl acetate (EVA) and polyamide are the two most commonly used hot-melt adhesives. Concern exists over their performance at reduced and elevated temperatures because cold temperatures in the zero range and moderately elevated temperatures of 50°C, are encountered during shipment, storage, and use (Forest, 2006).

Hot melt adhesives are solvent-free adhesives, which are characteristically solid at temperatures below 80°C, are low viscosity fluids above 80°C, and rapidly set upon cooling. The development of hot melt adhesive technology stemmed from the previous use of molten wax for bonding. When this method no longer satisfied performance needs, 100% thermoplastic systems were introduced. Hot melt adhesives form a strong bond quickly and simply upon cooling (Calif, 2000). Hot melt adhesives are used primarily for packaging, textiles, labels, and other pressure sensitive applications, disposable products, stamps and envelopes, and product assembly processes are compatible with most materials, and are clean and easy to handle. In general, hot melt adhesives are less water sensitive than other thermoplastic polymers, and are unaffected by water, moisture, or humidity, although if applied to a damp or wet surface the bonding may be poor. Hot melts can be formulated to increase their water sensitivity, as when used for stamps, envelopes and paper products that are to be recycled (Clif, 1991).

There are a number of hot melt adhesives in use, with the most common being those used for hot melt pressure sensitive adhesive applications: Ethylene vinyl acetate (EVA) copolymers, compatible with paraffin, the original hot melt, Styrene-isoprene-styrene (SIS) copolymers, Styrene-butadiene-styrene (SBS) copolymers, Ethylene ethyl acrylate copolymers (EEA) and Polyurethane reactive (PUR). Generally, these polymers do not exhibit the full range of performance characteristics required for an end product by them. Thus, a variety of resins, waxes, antioxidants, plasticizers, and other materials are added to the adhesive formulation to enhance the adhesive performance (Frisch, K.C & Reegen, S.L, 1971-1979).

#### **1.2.4 Polyurethane hot melt adhesives**

The latest advance in hot melt adhesive is termed PU adhesive, which is a 100% solid, one-component urethane prepolymer that "behaves like a standard hot melt until it reacts with moisture to crosslink or chain extend, forming a new polyurethane polymer. By curing the adhesive in this way, PUs have performance characteristics, superior to those of standard hot melts (Hughes et al, 1997). PUs are applied to a substrate as a dot or as a thin line, they set in seconds and are structurally rigid in minutes, following a final set. These adhesives have been accepted in many manufacturing industries, where they can be applied to small bond points to eliminate the use of mechanical fasteners, such as staples, screws, rivets, clips, snaps, nails or stitching (Dennis, 1997).

#### **1.2.5 Application and industrial usage of polyurethane hot melt adhesives**

A PU hot melt adhesive can compete with solvent-base products and is used in many applications. Hot melt adhesive can displace solvent based adhesives by virtue of their technical processing advantages. PU-Hot melts adhesive have applications in the production of footwear and functional textiles. These adhesives are used to manufacture automotive interior trims with the help of laminating processes and assembly joints. PUR-hot melts are also utilized in the production of panels. The other major field of application for these hot melt adhesives is to be found in furniture production, e.g. assembly bonding, edge and surface enhancement and in the manufacture of jacket window profiles, see Figure 1.2 (Thiele, 2007).

Table 1.1 shows common industrial application of PU hot melt adhesives. Today PU hot melt adhesives have a wide range of application from very advanced technology to everyday consumer products.

Table 1.1- Common Uses of Hot Melt Adhesives

Industry	Application
Construction	Manufacture of laminated wood panels; kitchen countertops.
Non-rigid Bonding	Bonding of woven and non-woven fabrics; manufacture of athletic shoes, books, and sporting goods.
Packaging	Manufacture of cartons, boxes and corrugated boards; bags, envelopes, disposable products (diapers, paper products); cigarettes; and labels, stamps.
Vehicles	Aircraft and aerospace structural assemblies; automotive, truck, boat, and bus assembly; mobile home manufacturing.

### **1.3 Project aim**

The major aim of this project was to investigate the durability and stability of adhesive bonding between the rigid PVC and the plasticised PVC film using a reactive hot melt polyurethane (PU) adhesive. The investigation was undertaken in order to develop a new methodology for the bonding between the rigid PVC and the PU reactive hot melt adhesive.

### **1.4 Project objectives**

The main objectives of the project include:

- 1- Characterise and investigate the properties of commercial PVC window profiles and pure PVC.
- 2- Investigate the degradation of pure and commercial PVCs under X-ray irradiation, by employing XPS, ToF-SIMS, Microtomy, Linescan XPS, EDX techniques.
- 3- Achieve optimum properties by modifying the surface of commercial PVC window profiles using flame treatment and hence characterise the chemistry and properties of the modified surfaces.

- 4- Evaluate the stability and lifetime of flame treated PVC window profiles.
- 5- Investigate the interfaces in the sandwich layers of PVC window profile/ PU hot melts adhesive/plasticised PVC, before and after flame treatment of the PVC window profile.

### **1.5 Research gap and previous research methodologies**

Although the surface modification of polymer with different surface modification technique such as ((plasma treatment, corona discharge and flame treatments) are studied and published, there has been no research done on surface modification of PVC with flame treatment. The only publication in this area is the patent obtained in the USA on PVC pallet, in which they have add flame treatment in the list of the claims, but there is no evidence of any practical work carried out. Surface modification of the PVC by flame treatment lasts longer than any surface treatment known so far and it does increase the surface free energy of PVC and reduce the contact angle between the surface of the PVC and water (changing the surface from hydrophobic to hydrophilic)

In order to investigate and determine any possible changes in the surface chemistry of the PVC after surface modification with flame treatment several surface characterisation techniques were carried. These include; XPS, EDX, ToF\_ SIMS, CAM, AFM, ULAM and DMA.

Few new methodologies in this project were developed:

One of the main surface analysis techniques employed in this project was XPS. Thus there will be X-ray degradation of the PVC while an XPS analysis is carried out. It is often observed that X-ray induced sample damage is common during the XPS analysis and can cause the spectrum to change with exposure time. Organic polymers exhibit a wide range of damage rates. The halogen containing polymers degrade fairly quickly, causing a change in surface chemistry at the surface region of these polymers.

Investigation of the X-ray degradation of pure PVC and commercial PVCs were carried out to determine the maximum time a PVC sample can be exposed to an X-ray source, such that the X-ray irradiation has minimal effect on the surface of the PVC. In many published works, PVC degradation has been assessed by considering the Cl/C ratio. The

majority work on PVC degradation changing in Cl/C ratio assumes to rise, by change in Cl concentration. However, no one to date has tried to distinguish between the Cl/C ratio changes caused by lower Cl concentration and an increase in C concentration. Such increase in C concentration could be caused by instrument contamination, this is always positive while it is out gassing of solvent or other impurities in the PVC. We have developed novel method to investigate whether C redeposition contribute changes to Cl/C ratio or whether change in Cl/C ratio is caused by the decrease on Cl concentration, by coating 1mm diameter of gold disk on to surface of PVC samples. Initially cryo-stage-Ultra low angle macrotomy (C-ULAM), XPS – line scan analysis, ToF-SIMS and EDX analysis were employed to find the depth of the degradation as function of X-ray exposure.

In this investigation, (buried interfaces) in order to characterise all the PVC specimens, surfaces and interfaces numbers of spectroscopic techniques have been employed. However, these spectroscopy techniques are restricted to the examination of interfaces at most a few hundred nanometres below the sample surface. The tapering of PVC specimens was performed in the manner described in chapter 1 by Hinder et al. However, in terms of tapering and sectioning of the polymeric PVC specimens, because they were very soft it was impossible to section them at room temperature. During sectioning pure PVC peeled from the sample instead of being sectioned. In this work the ULAM technique has been enhanced by in situ cooling of the samples using a cryo-stage (C-ULAM).

## **1.6 Research methodology**

The methodology adopted in this investigation is listed as follows:

A degradation study has been carried out to determine the maximum time a PVC sample can be exposed to an X-ray source during X-ray photoelectron spectroscopy (XPS) analysis. This is necessary as it was anticipated that XPS is the primary technique used to analyse PVC profile and it is known that PVC degrades under X-ray irradiation

Flame treatment has been used for surface modification of the surface of the commercial PVC window profile. Aerogen FT single burner flame treatment machine has been employed for the surface modification process.

To characterise the surface properties and chemistry of the modified PVC surface, several techniques have been used including XPS analysis, contact angle measurement, time of flight mass spectroscopy (ToF-SIMS) and atomic force microscopy (AFM) analysis.

To investigate the stability and lifetime of flame treated PVC window profiles, XPS and contact angle measurement has been used.

To study the changes in surface composition, as a function of time, for PU hot melt adhesives, XPS analysis has been carried out.

To investigate the interfaces in a PVC sandwich layer, cryo ultra-low angle microtomy (C-ULAM) has been employed to expose the interfaces. These interfaces has been characterised using XPS – line scan and SIMS analysis.

## **1.7 Thesis Structure**

The structure of the thesis, which covers six chapters, is discussed below:

Chapter 1 Introduction to the research field

Chapter 2 reviews the literature associated with the area of research. The aim is to provide a thorough background on the materials used in this project, including PVC window profile and PU hot melt adhesives.

Chapter 3 describes the methodology adopted in this project. This includes a full description of the materials used, the sample preparation and sample characterization. A full description of the degradation study is given including X-ray degradation study conducted on PVC. In this study the depth of the degradation was measured by cryo ultra low angle microtomy to expose the bulk of the PVC, the degradation depth was characterised by XPS linescan and ToF-SIMS. Furthermore description of how surface modifications were carried out on PVC by a LPG based flame treatment is included. The principal of the flame treatment and the parameters used during the flame treatment has been fully described here. This study focuses on characterising the PVC window profile

specimens before and after flame treatment. The longevity of the flame treated PVC surface was studied using XPS, ToF-SIMS, AFM, Contact angle measurements and DMA. Four different PU hot melt adhesives were characterised employing XPS analysis. The stability of PU hot melt adhesives as function of time was also investigated in this study. To study the PVC/PU interfaces it was necessary to develop a new technique to expose the buried interfaces of the sandwich layer specimens. This novel technique is described here and has been named as CULAM. The remainder of this chapter describes characterisation of the exposed interfaces and surfaces of the sandwich layer specimens employing XPS linescan, ToF-SIMS and DMA in order to study the inter layer penetrations as well as the effect of curing system on the viscoelastic properties of the Sandwich layers.

Chapter 4 describes the results and discussion.

Finally chapter 5 describes the main pertinent findings of the project including recommendations for further investigations.

Chapter 6 Appendix

# Chapter 2

## 2 Literature Review

In this chapter, the literatures associated with the area of research covered in this thesis are reviewed. The aim is to provide some background on the materials used in this project, including PVC window profiles and PU hot melt adhesives. The chapter will also introduce the different types of the surface modification techniques applied polymers, as well as the characterizations techniques use for analysis the surface properties and chemistries of the polymer materials. Finally, this chapter ends by describing techniques that can be used to expose the buried interfaces within laminated polymer system.

### 2.1 Polyvinylchloride

Poly vinyl chloride (PVC) is the second largest commodity polymer after polyethylene with a worldwide production of nearly eighteen million tonnes per year. PVC was discovered in the nineteenth century and ever since has been used in a diverse range of applications such as cable, pipe, construction and transport. More than half of the PVC produced goes to the construction industry for items such as windows and doors.

Pure PVC itself is a hard and rigid material; it is manufactured from the monomer, vinyl chloride. The raw materials for vinyl chloride are ethylene (from oil) and chlorine (from salt). The chemical process for making pure PVC involves two steps: first, production of the monomer, vinyl chloride and second the linking of these monomer units in a polymerisation process. The repeat unit structure of PVC is -  $[\text{CH}_2\text{-CHCl}]_n$  (Daning, 2001). Pure PVC has a glass transition temperature ( $T_g$ ) of approximately  $75^\circ\text{C}$  and a softening point close to the  $T_g$ . After polyethylene and polypropylene, PVC has one of the lowest  $T_g$  amongst all thermoplastic materials, which is one of the disadvantages of using PVC. Because of the low softening temperature, it is not really possible to use PVC in load bearing applications at temperatures above  $60^\circ\text{C}$  (Tseng,A.A et al, 1990). PVC blends with other polymer and additives are formulated to produce hard rigid PVC materials are known as unplasticised PVC (UPVC). Unplasticised PVC is very popular

for its use as a window frame material. Trocal (Troisdorf, Germany) was the first company in the world to innovate with windows and doors made from PVC. The first steps of work in this field dates back to 1954 (peter, 2003).

PVC can be made softer and more flexible by the addition of plasticizers, the most widely used being phthalates. Plasticizers work by embedding themselves between the chains of polymers, spacing the chains apart (increasing the "free volume"), and thus significantly lowering the glass transition temperature for the plastic and making it softer. In this form, PVC is used in clothing and upholstery, make flexible hoses and tubing, flooring, roofing membranes and electrical cable insulation. PVC is also commonly used in figurines and in inflatable products such as waterbeds, pool toys, and inflatable structures (Wypych, 2008). For plastics such as PVC, the more plasticiser added, the lower its cold flex temperature will be. This means that it will be more flexible, though its strength and hardness will decrease. The more flexible forms of PVC are produced by incorporating a liquid plasticiser in the PVC polymer to act as a plasticising agent (PPVC) (Wypych, 1977).

## **2.2 PVC Applications**

Blended PVC materials can be manufactured to possess a range of properties depending on the desired application. The intrinsic properties of PVC make it suitable for a wide variety of applications. It is biologically and chemically resistant, making it the plastic of choice for most household sewage pipes and other pipe applications where corrosion would limit the use of metal. With the addition of impact modifiers and stabilizers, it becomes a popular material for window and door frames. By adding plasticizers, it can become flexible enough to be used in cabling applications as a wire insulator (Wypych, 2008). Figure 2.1 shows different application of the PVC by type produced in Europe in 2007.

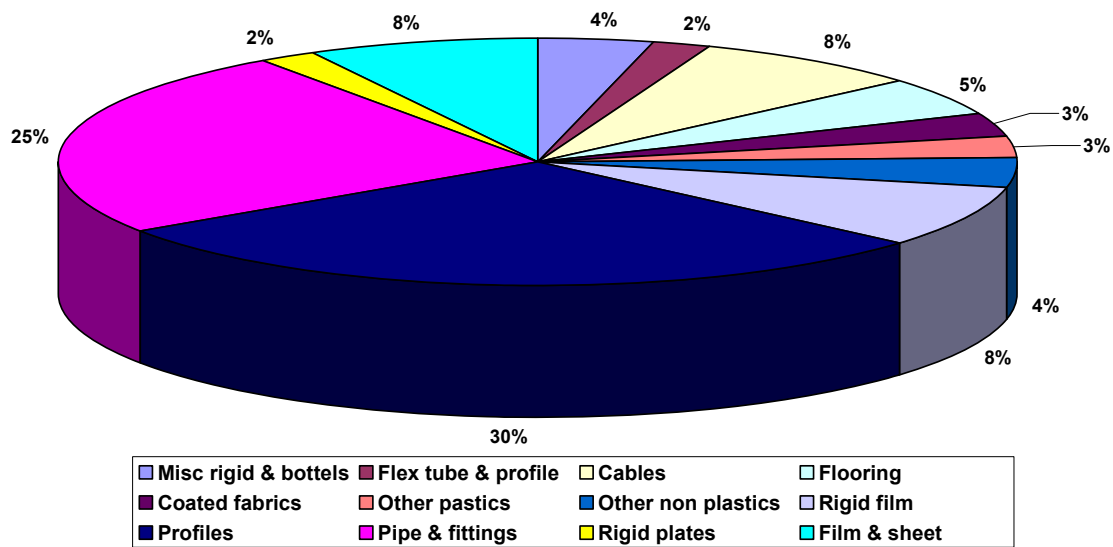


Figure 2-1 Sale of different products of PVC in Europe in 2007

PVC abrasion resistance, light weight, good mechanical strength and toughness are key technical advantages for its use in building and construction applications. PVC can be cut, shaped, welded and joined easily in a variety of styles. PVC is resistant to weathering, rotting, chemical corrosion, shock and abrasion. It is therefore the preferred choice for many customers for long-lived or outdoor products. In fact, medium and long-term applications account for some 85 per cent of PVC production in the building and construction sector (Michel, 1978).

Table 2.1 shows the list of some of the additives and stabilisers used with PVC for different applications.

Table 2.1 Types of Additives used in PVC

Additives	Main functions	Amount used/phr	Examples
Heat stabiliser	Essential to prevent Discolouration during processing	1-5	Basic lead compounds metal soaps and organotin compound
lubricant	Essential to reduce friction during processing	1-3	Waxes, glyceryl esters stearic acid and stearates
Plasticiser	To increase flexibility	30-120	Mostly esters- phthalates, adipates, phosphates
Filler	To increase bulk cheaply	15-100	Calk, synthetic calcium carbonate, china clay
Process aid	To improve fusion and flow in processing	1-5	polymethylmethacrylate
Colorant	To colour the product	0.1-4	Titanium dioxide (white), dyes and pigments
Impact modifier	To improve toughness	5-20	Rubber- EVA chlorinated PE, acrylics
Blowing agent	To produce cellular products	1-5	AZO- compounds
Antistatic agent	To prevent build-up of static charge	0.5-1	Quaternary ammonium salts
Antioxidant	To prevent oxidation of plastisiser	0.1-1	Hindered phenols
Fire retardant	To lower flammability	5-100	Antimony oxide aluminium hydroxide

It is estimated that PVC pipes will have potential in-service lives of up to 100 years. In other applications such as window profiles and cable insulation, studies indicate that over 60 per cent of them will have working lives of over 40 years. PVC has been a popular material for construction applications for decades due to its physical and technical properties which provide excellent cost-performance advantages. As a material it is very competitive in terms of price, this value is also enhanced by the formulation such as its durability, lifespan and low maintenance.

Excellent thermal insulation of PVC windows, cladding and roofing helps to significantly increase the energy efficiency of buildings. PVC products require comparatively less

energy and resource use during production, as well as in conversion to finished products. PVC products are lighter than those made of concrete, iron or steel while requiring less energy to transport and install. PVC products are also so durable that frequent replacement is unnecessary. PVC as a thermoplastic is relatively straightforward to separate from other plastics and hence can be easily recycled into new applications. Well established schemes ensure that a large proportion of the PVC used in construction applications, such as pipes, window profiles and flooring are now recycled at the end of their useful lives (Delassus,P.T & Whitman,N.F, 1999).

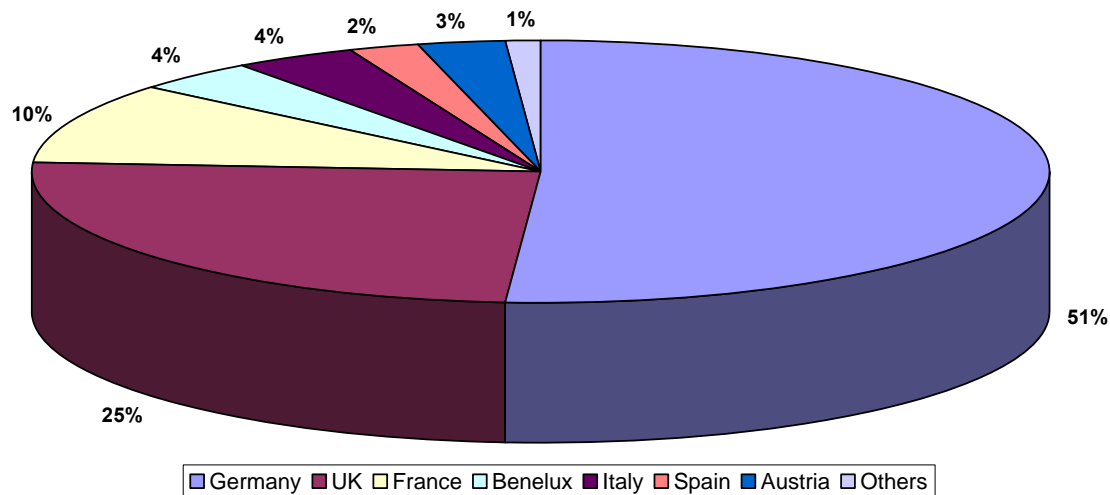


Figure 2-2 Amount of PVC window profiles used in west European in 1998

Figure 2.2 shows the usage of PVC window profiles in western European countries in 1998. The construction industry utilises 23% of the United Kingdom’s total plastic use, with unplasticised polyvinyl chloride (PVCu) accounting for over 80% of the construction plastics market via its widespread use in pipe, cable, cladding and joinery profiles (BPF, 1995).

Additives such as heat stabiliser, light stabiliser, slip agents, plasticisers and antioxidants represent some of the most common classes of compounds used to adapt polymer (PVC) properties for specific applications (Woodman,R.T et al, 1984). The global production of PVC is estimated at over 30 billion kg. In order to meet the conversion to, and performance expectations of this vast array of applications uses, a wide range of PVC additives are used. The global consumption of PVC additives, excluding plasticizer, reached 2 billion kg in 2004. Typical loading rates of lead salt based stabilisers range

from 2-6% in PVC resin. An initiative – Vinyl 2010 is expected to change the majority use of lead salt based stabilisers to more environmentally friendly calcium/zinc or organic based stabilisers within the next five years (Gonzalez, A et al, 1989). Table 2.2 shows the list of the additives and filler typically used in UPVC window profile products.

Recently new impact modifier have been introduced to the window profile industries product line – a series of all-acrylic, impact modifiers for PVC window extrusions. This new innovative product line enables users to choose from a suite of optimized products delivering specific performances to their PVC window profile product lines. Therefore, each product in this series offers a different balance of performance properties, such as impact and gloss and low temperature impact (Arias, G et al, 2006).

Table 2.2 shows the list of different additives used in UPVC formulation for window frame profiles.

Table 2.2 Additives used in UPVC window frame profiles

Ingredient	function	Phr
Mass or suspension PVC resin, K- value 60	polymer	100
Dibasic lead phosphate	Heat and light stabiliser	3
Dibasic lead stearate	Heat and light stabiliser	1.5
Calcium stearate	lubricant	0.5
Fatty alcohol	lubricant	0.4
Easter wax	lubricant	0.4
Synthetic calcium carbonate	filler	10
Acrylate rubber	Impact modifier	15
Titanium dioxide	White pigment	2.0

## **2.3 Polyurethane**

### **2.3.1 Introduction to polyurethane**

Polyurethane reactive hot melt adhesives are substances able to bond two identical or different substrates. They find applications in the bookbinding, packaging, automotive and construction industries where they are used to bond a large range of materials including wood and metal. They have many industrial applications due to their quality, innovation and properties. Polyurethane reactive hot melt adhesive are essentially prepolymers made by reacting a polyol with an isocyanate to form a urethane group (Figure 30). The polyurethane part reacts with moisture in the air or substrate being bonded, and crosslinks to form a far superior adhesive. In contact with moisture, there is an irreversible chemical reaction which gives this type of adhesive a resistance to high temperatures

One of the aims of this project was to study the stability and durability of four different PU hot melt adhesives using XPS analysis to study changing on surface composition of elements as function of time. This study enable us to know the best PU hot melt adhesives amongst four PU hot melting adhesives, in terms of chemical stability and durability to use it for bonding rigid PVC to plasticised PVC film. However, the right PU would be used to bond PVC V to plasticised PVC film to make sandwich layer. The final step of the work was to study the interface between the different substrates and the hot melt adhesives, as well as the substrates and the UV primer that had already been applied to PVC V in its cold liquid form. Ultra low angle microtomy (ULAM) was employed to expose the buried interface between the substrates and adhesives. XPS linescan analysis was used to investigate the degree of penetration between the substrates and adhesives.

### **2.3.2 Methylene diphenyl diisocyanate (MDI) adhesives**

Methylene diphenyl diisocyanate (MDI) has more than a 60 per cent share and toluene diisocyanate (TDI) has more than 30 per cent of global isocyanate production (Randall,D & Lee,S, 2002). These aromatic isocyanates are significantly more reactive than aliphatic isocyanates such as hexamethylene diamine (HDI) because the negative charge should be lone pair so that the negative charge on the nitrogen is distributed throughout the aromatic carbon and it results in reducing further the electron charge on the carbon of the isocyanate group. Besides, MDI and TDI are more economical to use. Only MDI was

used in this study. MDI has two isomers, 4, 4'-MDI and 2,4'-MDI, which may form polymeric MDI. Pure 4, 4'-MDI is a symmetrical molecule with two 2,4'-MDI groups of equal reactivity, and 2,4'-MDI is an asymmetrical molecule with two groups of different reactivity. The para position is more reactive than the ortho position, and most of isocyanate groups are located in the position. Figure 2.3 shows the structure of the three MDI forms.

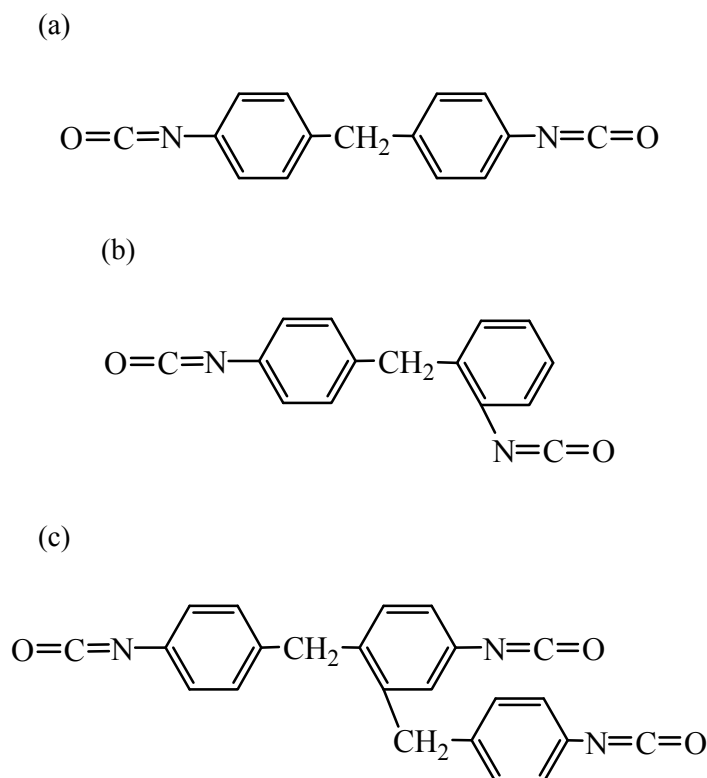


Figure 2.3: shows Structures of (a) 4, 4'-MDI, (b) 2,4'-MDI (c) an example of polymeric MDI

In the MDI production process, a complex mixture of di, tri, quarto, penta isocyanates are formed, and the NCO groups can be in the para or ortho position. Benzene is reacted with nitric acid and catalyst to form nitrobenzene, and then the nitrobenzene is catalytically hydrogenated to aniline. The aniline is reacts with formaldehyde and catalyst to form methylene dianiline (MDA) / diaminodiphenylmethane (DADPM). The MDA is then phosgenated to form polyisocyanate mixture. By distillation, a part of the diisocyanates are distilled off, and then purified further (crystallisation) in pure MDI (4,4-MDI) and mixed isomers (mixture of 4,4 and 2,4 MDI). The bottom fraction obtained after crude MDI splitting, labelled as polymeric MDI, contains a mixture of di-iso (30-50 wt.%), tri-

iso (20-30 wt.%) and small amounts of quato and penta isocyanates, as well as some impurities such as urea and biurets (Dillingham,R.G & Moriaty,C, 2003).

### **2.3.3 Polyurethane chemistry**

The isocyanate group reacts with compounds that contain active hydrogen such as hydroxyl, water, amine urethane and urea, but also with other isocyanates (Chehimi,M.M & Watts,J.F, 1992). The most important reactions are with hydroxyl groups and with water. In the first reaction, the polyurethane is formed with the reaction of an isocyanate group (-NCO) and a hydroxyl group (-OH) of polyol in the presence of catalyst and other additives, and this reaction is exothermic and reversible, as shown in Figure 1.2. In the second reaction, the isocyanates react with water to produce a carbamic acid in the presence of a catalyst. The carbamic acid is thermally unstable so breaks down into an amine and carbon dioxide, then the amine reacts immediately with another isocyanate to form a substituted urea.

The isocyanates also react with urea to form biurets via active hydrogen's, while the reaction with urethane forms an allophanate and both reactions are reversible upon heating. The former reaction is much faster than the latter reaction and takes place above 100°C compared with about 120 to 140° for the allophanate scheme.

The isocyanates can react with themselves to form dimers and trimers. The dimerisation is reversible and the dimer is thermodynamically stable at room temperature. The reaction rapidly increases with temperature. The dissociation is almost complete above 190°C and thus the dimer can go back to isocyanate by quenching to about 80°C after heating to 200°C. The trimerisation generally occurs in the presence of catalyst such as alkali metal alkoxides and carboxylic acid salts, and this reaction is exothermic and ends when all isocyanate groups have reacted. The trimer is thermally stable and the reaction is irreversible.

The isocyanates also produce carbodiimide and carbon dioxide by reacting with themselves above 180°C and the carbodiimide then slowly reacts with another isocyanate to form uretoimine at lower temperature. The former reaction is not reversible due to the loss of carbon dioxide whereas the latter one is reversible. Adhesion theory

There are mainly four mechanisms of adhesion: mechanical interlocking, diffusion theory, electronic theory and adsorption theory.

### 2.3.4 Mechanical interlocking

Mechanical interlocking of the adhesive into the pores, holes and other irregularities of the substrate surface is the major source of intrinsic adhesion as a result of increasing interfacial contact. One example of true mechanical interlocking is in the use of mercury amalgam for filling tooth cavities, where the dentist drills out the tooth material to create a pit with an undercut angle of about 5°. The adhesives have to flow into the pores and interstices of the materials to establish mechanical interlocking. The embedded adhesives solidify and become inextricable. However, the attainment of good adhesion between smooth surfaces exposes the theory as not being widely applicable. For example, the adhesion between two atomically smooth mica surfaces and the adhesion between two optically smooth rubber surfaces (Kinloch, 1995).

The adhesive strength depends on the topography of the substrate surface. The substrate has to be pre-treated to obtain appropriate roughness by mechanical or chemical pre-treatments. Mechanical pre-treatment involve scrubbing, polishing with abrasive paper and grit blasting, while chemical pre-treatment involve etching, polishing, anodizing and plasma treatment.

As two polymer surfaces are close enough to contact, parts of the long chain molecules diffuse across the interface, then interpenetrate and eventually the interface disappear. The diffusion theory requires that both adhesives and adherent are chain segments of the polymers, which have sufficient mobility and are mutually soluble. The solubility parameter,  $\delta_s$ , can be defined by the following equation, and is applicable to organic solvents:

$$\text{Equation 2 } \delta_s = \{(\Delta H_v - RT) / V\}^{1/2}$$

Where  $\Delta H_v$  is the molar heat of vaporization, R is the gas constant, T is the temperature in K and V is the molar volume. The solubility parameter is an index of the compatibility of two components. If adhesives and adherent possess similar value they will form a solution. However, in case they do not have similar values or one polymer is highly crosslinked,

crystalline or below its glass transition temperature, interdiffusion will not be as significant. (Kinloch, 1995).

### 2.3.5 Diffusion theory

As two polymer surfaces are close enough to contact, parts of the long chain molecules diffuse across the interface, then interpenetrate and eventually the interface disappears. The diffusion theory requires that both adhesives and adherent are chain segments of the polymers, which have sufficient mobility and are mutually soluble. The solubility parameter,  $\delta_s$ , can be defined by the following equation, and is applicable to organic solvents:

Where  $\Delta H_v$  is the molar heat of vaporization, R is the gas constant, T is the temperature in K and V is the molar volume. The solubility parameter is an index of the compatibility of two components. If adhesives and adherent possess similar value they will form a solution. However, in case they do not have similar values or one polymer is highly crosslinked, crystalline or below its glass transition temperature, interdiffusion will not be as significant. When certain metals are evaporated or sputtered on polymer surfaces, interdiffusion can be induced and interphase region created to enhance the interfacial adhesion. For instance, interdiffusion occurs at copper/polyimide interface. In this case, the chemisorption provides the intrinsic adhesion forces but also the interdiffusion of copper into the polyimide surface regions enhanced (Petrie, 2002).

### 2.3.6 Electronic theory

The electronic adhesion is based on the electrostatic double layer (EDL) theory (Lee, 1991). If adhesives and adherents have different electronic band structures, electron will be transferred from one to the other. This transfer results in the formation of a double layer of electrical charge at the interface. In Deryaguin's study, the condenser discharge energy ( $A_c$ ) that is required to separate the double layer can be described by the following equation:

$$\text{Equation 3 } A_c = h_c \epsilon_d / (8\pi) (dV_c / dh_c)^2$$

Where  $V_c$  is the discharge potential at the discharge gap,  $h_c$ , and  $\epsilon_d$  is the dielectric constant.

In the case of zirconium-coated gold sphered on cadmium sulphide single crystal substrates, the electrostatic properties of the photo conducting CdS samples were changed so that the EDL force at the interface was varied.

### **2.3.7 Adsorption theory**

The adsorption theory of adhesion is the most applicable theory. Sufficiently intimate molecular contact is achieved at the interface. The interatomic and intermolecular forces are established between the atoms and molecules in the surfaces of the adhesive and substrate, so they lead the materials to adhere (Watts, J.F & Castle, J.E, 1999).

Adsorption can be classified into physisorption and chemisorption according to the bond energies involved. Physisorption and chemisorptions are bonds on the thermodynamics of the adsorption process. Physisorption is often dispersion forces which are non-specific chemical bonding at the interface. In physisorption, the bonding is associated with van der Waals forces. The enthalpy of adsorption is less than  $-25 \text{ kJ mol}^{-1}$ . Chemisorption is characterised by primary bond and donor-acceptor bonds. The donor-acceptor bond such as Bronsted acid-base interaction and Lewis acid-base interaction may be formed across the interface and have higher bonding energy than physical forces. In addition, primary bonds such as ionic and covalent bonds may also be formed across the interface. Primary bonds have higher bonding energy than other bond types. The enthalpy of adsorption is greater than  $40 \text{ kJ mol}^{-1}$

## **2.4 X-ray photoelectron spectroscopy**

XPS is widely used as surface analysis technique, and is also called electron spectroscopy for chemical analysis (ESCA). XPS is utilized to determine all elements apart from H and He, and their chemical bonds. The information is obtained from the first few atomic layers, and the detection limit is about 0.1 atomic %.

## **2.5 Process of photoemission**

In XPS analysis, the primary excitation is accomplished by irradiating a sample using soft X-rays such as Mg  $K\alpha$ , Al  $K\alpha$ , Si  $K\alpha$ , Zr  $L\alpha$  and Ag  $L\alpha$ . The most common used anodes are Mg  $K\alpha$  of energy 1253.6 eV and Al  $K\alpha$  of energy 1486.6 eV. A photon with well-defined energy,  $h\nu$ , is targets the sample and then it is absorbed by an atom. As the

photon energy is high enough, the excited electron escapes from the surface and the binding energy of the electron,  $E_B$ , is:

$$\text{Equation 4 } E_B = h\nu - E_K - W$$

Where  $E_K$  is the kinetic energy of the electron and  $W$  is the spectrometer work function. Figure 2.3 illustrates the schematic of the XPS photoemission process. The photoelectron spectrum will reproduce the electronic structure of an element accurately within the limit of energy accessible.

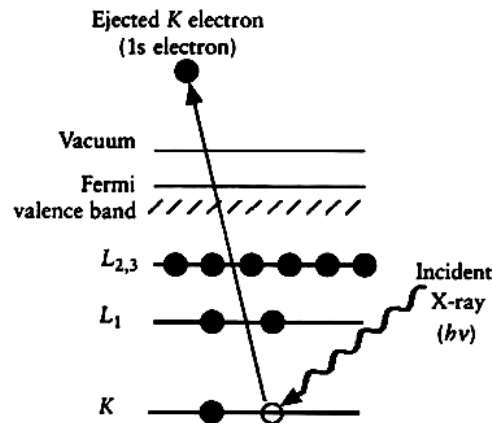


Figure 2-3 Schematic diagram of the XPS process, showing photoionization of an atom by the ejection of a 1s electron (Watts & Wolstenholm, 2003)

Once a photoelectron has been emitted in the photoelectron process, either Auger electrons or X-ray photons are emitted due to relaxation of the excited ions remaining after photoemission. Figure 2.4 describes the process of the emission of an Auger electron. An outer electron falls into an inner orbital vacancy, and a second electron is simultaneously emitted, carrying off the excess energy.

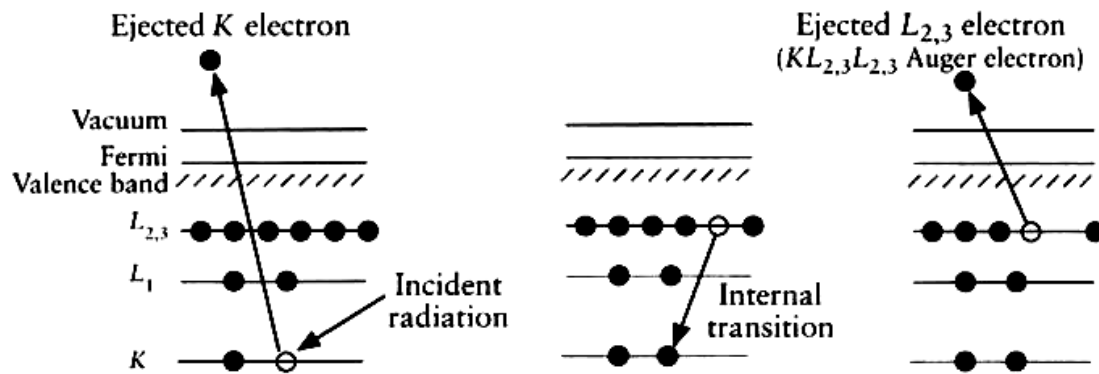


Figure 2-4 : Relaxation of the ionized atom of Figure 11 by the emission of a  $KL_{2,3}L_{2,3}$  Auger electron  
(Watts & Wolstenholm, 2003)

### 2.5.1 Depth of analysis

XPS can provide compositional information as a function of depth in either destructive or non-destructive way. In this study, non-destructive depth profiling method is used by manipulating the Beer-Lambert equation.

The relationship between a substrate of thickness,  $d$ , and electron intensity,  $I$ , exited from a depth in a substrate is expressed by the Beer-Lambert equation,

$$\text{Equation 2: } I = I_0 \exp(-d / \lambda \cos \theta)$$

Where  $I_0$  is the intensity from an infinitely thick layer,  $\theta$  is the angle for electron emitted to relative the surface normal and  $\lambda$  is the attenuation length of the electrons which is related to the inelastic mean free path (IMFP). The attenuation length is generally about 10 % less than the IMFP. The variation of electron intensity with depth is illustrated in Figure 2.4. When electrons emerge at  $0^\circ$  to the surface normal, 65 % of the electron signals emanates from a depth of less than  $\lambda$ , 85 % from a depth of less than  $2\lambda$  and 95 % from a depth of less than  $3\lambda$ . Therefore, the depth of analysis depends on electron angle of emission. Figure 2.5 shows the sampling ( $3\lambda \cos \theta$ ) depth at different take-off angles.

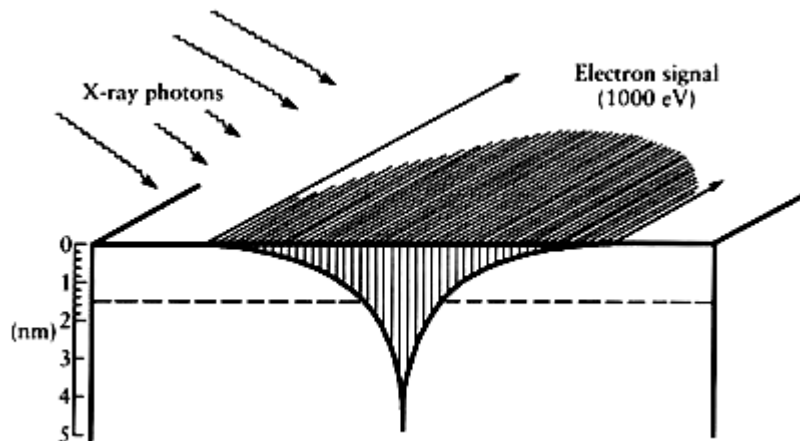


Figure 2-5: Relaxation of the ionized atom of Figure 11 by the emission of a  $KL_{2,3}L_{2,3}$  Auger electron (Vickerman, 1998)

## 2.5.2 Instrumentation

### 2.5.3 Vacuum system

XPS analysis must be carried out in the UHV range of  $10^{-8}$  to  $10^{-10}$  mbar. There are two principal reasons why the UHV system is required.

The first reason is permitting the analytical signal of low energy electrons to reach the detector without under interference from gas phase scattering, which will interact an ejected photo electron. A pressure of  $10^{-6}$  mbar will provide a long enough mean free path for the electron to carry out reliable analysis.

The second reason is more important. Photoelectron spectroscopic techniques analyse only the top few atomic layers with a sensitivity of a few atomic percent so that the surface is to be maintained in a contamination-free state during the experiment. At  $10^{-6}$  mbar, it is possible for a monolayer of gas to be adsorbed onto a solid surface in about 1 second. Therefore, a pressure of  $10^{-9}$ - $10^{-10}$  mbar needs to be achieved to obtain less than 1 % of a monolayer of contamination during the course of the experiment.

## 2.6 X-ray sources

### 2.6.1 Twin anodes

X-rays are generated by bombarding an anode material with high-energy electrons. The efficiency of X-ray emission from anode is determined by the electron energy, relative to the X-ray photon energy. Aluminium and magnesium are the most popular anode

materials, and are supplied in a single X-ray gun with a twin anode configuration providing Al K $\alpha$  or Mg K $\alpha$  photons of energy 1486.6 eV and 1253.6 eV respectively.

The twin anode assemblies are useful in case Auger and photoelectron peaks overlap in one radiation. XPS peaks change to a position 233 eV higher on a kinetic energy scale by switching from Mg K $\alpha$  to Al K $\alpha$  while Auger peak remains constant.

In addition, the higher energy X-ray radiation provides a non-destructive means of increasing the analysis depth; therefore, a depth profile can be deduced by changing the X-ray source. For instance, the analysis depth of the carbon 1s peak in a polymer is approximately  $7 \cos\theta$  nm for electrons excited by Al K $\alpha$  while Mg K $\alpha$  is  $6 \cos\theta$  nm (Watts & Wolstenholm, 2003).

### 2.6.2 X-ray monochromators

An X-ray monochromator can produce a narrow X-ray line, remove the X-ray satellites, and improves signal-to-background ratio by eliminating the Bremsstrahlung continuum, and selects an individual X-ray line from the unresolved K $\alpha_{1,2}$  doublet by using diffraction in a crystal lattice. The most popular source combines an Al anode with a quartz crystal (1010 orientation). X-rays strike the parallel crystal planes at an angle  $\theta$  and are diffracted at the same angle. If the distance between the crystal planes is equal to an integral number of wavelengths, the X-ray interferes constructively, but if not destructive interference takes place. It is governed by the Bragg equation:

$$\text{Equation 5: } n\lambda = 2d \sin\theta$$

Where  $n$  is diffraction order,  $\lambda$  is the X-ray wavelength,  $d$  is crystal lattice spacing and  $\theta$  is angle of diffraction.

Figure 2.6 illustrates the principle of X-ray monochromators. The quartz crystal (1010) is placed on the Rowland circle and the X-ray source is placed at another point on the circle. When X-ray source strikes the quartz crystal the K $\alpha$  X-rays are dispersed by diffraction and focused at another point on the Rowland circle where the sample is placed. Therefore, the K $\alpha_1$  component of the principal Al K $\alpha$  line can be obtained as the angle between incident and diffracted rays is 23°.

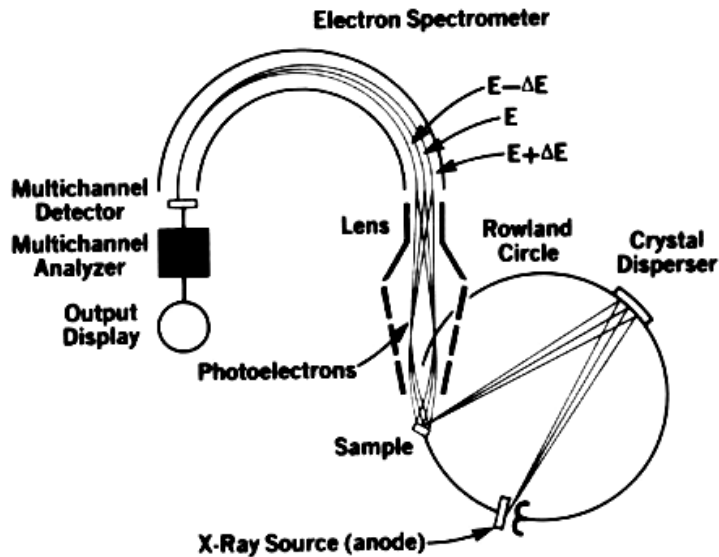


Figure 2-6 Principle of X-ray monochromator (Biriggs,D & Seah, M.P, 1987)

## 2.7 Time of flight secondary ion mass spectrometry

ToF-SIMS is a method for analysing the elemental and chemical composition of the outermost molecular or atomic layer of a solid surface. The sensitivity is extremely high for all elements.

### 2.7.1 Principle of the technique

A solid surface is bombarded with a high energy beam of primary ions. The primary ions penetrate the material and transfer their kinetic energy to the target atoms by a billiard-ball type collision process, which is called collision cascade. The collision cascade is classified into three types of regimes: a single knock on, the linear cascade and a spike regime. In the single knock on regime only small energy is transferred to individual atoms. As the linear cascade regime large energy, a few hundred eV, is transferred to atoms in the surface target so the collisions take place between a small region of moving atom and an atom at rest. The spike regime is for a large region of moving atoms due to a high energy (up to 10 keV) being transferred. As a result of the collision cascade, atoms, clusters and molecules are emitted from the surface, besides over 95 % of these secondary particles originates from the top two atomic layers of surface (Vickerman, 1998). The vast majority of emitted particles are neutral in charge but a small proportion is positively or negatively charged, and these ionized particles are accelerated to a constant kinetic energy and then allowed to pass a certain distance in a field free space before they are

collected on an intensity sensitive detector (Walls, 1990). Figure 2.10 illustrates the schematic diagram of the SIMS process.

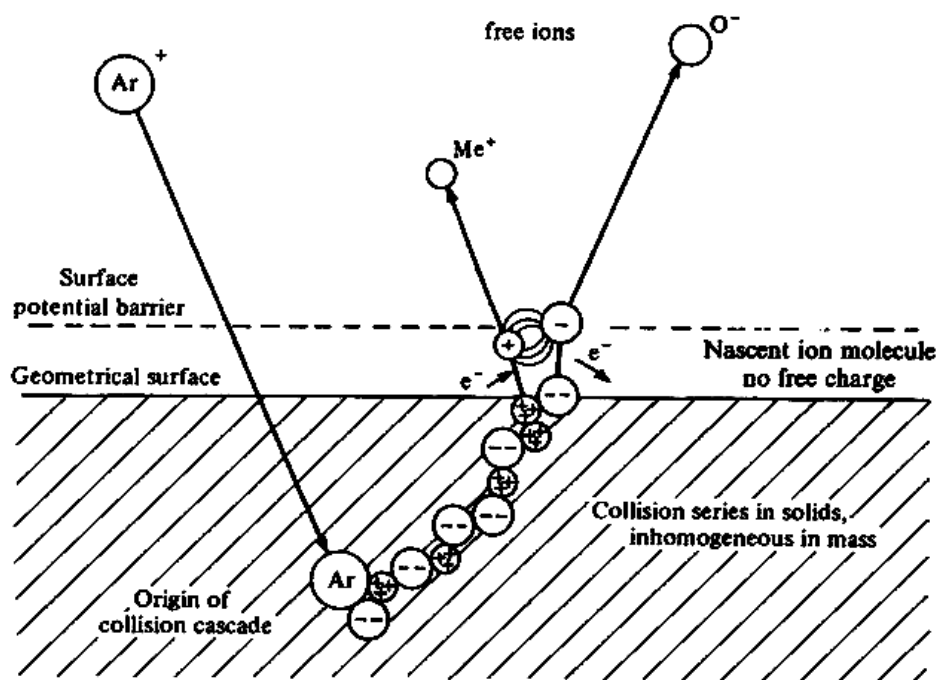


Figure 2-7 Schematic diagram of a modern HAS and transfer lens (Watts & Wolstenholm, 2003)

The static SIMS mode can maintain the integrity of a surface layer during the lifetime of the analytical experiment. A low primary beam dose, typically up to  $1 \text{ nA cm}^{-2}$ , is used to minimize surface damage.

## 2.7.2 Instrumentation

The basic components of a SIMS system are a primary ion gun and a mass analyser in a UHV system.

## 2.7.3 Primary ion beam sources

A range of primary beam sources has been used in SIMS and it can be classified into four basic types: electron bombardment, plasma, surface ionisation and field ionisation. The important ion source parameters are brightness, extractable current and energy spread so each type of source gives different performances such as spatial resolution, ease/speed of use, sensitivity, coping with insulating materials and beam induced damage. Table 2.2 summarizes the typical operating parameters for these type ion sources.

Table 2.3 Operating parameters for common sources (Vickerman, 1998)

Parameter	Electron bombardment	Plasma	Surface ionization	Field ionization
Source	Ar, Xe, C <sub>60</sub>	Ar, Xe, Ne, O <sub>2</sub>	Cs	Ga, Bi, Au
Acceleration voltage	0.1 – 5 keV	10 keV	10 – 20 keV	5 – 35 keV
Beam size at the best condition	0.1 – 2 mm	2 – 100 $\mu\text{m}$	$\geq 200 \text{ nm}$	$< 100 \text{ nm}$
Current density	4 mA cm <sup>-2</sup>	20 mA cm <sup>-2</sup>	100 mA cm <sup>-2</sup>	1000 mA cm <sup>-2</sup>

#### 2.7.4 Electron bombardment

In electron bombardment ion sources, electrons from a heated cathode are accelerated towards an anode to give them sufficient energy to ionise the source gas, which is usually argon or xenon. The design of source region and associated electrodes produce multiple passes of the electrons through the ioniser, and hence increasing the extractable ion current. The energy is variable from 0.1 to 5 keV and it leads to spatial resolution from 50  $\mu\text{m}$  to several mm. The brightness is about  $10^{-2} \text{ A cm}^{-2} \text{ Sr}^{-1}$  and the maximum current density is about  $1 \text{ mA cm}^{-2}$ .

This source is also used in a pulsed ion gun for ToF-SIMS. 10 keV argon ions in pulses of 0.8 ns half-width give spatial resolution between 4 and 10  $\mu\text{m}$  and 500 to 1000 primary ions per pulse (Beamson, G & Briggs, D, 1992).

#### 2.7.5 Time of flight mass analyser

All the secondary ions produced are extracted with the same kinetic energy so ions of differing mass to charge ratio have different velocities. A time-of-flight (ToF) mass analyser measures the mass-dependent time it takes ions of different masses to move from the ion source to the detector. They are left to drift through the flight tube of the

spectrometer and the heavier ions, which are higher mass ions, take longer to reach the detector than the lighter ions. The measured flight time,  $t$ , of ions of mass-to-charge ratio,  $m/z$ , accelerated by potential,  $V$ , down a flight path of length,  $L$ , gives a simple means of mass analysis:

$$\text{Equation 6: } t = L (m / 2zV)^{1/2}$$

The timing events require picosecond accuracy so the parallel detection combined with the high transmission gives high sensitivity. Although the mass range is unlimited, high mass ranges require slower pulse frequencies and longer analysis time and hence the mass range is in practice about 10000.

SIMS images can be obtained by rastering the primary ion beam with parallel acquisition, and imaging resolution is in a range of 0.1 to 4  $\mu\text{m}$  for the pulsed ToF SIMS beam.

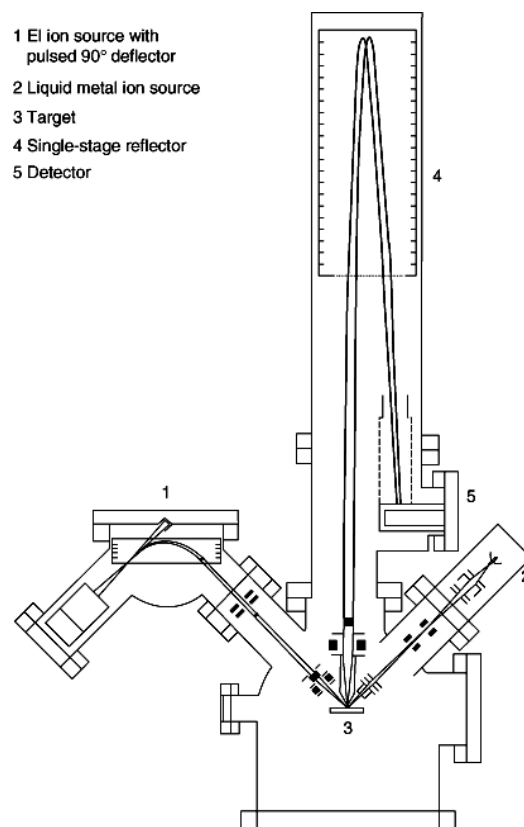


Figure 2-8 Schematic diagram of reflectron ToF-SIMS instrument (Hanton,S.D & Clark,P.A.C, 2000)

## 2.8 AFM

The Atomic Force Microscope (AFM ) is being used to solve processing and materials problems in a wide range of technologies affecting the electronics, telecommunications,

biological, chemical, automotive, aerospace, and energy industries. The materials being investigated include thin and thick film coatings, ceramics, composites, glasses, synthetic and biological membranes, metals, polymers, and semiconductors. The AFM is being applied to studies of phenomena such as abrasion, adhesion, cleaning, corrosion, etching, friction, lubrication, plating, and polishing. By using AFM one can not only image the surface in atomic resolution but also measure the force at nano-newton scale.

The Atomic Force Microscope (AFM) is one type of scanning probe microscopes, which is used to image surface structures (on a nm or even sub-nm scale) and to measure surface forces.

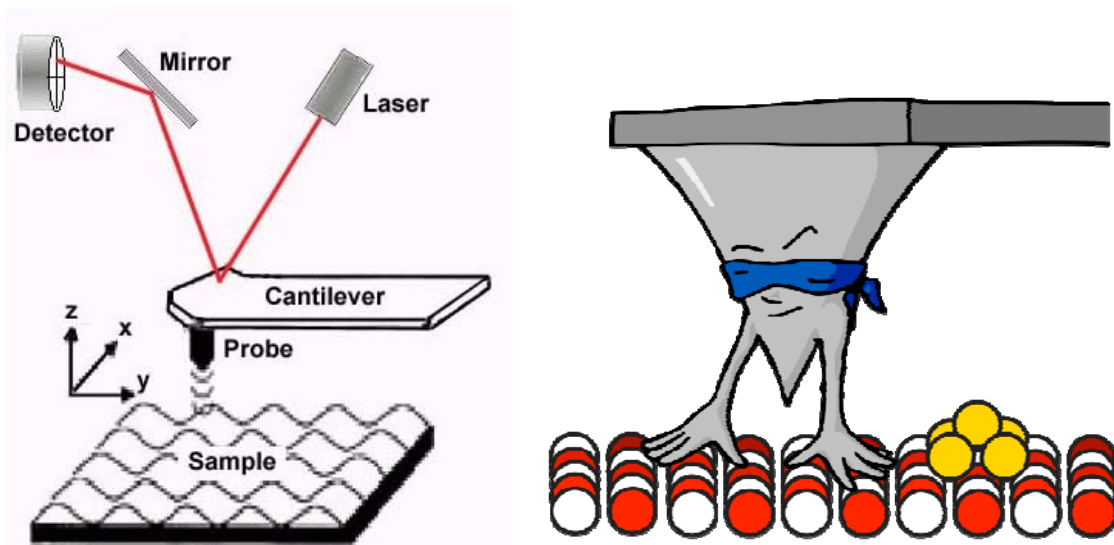


Figure 2-9 A schematic image of the AFM processing

The standard AFM contains a microscopic tip (curvature radius of  $\sim 10\text{-}50\text{nm}$ ) attached to a cantilever spring.

The underlying principle of AFM is the detection of the bending of this cantilever spring as a response to external forces. In the case of adhesive interaction between the tip and a surface, these forces are of the order  $0.1 - 1 \text{ nN}$ . To measure such small forces one must use not only very sensitive force-measuring springs but also very sensitive ways for measuring their bending.

In order to detect this bending, which is as small as 0.01 nm, a laser beam is focused on the back of the cantilever. From there the laser beam is reflected towards a position-sensitive photo detector. Depending on the cantilever deflection, the position of the reflected beam changes. The photo detector converts this change in an electrical signal.

A way to get information on the surface forces which are acting in a given system and to illustrate the functioning of an AFM is to use the Force Mode. This is done by moving the tip towards and away from the surface.

## 2.9 Contact angle measurements

Understanding and determination of surface free energies of both liquid and solid surfaces play an important role in a wide range of scientific and industrial areas, such as material sciences, polymers and particles, sprays and coatings, textiles and adhesives, soaps and detergents, oil recovery, printing industry, semiconductor industry, paper industry, food industry, cosmetics, pharmaceuticals, and biocompatibility of medical implants. The surface free energy of a liquid is measured by its surface tension and the surface free energy of a solid surface can be revealed by contact angle measurements.

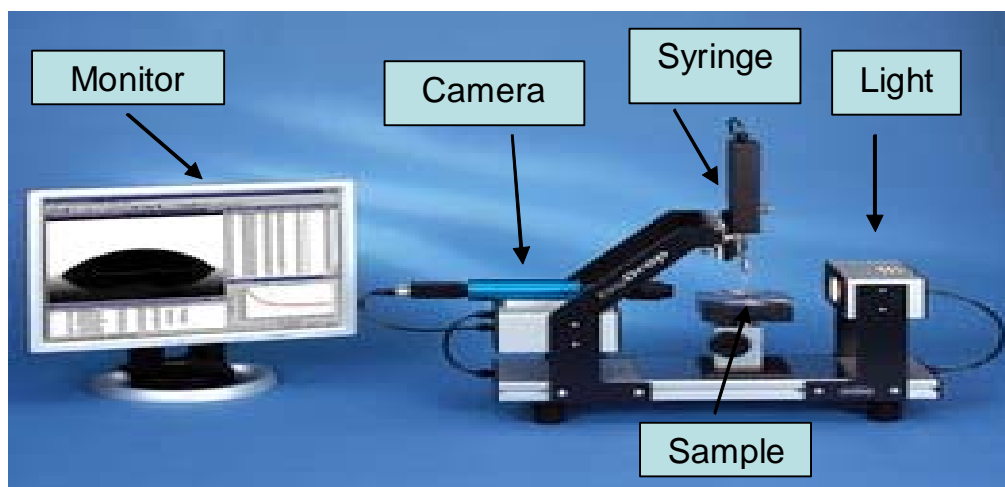


Figure 2-10 Contact angle measurement instruments

The contact angle is the angle, conventionally measured through the liquid, where a liquid/vapor interface meets a solid surface. It quantifies the wettability of a solid surface by a liquid via the Young equation. A given system of solid, liquid, and vapour at a given temperature and pressure has a unique equilibrium contact angle.

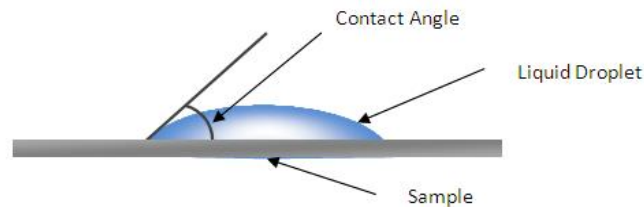


Figure 2-11 image of a liquid droplet on a sample surface

Water contact angle measurement is the most common method for determining a material's wettability, and the sessile drop approach is the most frequently used.

In many applications the wettability of a surface or ability of liquids to wet surfaces can be a key factor in a product's performance or be a significant issue in a manufacturing process. Measurement of wettability is primarily achieved by measuring the contact angle of a liquid on a surface.

In addition by combining the contact angle measurements with other surface analysis techniques available, Services such as XPS, SIMS and AES, a deeper understanding of the surface chemistry can be obtained.

Investigating properties of a manufactured polymer film, a coated item or the behaviour of a polymer melt requires a qualitative and quantitative appreciation of the interaction at all surfaces. The polymer / air, polymer / substrate interactions are crucial.

Contact angle measurements are important as is the understanding of surface chemical analytical techniques such as XPS and SIMS. Plasticisers and mobile low molecular species can affect wetting characteristics too.

For adhesives determination of the correct production methods and storage of a formulated liquid adhesive, the manufacture and application of a hot-melt or the long term stability of a coated product (eg. on a label) are all advisable.

A qualitative and quantitative appreciation of the interaction at all surfaces (liquid / liquid, adhesive / substrate) by a combination of contact angle and surface chemical techniques such as XPS is advisable to ensure good wetting characteristics as well as strong and robust bonding.

## **2.10 Flame treatment**

A Flame Treatment is a method of chemically changing the surface molecular structure of a substrate in a controlled manner to:

Increase "Surface Energy" Increase "Wettability", and therefore compatibility with coatings and materials

Flame treatment can be applied to any olefin based plastic or metallic component, like bumper fascias, body side mouldings, wheel covers, air spoilers, air scoops, door handles, door panels, consoles, dashboards, post trims, and carpet backing.

Flame treatment of components has for years always been troublesome in a high volume production environment. As such the common choice of manufacturing plants has been either the use of Adhesion Promoting Primers or the use of Flame Treatment, and in many cases a combination of both. Decisions on what method of surface treatment to use have always been a compromise.

With Adhesion Promoters, such concerns are environmental (High VOC emissions and clean-up costs), introductions of dirt, high maintenance costs, and safety. Chlorinated solvents, most commonly used in Adhesion Promoters, are highly flammable and toxic which in turn is dangerous to plant and personnel alike.

Flame Treatment provides a lower cost, high quality solution for surface treatment applications. Unfortunately, this technology has failed to keep pace with the advances made within manufacturing processes used in modern high production environments. Considerations of manufacturing engineers as to the use of flame as a method of surface treating have been based around cycle times, when the geometry was measured immediately.



Figure 2-12 Picture of Single Aerogen flame treatment machine

## **2.11 Why Flame Treatment**

In all instances the flame treatment offer superior results to other methods such as corona or plasma.

Flame treatment offers higher treatment levels and no decay of treatment.

The treatment level remains virtually indefinitely.

### **2.11.1 Applications of Flame Treatment**

- Automotive For painting and bonding of car bumpers and instrument panels etc.
- Converting/Printing - Web treatment or conditioning improves adhesion for laminating, coating and printing.
- Plastics - Flame treatment offers enhanced adhesion solutions for cups, caps, cables and containers when printing or labelling.
- Film - Printing for gift wrapping, confectionary, snack foods etc.
- Bakery - Baking of bread, cakes, pizza's, biscuits and searing or branding.

Implementing flame treatment will enhance product quality and durability, leading to a reduction in raw materials, waste and overall manufacturing costs. Due to the efficient low cost gas consumption and time savings in the production process can be

Flame treatment of plastics encompasses an infinite range of extruded or moulded products. Different applications are covered within this market sector including: bottles, containers, mouldings, components, extruded pipes and cable covers, etc. Flame treatment can be utilized to promote the adhesion of labels or print enhancing product quality. This is most beneficial for printing and labelling and insuring that there is no damage to such applications from transit or handling of the product ensuring a products visual integrity and "sale ability" is intact when reaching the supermarket shelf.



Figure 2-13 shows some sample of the products treated with flame for labelling

### 2.11.2 Benefits of flame treatment

- Improved print and label durability
- Reduce reject rates
- Enhanced product quality
- Versatile Treatment.
- Reliable
- Repeatable
- Low Costs
- Low Maintenance
- No Primers

Where gas flame has an advantage over corona is in the ability to treat differing Profiles and shapes. Corona is still regarded as the treated of choice when it comes to reel applications for most substrates. A gas flame is the combustion between an oxidizing element (air) and a fuel. The fuel in this case can be Methane, Propane or Butane.

## **2.12 Dynamic mechanical analysis (DMA)**

DMA is a technique in which either the modulus or damping or both of a substance under oscillatory load or displacement is measured as a function of temperature, frequency or time or combination thereof (Menrad, 1999).

DMA test is intended to provide a means for determining the transition temperatures, elastic and loss modulus of polymers over a range of temperatures, frequencies or time by free vibrations and resonant or non-resonant forced vibration techniques.

The stress consists of two components, one in phase with the strain (elastic response or storage modulus,  $E'$ ) and one out of phase with the strain (viscous response or loss modulus,  $E''$ ). The storage modulus is related to the storage of potential energy, while the loss modulus is related to the dissipation of heat energy when deformation occurs (Huang, Y et al, 2004)

DMA can also measure the ratio of  $E''/E'$ , known as  $\tan \delta$  of a polymer over a temperature and frequency ranges. The  $E'$  can be thought of as the stiffness of the polymer, like flex modulus or tensile modulus. (Griffin, 2001) The DMA supplies an oscillatory force, causing sinusoidal stress to be applied to the sample, which generates a sinusoidal strain. By measuring; both the amplitude of the deformation at the peak of the sine wave and the lag between the stress and strain sine waves, quantities like the modulus, the viscosity, and the damping can be calculated.

DMA identifies the transition regions in polymers, such as the glass transition, and may be used for quality control or product development. DMA can recognize small transition

regions that are beyond the resolution of DSC. DMA examines how the behaviour of viscoelastic materials changes with temperature and frequency.

The term viscoelastic has been defined as the simultaneous existence of viscous (liquid) and elastic (solid) properties in all materials (Barnes,H.A et al, 1996). In the test, the material is subjected to a sinusoidal strain over a range of temperatures, and the response obtained can provide extremely useful information about the behaviour of the material. For linear viscoelastic materials, the output stress will also vary sinusoidally, but will be out of phase with the strain (Huang,Y et al, 2004).

The polymer rheology and viscoelastic behaviour of materials under sinusoidal load will be reviewed further in chapter 5. The applied stress and material response are shown in Figure 2.17 (Menrad, 1999).

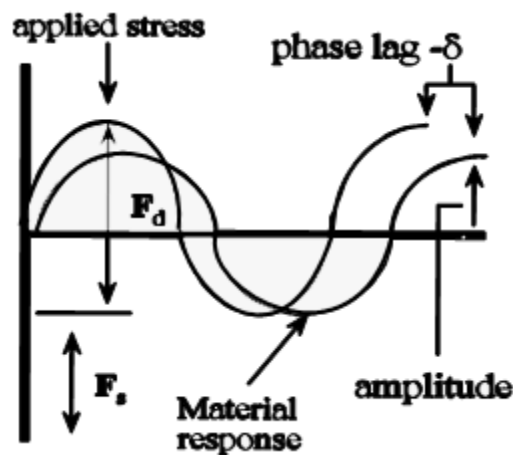


Figure 2-14 : *The DMA's oscillatory force*

### 2.12.1 Instrumentation

The DMA supplies an oscillatory force, causing sinusoidal stress to be applied to the sample, which generates a sinusoidal strain. By measuring; both the amplitude of the deformation at the peak of the sine wave and the lag between the stress and strain sine waves, quantities like the modulus, the viscosity, and the damping can be calculated.

### 2.12.2 Features of the DMA

Figure 4.18 shows the DMA unit consisting of oscillator and sensor, which can be moved in relation to the sample holder by means of the stepper motor. Static force can be applied to the sample and the device can be fit to a different sample height.

Some of the DMA features are as follows:

- Three-point bending
- Single and dual cantilever bending
- Compression – penetration
- Tension.

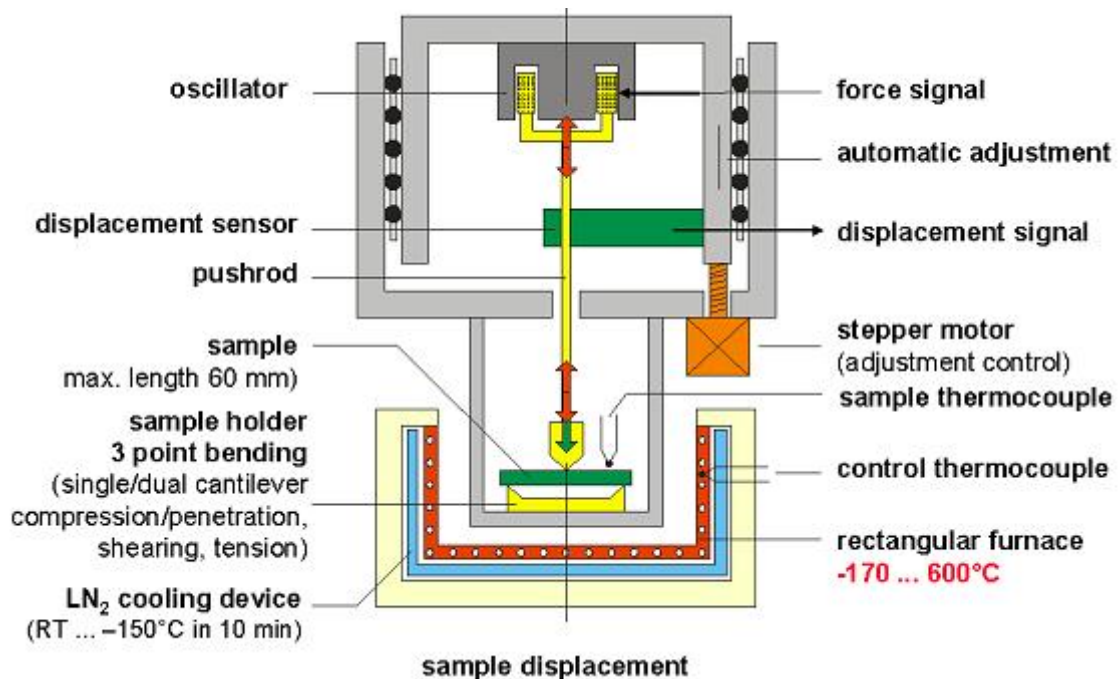


Figure 2-15 : DMA schematic diagram

### 2.12.3 Three point bending

In engineering mechanics, bending (also known as flexure) characterizes the behaviour of a slender structural element subjected to an external load applied perpendicular to an axis of the element. When the length is considerably larger than the width and the thickness, the element is called a beam (Saarela.O, 1992).

The three points bending flexural test provides values for the modulus of elasticity in bending, flexural stress, flexural strain and the flexural stress-strain response of the material. The main advantage of a three point flexural test is the ease of the specimen preparation and testing. However, this method has also some disadvantages: the results of the testing method are sensitive to specimen and loading geometry and strain rate (Tasi, 1987).

The sample is supported on two edges, while the cutting end of the push rod applies a load to the sample from above. The spacing between the two edges is in accordance with DIN 53457. Four different free bending lengths between 10 and 50 mm are available. This deformation mode is ideal for materials with a high storage modulus such as filled or reinforced thermoplastics and thermosets (composites) or metals and alloys (Bassali, 1957).

## **2.13 PVC and adhesives**

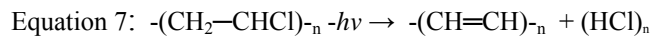
### **2.13.1 PVC Degradation**

PVC differs from many other polymer materials in that it possesses a low thermal stability. When PVC is exposed to heat, light such as ultra violet (UV) or radiation such as X-rays it will degrade with the loss of HCl. When polymeric materials are subjected to such irradiation, changes are observed in their molecular structure. Mainly chain scission that leads to a reduction in molar mass and reticulation which increases the molar mass but reduces solubility (Wypych, 2008).

The work of this these associated with analysis of PVC widow profile, X-ray photoelectron spectroscopy (XPS) is widely used for the quantitative surface analysis of polymer and polymer blends. The compositions of some polymers can change under X-ray exposure, influencing peak intensities and positions in XPS survey and high resolution spectra. In order to quantify spectra acquired after prolonged (>10 min) X-ray exposure, polymer degradation may need to be taken into account. Halogenated compounds, especially chlorinated, are known to degrade with X-ray exposure, resulting in a decrease in the halogen surface concentration and an increase in carbon surface concentration (Wypych, 1977).

As PVC degrades it also discolours and changes from transparent/white (when formulated) to pink, orange, red-brown and finally to black. Because of degradation, the intensity of Cl 2p peak will decrease as the PVC sample is exposed to a X-ray source. To resolve the degradation and discolouration problems of PVC, PVC has to be blended with other polymers, stabilisers and additives. For example, acrylic styrene acrylonitrile (ASA) is blended with PVC resulting in an increase in heat deflection temperature (HDT). The HDT of PVC is approximately 70°C and HDT of ASA is up to 105°C, by blending PVC with ASA the HDT of the blended PVC polymer rises to 90°C allowing the PVC blend to

be used in higher temperature applications (DeArmitt, 2004). PVC degrades by photo ionization, and the degradation is as follows:



Although X-rays cause changes in surface composition and chemistry at the surface of PVC based polymers, scientists could not determine any standard model to give comparative relation between the PVC degradation rate and the X-ray source flux. Yoshihara and Tanaka investigated the degradation of PVC, nitrocellulose and poly (tetrafluoroethylene) (PTFE) by X-rays in XPS instruments. Forty laboratories were involved in the study. The authors suggested PVC and nitrocellulose + cellulose acetate (NC +CA) are useful materials for comparison of X-ray source flux in different XPS instrument. The outcome of this investigation was that they could not find any standard way to calculate approximately the degree of degradation caused by the X-ray irradiation of polymers when the surface is analysed by XPS. The authors pointed out there would be good correlation between the rate constant of the degradation for PVC and that of NC + CA if analysis was carried out using achromatic X-ray rather monochromatic X-ray (Yoshiharal,K & Tanaka,A, 2002).

In 2003 Seah and Spencer investigated the degradation rate of PVC and nitrocellulose with cellulose acetate using XPS. The effects of the X-ray source and what the authors called “adventitious electrons”, on the degradation rate were studied. The “adventitious electrons” may arise either from the Al window of an unmonochromated X-ray source or from a non-ideal flood neutralization source for monochromated X-ray sources. Nitrocellulose with cellulose acetate, which has a degradation rate 4.65 times greater than PVC for unmonochromated, Al X-rays, has a degradation rate only 1.41 times higher than PVC for “adventitious electrons”. If the degradation rate measured involves similar adventitious electrons, the ratio of the degradation rates may be measured to be anywhere in the range 1.41– 4.65. The authors suggested for minimizing the degradation effects, a monochromated source should be used, provided that it is not focused to a spot of less than 300µm diameter. The degradation rate for Mg X-ray is 1.65 time that of Al X-ray. Mg source provide more intensity than Al source with same wattage, so with less wattage we can run Mg source and get same intensity that we can get higher wattage of Al source. Therefore, alternatively a Mg X-ray source should be used with the source emission at the

lowest setting compatible with the required signal quality (Seah, M.P & SPENCER, S.J, 2003).

Beamson and Briggs studied the X-ray degradation of PVC exposed to X-ray as function of time for 500min employing a monochromated X-ray source at a power of 140W. The use of a monochromated source resulted in low sample heating. Typically with an unmonochromated source the sample is much closer to the X-ray anode; hence it will receive more thermal radiation. The degradation index of PVC was calculated after PVC was exposed to X-ray for 500min using equation 2.1.

$$\text{Equation 8: } X_t/X_0 \times 100$$

Where  $X = \text{Cl/C}$  surface concentration ratio, where  $X_t$  is  $X$  at time  $t$ ,  $X_0$  is  $X$  at time 0, and  $t$  is the X-ray exposure time. In order to calculate the degradation rate they plotted the result from equation 2.1 against  $t$  (time/ (min)) ( $X_t/X_0 \times 100$  vs.  $t$ ). After 500min PVC was exposed to the X-ray, the X-ray degradation index for PVC was  $\sim 25\%$  (Beamson, G & Briggs, D, 1992).

Artyushkova and Fulghum (2001) investigated the surface composition of PVC-PMMA polymer blends using XPS in order to study X-ray degradation effects. They used XPS and XPS image analyses, the outcome of their work was that halogenated polymers, especially chlorinated, degrade with X-ray exposure resulting in a decrease in the Cl surface concentration and an increase in C surface concentration. For the period of the XPS analysis, dehydrochloration of PVC was evident with decreasing intensity of Cl2p and an increasing surface concentration of carbon. The increase in carbon concentration in pure PVC was twice that of the PVC-PMMA blend (50-50) 3.5% vs. 1.8%. Degradation analysis using XPS image analysis was promoted in this study by analysing images of the same sample (analysed using monochromatic X-ray XPS) before and after 12 h of X-ray exposure (Artyushkova, K & Fulghum, J.E, 2001). As result of PVC dehydrochloration, the maximum counts in images decreased for Cl2p from 7308 to 2150 counts, and from 10173 to 3813 counts in the O 1s image, where the maximum intensity in C 1s image increased from 7665 to 12504 counts.

Manfredini et al (2003) studied plasticised PVC, used for disposable biomedical products in the non-sterilized state, after irradiation with soft X-rays using an unmonochromated

X-ray source. The conclusion of this work was that X-ray irradiation for >10 min can degrade the plasticised PVC by more than 5%; Manfredini also found that the degradation was greater for 300 W Al than 240 W Mg. The Cl2p high-resolution spectrum confirmed that the degradation occurs via bond cleavage of C-Cl bond, releasing hydrogen chloride gas. Another suggestion was that during the X-ray exposure an oxidative reaction of the plasticiser molecules at the polymer surface occurs, increasing carbonyl and hence oxygen concentration at the PVC surface. The final point of the authors conclusions was that to overcome the X-ray degradation effects, XPS analysis of the plasticised PVC had to be performed within 8-10 min (under the experimental conditions employed) (Manfredini, M et al, 2003).

Arki and Balköse (2002) investigated the heat stability of PVC formulation including stabiliser based on an organotin (tin soap heat stabiliser). X-ray fluorescence spectroscopy, IR spectroscopy, differential scanning calorimetry (DSC), UV spectroscopy, and thermo gravimetric analysis were employed in this study. IR spectroscopy indicated that the concentration of carboxylate groups in the organotin stabiliser decreased with heating. At 160°C for 15min heating the PVC, containing 2.5% (Sn500K, from Farstab stabiliser company, Turkey), was more stable than PVC without the tin soap, however, for longer heating times the organotin heat stabiliser was less effective. At high temperature, (Sn500K) had no effect on the degradation behaviour (Arki, E and Balkose, D, 2002).

Atzei et al (2003) used angle- resolved X-ray photoelectron spectroscopy (ARXPS) to analyse a disposable medical device made of plasticised PVC, so as to investigate the effects of  $\beta$ -ray sterilization on the surface chemical composition. The ARXPS analysis of the non-plasticised PVC showed an obvious surface enrichment of the chlorine. The authors suggested that during the extrusion process, a thin layer of the PVC surface degrades and dehydrochloration occurs resulting in a surface layer depleted in chlorine. During irradiation (accompanied by heating), some hydrogen chloride gas is evolved from the surface of the plasticised polymer and polymer degradation may occur at greater depths (Atzei, D et al, 2003).

Gonzalez et al (1989) monitored the UV degradation of PVC window frames using micro hardness analysis. This paper was one of the few papers published on the subject of the degradation of commercial PVC. The investigation was undertaken by monitoring PVC samples exposed to UV light for up to 1000 h. The hardness and elongation at break of

the samples was measured as a function of time. The results showed a 30%-50% decrease in the elongation at break in the first 1000 h, which after that remained constant. The results from the micro hardness tests showed the same behaviour as thermal degradation of PVC. The authors suggested that during the initial period of irradiation a decrease in the micro hardness of materials occurs, that can be related to scission of structural elements and integration of stabilising groups to the PVC chain (Gonzalez, A et al, 1989).

DeArmitt investigated the raising of the softening point of PVC by blending PVC with other polymers. PVC materials are degraded by UV light and must be stabilized to be able to use them outdoors. PVC can be blended with a wide range of polymers (with similar polarity) and stabilisers to improve its stability, stiffness and softening point. The author suggested a blend of PVC/poly acrylonitrile-styrene-acrylate (ASA) is well suited to outdoor use. The heat distortion temperature (HDT) of PVC is approximately 70°C while that of ASA is up to 105°C, and the HDT of a blended PVC/ASA polymer is ~ 90°C. As the amount of ASA increases in the blend, it increases the HDT value of the blend<sup>3</sup>.

Berard and Ventresca (2006) investigated evaluating the processing window of impact modified rigid PVC formulation. This investigation was involved mixing the compound in bowl mixer at various temperatures and various levels of total work input. Although the investigation was concentrating on melting temperature and the mechanical property of the PVC window profile, the additives and the stabilisers they used in different formulations were the actual stabiliser and additives used to design the PVC window profile in PVC profile. The components they used to design 6 different PVC window profiles are as follows: PVC, Tin stabiliser, CaSt, PE Wax, Process aid, Metal release, Impact modifier, CaCO<sub>3</sub>, TiO<sub>2</sub>, Oxidized PE. This list shows that the PVC window profile made of blend polymer with different additives and stabilisers (Arias, G et al, 2006).

Fletcher (2005) has written his personal communication, which was a surface analysis of PVC flexible film and rigid PVC window profile samples. One of the analysis techniques he used to characterise the surface chemistry of the PVC samples was ToF-SIMS. One sample was analysed as received, the two other samples were analysed after solvent washing. The author suggested that the surface chemistry was consistent with the presence of a PVC/acrylate copolymer with butyl acrylate (BA) being the dominant acrylic monomer. Lead, possibly associated with a stabiliser, and a phosphate containing

material were also detected together with an anti-oxidant additive, identified as Irgafos 168. Author suggested the Irgafos 168 being material that had been transferred from the polyolefin based protective film. Solvent washing with iso-hexane and then methanol removed the Irgafos 168 material. Lead and calcium were still present, together with a low level of titanium (detected by XPS). Clearly this latter element was probably due to the titanium dioxide pigment used in the PVC. The only other material that remained on the PVC/acrylic surface was the phosphate containing material which again might imply the presence of a phosphate ester type material or the presence of some remaining, low level Irgafos 168 residues (Davies and, F.S & Fletcher, I.W, 2005).

Irgafos 168 and Irganox 1010 are stabilisers, to protect the polymer resin against oxidation during resin manufacture and processing (thermal curing and over baking). The manufacturers suggested they provides excellent protection against discolouration and changes to physical properties caused by heat or exposure (Davies and, F.S & Fletcher, I.W, 2005).

There is some published work on the segregation of the additives to surface of the polymers. Medard et al published three papers from 2002-2004 investigating the segregation of additives and antioxidants to polymer surfaces. They used ToF-SIMS to identify the additives at polymer surfaces. Although in these papers the materials investigated were not PVC, the additives and the antioxidant employed were Irgafos and irganox. In the first investigation the authors referred to the work of Calvert and Billingham as anticipated by, the surface segregation of additives occurs when the additive dispersion over passes its solubility in the polymer matrix. ToF-SIMS analysis has good sensitivity for the detection of additives at polymer surfaces. The authors suggested that the surface segregation of additives occurred during the first few days (5-10days) following sample preparation. After 15-20 days, the polymer surface composition was found to remain stable.

## ***2.14 PVC surface modification***

One of the disadvantages of polymeric materials, when compared to other materials such as metals and ceramics, is their low surface free energy and low wettability. Materials with low surface free energy do not possess good adhesion property, which can easily bond them to other materials. Polymeric materials in general are hydrophobic which

leads them to have high contact angle and low wettability. Often, when polymeric materials have to be bonded to other materials such as other polymers, polymeric coatings or an organic adhesive, the surface of the polymer substrate is modified to make it more hydrophilic or at least less hydrophobic. Therefore, polymers are often not suitable materials for bonding to other material without surface modifications of polymers. There are many surface treatment techniques which can affect surface modification of polymers. Surface modification techniques of polymers include corona discharge treatment (Borcia,D & Popa, 2001), remote argon plasma (Ru & Rong,J, 2006), etching by ultrasound (Zhao et al, 1998) and flame treatment. The effect of some treatments last much longer than that obtained with other surface modification techniques, they have different lifetime; from each other's some of them end very quickly and some of them last longer. For example the effect of corona discharge treatment last very quickly and the effect of flame treatment last longer than most of other treatments (Comyn, 1997).

There are some published work on the surface treatment of PVC available in the literature such as Zhao et al ultrasonic etching (Zhao et al, 1998), Dumitrascu et al corona discharge (Godbey,D.J et al, 1997) and Vladkova et al Ion-plasma treatment (Cohen, 1989). However, there is little published work on the surface treatment of PVC by flame treatment technique. One of the few works in this area was US Patent 5879495; in this patent Evans mentions flame treatment in his patent claim list, but he has not performed any experiments. The patent title is PVC pallets and the like, but there is no evidence of the performance of any experimental work in this patent. The author put the names of the available treatments plus many polymer materials in his patent (Evans, 1999).

Pascoe and Connell (2003) used an angled flame treatment employing a burner with natural gas (predominately methane) at an angle of 15° to PVC and polyethylene terephthalate (PET). They used XPS and contact angle measurement (CAM) for their analysis. Their results showed that both side of the PVC film (0.5 mm thick) were flaking and became hydrophilic after flame treatment. The virgin PET was more easily modified than the PVC, resulting in a difference in contact angle of 30° after a 0.135 s treatment. The affect of the variation in residence time within the flame on the contact angle of both polymers was similar. The authors mentioned that the flame treatment, led to increased oxygen surface concentration from 3 at% in untreated to 17 at% in treated PVC (Pascoe,R.D & Connell,B.O, 2003).

## **2.15 Contact angle measurements**

The important characteristic of a liquid wetting a material is its ability to freely wet the surface of the material. At the liquid-solid interface, if the molecules of the liquid have a stronger attraction to the molecules of the solid surface than to each other (the adhesive forces are stronger than the cohesive forces), wetting of the surface occurs. Alternately, if the liquid molecules are more strongly attracted to each other than the molecules of the solid surface (the cohesive forces are stronger than the adhesive forces), the liquid beads-up and does not wet the surface. Surface tension is the tendency of liquids to reduce their exposed surface to the smallest possible area. For liquids, the surface tension (force per unit length) and the surface energy density are identical. Water has a surface energy density of  $0.072 \text{ J/m}^2$  and a surface tension of  $0.072 \text{ N/m}$  (Chan, 1993). A drop of water, for example, tends to assume the shape of a sphere. This phenomenon is attributed to cohesion, the attractive forces acting between the molecules of the liquid (Bragg, 2004).

One way to measure, a liquid's surface wetting characteristics is to measure the contact angle of a drop of liquid placed on the surface of material. The contact angle is the angle formed by the solid/liquid interface and the liquid/vapour interface measured from the side of the liquid. Liquids wet surfaces when the contact angle is low (less than  $\sim 50^\circ$ ). For a wetting material to be effective, the contact angle should be as small as possible. The wetting ability of a liquid is a function of the surface energies of the solid-gas interface, the liquid-gas interface, and the solid/liquid interface. The surface energy across an interface or the surface tension at the interface is a measure of the energy required to form a unit area of new surface at the interface (Cartz, 1995). The contact (wetting) angle of a liquid with a solid surface plays the role of a sensitive contact angle can used to indicator of changes in surface free energy level and the chemical structure of modified surfaces (Zenkiewicz, 2000).

## **2.16 Production of jacket window profiles**

The jacketing of a PVC-window profile with a decorative film is a special field in profile modification. This technology is used in the production of PVC-window frames laminated with decorative film. Approximately 15-20% of the PVC profiles used in the production of windows today are film-laminated. The decorative film is mostly imitation wood, however plain colour film also available. The most commonly used jacketing film

is weather resistant, acrylate-coated PVC film and more recently, polyvinylidene fluoride (PVDF) based film, as shown in Figure 2.20. Almost 90% of these jacketed profiles are bonded using PU hot melt adhesives especially produce for this application. The adhesive are dispensed with rollers or slot nozzles. Before jacketing, the window profiles are primed inline to improve the adhesion of the surface, which is strongly influenced by the production process, and then laminated with the adhesive-coated film via a roller system. The primers used are mainly solvent-based products, either methylene chloride based or methyl ethyl ketone based.

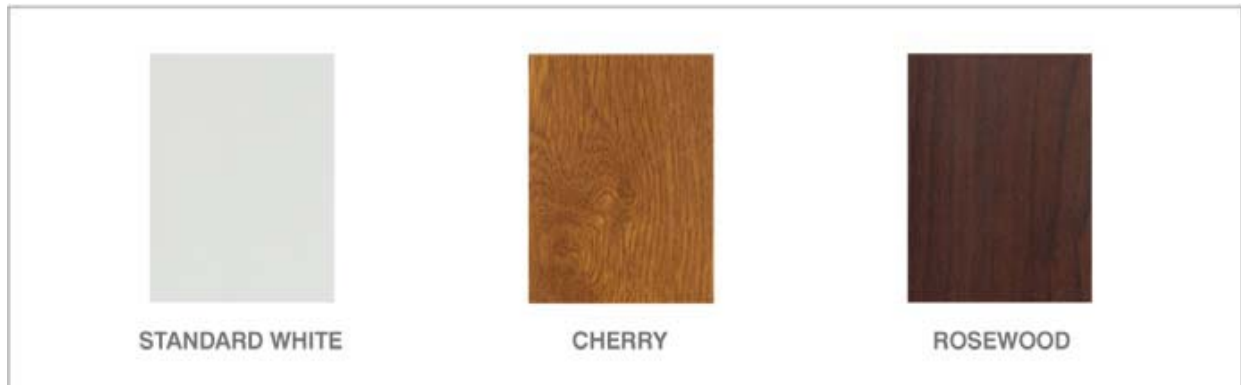


Figure 2-16 - PVC window profile without jacket window, at left and with jacket window in the middle and right

After the jacketing the adhesive needs ~ 1 to 2 days before it is fully cured. The products are then be stored for another 4 to 7 days before being use a in window production. The jacketed profile must have sufficiently high peel strength to ensure that during a peel test the film cannot be peeled from the profile, but tears after the laminate has been bonded to a window profile (Thiele, 2007).

Henkel is an international company, with more than 55,000 employees worldwide. Henkel a Brand in more than 125 countries around the world trust in innovative. Henkel adhesive and sealant systems and surface treatment products contribute to sustainable development in numerous industries, such as the automotive, packaging, aerospace, electronics, metal and solar energy sectors (Castel,J et al, 2003).

### **2.17PU Reactive hot melt adhesives and buried interfaces**

Polyurethane reactive hot melt adhesives are one of the fastest growing classes of adhesive worldwide. They can be used in many areas to replace solvent-borne adhesives

as they offer exceptionally high performance in terms of adhesion and toughness, coupled with extremely fast adhesive bonding. PU reactive hot melt adhesives are heated in order to apply them in a molten state. Upon cooling they solidify, forming a permanent bond. As has been discussed in the introduction, polymers have low wettability and low surface free energy. This renders them less able to easily bond to polymers or other materials without modification of the surface.

A number of techniques have been used to investigate buried interfaces, includes sum frequency generation vibrational spectroscopy (Chen, C et al, 2002), polymer/polymer interfaces, soft X-ray emission spectroscopy analysis of metal/Si interfaces (Wang,J & Wang,T, 2000) and XPS investigation of polymer/metal oxide interfaces (Kugler, T et al, 1999). Such techniques are restricted to the examination of interfaces, at the most, a few hundred nanometres below the sample surface. Leadley and Watts, however, used a different approach to probe the metal/polymer interface. Very thin (~2 nm) polymer film were cast onto metal substrates, they then used high-resolution XPS to monitor changes in the C1s spectrum as results of significant interactions at the interface (Leadley,S.R & Watts, J.F, 1997).

Walls et al (1979) used a ball-cratering device to achieve a well-defined spherical crater in a sample surface as show in Figure 3. A rotating, spherical, steel ball, coated in fine diamond paste, was used to grind a spherical crater in the sample. The depth and width of the crater could be accurately controlled. With this method depth profiling information was obtained either by point-by-point analysis down the sloping side of the crater wall or by using Auger linescan across the crater.

Using this method accurate depth profiles for metal samples can be obtained however, it is not a good technique for polymeric materials. Polymers are soft and using this technique on soft material leads to smearing and loss of depth resolution. (Wall,J.M et al, 1979). However, Cohen and Castle used the ball-cratering method with cryogenic cooling of substrate to good effect to expose the interface of a polymer/metal. Ball-cratering can produce excellent sections on hard materials, but often gives only a poor geometry when used on polymers. This arises from smearing and tearing of the polymer over the metal surface (Cohen,J.M & Castel,J.E, 1988).

Hinder et al (2004) developed ultra-low-angle microtomy (ULAM) to produce ultra low angle tapers through polymeric coating systems. Analysis across a buried polyvinylidene difluoride (PVdF) topcoat and polyurethane primer interface exposed by ULAM performed using XPS line scan analysis was demonstrated by the authors. Changes observed in the fluorine and nitrogen concentration across the interface suggested diffusion and penetration of fluorine-bearing component from the topcoat into the topmost nanometres of the underlying primer coating had taken place. Hinder et al published three more articles where ULAM was employed, Time of flight mass spectrometry (ToF-SIMS) was employed in two of them studies to analyse buried polymer/polymer interfaces (Hinder et al, 2004).

# Chapter 3

## 3 Experimental details

### 3.1 *PVC degradation study*

#### 3.1.1 Introduction to PVC

PVC differs from other polymer materials by its low thermal stability. When PVC is exposed to heat, light such as UV light or radiation such as X-rays will degrade it with the loss of HCl (dehydrochlorination). The process of dehydrochlorination takes place even at low temperatures. As the PVC degrades it also discolours and changes from transparent/white (when formulated) to pink, orange, red-brown and finally to black (Randall, D & Lee, S, 2002). UV light and heat will damage and degrade PVC, so by including additives and stabilisers into a PVC formulation, the PVC may be stabilised for outdoor use.

PVC degrades when it is exposed to X-ray radiation. In XPS, it is often observed that the X-ray radiation causes changes to the surface structure and chemistry of the surface region of organic materials. K. Yoshihara<sup>1</sup> and A. Tanaka summarized the radiation-induced chemical damage. Beamson and Briggs have worked on X-ray spectra of organic materials and X-ray degradation rates in 1992. The Organic Materials Group of the Surface Analysis Society of Japan reported degradation rates of nitrocellulose by x-ray radiation. The X-ray degradation of poly (vinyl chloride) and nitrocellulose in XPS and its effect on the change in composition of PVC –PMMA using XPS has been studied by M. P. Seah and S. J. Spencer (2003) and (K. Artyushkova and J. E. Fulghum 2001)

One of the main surface analysis techniques employed in this project is XPS. Thus there will be X-ray degradation of the PVC while an XPS analysis is carried out. It is often observed that X-ray induced sample damage is common during the XPS analysis and can cause the spectrum to change with exposure time. Organic polymers exhibit a wide range

of damage rates. The halogen containing polymers degrade fairly quickly, leading to changes in surface chemistry at the surface region of these polymers (Dillingham,R.G & Moriarty,C, 2003). Copperthwaite summarized the radiation-induced chemical damage (Chehimi,M.M & Watts,J.F, 1992). Beamson and Briggs investigated the effect of X-ray degradation rate of organic material including the PVC, as function of X-ray exposure and time for 500min employing a monochromated X-ray source (Beamson, G & Briggs,D, 1992). The Organic Materials Group of the Surface Analysis Society of Japan investigated the degradation rates of nitrocellulose by X-ray radiation (Wall,J.M et al, 1979). The degradation behaviour of poly (vinyl chloride) and poly (tetrafluoroethylene) was studied by Coullerez et al (Gonzalez, A et al, 1989). Thomas summarized the mechanism of photon beam damage in solids (Miki,N et al, 2000).

Investigation of the X-ray degradation of Pure PVC and commercial PVCs were carried out to determine the maximum time a PVC samples can be exposed to an X-ray source, where X-ray has minimum effect on the surface of PVC. In much published work the damage has been assessed by measuring the reduction in Cl relating to the intensity of Cl/C by assessing the Cl/C ratio. This does not distinguish by the carbon of Cl from reduction in Cl signal, because of C disposition in the form of contamination this is always positive though it's out gassing of solvent of other impurities in the PVC. A unique method used in this work to prove the decreasing of Cl in PVC is by coating 1mm diameter of gold on top of the specimens. In this work the ULAM technique has been enhanced by in situ cooling of the samples using a cryo-stage (C-ULAM). Initially (C-ULAM), XPS linescan analysis, ToF-SIMS analysis were employed to find depth of the degradation as function of time and X-ray exposition.

In the investigation of buried interfaces number of spectroscopic technique have been employed. However, these spectroscopes techniques are restricted to the examination of interfaces at most a few hundred nanometres below the sample surface. The tapering of PVC specimens was performed in the manner as described in chapter 1 by Hinder et al (Hinder,S.J et al, 2004) However, in terms of tapering and sectioning of the polymeric PVC specimens, because they were very soft it was impossible to section them at room temperature. During sectioning pure PVC peeled from the sample instead of being sectioned. So cryo-stage (C-ULAM) was employed instead of (ULAM).

## **3.2 Experimental**

### **3.2.1 Materials used**

The pure PVC powder used in this project is 189588 (25g) which was supplied by Sigma Aldrich (Gillingham, UK). The Hexane solvent was supplied by Fisher Scientific (UK). Tetrahydrofuran (THF) was supplied by Fisher Scientific (UK).

Two commercial rigid PVC window profile samples manufactured by Veka (named as PVC-V) AG Sendenhorst, (Germany) and Rehau (named as PVC-R) AG Bavaria, (Germany) were supplied by National Starch & chemical Slough, (UK). The PVC window profiles were supplied with a protective film of low density polyethylene (LDPE) on one side of the profiles.

An extruded plasticised PVC film with a thickness of 0.2 mm (200 $\mu$ m) was also supplied by National Starch.

### **3.2.2 Sample preparation**

In order to prepare a specimen of pure PVC powder (as a reference sample) for XPS analysis, the PVC powder was dissolved in THF and drop cast on to aluminium foil. The THF evaporated and a PVC film remained on the aluminium foil. A desiccator was then used to dry the pure PVC. Cleaned scissors were then used to cut the pure PVC film into specimens of  $\sim 1\text{cm}^2$  for the degradation study.

A Pratt- Whitney hand punch with a  $\sim 1\text{cm}$  diameter aperture was used to prepare disc shaped specimens of rigid PVC samples and the extruded plasticised PVC film Figure 3-1. The rigid PVC samples were covered with a protection film, which was removed just before the sample was introduced in to the instrument. In order to remove the release agent from surface of PVC R and V samples, the surface of the PVC samples was washed with hexane solvent. Hexane was applied with a Kimtech tissue.



Figure 3-1 – Picture of Samples from PVC Profile left and Plasticized PVC right

An Emitech K775X Peltier Cooled coater (E.M. Technologies Ltd Kent, UK) was employed to deposit gold onto PVC samples. 1 mm diameter gold discs, with a thickness of 4 nm, were deposited on the surface of the PVC V and R and extruded plasticised PVC film. Before the gold was deposited on the surface of the samples, the surface of PVC V and R profile was cleaned with hexane to remove any release agent.

### **3.3 XPS analysis**

XPS analyses were performed on a modified ESCALAB MKII (Thermo Scientific, East Grinstead, UK) instrument Figure 3.2. The Al side of a twin anode X-ray source was employed at a power of 300 W. All survey spectra were recorded at an analyser pass energy of 200 eV. The reason why pass energy of 200 eV was chosen was to have a greater intensity of peaks. The instrument software was setup to serially run 40 survey spectra with no intervene gap. This was in order to minimise X-ray exposure time between the surveys spectra.

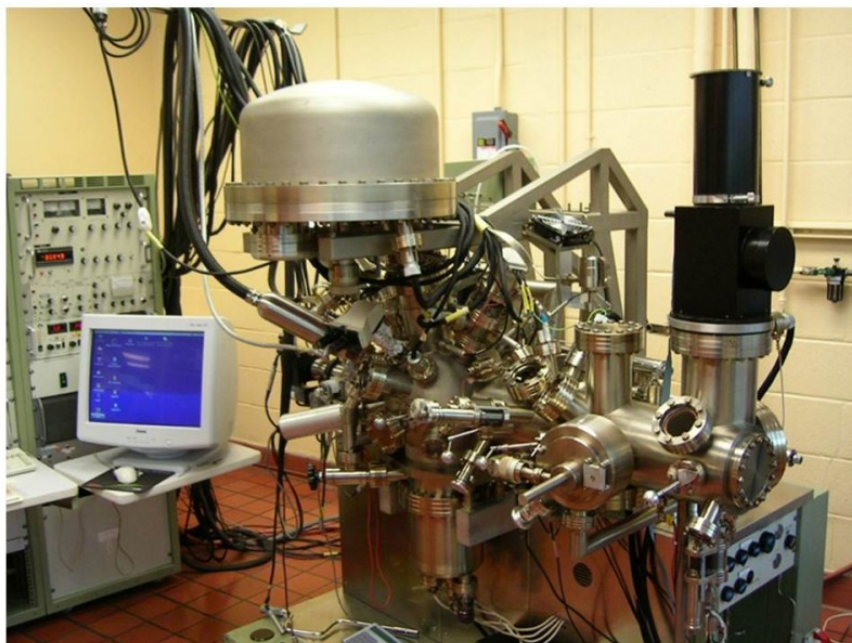


Figure 3-2 Picture of ESCALAB MKII (Thermo Scientific, East Grinstead, UK) instrument

Once the sample was moved under the X-ray source, the recording of the survey spectra started, and each survey spectrum took 2-3 minutes to complete. The number of scans for each survey spectra was one and the step size employed was 1 eV. This was the method of degradation study employed for analysis of all the samples during this investigation.

### **3.4 EDX analysis**

Energy dispersive X-ray spectroscopy (EDX) analysis of pure PVC film that has been exposed to X-rays (Using modified ESCALAB MKII (Thermo Scientific, East Grinstead, UK) as a function of time was performed using a Hitachi – S 3200N scanning electron microscope. Instrument environmental SEM at a chamber pressure of 5 Pa and the energy of the electron beam was 15 kV.

EDX analysis of the PVC samples, that were expose to X-ray irradiation carried out, in order to get optimum result for degradation study of the PVC samples, and compare that with result of XPS analysis.

Because the depth of the analysis in XPS is almost 5nm, but in EDX the X-rays are generated in a region about 2 microns in depth, and thus EDX is not a surface science technique.

The PVC sample, those exposed to X-ray irradiation by XPS as function of times, were gold coated and analysed by EDX to monitor the C/Cl ratio of these samples as a function of time.

The temperature of the outside of the chamber (in the lab) was room temperature during the analysis, but temperature inside the chamber was always cooled down by liquid nitrogen.

### **3.5 Microtomy**

Hinder and et al (Hinder et al, 2004) developed ULAM processing for exposing the buried interfaces of sandwich layers by employing the microtome, that equipped with a standard specimen clamp and a tungsten carbide knife. Ultra-low- angle blocks were manufactured in house from stainless steel with taper angles from 0.4°, to 2°. For taper sectioning of the sample a block of polyethylene (PE) was placed in the microtome sample clamp and trimmed with the tungsten-carbide knife until the section comprised the complete face of the PE block. An angled sectioning block was attached to the PE block with double-side adhesive tape, and then the sample was attached to the angled sectioning block. In this investigation during the sectioning the PVC peeled off from the sample instead of being sectioned. Two problems were encountered, a PE block does not have good thermal conductivity, the second problem is that the angled sectioning block needs to be positioned on the cooling stage, and otherwise it is impossible to taper the sample at a precise angle. So the material used as alternative to the PE block should have overcome the two problems; have a good thermal conductivity and stick to the double sided adhesive easily.

A number of techniques were tried to develop a new way of transferring the cold from the cooling stage to the specimens. This included placing a block of copper in the middle of a PE block and using a graphite block. When a block of copper was placed in the middle of the PE it could not reduce the temperature of the sample because the size of the PE block was larger than the copper. The graphite block had a very good thermal conductivity, but it presented an adhesion problem and double sided adhesive tape would not adhere to the graphite block. Finally, the PE block was replaced by a copper block. A spirit level was used to level the copper block in the vertical and horizontal direction (as reference points), then as a substitute for the ULAM angled section block, the specimen clamp with copper block was adjusted to set the block of copper to the desired angle. A clock gage with a magnetic base was used to set up the desired angle for the

copper block, in this case the copper block was tilted, so that the outer edge of the copper block was increased by a height of 250µm compared to the opposite edge. Hence, the difference in height between the two edges of the copper block was 250 µm; therefore, the angle of the slope between the two edges of the copper block can be calculated using the equation, in Figure 3.3.

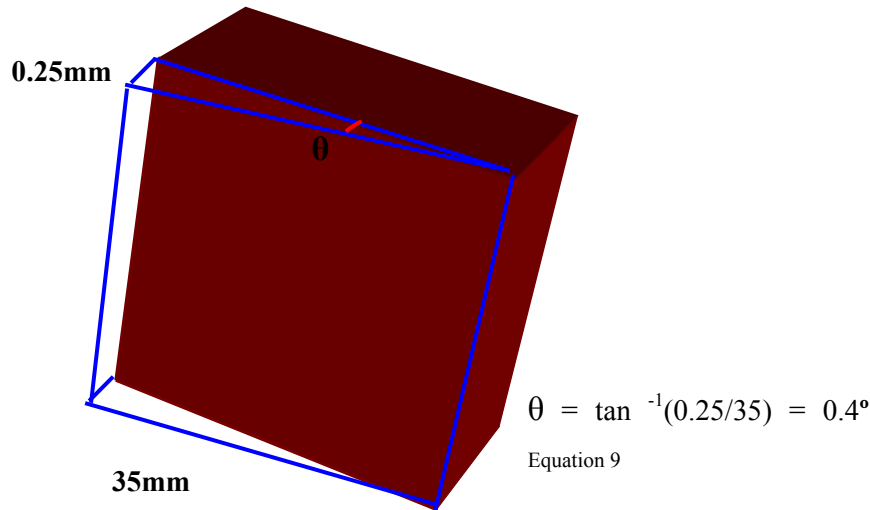


Figure 3-3 - Schematic diagram of the copper block with an angle of 0.4°

After the PE block was replaced by a copper block the temperature of the samples could be reduced to  $-2^\circ\text{C} \pm 2^\circ\text{C}$ , therefore, specimens of pure PVC were sectioned at  $-2^\circ\text{C} \pm 2^\circ\text{C}$ , with a taper angle ( $\theta$ ) between  $0.4^\circ - 0.8^\circ$ . The Cryo-Ultra low angle microtomy (C-ULAM) processing of the samples was carried out on a Microm HM355S motorised rotary microtome with a K 300 freezing unit (Optech Scientific Instruments, Thame, UK).

Figure 3.4 is a picture of the Microm HM355S motorised rotary Microtome with the copper block and cooling stage, which are used for C-ULAM tapering of the specimens, in place after replacing, the PE block by the copper block the temperature of the samples could be reduced to  $-2^\circ\text{C} \pm 2^\circ\text{C}$ . Specimens of pure PVC were sectioned at  $-2^\circ\text{C} \pm 2^\circ\text{C}$ .

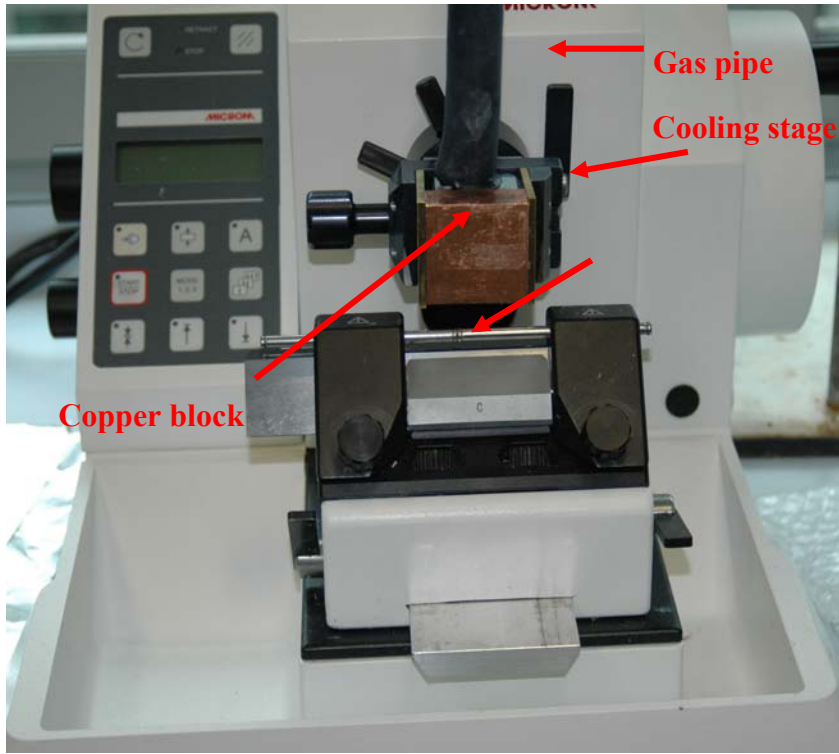


Figure 3-4 – Picture of Microtome motorised rotary microtomy (HM355S), setup for C-ULAM.

Figure 3.5 shows a schematic of the C-ULAM set up as employed in production of the Cryo-ultra-low angle tapers. This schematic image shows how the components of C-ULAM were assembled, such that the cooling stage can cool the samples.

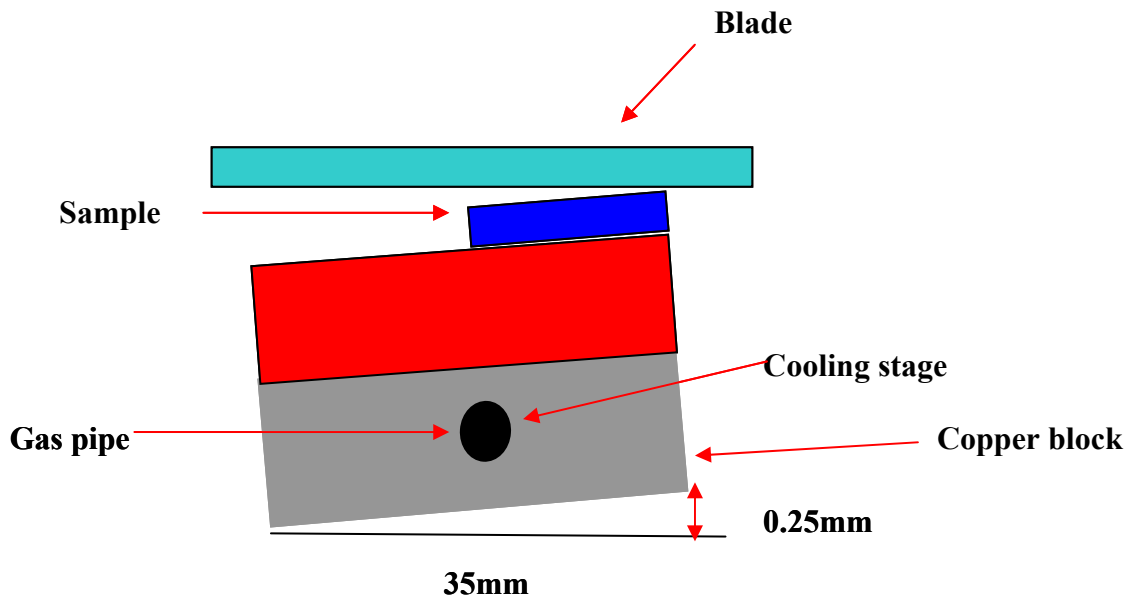


Figure 3-5 – Schematic diagram of assembled C-ULAM components.

### 3.6 XPS - line scans

XPS – line scans analyses were performed using a monochromated X-ray source, in order to characterise the variation in concentration of PVC components across a C-ULAM produced taper through pure PVC, which has been exposed to X-ray radiation as a function of time. To find the depth of degradation on the pure PVC sample, cryo-ultra low angle microtomy was used to section the PVC sample. Hinder et al tapered and sectioned their samples at room temperature (Hinder,S.J Et al, 2005), but a cryo unit was employed in this project to cool the sample down to  $-2^{\circ}\text{C} \pm 2^{\circ}\text{C}$ . The cryo-ultra-low angle microtomy (C-ULAM) technique was employed to impart an ultra-low angle taper through a pure PVC film (that had been exposed to X-rays for 70 minutes). XPS linescan analyses were performed on a Sigma Probe spectrometer VGScientific, shown in Figure 3-6.



Figure 3-6 Picture of Sigma Probe spectrometer VG Scientific

The instrument includes a monochromated Al  $K\alpha$  X-ray source ( $h\nu = 1486.6 \text{ eV}$ ) which was used at 140W. The area of analysis (X-ray spot size) was approximately  $200\mu\text{m}$ . In diameter and there were twenty points of analysis and the step size was  $230\mu\text{m}$ . Each successive analysis point increased the analysed depth by  $1.6 \mu\text{m}$ .

### **3.7 ToF-SIMS analysis**

The ToF-SIMS analyses were carried out on an IONTOF GmbH (Münster, Germany) ToF.SIMS 5 system figure 38. The instrument is equipped with a reflectron type analyser and a micro channel plate detector. A Bi liquid metal ion source (LMIS) was employed for mass data acquisition. Mass data was acquired using the  $\text{Bi}_3^+$  cluster ion. Mass data acquisition was performed by raster scanning the primary ion beam over  $100 \times 100 \mu\text{m}^2$  area. A 25 keV  $\text{Bi}_3^+$  primary ion beam delivering 0.4 pA of current was used. A cycle time of  $100\mu\text{s}$  was employed for mass data acquisition Figure 3.7.



Figure 3-7 Picture of IONTOF GmbH (Münster, Germany) ToF.SIMS 5

### **3.8 Treatment and Modification**

#### **3.8.1 Introduction**

Most polymeric materials have a very low surface energy and low wettability. In terms of bonding, coating and using adhesives, it is difficult to work with materials with low surface energy and low wettability. Often when polymeric material have to be bonded to other materials such as other polymers, polymeric coatings or an organic adhesive, the

surface of the polymer substrate has to be modified to make it hydrophilic or at least less hydrophobic. Therefore, polymers are often not suitable materials for chemical bonding between an adhesive and a substrate without surface modification and surface treatment of the polymer substrate. There are many surface treatment techniques which can affect surface modification of polymers. Surface modification techniques of polymers include corona discharge treatment (Purdy, 1997), ion-plasma modification (Castel, J et al, 2003), remote argon plasma (Lee, 1991), etching by ultrasound (Beamson, G & Briggs, D, 1992) and flame treatment. The effects of each of these treatments have different life times; some of them end very quickly and some of them last longer (Comyn, 1997).

When window profiles are treated, they may be stored in a warehouse for a long time before being used and bonded to a plasticised PVC foil. The effect of the flame treatment lasts much longer than that obtained with other surface modification techniques (Shingley, J.E, 2003). However, the flame treatment was carried out to modify the surface of the commercial PVC window profile and improve its wettability and adhesion properties. The flame is typically applied to the surface from above and in some cases, such as bottles, from the side; also there is another option where by two burners apply their flames to the product. Before any surface treatment, the wettability of the polymer have to be measured, this measurement allows us to determine the effect of flame treatment on the surface of PVC window profile by comparing the surface free energy before and after flame treatment. Contact angle, ( $\theta$ ) is a measure of the wetting of a solid surface by a liquid. Another important test usually undertaken before and after the flame treatment is the water break test. The water break test employs before the flame treatment to find the dyne level of the specimen and after the flame treatment determine the effect of flame treatment on the surface. As has been described in the previous chapter, the materials chosen for this project are commercial PVC window profiles from Veka AG (Sendenhorst, Germany) and Rehau AG (Bavaria, Germany) and a plasticised PVC foil.

### **3.9 Flame treatment**

The surface modification of PVC samples were done in two parts. In order to gain knowledge of flame treatment and the effect of that on surface of PVC window profile, the initial study of flame treatment was carried out. In initial study flame treatment

technique with different parameters was employed to modify surface of the PVC profile Veka (V), samples. In later study flame treatment technique with fixed parameters were employed to modify surface of PVC profiles V and Rehau (R).

The approach in first part (Initial part) was that, all the parameters of the flame treatment equipment such as (Gap between burner and sample, % of gas and oxygen, speed of conveyer, etc.) were adjusted to reach the optimum surface free energy for PVC samples.

The approach of second (Final part) was that, the flame treatment carried out with fixed parameters employed to modified surface of PVC profiles V and Rehau (R).

### **3.9.1 Materials**

The material used for flame treatment includes; commercial, rigid PVC window profile manufactured by Veka (PVC-V) AG (Bavaria Germany) and supplied by National Starch and Chemical Ltd (Slough, Uk). Each window profile was supplied with a protective film of low density polyethylene (LDPE) on one face of the profile. The solvent used was Hexane, supplied by Fisher Scientific (UK). Deionised water was obtained from a Purite instrument (Ondeo Industrial Solution, UK) and was used as the liquid phase for contact angle measurement. The ink kit used before and after flame treatment was Dyne Test Inks (levels 30-56 Dynes/cm) supplied by Dyne Technology Ltd (Lichfield, Staffordshire, UK).

### **3.9.2 Sample preparation**

In order to prepare samples for XPS analysis a puncher with an aperture of approx. 1cm in diameter was used to punch out a disc from the rigid PVC V sample.

In order to prepare samples from PVC-V for contact angle measurement, a hacksaw was employed to cut the PVC V in to section of 1cm<sup>2</sup>. The effect of release agent was investigated on the contact angle measurement of PVC V, therefore, two samples were prepared for contact angle measurement, one sample with release agent intact on the surface of the PVC sample, and the surface of the second sample was cleaned with hexane to remove the release agent.

A band saw was used to cut specimens with size of 30 x 6 cm with thickness of 3mm from each side of the PVC V window profile as flame treatment specimens. In total five

samples were prepared for flame treatment, four samples from the sides of the sample without release agent and one sample from the face of the profile with release agent.

A puncher with a diameter aperture of approx. 1cm was used to punch out discs specimens of the rigid PVC V samples before and after flame treatment, in order to characterise the surface properties and topography of the PVC V samples before flame treatment, and the effect of flame treatment on the surface by atomic force microscopy (AFM).

### **3.10 Contact Angle Measurements**

Contact angles were measured by employing an Easy Drop –KRUSS Standard TR30R instrument with deionised water as the liquid phase. To measure the contact angle a 1µl drop of water was placed on the surface of a sample via an automated syringe. The contact angle between the material surface and the water droplet was measured using the drop shape analysis (DSA) software. The contact angle of the pure PVC was measured as a reference sample. Contact angles from 10 different areas of a sample surface were measured and an average value was determined, with standard deviation of  $\pm 2^\circ$ .

### **3.11 XPS Analysis**

XPS analysis was performed using ESCALAB MKII (Thermo Scientific, East Grinstead, UK) instrument. The aluminium side of a twin anode X-ray source was employed with a power rating of 300 W. All survey spectra were recorded as an analyser pass energy of 100 eV. The degradation background as described in Section 3.1.1 suggests that a XPS analysis of PVC should not be carried out for more than 10 minutes using a twin anode X-ray source, because after 10-minute of X-ray exposure the PVC samples start to degrade rapidly. In order to minimise X-ray exposure time, two specimens of each sample were characterised by XPS. The initial sample was characterised by XPS recording survey spectrum, and the second sample was characterised by XPS recording high resolution C1s spectrum. Peak fitting of the high resolution C1s spectra was carried out using the manufacturers Advantage software.

In order to study the effect of the flame treatment on surface chemistry of the PVC V samples, two PVC V samples were characterised as reference samples before flame treatment, with and without release agent. The protection film of rigid PVC profile

samples were removed just before the sample was introduced in to the XPS instruments sample entry chamber. In order to wash off the release agent from surface of PVC V sample the hexane solvent was applied on surface of PVC V samples using a Kimtech tissue.

The surface of the treated PVC V samples were characterised by XPS in the same manner used to characterise untreated PVC V samples. This method of analysis with XPS was employed to study the variation of surface chemistry of the treated PVC V over time.

### **3.12 Water Break Test**

The wettability of the substrates was measured using Dyne ink test with a range of dyne ink levels from 30-56 before and after flame treatment, Figure 3.8. The parameters of the flame treatment machine were changed in order to achieve the greater surface free energy and better wettability on surface of PVC V samples. The ink was applied by a cotton wool bud, using a separate applicator for each ink (cotton buds were discarded after each test) to make sure that cotton buds were not contaminated by more than one ink. The surface free energy of the rigid PVC is  $0.038 \text{ J/m}^2$  (test, n.d.). For maximum accuracy, the test was started using the dyne ink with a level equal to that of the surface free energy of PVC  $0.038 \text{ J/m}^2$ . When the dyne ink wetted the surface within 2 second without forming globules, the surface free energy of the specimen is either higher than, or exactly that of the ink.



Figure 3-8 Picture of Dyne ink kit for measuring the level of dyne in samples

### **3.13 Flame Treatment**

The surface of the PVC V window profile samples was modified by flame treatment technique with propane liquid gas using a single burner Aerogen flame treatment instrument supplied by Aerogen Ltd Alton, Hampshire, UK. The parameters of the flame treatment instrument such as gas flow ( $\text{dm}^3\text{mi}^{-1}$ ), air flow ( $\text{dm}^3\text{min}^{-1}$ ), oxygen (%), the gap between burner and sample (mm) and the conveyer speed ( $\text{mm}/\text{min}^{-1}$ ) were adjusted to achieve the dyne level of  $0.056 \text{ J}/\text{m}^2$ . The parameters of the flame treatment were then kept constant and repeated for the main specimen, which was PVC V with release agent.

The Table 3.1 shows the variation of parameters of flame treatment instrument employed to modify the surface of the PVC V samples. The face of the PVC V profile, which the protection film was applied to it (raw 5 of Table 3.1), was the face that required surface modification by flame treatment, and our studies have concentrated on that side. The Table 4.1 shows that the PVC sample was divided to five specimens, the numbers of specimens are after the number of the parameter of flame treatment instrument used to modify the surface of each samples. PVC 1, 2, 3, 4 which they were from the side of the PVC profile without the release agent and PVC 4 with release agent from the surface of the profile that was covered by the protection film. There were two PVC samples which were flame treated with parameter number 4, one of them was from the side of the PVC profile without release agent and second one was from surface of the PVC profile with release agent on the surface of sample. The protection film was removed from the surface

of sample just before flame treatment; however, some release agent remained on the sample when the sample was flame treated.

Table 3.1-Parameters used for flame treatment of PVC window profile Veka

<b>Sample</b>	<b>Gas flow /dm<sup>3</sup>min<sup>-1</sup></b>	<b>Air flow dm<sup>3</sup>min<sup>-1</sup></b>	<b>Oxygen/ %</b>	<b>Burner gap /mm</b>	<b>Conveyer speed /m min<sup>-1</sup></b>	<b>Release agent</b>
<b>1</b>	<b>8.2</b>	<b>256</b>	<b>1.9</b>	<b>75</b>	<b>40</b>	
<b>2</b>	<b>6.3</b>	<b>200</b>	<b>1.9</b>	<b>75</b>	<b>30</b>	
<b>3</b>	<b>6.3</b>	<b>200</b>	<b>1.8</b>	<b>60</b>	<b>30</b>	
<b>4</b>	<b>10</b>	<b>328</b>	<b>1.7</b>	<b>60</b>	<b>40</b>	
<b>4</b>	<b>10</b>	<b>328</b>	<b>1.7</b>	<b>60</b>	<b>40</b>	<b>✓</b>

Figure 3.9 shows images of the Aerogen FT single burner flame treatment instrument while a flame treatment of PVC samples was carried out. The arrows point at the parameters which were changed for different samples. To avoid contamination on surface of flame treated samples, all of the samples were wrapped in clean aluminium foil immediately after flame treatment.

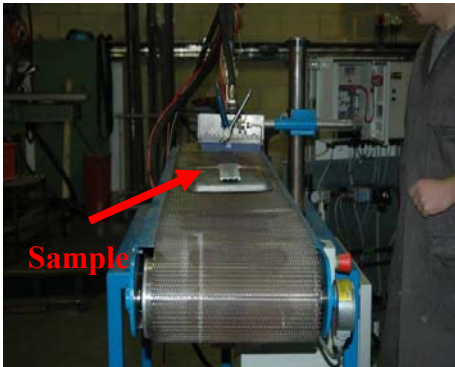
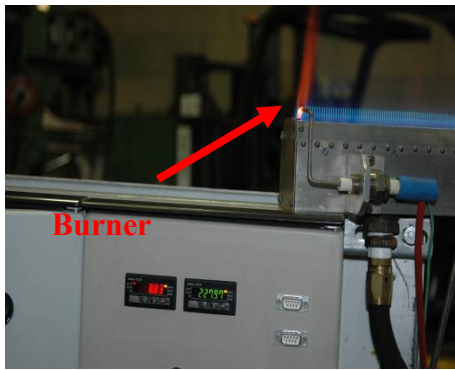


Figure 3-9 Pictures of flame treatment machine (Aerogen FT single burner), with parameters pointed out by arrows

### **3.14 AFM Analysis**

The surface properties and topography of the modified and unmodified PVC samples surfaces were characterised by atomic force microscopy (AFM). A Nanoscope III microscope (USA) was employed in all AFM experiments. Topographic and phase images were obtained for all samples from three different areas. In the case of PVC samples with release agent, in order to obtain the topographic and phase images from the surface of the release agent as well as the surface of the PVC sample beneath the release agent, low tapping amplitude employed for characterising the surface of release agent, and tapping amplitude increased 2 to 3 times for surface of the underneath PVC

### **3.15 Dynamic mechanical analysis of samples before and after surface modification**

In order to study the effect of the surface modification of the PVC by flame on mechanical property of the PVC samples, the Dynamic mechanical analysis (Three point

bending/ DMA) of the modified and unmodified PVC samples were carried out 19 months after surface modification of PVC samples.

A DMA Q800 V7.5 Build 127 model multi-frequency- strain with dual cantilever figure 3.10 was employed to carry out all DMA experiments Figure 3.10. Storage Modulus, Loss Modulus, and Tan Delta of the treated and untreated PVC samples were tested to determine the effect of the flame treatment on the parameters.

The band saw was employ to cut the samples of the rigid PVC with size of 60 x 10 x 2.9mm as DMA specimens. The instrument was setup in method temperature between (-40°C and 120°C).



Figure 3-10 shows DMA.Q800 V7.5 Build 127 model in left and Dual cantilever at right

### **3.16 Polyurethane hot melt adhesives**

#### **3.16.1 Materials used**

Rigid PVC Veka (PVC-V) window profile coated with polyurethane (PU) hot melt adhesive (FRD-740-29- 4) and a rigid PVC Veka window profile coated with UV primer (5µm thick) were supplied by National Starch. PVC Veka window profile and a plasticised PVC film (with a thickness of 0.2 mm) were supplied by National starch.

Four PU hot melt adhesives with national starch designate (FRD-740-29-1, 2, 3 and 4) were supplied in metallic can as they were in the solid phase by National Starch.

FRD 740-29-1 is Voranol P2000 MDI, FRD 740-29-2 is Voranol P2000 Dynacoll 7360 MDI, FRD 740-29-3 is Dynacoll 7231 MDI and FRD 740-29-4 is Dynacoll 7231 Dynacoll 7360 MDI.

### **3.16.2 PU Sample preparations**

XPS was employed to study the change in surface composition of elements as a function of life time of the PU (FRD-740-29-1,2,3 and 4) adhesives. In order to prepare sample for XPS analysis, a thin layer of the adhesive deposited on the aluminium foil substrate with the help of a calibrated cube. A 25mm Cube Applicator manufactured by Sheen Instruments Ltd with film width of 16mm and two standard gaps of 37 and 75 $\mu$ m was employed to deposit a thin film of adhesive on to aluminium foil. First, the PU adhesives were heated in an oven at 130°C for 30 minutes at which point they were liquid. To avoid the adhesive sticking to the applicator cube and also to balance the temperature between the cube and the adhesive, the cube was heated in the oven alongside the adhesives (Figure 3.11). When the adhesive was liquid, it was removed from the oven and a small quantity was poured into the cube. The cube was then drawn across the aluminium foil and a layer of adhesive, with a thickness of 37 $\mu$ m, was deposited on the foil. To avoid any contamination of the still soft adhesive film during its curing process, samples were covered with aluminium foil taking care not to touch the adhesive samples or allowing the foil to come into contact with the specimen surface. While the adhesives were still liquid a thin film of each adhesives was deposited on sample stub for XPS analysis as a reference (time zero) sample. For the rest of the study,

Samples of  $\sim 1\text{cm}^2$  were cut from the adhesive thin films deposited on aluminium foil and analysed by XPS as a function of time.



Figure 3-11 - (a) picture of the resin tin and cube inside of the oven, (b) melted resin with tapered cube, (c) coating of the substrate by resin

### 3.16.3 Preparation of Microtomy specimen

In order to preparing specimens made of PVC 4 with release agent (see Table 3.1), three months after surface treatment, the FRD 740-29-4 PU adhesive was heated in an oven and coated on to the surface of PVC 4 with release agent. The applicator cube with a gap of 75  $\mu\text{m}$  was employed to deposit the adhesive on to the surface of PVC V 4 with release agent. The cube with liquid adhesive was drawn across the substrate and a thick layer of adhesive deposited on the substrate.

In the case of the sandwich layer, which, was made of PVC 4 with release agent bonded to the plasticised PVC film by PU 740-29-4 (Figure 3.12). The PU adhesive was deposited on to the PVC 4 with release agent substrate and then the plasticised film was bonded to the adhesive. To avoid contamination all the samples were kept in desiccators to cure at room temperature. When the samples were cured, a band saw was used to cut the specimens to a size of  $2\text{cm}^2$  to be used as microtoming samples.

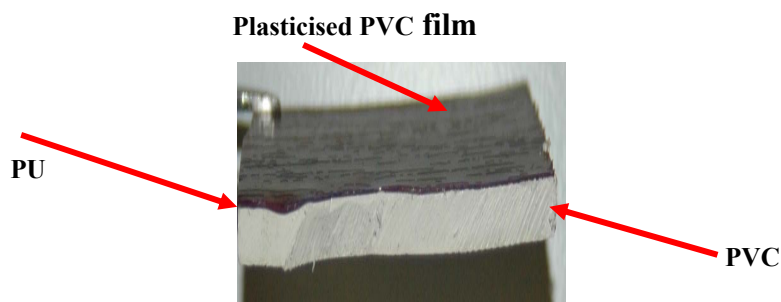


Figure 3-12 - Image of sandwich layer of PVC 4 with release agent bonded to PVC plasticised film by PU 740-29-4

### **3.17 XPS analysis of PU adhesives**

XPS analysis was employed to characterise surface chemistry of PU hot melt adhesives as a function of variation of surface concentration with time. XPS analysis was performed on an ESCALAB MKII (Thermo Scientific, East Grinstead, UK) instrument. The Al twin anode X-ray was employed as a source with power of 300 W. All survey spectrum were enquired using the constant analyser with pass energy of 100 eV. High-resolution spectra of all observed elements were recorded with pass energy of 20 eV. Quantitative surface analyses were taken for each specimen using the peak areas of the high-resolution spectra of element. For all specimens, the reference C1s peak was shifted at 285.0 eV. Peak fitting of the high-resolution C1s spectra was performed using the Avantage software.

### **3.18 Microtomy process**

C-ULAM processing of the samples was carried out using a Microm HM355S motorised rotary microtome with a K 300 freezing unit (Optech Scientific Instruments, Thame, UK) with same methodology used explained in chapter 4.

After replacing, the PE block by the copper block the temperature of the samples could be reduced to  $-2^{\circ}\text{C} \pm 2$ . Specimens of the PVC Veka coated with the PU 740-29-4, PVC 4 with release agent coated with PU740-29-4 and PVC 4 with release agent bonded to a plasticised PVC film by PU 740-29-4 were sectioned at  $-2^{\circ}\text{C} \pm 2$ .

It was possible to section the specimen of PVC Veka coated with UV primer using microtomy at room temperature ( $20^{\circ}\text{C}$ ) in addition to the temperature of  $-2^{\circ}\text{C}$ . A schematic of the ULAM set up as employed in production of the ultra-low angle tapers is presented in Figure 4.6.

### **3.19 XPS linescan analysis of Interface**

XPS linescan analyses were performed on a Thermo VGScientific Sigma Probe spectrometer. The instrument includes a monochromated Al K $\alpha$  X-ray source ( $h\nu = 1486.6$  eV) which was used at [140 W power]. The area of analysis was approximately 100 $\mu\text{m}$  diameter for all the samples. The pass energy was set at 100eV for high resolution spectra of all elements of interest. Charge compensation was achieved using a low energy electron flood gun. To aid charge compensation during the line scan analysis across the PVC/UV primer, PVC/PU 740-29-4 and PVC/PU/PVC plasticised brown/ black polymer

film interfaces, the straight-line edge of an aluminium grid was placed such that it was at right angle to the interface region to be analysed. The aluminium grid was held in place by sprung Cu/Be clips which were positioned so as to be at right angle to the interface to be analysed. This combination of aluminium grid and Cu/Be clip geometry promotes stable charge compensation across the interface to be analysed.

### **3.20 ToF SIMS analysis**

ToF Sims has employed with same condition that done to characterise the modified PVC samples, to characterise the surfaces and interfaces of sandwich layers which was exposed by microtomy (see section 3.6)

#### **3.20.1 Dynamic mechanical analysis of sandwich layered samples with different curing systems**

In order to study the mechanical property of sandwich layer samples, made of (Rigid PVC/PU adhesive/ Plasticised PVC), with different curing system the Dynamic mechanical analysis (Three point bending/ DMA) of all sandwich layer and samples were carried out 19 months after they have bonded together. DMA analysis was employed to investigate the effect of the different curing system of mechanical property of the sandwich layer same manner was used in section 3.14.

# Chapter 4

## 4 Results and Discussion

### 4.1 XPS analysis of pure PVC

One of The parameters that can affect the rate of PVC degradation is the distance between the source and the sample. As the distance between the X-ray source and the sample increases, the intensity of the peaks in a spectrum is expected to decrease. Therefore, initially the X-ray source was adjusted to its maximum adjustment with the maximum distance between the sample and the X-ray source. This resulted in low intensity peaks in the survey spectra. The analyses were then repeated with the minimum distance between the sample and the source. By comparing the survey spectrum acquired, the minimum distance between the source and sample was employed for all degradation studies.

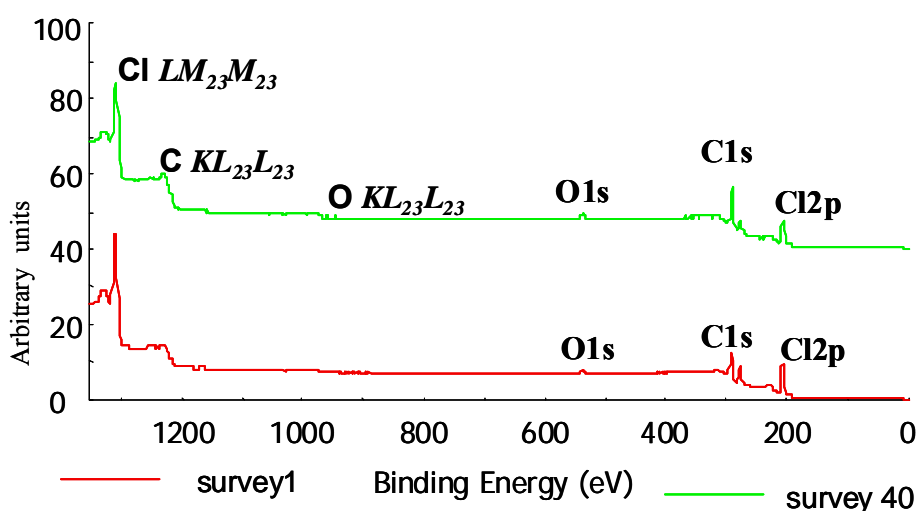


Figure 4-1 -XPS Survey spectrum number 1 at the top and 40 below of pure PVC film

Figure 4.1 is the XPS survey spectra number one and forty of a pure PVC film reference sample. The repeat unit of PVC is  $(-\text{CH}_2-\text{CHCl}-)_n$ ; hence the only elements present in a pure PVC film are C, Cl and H. The hydrogen is not observable in XPS. In Figure 3.4, survey spectra which was acquired from the pure PVC film, shows Cl2p at 200eV, Cl2s at 270eV, C1s at 285eV and O1s at 532 eV. The oxygen observed is due to oxidation of the polymer chain, as described by Beamson and Briggs (Beamson, G & Briggs,D, 1992). By comparing of initial survey (number one) and final survey (number forty), it is

observed that, there was evidence of decreased in surface concentration of the Cl and increase in surface concentration of carbon.

Table 4.1 shows XPS quantitative surface compositions of C, O and Cl of the initial and final survey spectra (survey 40). These data were obtained from the XPS surface analysis degradation study of pure PVC.

4.1 XPS quantitative surface analyses and degradation study of pure PVC.

Sample	Elapse time/min	Surface compositions/atomic %		
		C	O	Cl
Survey 1	2.3	66	19	15
Survey 40	90	79	14	7

The ratio of chlorine to carbon ( $\frac{Cl}{C}$ ) in the surveys spectrum were measured at different times of analysis. Then the degradation index after 93min was calculated using equation 11.

$$\text{Equation 10: } X_t/X_0 \times 100$$

Where  $X = Cl/C$  ratio and  $X_t$  is  $X$  at time  $t$ ,  $X_0$  is  $X$  at time 0, and  $t$  is the X-ray exposure time. In order to determine the degradation index, the result from the equation <3.1> is plotted against  $t$  (time/ min) ( $X_t/X_0 \times 100$  vs.  $t$ ).

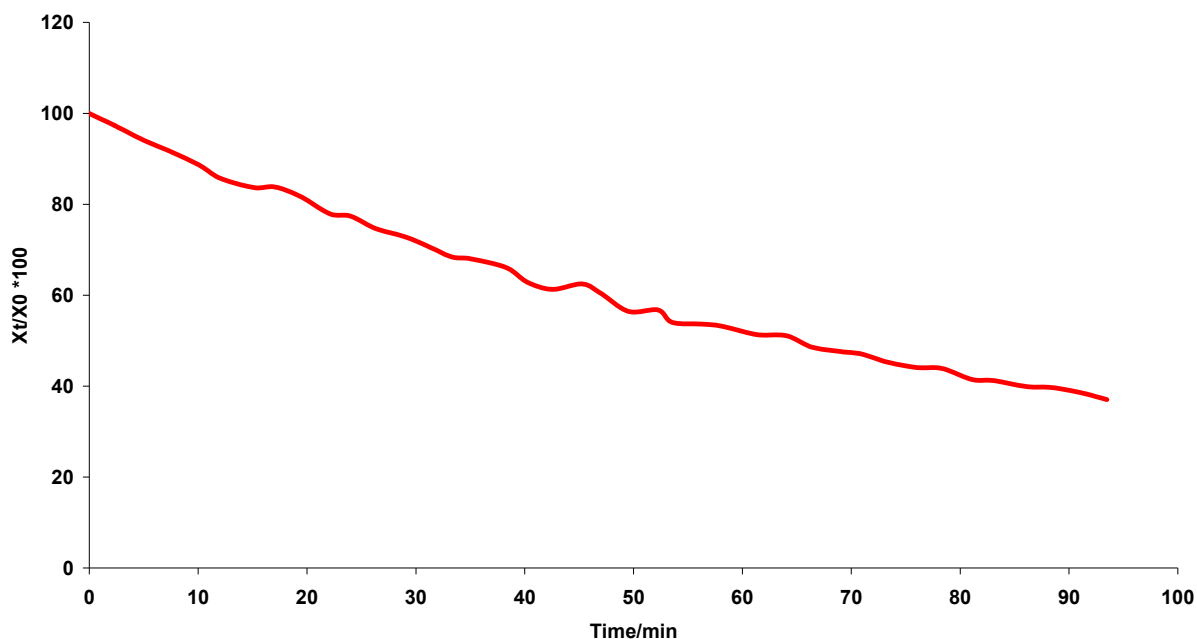
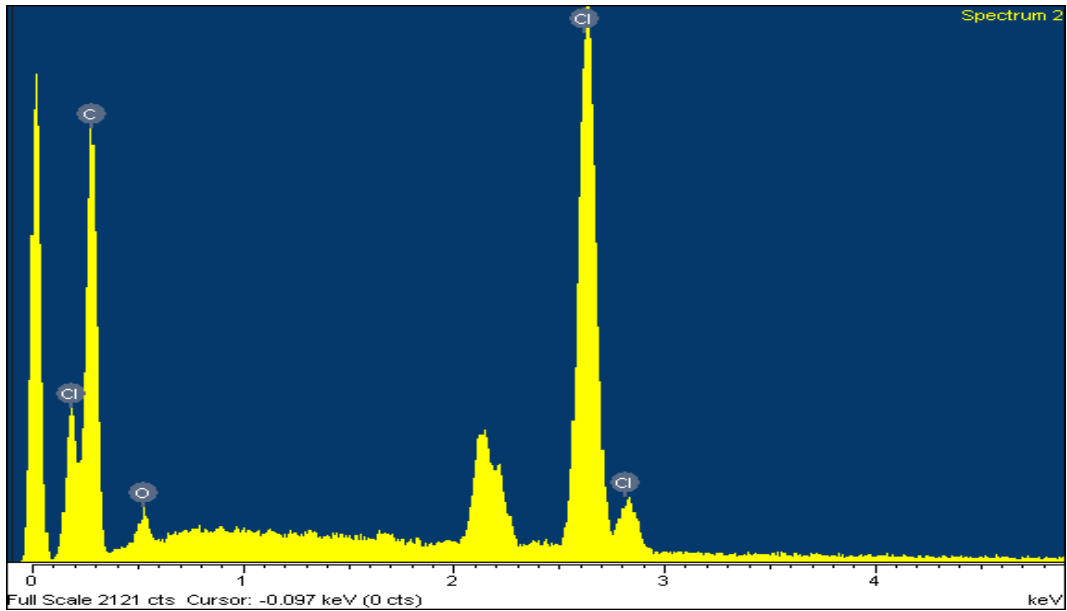


Figure 4-2 - Degradation index of pure PVC, reference sample as function of time

Figure 4.2 shows the results of the degradation study of pure PVC as a function of time and hence X-ray exposure. The graph has been plotted using equation <3.1> against the X-ray exposure time. The degradation index was obtained from equation <3.1> plotted against t (time/(min)) ( $X_t/X_0 \times 100$  vs. t). The degradation index of the pure PVC after 10minute, X-ray exposure was 5% and the final degradation index after 93 minutes X-ray exposure was 63%. This result from study was similar to the reported degradation study of PVC by Beamson and Briggs (Beamson, G & Briggs,D, 1992).

## 4.2 EDX analysis of pure PVC

Five samples of pure PVC powder (drop cast in THF, on to aluminium foil) were exposed to X-ray radiation for 0, 10, 30, 50 and 70 minutes. The ratio of chlorine to carbon for each sample was determined. Then the degradation index after 70 min was calculated using equation <3.1>. In order to determine the degradation of pure PVC, the result from equation <3.1> was plotted against t (time/ (min)) ( $X_t/X_0 \times 100$  vs. t). Figure 4.3 shows the result of an EDX analysis of pure PVC before the sample was exposed to X-rays (time zero), the Cl/C ratio at  $X_0$  was 0.3.



Figur4-3: shows EDX analysis of a pure PVC before the sample was exposed to X-rays (time zero,  $X_0$ )

Figure 4.4 shows the result of EDX analysis of pure PVC after the PVC was exposed to X-rays for 70 minutes. The EDX survey shows the loss of chlorine after 70 minutes X-ray exposure. The Cl/C ratio of this sample at 70min was 0.19, thus it shows decrease in Cl/C ratio from 0.3 at time zero to 0.19 at 70min.

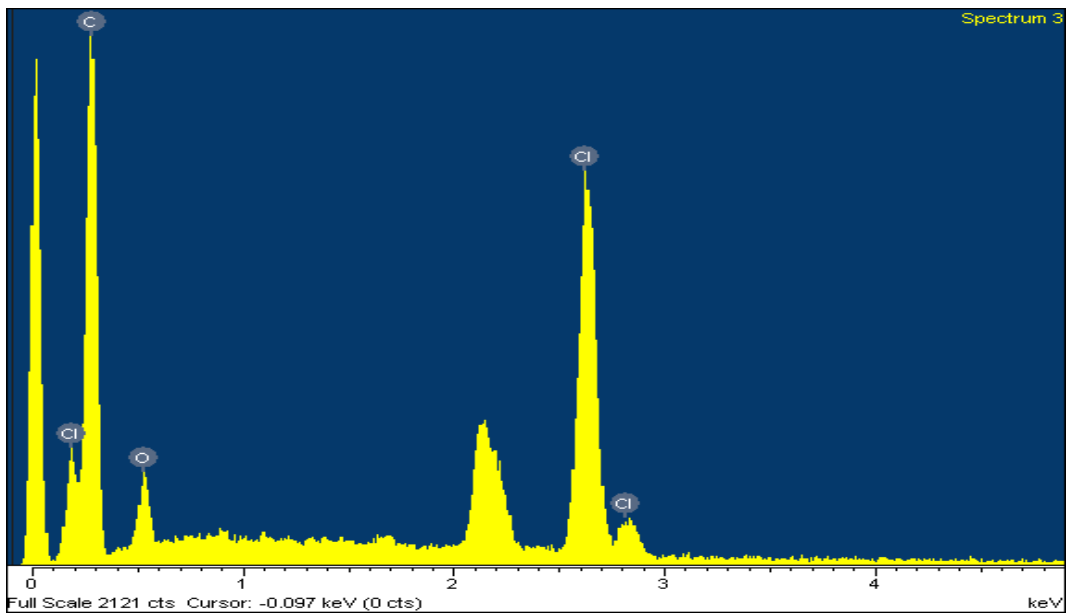


Figure 4-4 EDX analysis of pure PVC after seventy minutes X-ray exposure

Figure 4.5 contains the degradation index of pure PVC as a function of X-ray exposure after 70 minutes of X-ray exposure. The percentage degradation index of pure PVC after 10 minutes was 5% and the final degradation index after 70-minutes of X-ray exposure was 37.7%. By comparison of the results from XPS and EDX degradation study of PVC samples which have been exposed to X-ray irradiation using the same X-ray source and same power. The degradation index of the XPS and EDX analysis of the pure PVC in the first 10 minutes was similar. After 70 minutes of X-ray exposure the degradation index obtained from XPS was 53%, and while that from EDX was 30%. In XPS, the analysis depth is approximately 5nm while the depth of analysis in EDX is a few  $\mu\text{m}$ .

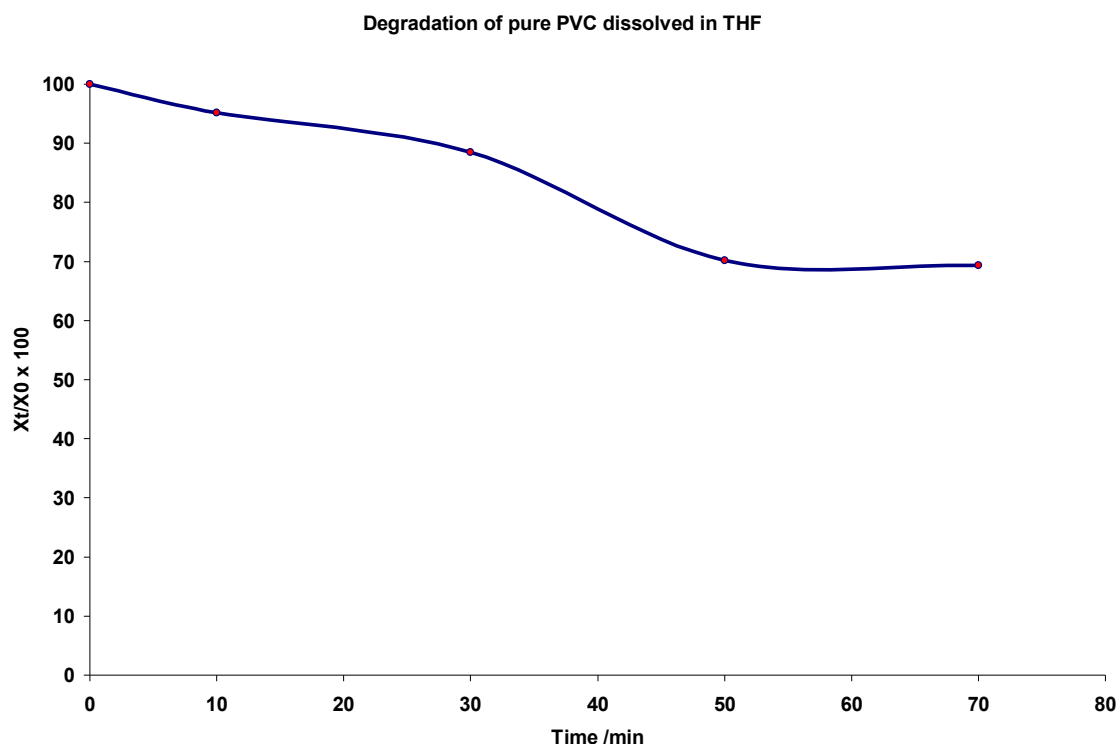


Figure 4-5 - Degradation index of pure PVC by EDX up to 70 minutes of X-ray exposure (By twine anode Al source)

### 4.3 Line scans analysis of pure PVC

A XPS – line scans analysis along a C-ULAM taper through a pure PVC film was carried out in order to determine the depth of PVC degradation after 70 minutes X-ray exposure. Figure 4.6 shows the result of a compositional depth profile through pure PVC, obtained by performing an XPS linescan analysis along a C-ULAM taper through the PVC exposed to X-ray for 70 minutes. The area of analysis (X-ray spot size) was 200  $\mu\text{m}$ .

The insert in Figure 3.9 is an optical micrograph of the C-ULAM taper, the right hand corner of the inset is bulk of PVC region and the left hand corner is the degraded region of the PVC. The depth of the degradation was calculated using Equation this depth was approximately 17.6 $\mu\text{m}$ , and also indicated an increase of Cl intensity in degraded region.

$$\text{Equation 11: } \theta = \tan^{-1}(\text{depth/distance}),$$

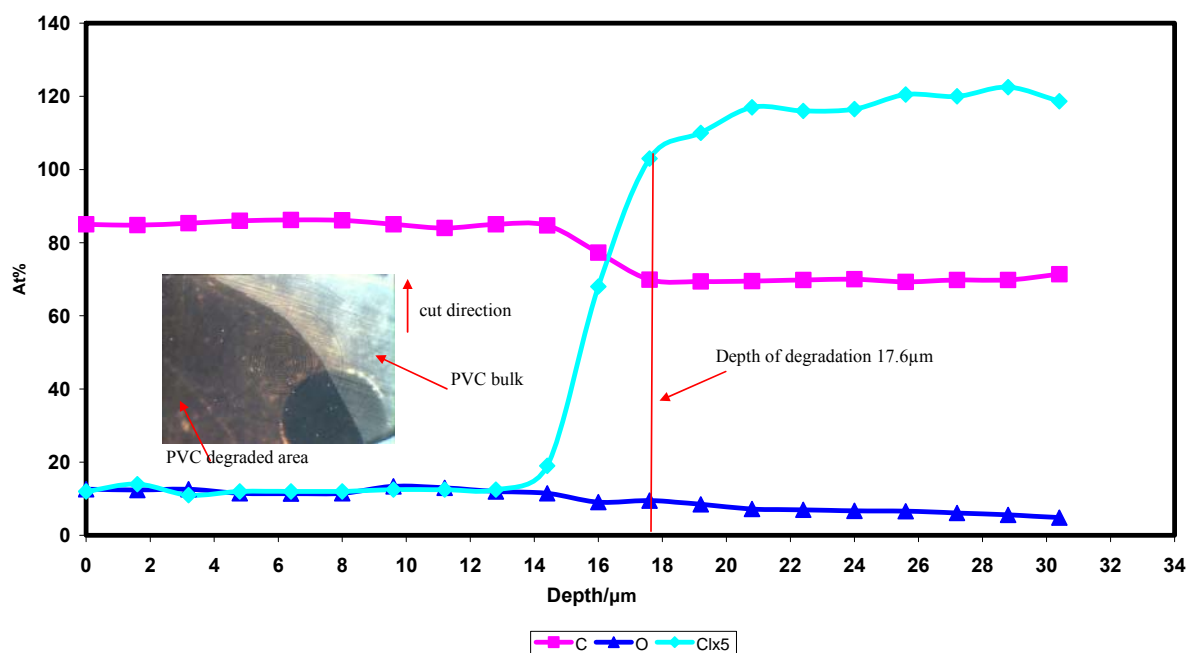


Figure 4-6 - Compositional depth profile of pure PVC, obtained by performing an XPS line scan analysis along a C-ULAM taper through the PVC exposed to X-rays for 70 minutes. Inset is an optical micrograph of the degraded pure PVC

#### 4.4 ToF-SIMS analysis of pure PVC

Here the results of the ToF-SIMS were compared together using data manager to overlay the ToF-SIMS spectrum of bulk PVC region and degraded PVC region. In order from top to bottom, are spectra of bulk PVC region and degraded region of PVC. Because the degradation of PVC is associated with dehydrochlorination, this study focused on the isotopes of Cl and  $\text{Cl}_2$  and  $\text{Cl}_2$  in both regions. The isotopes of Cl have numerical masses of 35 (75.77%) and 37 (24.23%). The  $\text{Cl}_2$  are at masses of 70 (57%), 72 (36.718%) and 74 (5%). Figure 4.7 shows the result of negative ToF-SIMS analysis of the bulk of a pure PVC region and from X-ray degraded region. These results are associated with the

dehydrochlorination of the PVC after seventy minutes exposure to X-rays. The relative intensities of the Cl and Cl<sub>2</sub> species in negatives ion spectra from both regions have been compared. The results indicate that there is a significant intensity change in all Cl and Cl<sub>2</sub> species. The intensity of all Cl and Cl<sub>2</sub> species decreased in the negative ion spectra from the degraded region. The chlorine intensity in the ToF-SIMS spectra from the bulk of the PVC is much greater than the intensity of chlorine in the degraded region.

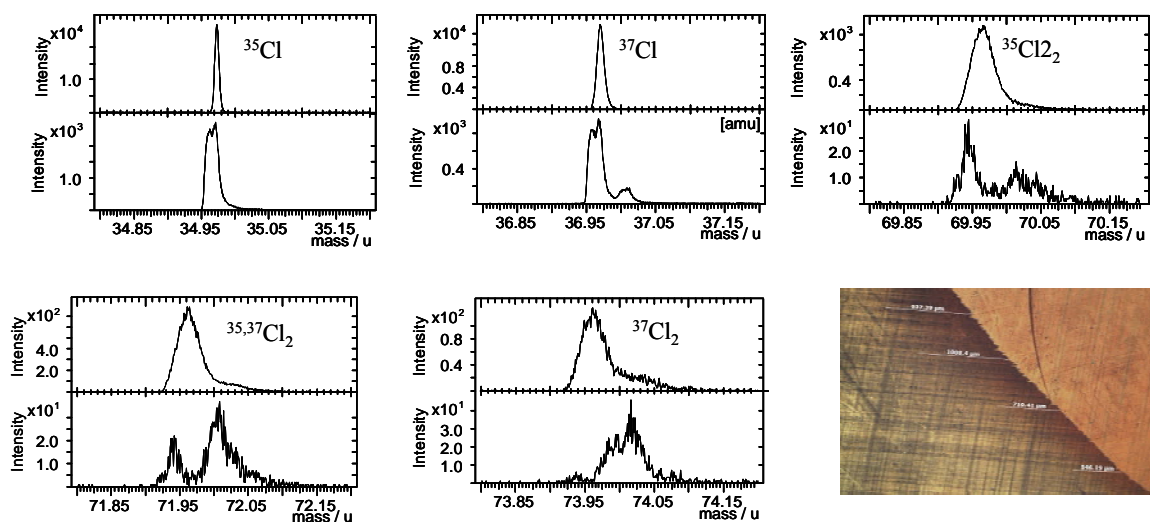


Figure 4-7 - shows Negative ToF-SIMS spectra from the bulk region of pure PVC (upper spectra) and from a degraded region (lower spectra). The inset is an optical micrograph of the specimen.

#### 4.5 X-ray degradation study of PVC window profile

XPS analysis of PVC V, PVC R and the plasticised PVC as a function of the time of X-ray irradiation of the sample was performed employing the same method used to analyse pure PVC. In the case of PVC V and R, these were supplied with one side of the PVC profiles was covered by a PE protective film. The protection film was removed pre XPS analysis. Although the protective film was removed from the surface of the PVC V and R profile samples some of the release agent remained on surface of PVC V and R profiles samples. The reason why surface analysis of the PVC R and V profiles with release agent was carried out is that when bonding and coating of the surface of the PVC profile is carried out commercially, the release agent is not removed from the surface of the PVC profile. The XPS analysis surface analysis of PVC V and R profiles samples carried out

once the release agent was remained on surface of the samples, and while the surface of the samples was washed by hexane. The Figure 3.11 shows number one and forty XPS survey spectra of PVC V with and without release agent on the surface of the sample. The two surveys spectra at the bottom of the Figure are survey spectrum number one and number forty acquired from PVC V while release agent was remained on the surface of the PVC V profile sample. Also two surveys spectra at the top are the survey spectrum number one and forty of PVC V while the surface of the PVC V profile was washed by hexane. The intensity of the Cl<sub>2p</sub> peak in survey spectrum that was occurred from the PVC V with release agent was very low. The reason of the low intensity in Cl<sub>2p</sub> was, because the PVC material is buried beneath the release agent. When photo electrons pass through the release agent layer they lose their kinetic energy. Therefore, the elements peaks will have a lower intensity. As the depth from which information can be obtained in XPS is of the order of a few nanometres, ~ 5nm (Watts & Wolstenholm, 2003), as the first two survey spectrum at the bottom of Figure 4.8 showed the PVC was buried under release agent. In order to characterise the PVC samples without release agent, the XPS analysis of both rigid PVC V and R was carried out after the release agent had been removed from the surface of the PVC samples using hexane solvent.

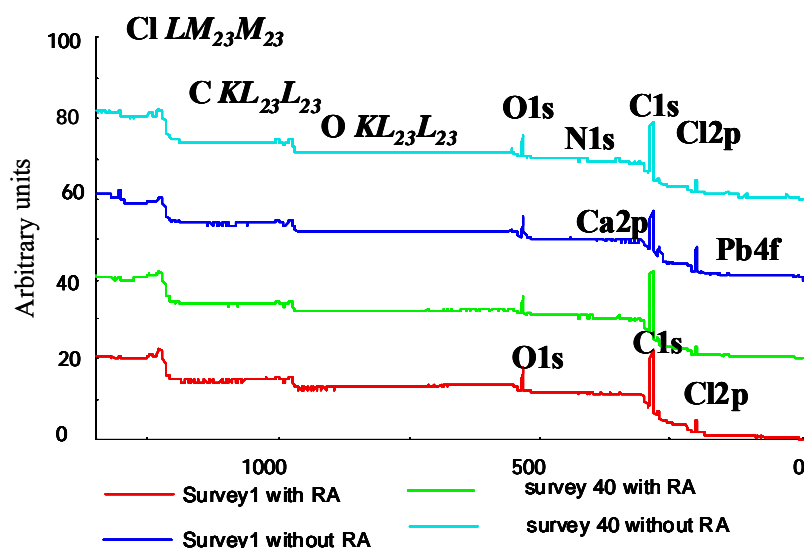


Figure 4-8 - XPS Survey spectrum of PVC-V with and without release agent

The outcome of that was surface concentration of the Cl increased and peaks for Pb and Ca became visible on the survey spectrum of the PVC V. The lead salt is added to PVC as a heat and light stabiliser (UV stabiliser) because PVC V and R are designed for

outdoor use. Both commercial PVC window profiles are blended polymer and they are blended with other polymers<sup>2</sup>.

Table 3.2 is the result of quantitative surface analysis from the degradation study of the PVC V, with and without release agent. When the release agent was removed from the surface of PVC V, it resulted in a decrease in the surface concentration of C from 81 to 50 at% and an increase in the surface concentration of Cl from 5 to 10 at%. As PVC V was analysed while the release agent remained on the surface of PVC, the surface concentration of C was higher than when the release agent removed from the surface of PVC profile. Thus, the C in this survey spectrum contributed from the PVC and the release agent. When pure PVC analyse by XPS the surface concentration of PVC would be up to 30 at%, but the commercial PVC are blended polymer. Also peaks from the elements of the filler and additives included in the PVC formulation, such as lead and calcium were in the survey spectra after removing the release agent. In both PVC profile samples, with and without release agent, after 93 minutes of X-ray exposure (survey 40), there was evidence of the dehydrochlorination of PVC.

Table 4.2 Quantitative XPS surface analyses from the degradation study of the PVC-V samples.

Sample	Surface compositions/atomic %					Release agent
	C	Pb	O	Cl	Ca	
Survey1	81	0	12	5		✓
Survey 40	86	0	10	3		✓
Survey 1	50	0.1	39	10	0.5	
Survey 40	60	0.2	35	5	0.6	

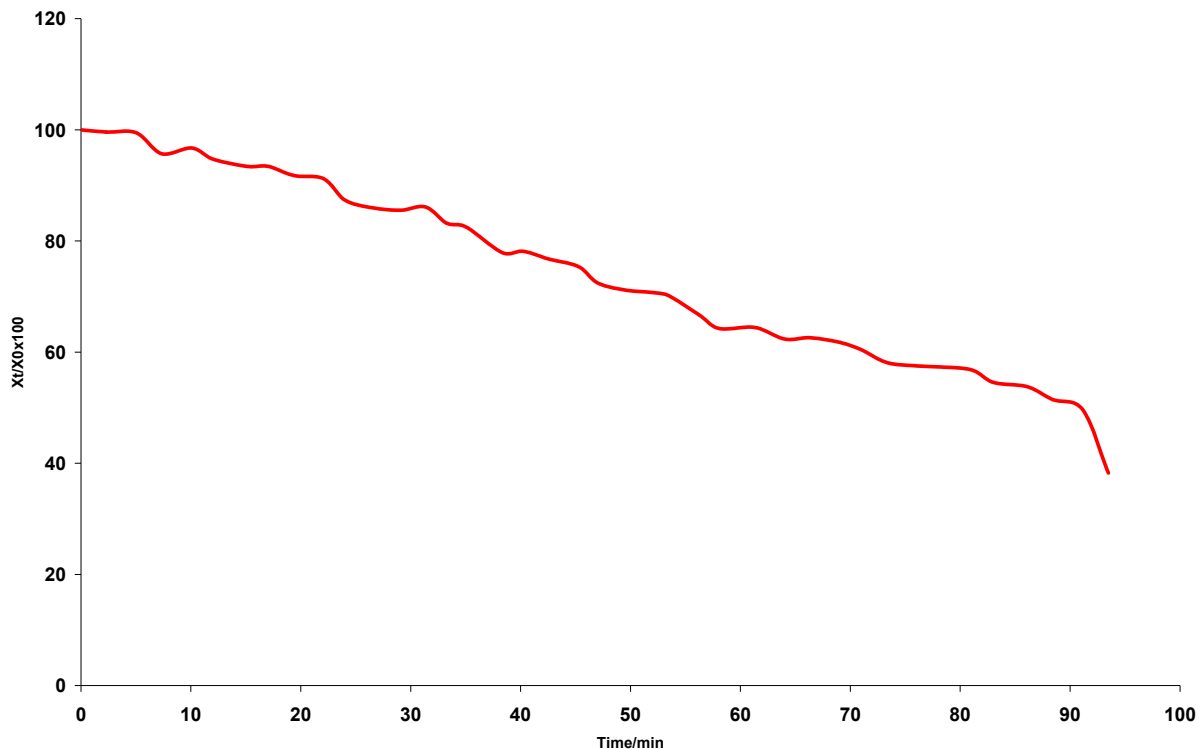


Figure 4-9 – shows the Degradation index of PVC-V with release agent

Figure 4.9 shows the results of the degradation study of PVC V with release agent after 93minutes of X-ray exposure. The degradation index of PVC V with release agent after 10 minutes was 3% and at the end of the analysis after 93 minutes it was 62%. The degradation index of the pure PVC after 10 minutes X-ray exposure was 5% (see figure 4.5), it was about 2% higher than PVC V with release agent. The surface concentrations of PVC elements such as Cl in the surface of pure PVC are greater than in commercial PVC which is blended with other polymer and the additives.

Figure 4.10 shows the result from the degradation study of PVC V without release agent. The degradation index after 10 minutes was 12% and finally after 93 minutes was 63%. The result from Figures 4.9 and 4.10 shows, dehydrochlorination on PVC V samples with and without release agent. The results of the degradation studies were different for the PVC V samples with release agent and without in the first thirty minutes of X-ray exposure. After 93 minutes of X-ray exposure the result of the degradation was almost the same. In fact after 30 minutes of X-ray exposure on surface of the PVC with release agent, the heat of the source will damage the release agent and it cause Cl enrichment on surface of PVC and increasing the degradation index.

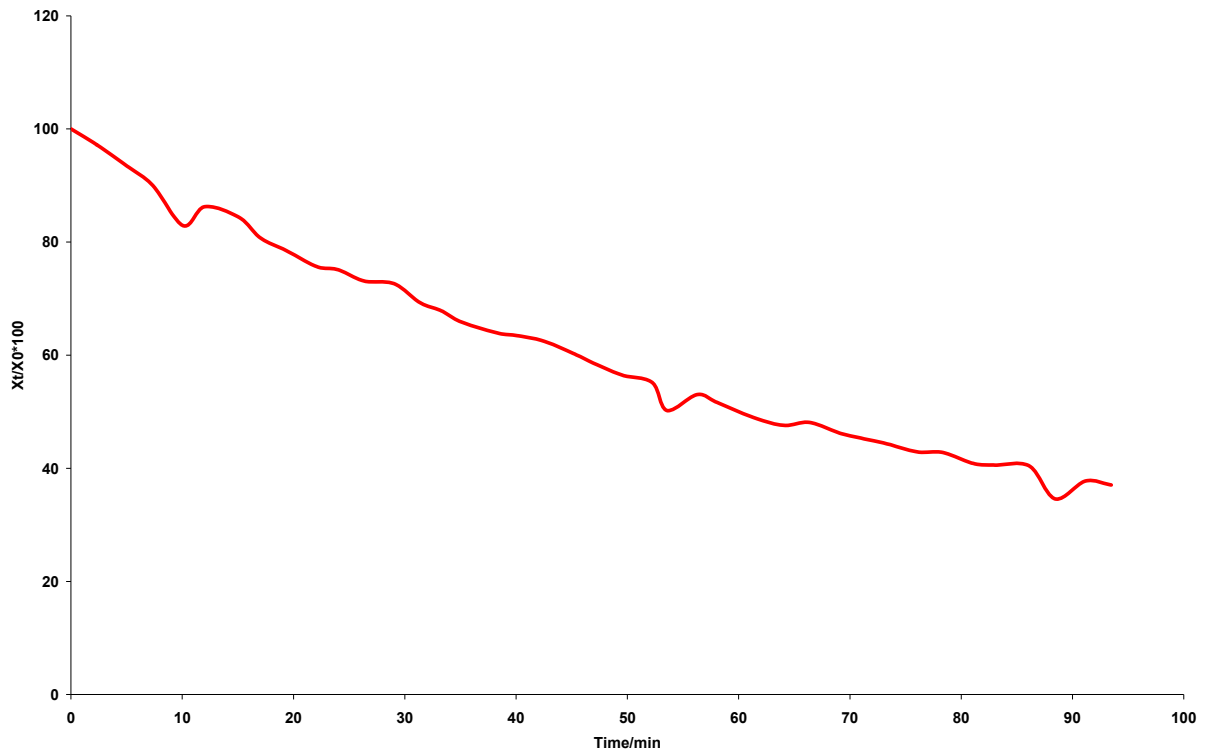


Figure 4-10– shows the Degradation index of PVC-V without release agent

Figures 4.11 and 4.12 show the degradation index of PVC R with and without the release agent respectively. The degradation index of PVC R with release agent (Figure 411) after 10 minutes was 1%, and after 93 minutes of X-ray exposure was 34%. After the release agent was removed from the surface of PVC R (Figure 4.12), the degradation index of PVC R increased. After 10 minutes X-ray exposure on PVC R without release agent the degradation index of the sample was 9%, and finally after 93 minutes X-ray exposure was 61%.

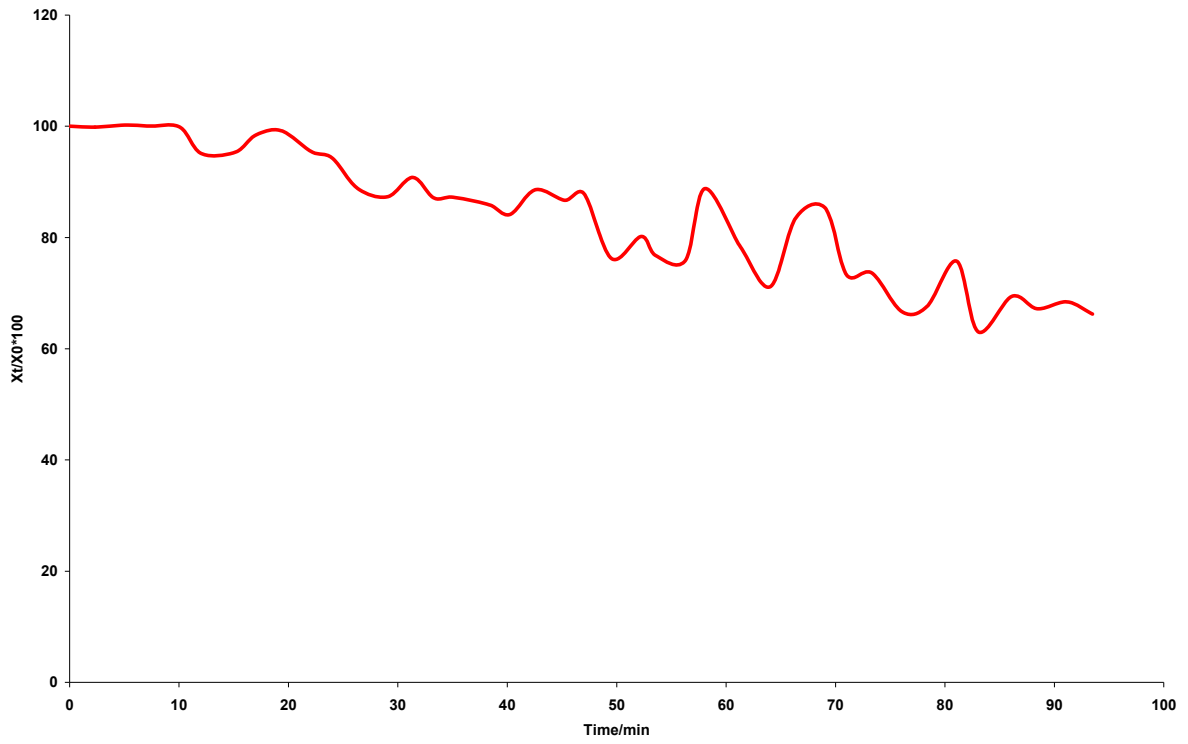


Figure 4-11—shows the Degradation index of PVC-R with release agent

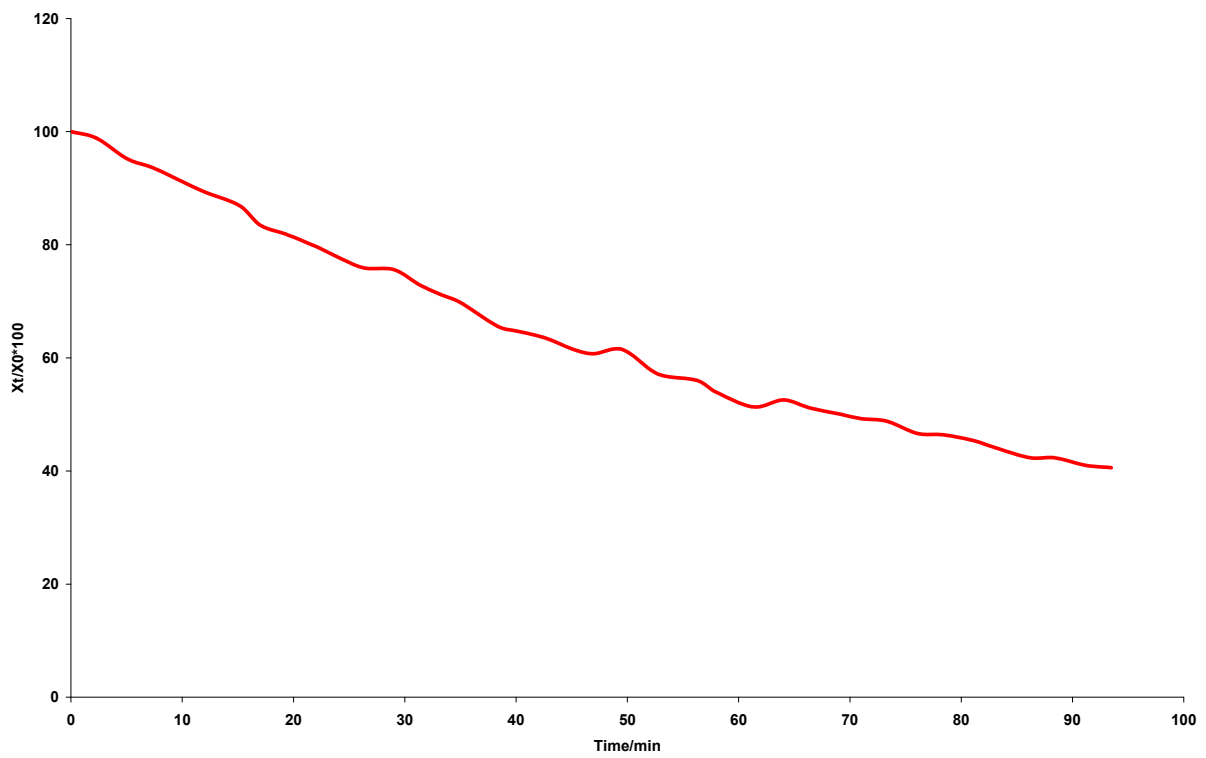


Figure 4-12 shows the Degradation index of PVC-R without release agent

Table 4.3 presents the XPS quantitative surface analysis from the degradation study of PVC R with and without release agent. Two samples of PVC R were analysed as a function of time and hence X-ray exposure, one with release agent on the surface of the PVC and one without release agent. When the release agent was removed from the surface of the PVC R, this resulted in a decrease in the surface concentration of C from 78 to 72 at%, and an increase in the surface concentration of Cl from 1.2 to 5/at%. Calcium carbonate and the zinc oxide are two additives used in the formulation of PVC R. The purpose of using calcium carbonate is the same as PVC V (impact resistance and increase bulk cheaply). Zinc oxide is used in the PVC R formulation as a heat and light stabiliser (UV stabiliser) instead of lead salt (as was in PVC V). After the release agent was removed from the surface of PVC V and R in both cases an increase in surface concentration of the oxygen was observed. As it was mentioned before these PVC window profile are blended polymers, so by removing the release agent the surface concentration of the elements obtains from other polymers such as (acrylic impact modifier) will increase.

Table 4.3 XPS Quantitative surface analyses from the degradation study of PVC- R samples

Sample	Surface compositions/atomic %					Release agent
	C	O	Zn	Cl	Ca	
Survey1	78	20	0.2	1.2		✓
Survey 40	82	17	0.1	0.8		✓
Survey 1	72	22	0.3	5	0.4	
Survey 40	78	19	0.4	2.5	0.4	

Table 4.3 indicates when the release agent was on the surface of the PVC, the surface concentration of carbon was 78 at% and the chlorine surface concentration was 1.2 at%. When the sample was exposed to X-ray for 93 minutes the surface concentration of chlorine was reduced to 0.8 at % and the surface concentration of carbon increased to 82 at%. After removing the release agent from the surface of PVC R, the surface concentration of chlorine increased to 5 at %, and the surface concentration of carbon decreased to 72 at%. When the PVC R without release agent sample was exposed to X-rays for 93 minutes the surface concentration of chlorine was reduced to 2.5 at % and the surface concentration of carbon increase to 78 at%.

#### 4.6 X-ray degradation study of plasticised PVC foil

A degradation study on a plasticised PVC film was carried out using XPS in a manner similar to that used to investigate the PVC V and R profiles. The plasticised PVC foil exhibited a lower degree of degradation than the two rigid PVC profiles (V&R). The reason why the plasticised PVC foil had a lower degradation index was that the plasticised film was laminated with additional polymer film layers. The total thickness of the laminated foil was  $213\mu\text{m}$ , with the thickness of the PVC layer of  $\sim 127\mu\text{m}$ . The plasticised PVC layer was between the thin polymer film with thickness of ( $3.88\mu\text{m}$ ) and another film with a thickness of  $68.98\mu\text{m}$  Figure 4.13.

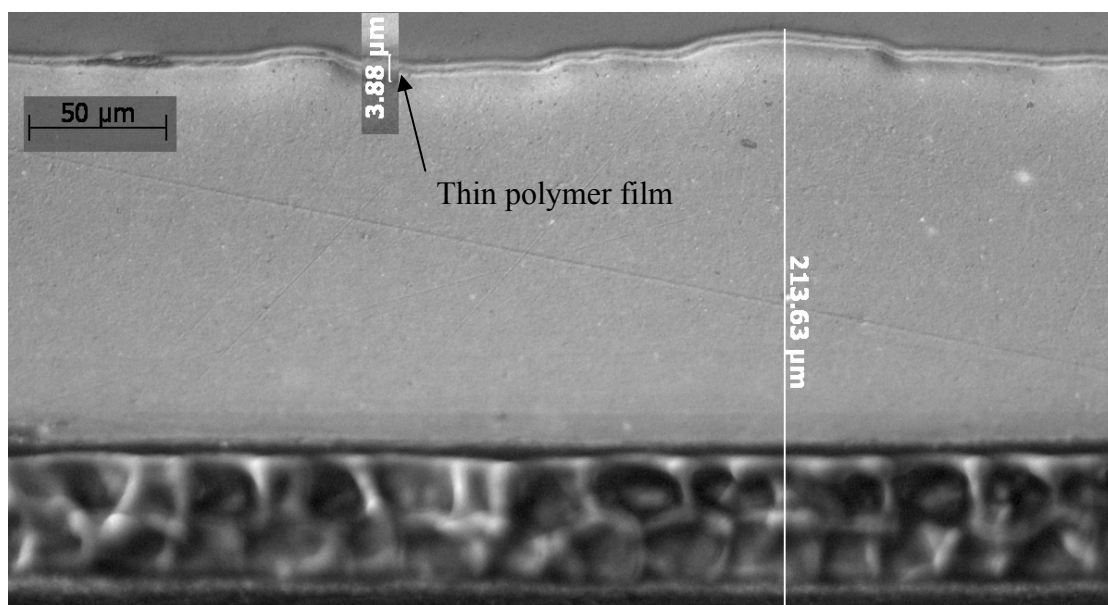


Figure 4-13 –Picture of Optical micrograph of a cross section through plasticised PVC film mounted in resin.

While the plasticised PVC sample was exposed to X-ray source during the XPS analysis, the plasticised PVC layer under the thin polymer experienced thermal degradation caused by the heat of the X-ray source. As the depth of degradation of pure PVC, obtained by performing an XPS - line scans analysis along a C-ULAM taper was 17.6 . Indeed, the chlorine, which came from the degradation of the PVC layer beneath the top polymer film, was moved to the surface of the specimen, resulting in chlorine enrichment on the surface of specimen. Figure 4.14 shows the degradation index of the plasticised PVC after 93 minutes, while Table 3.5 shows the XPS quantitative surface analysis of the plasticised PVC film.

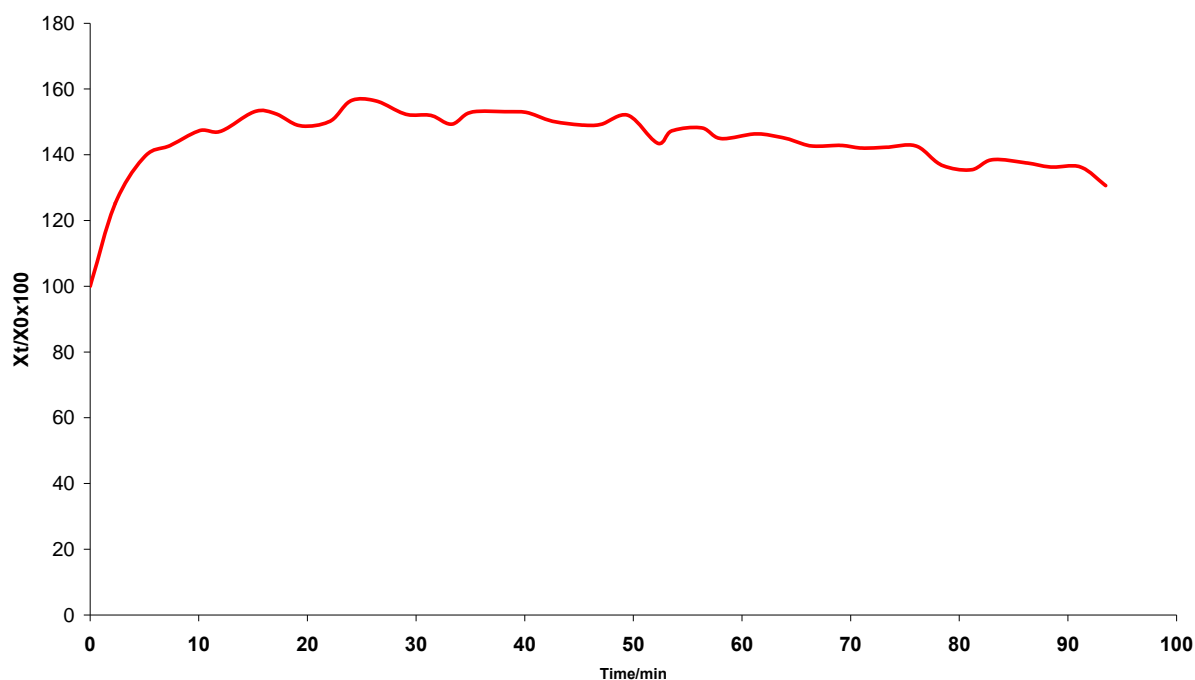


Figure 4-14 - shows the Degradation index of plasticised PVC

Table 4.4 XPS Quantitative surface analyses from the degradation study of a PVC-Plasticised foil sample.

Sample	Surface compositions/atomic %								
	C	Ca	O	N	Cl	Si	Co	Zn	Na
Survey1	75	0.4	16	1.2	3	1.5	0.7	1.2	1.3
Survey 40	75	0.5	14	0.9	4.3	1.5	1.5	0.6	1.6

#### 4.7 X-ray degradation study of PVC with gold disc

To distinguish between the Cl/C ratio changes due to lower Cl concentration and increase in C concentration. A further degradation study was under taken by developing novel method to investigate whether C redistribution contribute to changes in Cl/C ratio or whether change in Cl/C ratio cause by decrease on Cl concentration, by 1mm diameter gold disc was sputter coated on to all PVC samples surfaces. However, the Au/C ratio remained constant suggesting there was no redeposition of C on to the PVC profile samples surfaces. Degradation of PVC takes place when PVC lose Cl-H. Before depositing the gold on to the sample surface, the surface of PVC V and R profile were wiped with hexane to remove the release agent. Then the samples were analysed in the same manner that specimens were analysed before with XPS in this study. Figures 4.15,

3.16 and 3.17) shows result of degradation study of PVC V, R and plasticised PVC foil while 1mm disc gold was coated on to the surface of the samples.

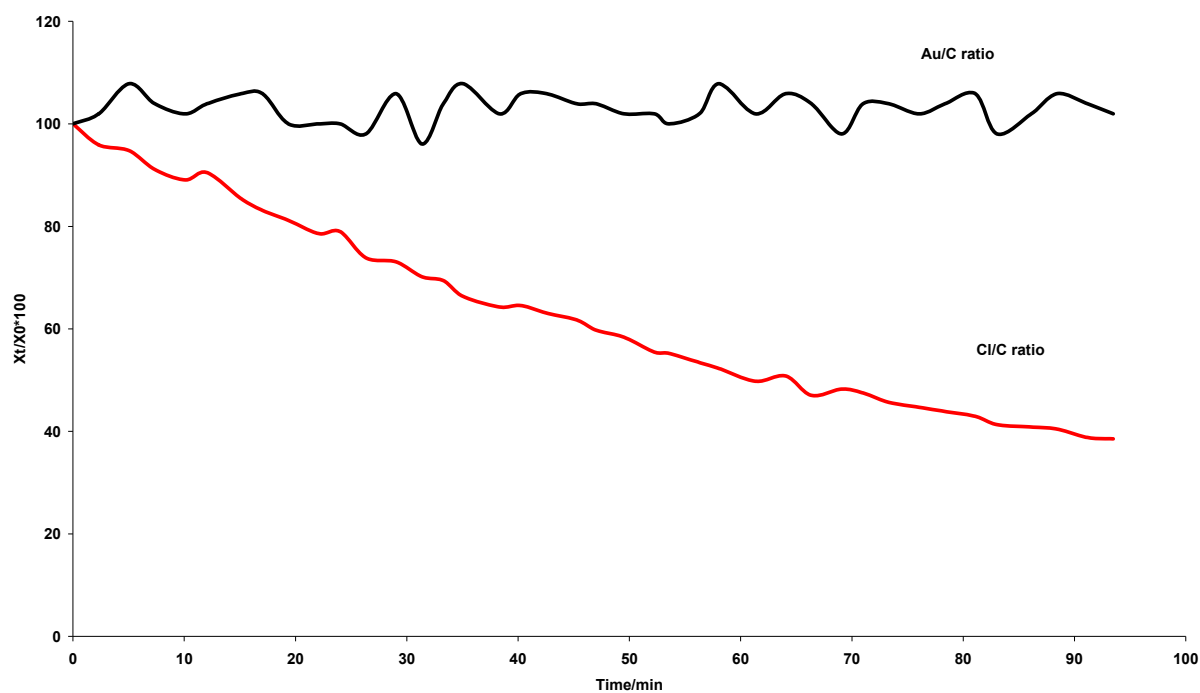


Figure 4-15 – shows the Degradation index of PVC-V with gold disc

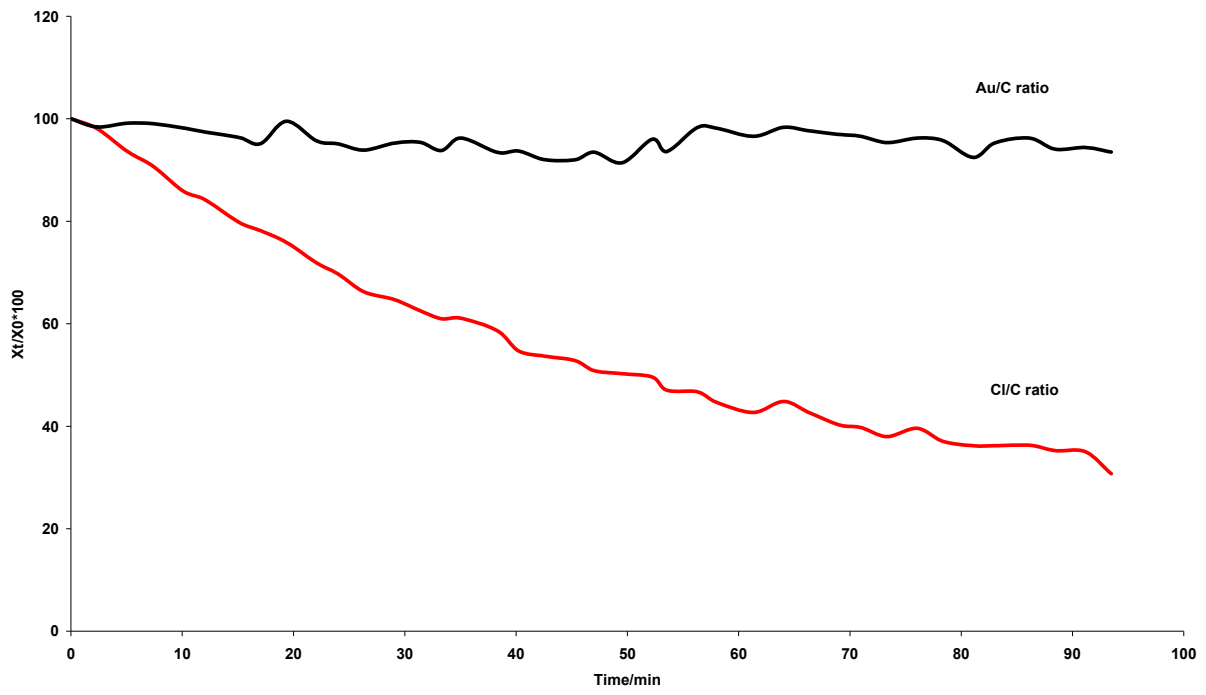


Figure 4-16 – shows the Degradation index of PVC-R with gold disc

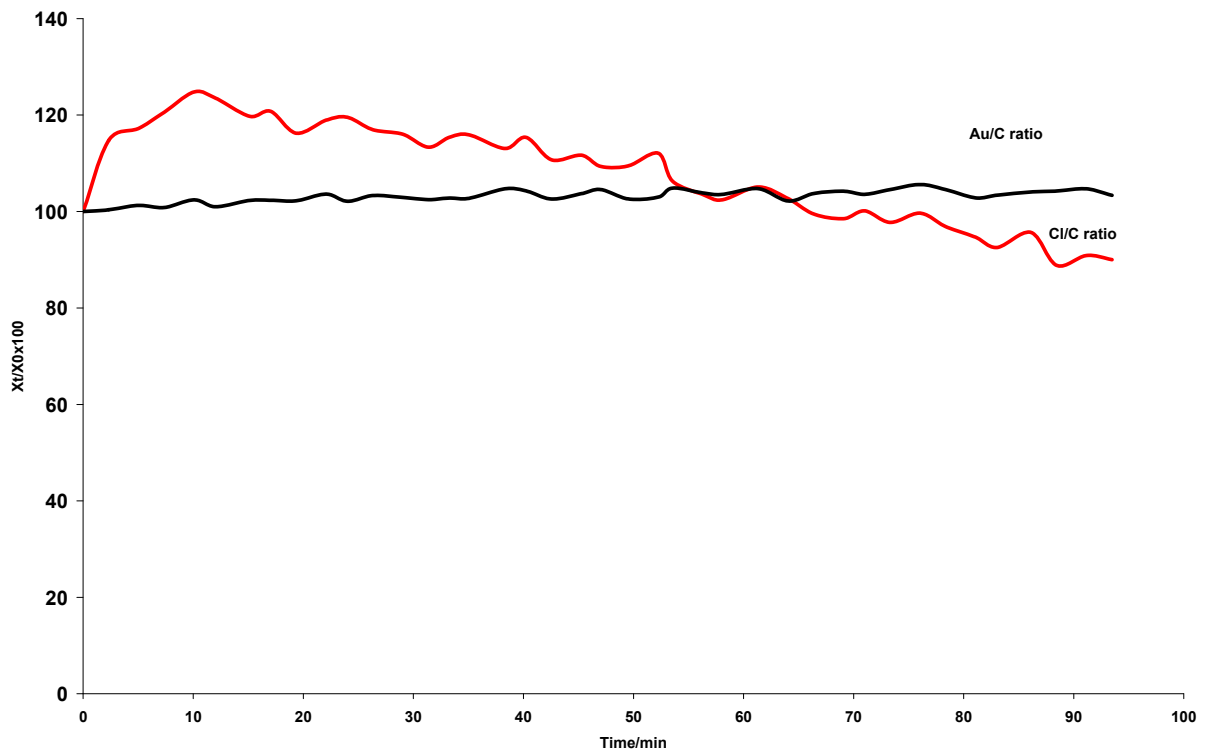


Figure 4-17 - shows the Degradation index of plasticised PVC with gold disc

Figures 4.15, 4.16 and 4.17 are the result of the degradation study of PVC V, R and plasticised PVC with a gold disc deposited on to the surface of the PVC samples, respectively. The surface concentration of Au on all the samples was constant after 93 minutes of X-ray exposure. After gold disc was coated on to the surface of the plasticised PVC, it was significant change on Cl/C ratio of plasticised PVC. As the plasticised PVC was analysed with gold coat on top by XPS after 93 minutes X-ray exposure the degradation index of the sample was 9%. This degradation index of this sample was -39 before gold was deposited on the surface sample.

Table 4.5 is a XPS quantitative surface analysis of the three types of PVC (V, R and plasticised film) after a 1mm diameter gold disc was deposited on the surface of the samples. By comparing the initial survey (survey 1) and the final survey (survey 40) for each sample, there is evidence of a decrease in the Cl/C ratio for PVC V and R, resulting from a decrease in the surface concentration of Cl. The Cl/C ratio of the plasticised PVC changed after 93 minutes of X-ray exposure, resulting from an increase in the C surface concentration. The surface concentration of gold was constant for all the samples and it did not change after 93 minutes of X-ray exposure.

Table 4.5 XPS Quantitative surface analyses from the degradation study of PVC V, R and plasticised PVC after a gold disc was deposited on the surface of samples.

Sample	Surface compositions/atomic %									
	C	Pb	O	N	Cl	Si	Co	Zn	Ca	Au
Survey 1 V	70	0.03	9	0.1	16	0.4	0.6		0.4	0.6
Survey 40 V	82	0.04	11	0.1	7	1.5	0.7		1.5	0.7
Survey 1 R	75		14	0.1	9					1
Survey 40 R	84		12	0	3					1
Survey 1 Plas	72	0.01	18	0.2	7	0.4	0.8	0.9	0.8	1.8
Survey 40 Plas	74	0.01	14	0.2	7	0.3	0.3	1.2	0.3	2

Figure 4.18 gives a summary of the degradation study data for all of the samples (pure PVC, PVC V, R and plasticised PVC film) after 93 minutes of X-ray exposure. The degree of degradation of the PVC relates to how pure the PVC is because different additives and fillers affect the degradation of the PVC. In this investigation Cl that occurred from survey spectrum of pure PVC had greatest surface concentration amongst of the four samples 15at% at time zero ( $X_0$ ), due to the purity of this PVC. PVC profiles V and R were commercial blended polymers, those blended with other polymers and

additives. The plasticised PVC film was a laminated specimen made from a plasticised PVC layer and 2 other polymeric layers.

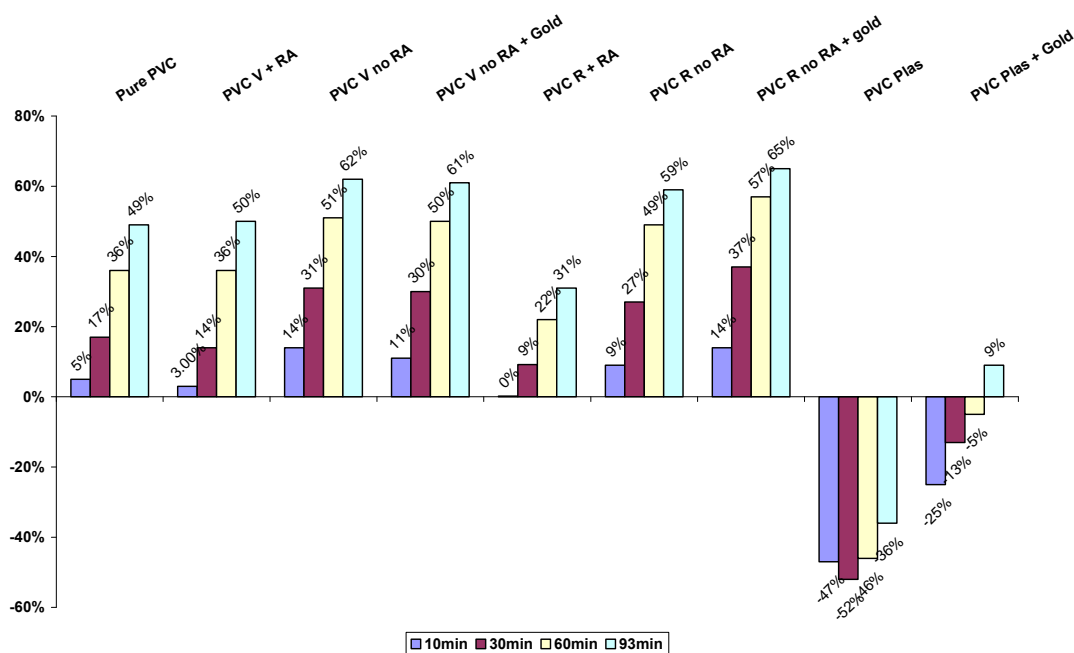


Figure 4-18 - shows the Degradation index of the PVC-V, PVC-R and plasticised PVC samples

#### 4.8 XPS analysis before surface modification

The XPS analysis of the PVC V and R samples before flame treatment enables us to determine the effect of the flame treatment on the surface chemistry by comparison with the results of the surface analysis of the PVC samples after surface modification

As PVC is known to undergo dehydrochlorination during XPS analysis, a very rapid XPS analysis has been used so that the dwell time. PVC sample V1, V2, R1 and R2 had protection film on the surface of the samples. In order to investigate these PVC samples, the XPS analysis of these samples was carried out twice; first with the release agent on the surface of the samples, and second hexane solvent applied to the surface of the samples to remove the release agent. For each samples (with and without release agent) two specimens were prepared for XPS analysis, first sample was analysed by recording just survey spectrum and the second sample analysed by recording high resolution spectrum of C1s only.

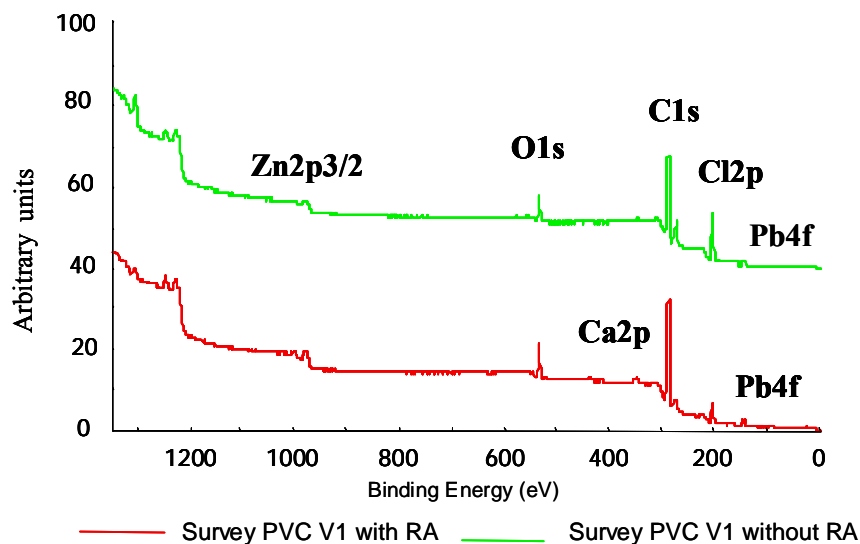


Figure 4-19 - shows the Survey spectra of PVC V 1 with and without RA before FT

Figure 4.19 shows the survey spectra of PVC V 1 before flame treatment. The survey spectrum of PVC V 1 has seven characteristic peaks: Pb4f (138 eV), Cl2p (200eV), Cl2s (270eV), C1s (285 eV), Ca2p (347eV), O1s (532eV), and Zn2p<sub>3/2</sub> (1022eV). The Pb and Zn are additives used as a heat and UV stabiliser in PVC window profile, Cl2p is from PVC, the C1s and O1s peaks have contributions from both the PVC and the release agent, the Ca comes from window PVC profile formulation it is one of PVC filler to improve impact resistance and also to reduce the price of the PVC. Table 5.7 shows quantification of XPS analysis of PVC V samples before flame treatment.

While the release agent was removed from the surface of PVC V1, it resulted in an increase in the surface concentration/at% of the Cl from 5.4 to 14 at%, and decrease in the surface concentration of C from 82 to 75 at% and O from 12 to 9.5 at %. The cause of the decrease in the surface concentration of C and O were after removing release agent from surface of PVC, in fact just the surface of PVC was analysed. So Cl surface concentration that contributed from PVC surface increased sharply.

High-resolution C1s spectra for all samples have been peak fitted with three curves Figure 4.20 shows the high resolution spectra for C1s of PVC V1 with and without release agent before flame treatment. It is observed in Table 5.8 that while the release agent is removed from the surface of the PVC V1 samples it has an increase on surface concentration of C-O/ C-Cl component from 10.6/at% to 18/at%. Also removing release

agent resulted decreasing on surface concentration of CH/C-C component from 86/at% to 78.7/at%.

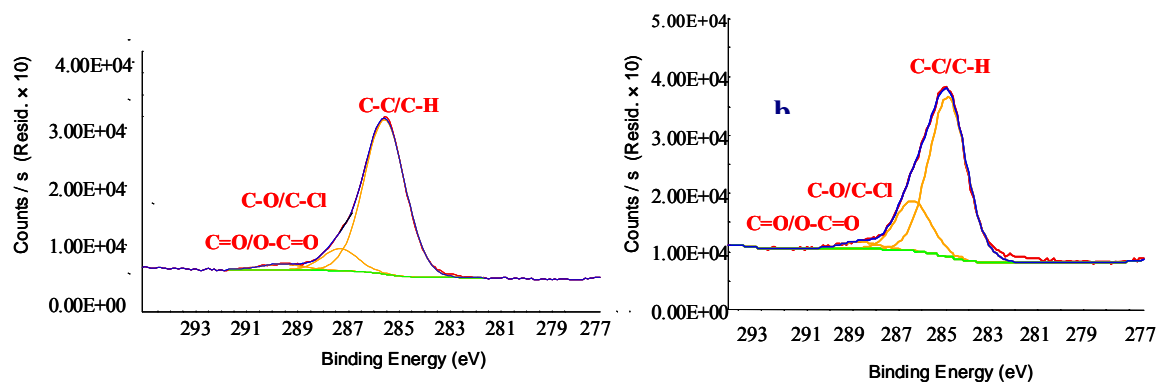


Figure 4-20 shows the High resolution spectrum of C1s of PVC V 1 with and without Ra before FT

Figure 4.21 shows the survey spectrum of PVC V2 with and without release agent before flame treatment. The PVC V1 and PVC V2 had similar surface composition but different surface concentration of element. After removal of the release agent from the surface of PVC V2 by hexane solvent, the surface concentration of C and O decreased while the surface concentration of Cl increased.

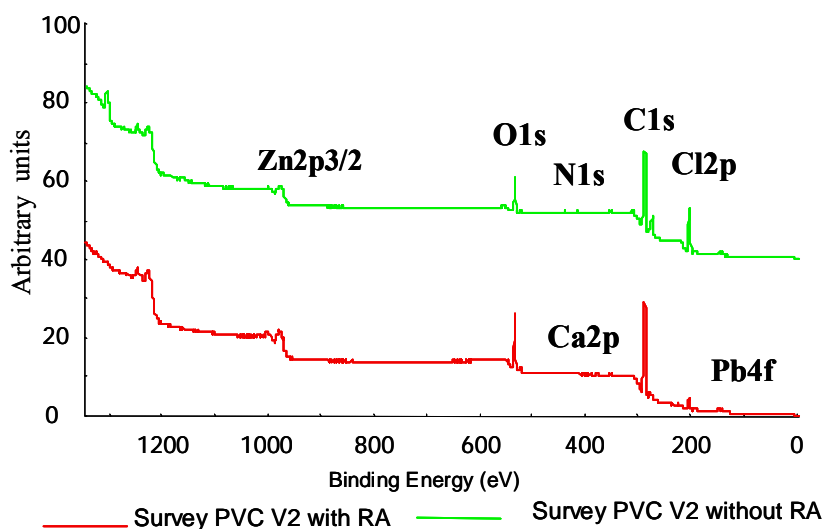


Figure 4-21 - shows the Survey spectrum of PVC V 2 with and without RA before FT

Figure 4.22 shows the high resolution spectra for C1s for PVC V 2 with and without release agent before flame treatment. By removing the release agent from the surface of

the PVC V2, resulted an increase on surface concentration of C-O/C-Cl component from 11.3/at% to 25/at%, removing the release agent also resulted on surface concentration of CH/C-C component from 84.6/at% to 70/at%.

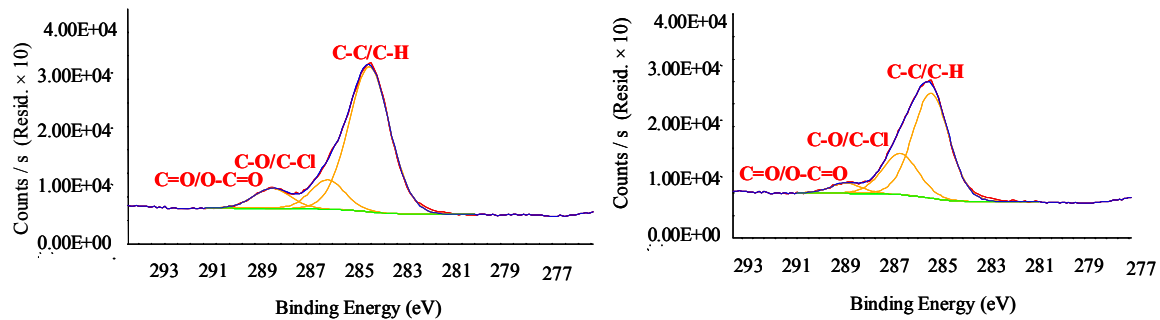


Figure 4-22 - shows the High resolution spectra of C1s of PVC V2 with and without RA before FT

Figure 4.23 shows survey spectrum of PVC V 2 plain, and high resolution spectrum for C1s of PVC V2 plain before flame treatment. The survey spectrum of PVC V 2 plain has nine characteristic peaks: Pb4f (138eV), Cl2p (200eV), C1s (285eV), Ca2p (347eV), N1s at (400eV), O1s (532eV), Zn2p<sub>3/2</sub> (1022eV) and Na1s at (1072eV). The different between PVC V2 plain and two previous PVCs (V1, V2) was that, the PVC V 2 plain did not have any protection film on the surface of the sample. Thus the entire element observed by XPS analysis that showed on survey spectrum contributed from PVC V2 plain profile formulation. The N1s peak (400 eV) and a Na1s peak (1072 eV) were identified in this sample. The nitrogen could contribute from impact modifier in PVC V2 plain profile. Although sodium peak visible in many XPS survey spectra as contamination element in surface of material, here the sodium is not contamination. It has got quite auger peak and as it will show in treatment section in XPS analysis after flame treatment that sodium visible of survey spectrum after flame treatment.

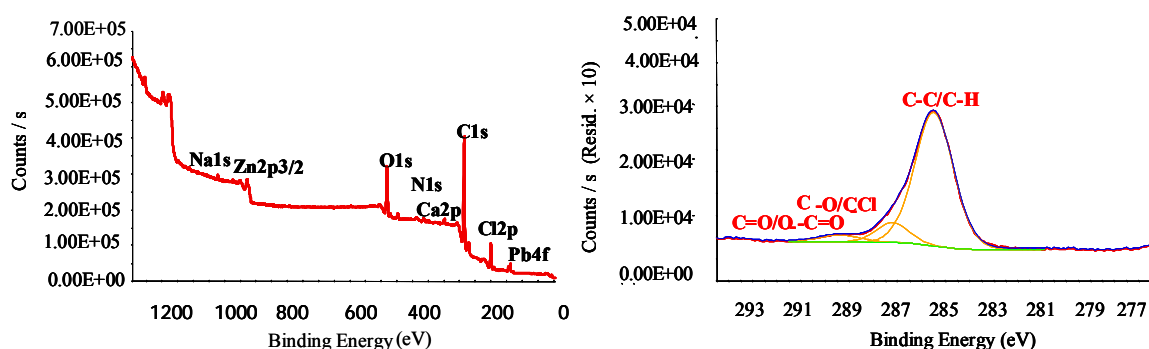


Figure 4-23 - shows the High resolution spectra of C1s of PVC V2 with and without RA before FT

The high resolution C1s spectrum of PVC V 2 plain before flame treatment was fitted in the same manner as PVC V1 and V2 by 3 curve. The curve with component CH/C-C (285 eV), curve of component C-O /C-Cl (286.7 eV) and component C=O/O-C=O (288.9 eV).

Table 4.6 Quantitative of XPS surface analyses of PVC (V) samples before flame treatment

Sample	Surface compositions/atomic %							Release agent	No release agent
	Pb	Cl	C	Ca	N	O	Zn		
PVC V 1	0.2	5.4	82	0.7		12	0.2		✓
PVC V 1	0.07	14	75	0.8		9.5	0.7		✓
PVC V 2	0.2	5.5	81	0.6		12	0.2		✓
PVC V 2	0.1	15.5	72	0.5		12	0.7		✓
PVC V 2 Plain	0.2	5.6	76.6	0.6	1.2	14	0.2	1.5	

Table 4.6 is the result of quantitative XPS surface analyses of PVC V samples before flame treatment. As was mentioned above it is clear for the PVC V1 and V2 samples that after removing the release agent (by hexane) the surface concentration of C and O/at% decreased and the surface concentration of Cl/at% increased. As the result shows on the one hand, by removing the release agent, from the surface of the PVC V1 and V2 that was buried under the release agent, it would be greater surface concentration of Cl/at% on survey spectrum of XPS analysis. On the other hand when release agent was deposited on the surface of the PVC the carbon and oxygen were contributed from the release agent and PVC surface, so by removing release agent less carbon and oxygen would be on survey spectra of the PVC because this analysis is result of the surface analysis of PVC only.

Table 4.7 Results of C1s peak fitting of PVC V samples before FT

Sample No	Hexane	Functional groups/%		
		C-C/C-H	C-O/C-Cl	C=O/O-C=O
PVC V 1		285 (86%)	286.8 (10.6%)	289.1 (3.4%)
PVC V1	✓	285 (78.7%)	286.4 (18%)	288.4 (3.3%)
PVC V2		285 (84.6%)	286.7 (11.32%)	289.1 (4.1%)
PVC V2	✓	285 (70.2%)	286.3 (25.1%)	288.6 (4.7%)
PVC V2 plain		285 (84.9%)	286.7 (10.8%)	288.9 (4.4%)

Table 4.7 shows the results from the peak fitting of the high resolution C1s spectra for all of the PVC samples, before flame treatment. Once again while release agent was removed from the surface of the PVC V1 and V2 samples it was an increase in C-O/C-Cl component and also decrease in C-C/C-H component.

Figure 4.24 shows the survey spectra of PVC R 1 with and without release agent before flame treatment.

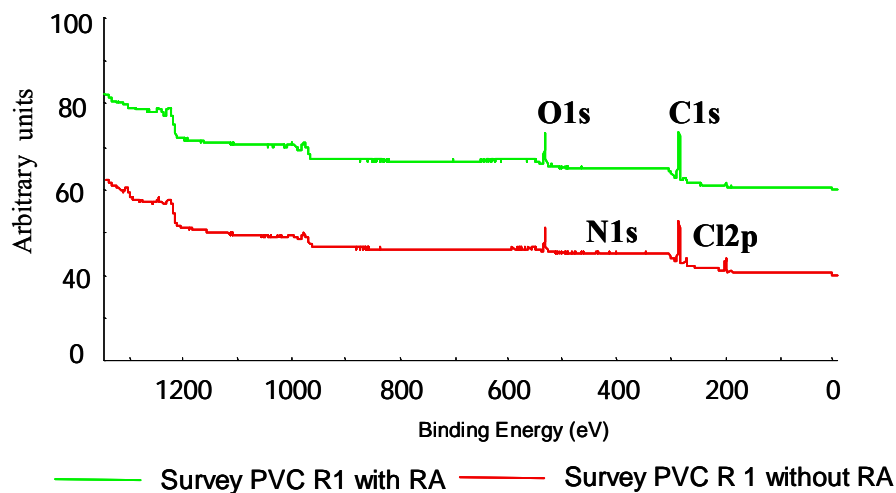


Figure 4-24 the Survey spectrum of PVC R1 with and without RA before FT

The survey spectrum of PVC R 1 with release agent has four characteristic peaks: Cl2p (200eV), C1s (285eV), N1s (400eV), and O1s (532eV). While release agent was removed from the surface of the PVC R1, the surface concentration of Cl increase on surface of PVC R1, also it has resulted Cl2s peak at 270ev observed on survey spectrum. By removing the release agent a very low intensity Pb4f peak at (138eV) is observed on survey spectra of PVC R 1 washed with hexane.

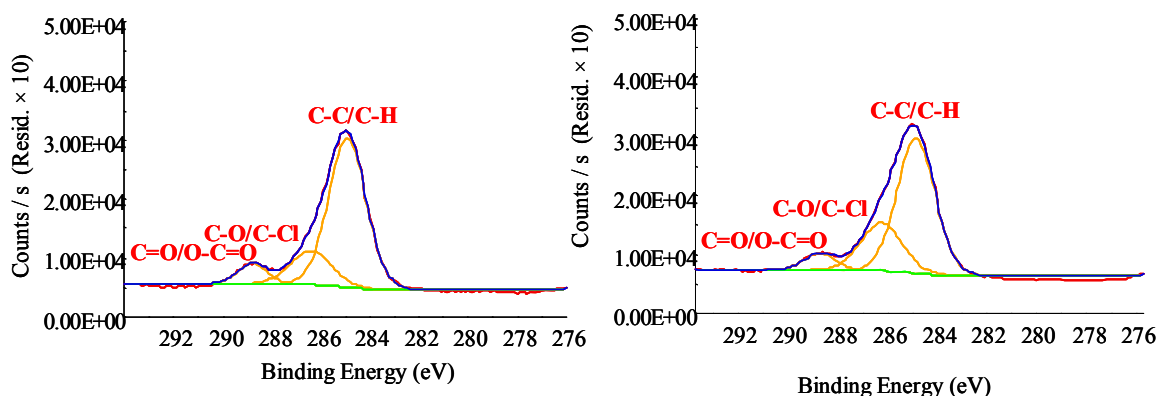


Figure 4-25 -shows the High resolution spectrum of C1s of PVC R 1 with and without RA before FT

Figure 4.25 contains high resolution spectra of C1s for PVC R1 with and without release agent before flame treatment. Table 4.10 exhibits while the release agent removed from the surface of the PVC R 1 the surface concentration of the Cl increased and the surface concentration of C and O decreased. This observed increase on component C-O /C-Cl from 13.6 to 16.4/at% and decreasing on component CH/C-C from 76 to 67/at%.

Figure 4.25 shows the survey spectra of PVC R2 with and without release agent before flame treatment. The survey spectrum of PVC R 2 with release agent contain six characteristic peaks, Pb4f (138eV), Cl2p (200eV), C1s (285eV), Ca 2p (347eV), N1s (400eV), O1s (532eV) and Zn2p3/2 (1022eV). As release agent removed from surface of PVC R2 the Cl2s peak appeared at 270eV.

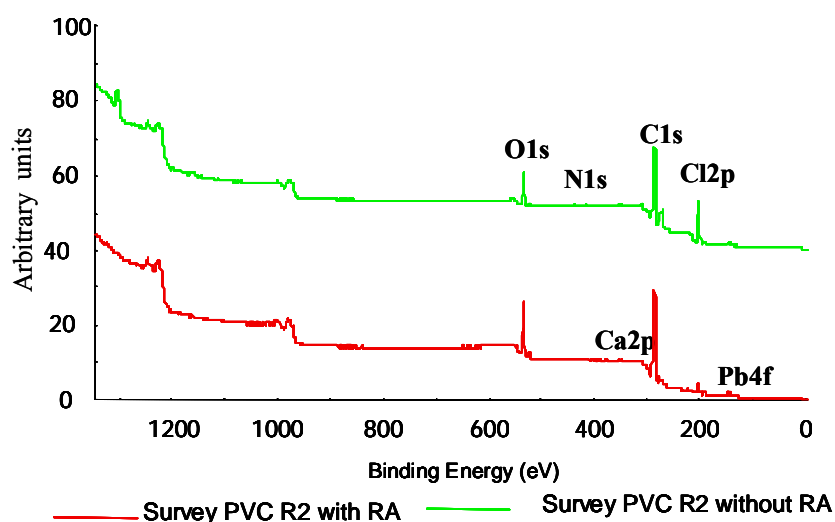


Figure 4-26 - shows the survey spectrum of PVC R2 with and without RA before FT

Figure 4.27 shows the high resolution spectra of C1s for PVC R2 with and without release agent before flame treatment. While release agent cleaned from the surface of PVC R2 by hexane, it resulted in an increase in C-O/C-Cl component from 13 to 26/at%. The removing release agent also resulted in a decrease on C-C/C-H and C=O/O-C=O components from 77.4 to 68.4 at% and from 9.6 to 5.4 at% respectively.

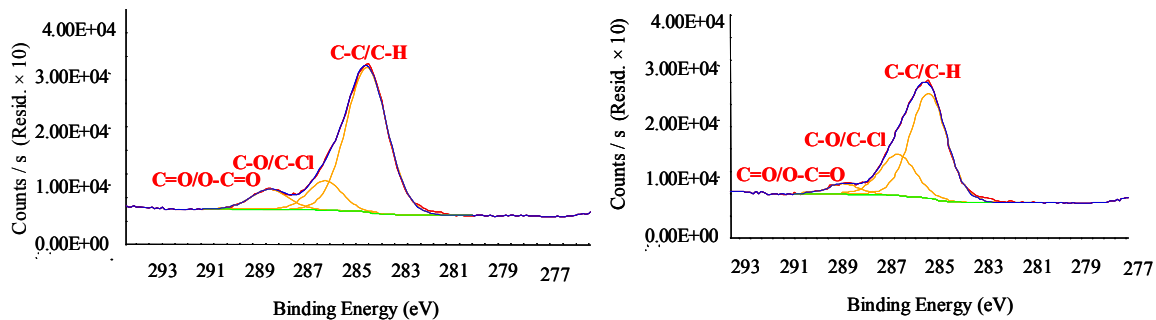


Figure 4-27 shows the High resolution spectrum of C1s of PVC R2 with and without RA before FT

Figure 4.28 shows the survey spectrum of PVC R2 plain and the high resolution spectrum of C1s for PVC R2 plain before flame treatment. The survey spectrum of PVC R2 plain contains eight characteristic peaks, Pb4f (138eV), Cl2p (200eV), Cl2s (270eV), C1s (285eV), Ca2p (347eV), N1s (400eV), O1s (532eV), Zn2p<sub>3/2</sub> (1022eV) and Na1s (1072eV). This sample did not have any protection film on the surface.

The high resolution spectrum of C1s for PVC R2 plain in figure 4.19 has been peak fitted with three curves.

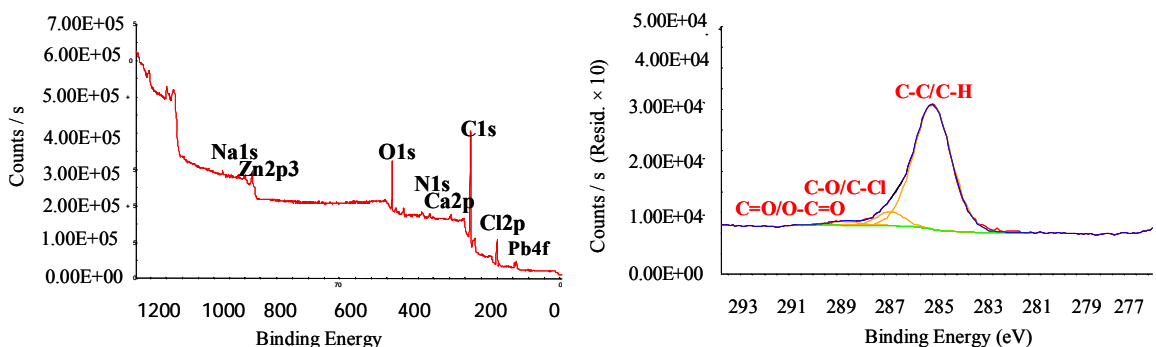


Figure 4-28 shows the Survey spectra and high resolution spectra of PVC R2 plain before TF

Table 4.8 is the result of quantitative XPS surface analysis of PVC R samples before flame treatment. Although the PVC V and R samples had different formulation, the effect of hexane on the surface of the samples was the same. The release agent removed from the surface of the PVC R1 and R2 resulted in an increase in Cl surface concentration and also a decrease in the surface concentration of C and O.

Table 4.8 Quantitative of XPS surface analyses of PVC (R) samples before flame treatment

Sample	Surface compositions/atomic %								Release agent	Hexane
	Pb	Cl	C	Ca	N	O	Zn	Na		
PVC R 1		1.8	76		1	21			✓	
PVC R 1	0.05	8	73.5	0.3	1	17				✓
PVC R 2	0.1	3	76	0.2	0.6	20			✓	
PVC R 2	0.1	13	72	0.4		14				✓
PVC R 2 plain	0.2	5.6	77	0.6	1.2	14	0.2	0.7		

Table 4.9 shows the result of the peak fitting of the high resolution C1s spectrum of PVC R samples before flame treatment. It is clear that C-O/C-Cl component concentration increased after removing the release agent from PVC R1 and R2. The removal of release agent also resulted in a decrease in percentage of components C-C/C-H and C=O/O-C=O, concentration after release agent was removed from the surface of the PVC R samples.

Table 4.9 Results of C1s peak fitting of PVC R samples before FT

Sample No	Hexane	Functional groups/%		
		C-C/C-H	C-O/C-Cl	C=O/O-C=O
PVC R1		285 (76%)	286.6 (7.6%)	288.8 (16.4%)
PVC R1	✓	285 (67%)	286.5 (26%)	288.7 (6.8%)
PVC R2		285 (77.4%)	286.7 (13%)	288.8 (9.6%)
PVC R2	✓	285 (68.4%)	286.3 (26.2%)	288.8 (5.4%)
PVC R2 plain		285 (89.5%)	286.8 (7.5%)	288.9 (4%)

#### 4.9 XPS analysis after surface modification

The same method and manner of analysis employed to analyse the samples before flame treatment was used to analyse the modified samples. XPS surface analysis of the modified samples was carried out as a function of time for more than three months. Additionally to investigate the effect of solvent on the surface of the modified samples, three months after surface modification the surface of all modified samples washed by hexane solvent then surface chemistry of the samples were characterised by XPS analysis.

Figure 4.20 shows the survey spectrum of the PVC V1 one day after flame treatment, twelve weeks after flame treatment, also and twelve weeks after flame treatment while surface of sample was washed by hexane. The survey spectrum of PVC V 1 one day after flame treatment has seven characteristic peaks: Pb4f (138 eV), Cl2p (200eV), Cl2s

(270eV), C1s (285 eV), Ca2p (347eV), O1s (532eV), Zn2p<sub>3/2</sub> (022eV) and Na1s (1072eV).

In step one of flame treatment oxygen surface concentration was increasing week after surface of the samples was modified by flame treatment technique. Here by employing new parameters for flame treatment machine (see section 4.7.4) the surface concentration of oxygen increased immediately after flame treatment.

The surface concentration of C, O and Cl of PVC V1 window profile before surface modifications by flame treatment technique were 82, 12 and 5.4/at% respectively. These surface concentrations changed after flame treatment to 70, 22.4 and 5/at% respectively, these results remained constant afterwards. The surface of the modified PVC 1 sample washed with hexane three months after surface modification, this resulted in an increase in surface concentration of Cl from 5 to 13.6 at% and a decrease in surface concentration of O from 22.4 at% to 15.5 at%. Although the hexane solvent had an effect on the surface concentration of the PVC V1 elements, the hexane solvent could not remove the effect of the surface modification by flame treatment technique.

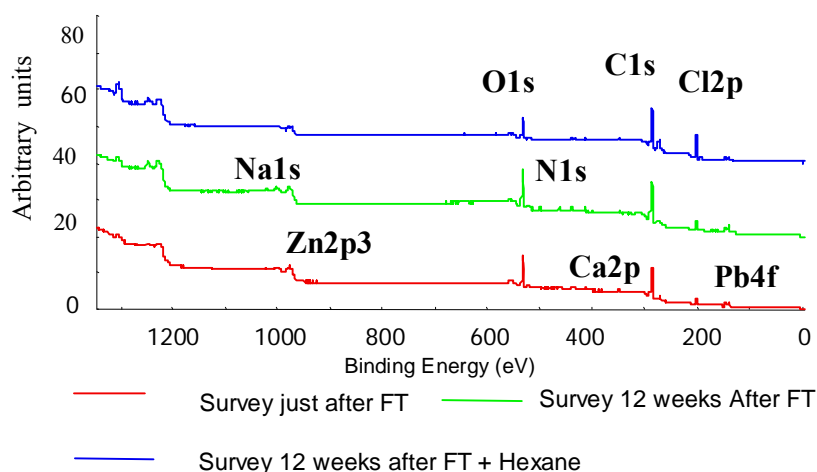


Figure 4-29 Survey spectrum of PVC V1 just after FT, 12 weeks after FT and 12 weeks after with hexane

Figure 4.29 shows high resolution spectra of the C1s of PVC V1 one day after flame treatment and twelve weeks after flame treatment while the surface of the treated sample was washed by hexane solvent. The high resolution C1s spectra were peak fitted with three curves in the same manner of peak fitting before flame treatment (see section 4.8). The components C-C/C-H (285eV), C-O/C-Cl (286.7eV) and C=O/O-C=O (288.8eV).

By washing the surface of PVC V1 with hexane resulted in an increase in C-O/C-Cl component from 16 to 35/at%, and a decrease in C-C/C-H and C=O/O-C=O components from 75.5 to 59.5 at% and 8.5 to 6 at% respectively.

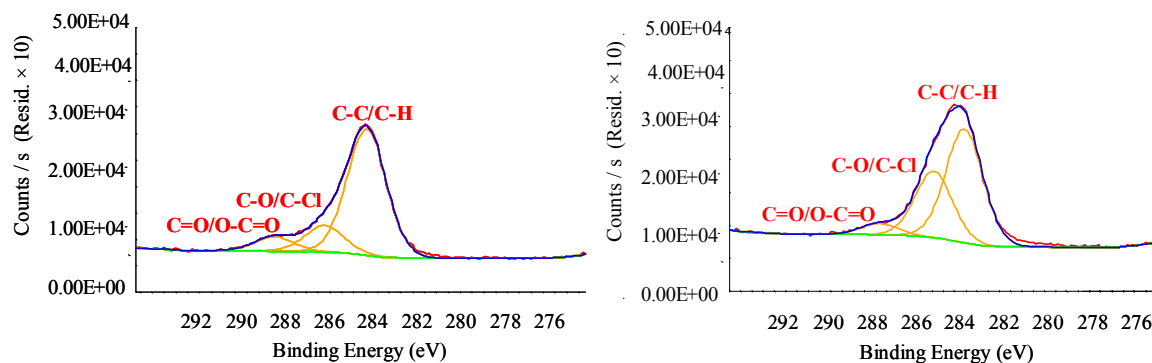


Figure 4-30 High resolution spectrum of C1s of PVC V1 just after FT and 12 weeks after FT with Hexane

Figure 4.30 shows XPS survey spectra of PVC V2 just after flame treatment, twelve weeks after flame treatment and twelve weeks after flame treatment when surface of the PVC was washed by hexane solvent. The survey spectrum of PVC V2 one day after flame treatment has nine characteristic peaks: Pb4f (138eV), Cl2p (200eV), Cl2s (270eV), C1s (285 eV), Ca2p (347eV), N1s (400eV), O1s (532eV), Zn2p<sub>3/2</sub> (1022eV) and Na1s (1072eV) (See section 4.8).

Surface concentration of C, O and Cl for PVC V2 before surface modifications by flame treatment technique were 81, 12 and 5.5/at% respectively. These results have changed immediately after flame treatment to 68, 25 and 5.4/at% respectively, and remained constant afterward. The surface of the treated PVC V2 washed with hexane three months after surface modification showed the surface concentration of the C,O and Cl changed to 71,13 at% and 14.8/at% respectively. Although the hexane solvent had an effect on the surface concentration of the treated PVC V2 elements, the surface concentration of the element was not the same as the result before flame treatment. Here again by washing the surface of PVC V2 with hexane solvent twelve weeks after flame treatment the peaks of Zn2p<sub>3/2</sub> (1022eV) and Na1s (1072eV) were not observe on the survey spectra of treated PVC V2 washed with hexane twelve weeks after flame treatment.

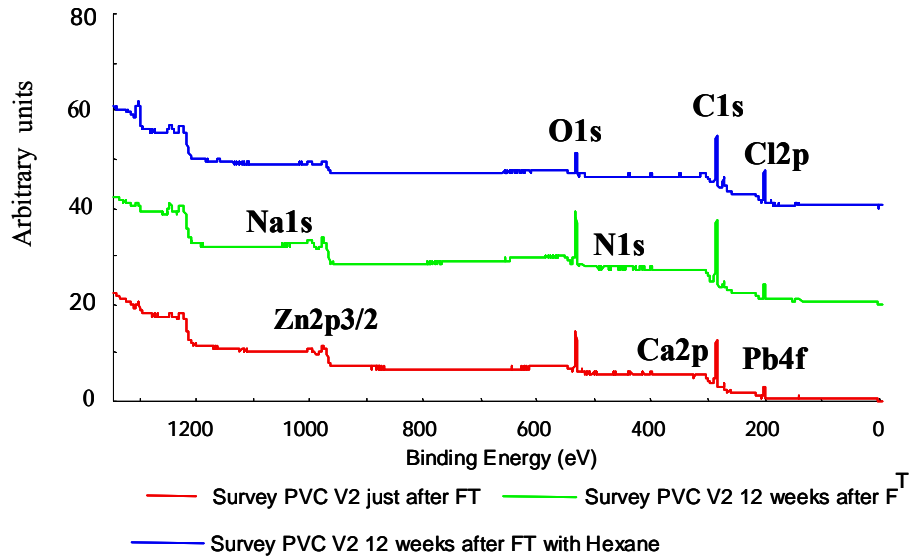


Figure 4-31 Survey spectrum of PVC V2 just after FT, 12 weeks after FT and 12 weeks after flame FT with hexane

Figure 4.31 shows the result of peak fitting of high resolution spectra of C1s of treated PVC V2 one day after flame treatment and twelve weeks after flame treatment while the surface of the sample washed with hexane. The high resolution C1s spectrum peak fitted with three curves in the same manner of peak fitting (see section 4.8). While the surface of the treated PVC V2 sample washed with hexane, it's lead to an increase in C-O/C-Cl component from 21.6 to 33.4/at%. Also decrease on components C-C/C-H and C=O/O-C=O from 69 to 61 and from 9.2 to 5 at% respectively.

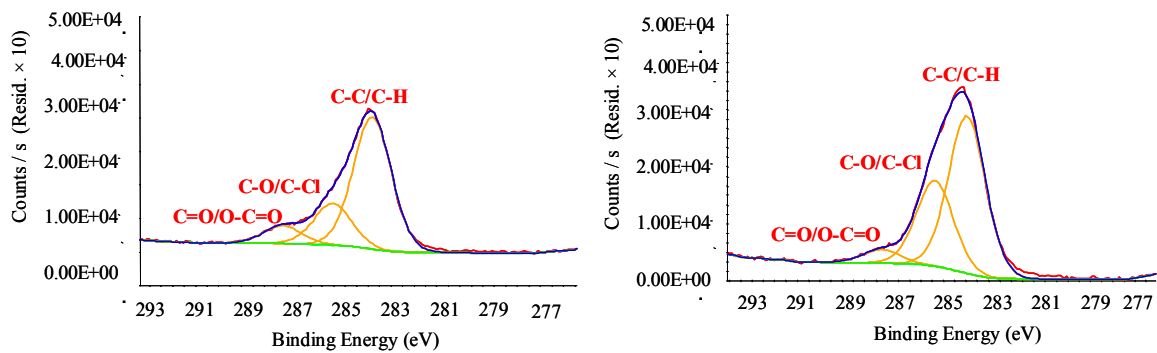


Figure 4-32 High resolution spectrum of C1s of PVC V2 just after FT and 12 weeks after FT with hexane

Figure 4.33 shows XPS survey spectra of treated PVC V2 plain one day after flame treatment, twelve weeks after flame treatment and while the surface of the treated PVC V 2 plain was washed with hexane twelve weeks after treatment. The survey spectrum of treated PVC V2 plain has nine characteristic peaks: Pb4f (138eV), Cl2p (200eV), Cl2s (270eV), C1s (285 eV), Ca2p (347eV), N1s (400eV), O1s (532eV), Zn2p<sub>3/2</sub>(1022eV) and Na1s (1072eV) (see section 4.8)

The surface concentration of C, O and Cl, for untreated PVC V2 plain before surface treatments were 76.6, 14 and 5.6/at% respectively. These surface concentrations have changed after flame treatment to 72, 21 and 5/at% respectively, and were remained constant afterward. While the surface of the treated PVC V 2 plain was washed with hexane twelve weeks after flame treatment, the surface concentration of the C, O and Cl changed to 69, 16 and 13.6/at% respectively. As hexane solvent was applied on to the surface of the PVC V2 plain the peaks of Zn2p<sub>3/2</sub> at 1022ev and Na1s at 1072 ev disappeared from the XPS survey spectra of PVC V2 plain three months after flame treatment with hexane.

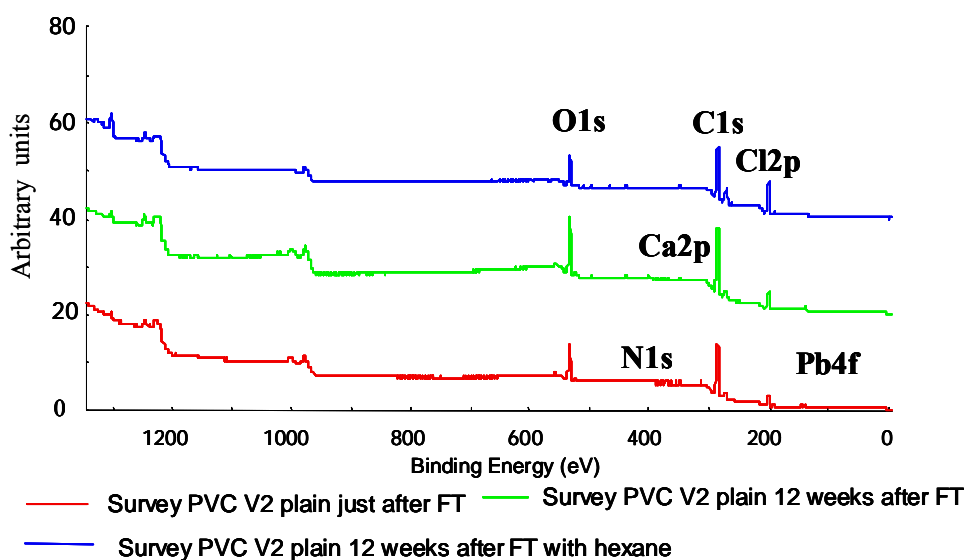


Figure 4-33 Survey spectrum of PVC V2 Plain just after FT, 12 weeks after FT and 12 weeks after FT with hexane

Figure 4.33 shows high resolution survey spectra of C1s of PVC V2 plain one day after flame treatment and twelve weeks after flame treatment while the surface of the treated

sample washed with hexane. The high resolution C1s spectra were peak fitted with three curves in the same manner of peak fitting (see Section see section 4.8) The High resolution C1s spectra fitted with cures of components of C-C/C-H (285eV), C-O/C-Cl (286.7 eV) and C=O/O-C=O (288.6 eV). While the surface of treated PVC V2 plain washed with hexane resulted an increase in C-O/C-Cl component from 16 to 34/at%, and decrease on C-C/C-H and C=O/O-C=O components from 74 to 61 and 9.7 to 5 at% respectively.

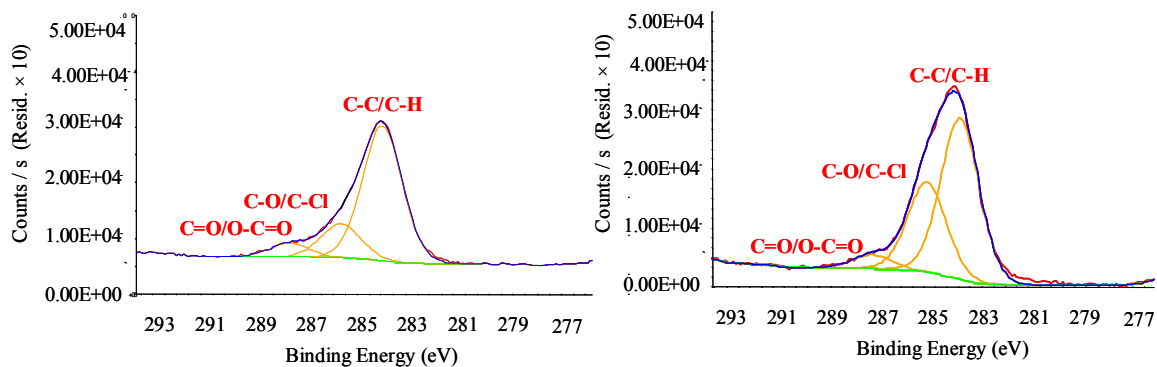


Figure 4-34 High resolution spectrum of C1s of PVC V2 plain just after FT and 12 weeks after FT with hexane

Table 4.34 are the results of the XPS quantification of PVC V samples one day flame treatment. By comparing Table 4.7, which is quantification table of PVC V samples before flame treatment with Table 4.10, we can see immediate changes in surface concentrations of C, O and Cl. These were immediately increased on surface concentration of O for treated PVC V1, V2 and V2plain from 13 to 22.4, 13.5to 25 and 14 to 21 at% respectively. The effect of the flame treatment also decreased surface concentration of carbon and chlorine immediately after flame treatment. The surface concentration of carbon in PVC V1, V2 and V2 plain reduced from 80 to 70, 79 to 68 and 77 to 72 respectively. The Cl surface concentration on PVC V1, V2, and V2 plain reduced immediately after flame treatment from 6 to 5, 6 to 5 and 7 to 5 at % respectively.

Table 4.10 XPS quantification table of PVC V samples after flame treatment

Sample	Surface compositions/atomic %								Release agent
	Pb	Cl	C	Ca	N	O	Zn	Na	
PVC V 1	0.4	5	70	0.6	1.2	22.4	0.1	0.3	✓
PVC V 2	0.05	5.4	68	0.4	1.5	25			✓
PVC V 2 Plain	0.08	5	72	0.3	1.7	21			

Figure 4.35 exhibits XPS survey spectra of treated PVC R1 one day after flame treatment, twelve weeks after flame treatment, also twelve weeks after flame treatment while the surface of the treated sample washed with hexane. The survey spectrum of PVC R1 one day after flame treatment has six characteristic peaks: Cl2p (200eV), C1s (285 eV), N1s (400eV) and O1s (532eV).

The surface concentrations of C, O and Cl of PVC R 1 before surface modification were 86, 21 and 1.8/at% respectively Table 4.9. The effect of flame treatment have changed these result to 64, 31 and 2/at% respectively Table 4.11. These surface concentrations were remained constant afterward. While the surface of the treated PVC R1 washed with hexane the surface concentration of C, O and Cl change again to 70,18.8 and 9.7/at% respectively Table 4.12. By comparing the surface concentrations of C, O and Cl of untreated PVC R1 Table 4.9 with surface concentrations of the same element for treated PVC V1 while the surface of the sample was washed with hexane, although applying the hexane on the surface of the treated sample observed that, the surface concentration of these elements has changed, these surface concentration did not go back to the concentration before treatment.

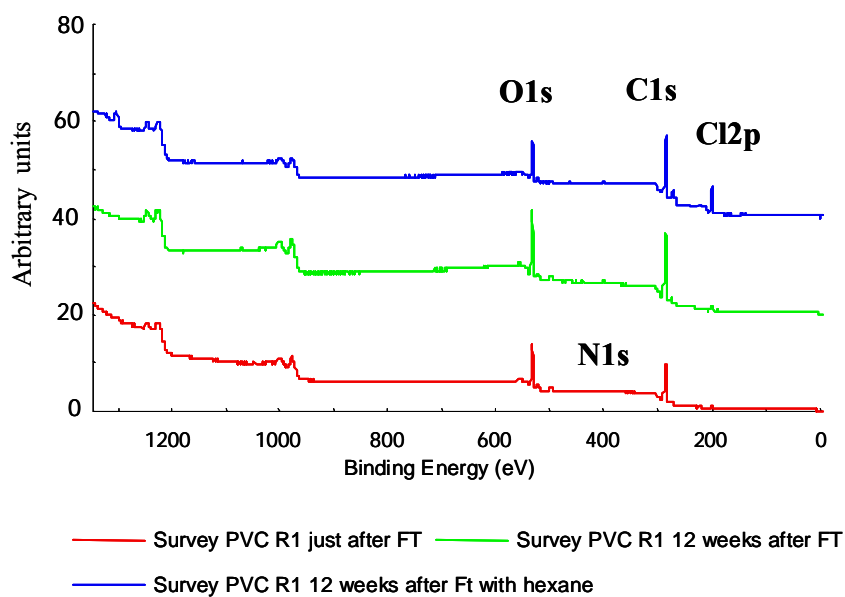


Figure 4-35 Survey spectrum of PVC R1 just after FT, 12 weeks after FT and 12 weeks after FT with hexane

Figure 4.36 shows high resolution spectra of C1s peak fitted of treated PVC R1 one day after flame treatment and twelve weeks after flame while the surface of the treatment

sample washed with hexane. The high resolution C1s spectrum of PVC R1 peak fitted with three curves in the same manner of peak fitting chapter 3. While the surface of the treated PVC R1 sample washed with hexane, that cause an increase in C-O/C-Cl component from 18 to 24/at%. Also decrease on components C-C/C-H and C=O/O-C=O from 73 to 67 and 8.4 to 8.6 at% respectively.

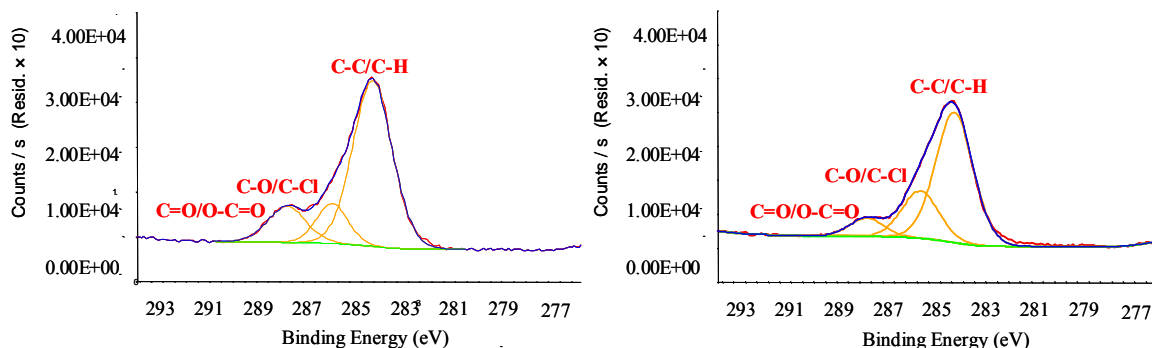


Figure 4-36 High resolution survey spectrum of C1s of PVC R1 just after FT and 12 weeks after FT with hexane

Figure 4.37 shows XPS survey spectra of treated PVC R2 one day after flame treatment, twelve weeks after flame treatment and twelve weeks after flame treatment the surface of the treated PVC R2 was washed with hexane. A survey spectrum of treated PVC R2 one day after flame treatment has got four characteristic peaks: Pb4f (138eV), Cl2p (200eV), C1s (285 eV) and O1s (532eV).

The surface concentration of C, O and Cl for PVC R2 before surface modification Table 4.9 were 78 ,16.9 and 4/at% respectively. These results have changed after flame treatment Table 4.11 to 65.5, 29 and 2.6 /at% respectively, and remained constant afterwards. While the surface of the treated PVC R2 after twelve weeks washed by hexane, it resulted change in the surface concentration of the C, O and Cl to 70, 14 and 14/at% respectively. Although when the surface of the treated PVC R2 washed by hexane did changed the surface concentration of the C, O and Cl, the surface concentration of these element were not the same as for untreated PVC R2, however the effect of the flame treatment was strong which was not removed fully by solvent.

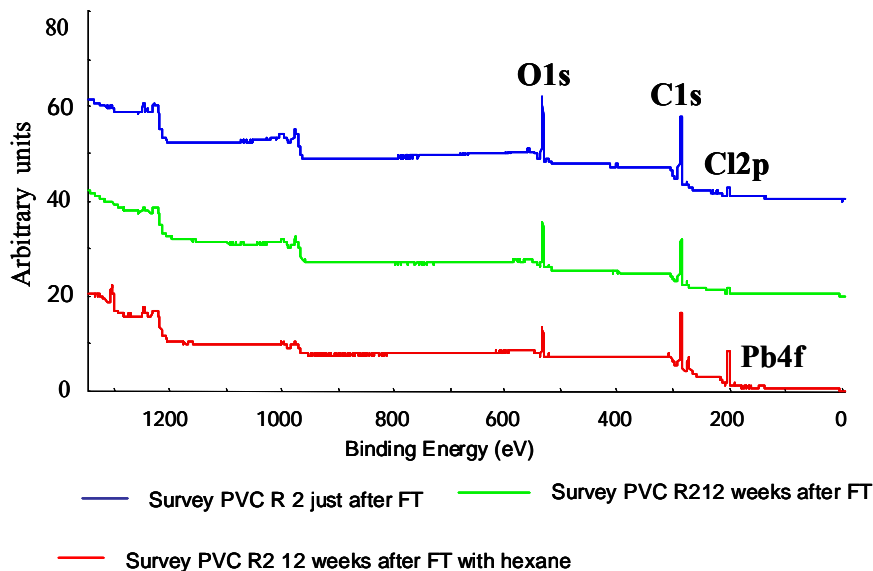


Figure 4-37 Survey spectrum of PVC R2 just after FT, 12 weeks after FT and 12 weeks after FT with hexane

Figure 4.38 shows high resolution spectra of C1s peak fitted of treated PVC R2 one day after flame treatment and twelve weeks after flame while the surface of the treatment sample washed with hexane. The high resolution C1s spectrum of PVC R2 peak fitted with three curves in the same manner of peak fitting (see section 8.4). While the surface of the treated PVC R2 sample washed with hexane, it was resulted an increase in C-O/C-Cl component from 22 to 34/at%. Also decrease on components C-C/C-H and C=O/O-C=O from 59 to 60 and 14.9 to 6 at% respectively.

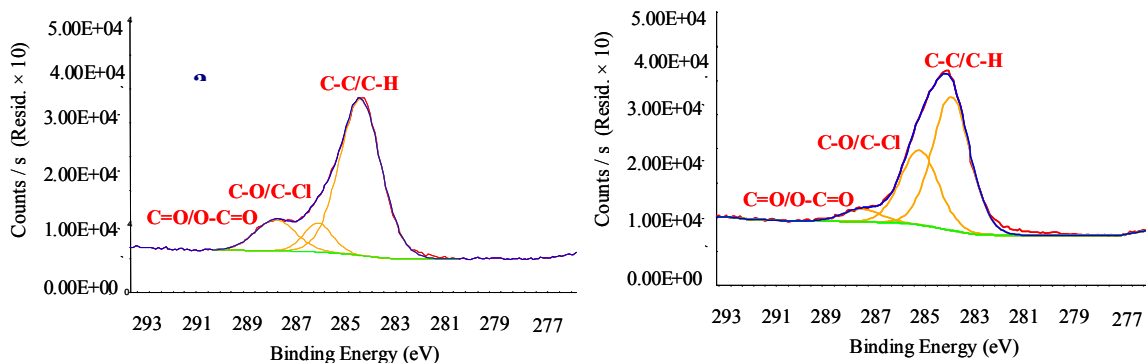


Figure 4-38 High resolution spectrum of C1s of PVC R2 just after FT and 12 weeks after FT with hexane

Figure 4.39 shows XPS survey spectra of PVC R2 plain just after flame treatment, twelve weeks after flame treatment, also twelve weeks after flame treatment while the surface of

the treated PVC R2 plain washed with hexane. The survey spectrum of PVC R2 plain after flame treatment has five characteristic peaks: Pb4f (138eV), Cl2p (200eV), C1s (285 eV), Ca2p (347eV) and O1s (532eV).

The surface concentration/at% of C, O and Cl before surface modification Table 4.9 were 72, 12 and 12 /at% respectively. While the surface of the PVC R2 plain treated by flame, these results were changed to 68.5, 29 and 4.4 /at% respectively and it remained afterward. Once the surface of the treated PVC R2 plain after twelve weeks was washed with hexane, the surface concentration of the C, O and Cl changed to 68.5, 17.5 and 11.5 /at% respectively. When the surface concentration of C, O and Cl for untreated PVC R2 plain compare with surface concentration of treated PVC R2 plain twelve weeks after treatment while the surface of treated sample was washed by hexane, it observed that the surface concentration of C, O and Cl for untreated PVC R2 were not similar to surface concentration of same elements for treated PVC R2 plain even after washing the surface of the treated sample with hexane. Thus the effect of the flame treatment was robust and solvent could not remove that.

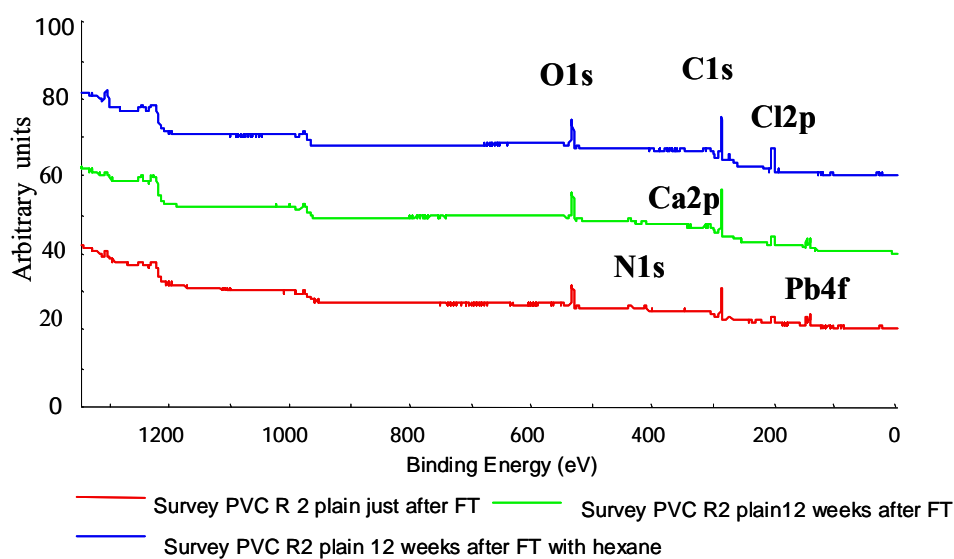


Figure 4-39 Survey spectrum of PVC R2 plain just after FT, 12 weeks after FT and 12 weeks after FT with Hexane

Figure 4.40 shows result of high resolution spectra C1s peak fitting for treated PVC R2 plain one day after treatment and twelve weeks after flame treatment while the surface of treated PVC R2 plain was washed with hexane. The high resolution C1s spectrum of PVC R2 peak fitted with three curves in the same manner of other C1s peak fitting for PVC R

and V samples. While the surface of the treated PVC R2 sample washed with hexane, it resulted in an increase in C-O/C-Cl component from 14.5 to 30/at%. Also decrease on components C-C/C-H and C=O/O-C=O from 78 to 63 and 7 to 6 at% respectively.

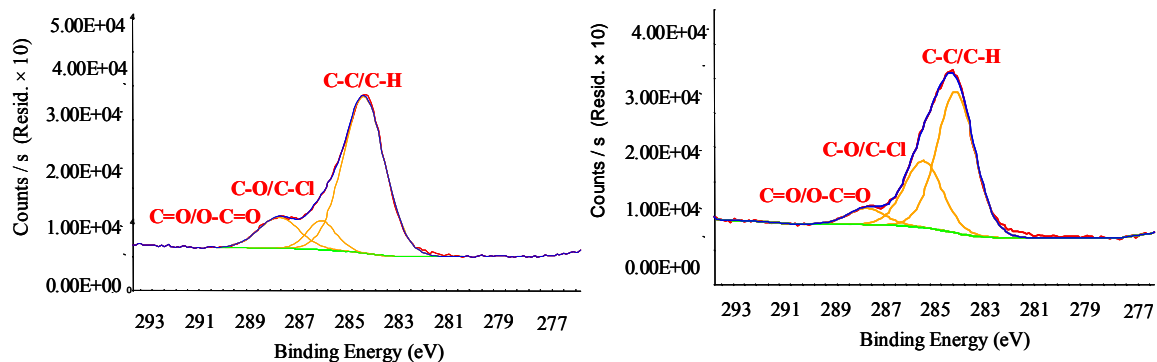


Figure 4-40 High resolution spectrum of C1s of PVC R2 plain just after FT and 12 weeks after FT with hexane

Table 4.11 shows results of XPS quantification of PVC R samples after flame treatment. By comparing the results of Table 4.9, XPS quantification of untreated PVC R samples, with Table 4.11 XPS quantification of treated PVC R samples. It is clear that it was an increase in surface concentration of the oxygen and decrease in surface concentration of carbon and little decrease on surface concentration of Cl Immediate after flame treatment. Surface concentration of oxygen for treated PVC R1, R2 and R2 showed an increase in comparison to untreated PVC R1, R2 and R2 plain from 20 to 30, 17 to 29 and 14 to 22/at% respectively. It was decrease in surface concentration of the carbon for treated PVC R1, R2 and R2plain in comparison with untreated PVC R1, R2 and R2 from 76 to 64, 76 to 65.5 and 77 to 68.5 respectively.

Table 4.11 XPS Quantification table of PVC R samples after FT

Sample	Surface compositions/atomic %								Release agent
	Pb	Cl	C	Ca	N	O	Zn	Na	
PVC R 1		2	64		2	31.4	0.1	0.6	✓
PVC R 2	0.06	2.6	65.5			29	0.1	0.3	✓
PVC R 2 plain	0.8	5.4	68.5	0.6	2	22	0.2	0.3	

Table 4.12 shows the result of XPS quantification of treated PVC V and R samples 12 weeks after flame treatment before and after surface of treated samples was washed with hexane. The surface concentration of the elements for treated PVC V and R after treatment was remained steady. While the surface of treated PVC V and R samples were

washed by hexane, that resulted in an increase in the surface concentration of Cl and a decrease in surface concentration of oxygen. Although the surface of all treated samples were washed by hexane, the effect of the flame treatment on the surface of the PVC V and R was robust and the hexane could not remove the effect of the flame treatment from the surface of the samples.

Table 4.12 -XPS quantification table of PVC V and R samples 12 weeks after flame treatment and 12 weeks after flame treatment with hexane

Sample No.	Surface compositions/atomic %								
	Pb	Cl	C	Ca	N	O	Zn	Na	Si
PVC V 1	0.5	5.4	68	0.6	1.5	24	0.1	0.05	
PVC V 1	0.3	13.6	69.6	0.8	0.3	15.5	-	-	
PVC V 2	0.1	5.5	70	0.4	1.6	22	0.01	0.07	
PVC V 2	0.08	14.8	71	0.5	0.6	13	-	-	
PVC V 2 plain	0.2	5.4	69.4	0.4	1.6	23	0.1	0.04	
PVC V 2 plain	0.1	13.6	69	1	0.2	16	-	-	
PVC R 1	0.04	1.7	69	-	1.7	27.4	0.01	0.4	
PVC R 1	0.05	9.7	70	0.1	1	18.8	-	0.4	
PVC R 2	0.1	2.4	69	0.2	2	26	0.05	0.2	
PVC R 2	0.2	14	70.5	0.4	0.5	14	-	0.1	
PVC R 2 plain	0.7	5	73.6	0.7	1.4	17	1.4	0.2	0.1
PVC R 2 plain	0.2	11.5	68.5	0.5	1.7	17.5	1.7	-	0.5

#### 4.10 Contact angle measurements

Contact angles of all the untreated and treated PVC V and R samples have been measured in the same manner of (see section 2015). Contact angle measurements of the untreated PVC samples were carried out in order to have this measurements as reference point, so by comparing the result of contact angle measurements of untreated sample with contact angle of treated sample it would be easy to find the effect of the flame treatment on surface of the PVC samples. In order to study the surface wettability of PVC samples as a function of time, contact angle measurements of PVC samples were acquired for up to three months after flame treatment.

The surface of all the PVC V samples before flame treatment was hydrophobic surface, hence the contact angle between the surface of the PVC window profile V samples and the Liquid (ionized water) were above 90°. While the surface of the PVC samples modified by flame treatment technique, the surface free energy of the PVC window profile increased. However, the surface of the PVC profile became more polar by introducing oxygen functional group on surface of the PVC samples.

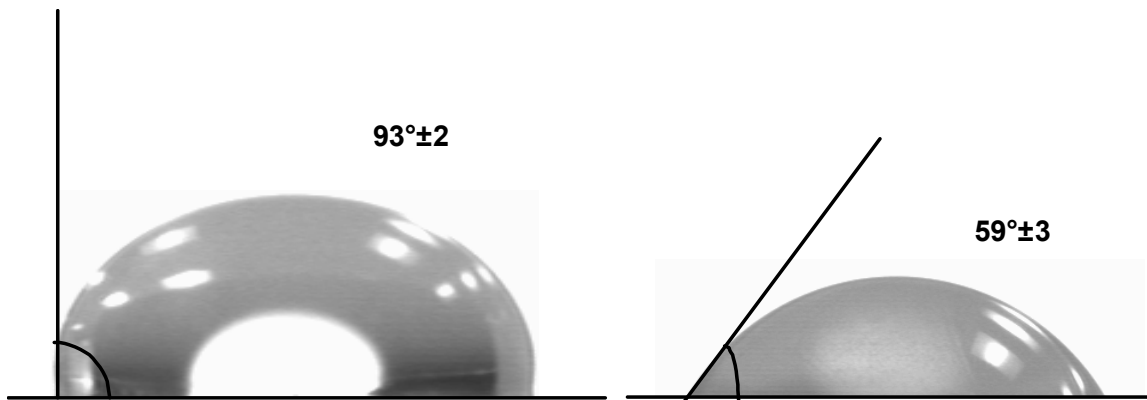


Figure 4-41 Image of contact angle of PVC R Before and after flame treatment

This polarity allow the liquid (water) to wet the surface of the PVC samples by reducing the contact angle between the surface of the samples and liquid (water). The greater surface free energy will have lower contact angle and better wettability and adhesion property. It was decrease in contact angle of all treated PVC samples by as much as  $30^{\circ}$  in comparison with contact angle of untreated PVC samples. The surface of the PVC profile samples became more hydrophilic, better wettability easier to apply adhesives and coating on surface of samples.

Table 4.13 shows contact angle results of untreated and treated PVC V, the rows 1 to 5 are the results of contact angle of untreated PVC V samples. Although the surface of the all samples that had release agent on the surface were modified while the release agent was on the surface of the samples, in order to study effect of the release agent on contact angle of the PVC V samples, the contact angle of PVC V1 and V2 once when the release agent was on the surface on the samples and second time while the surface of the samples was washed with hexane. The row 1 to 4 are the result of contact angle for untreated PVC V1 and V2 with and without release agent respectively. The PVC V2 plain did not have any protection film and release agent on the surface. The result of contact angle between PVC V1 and water before flame treatment with and without release agent were  $91^{\circ} \pm 3$ ,  $90^{\circ} \pm 1$  (row 1 and 2) respectively, the effect of the flame treatment resulted decrease in contact angle of treated PVC V1 from  $91^{\circ} \pm 3$  to  $59^{\circ} \pm 3$ . While the surface of the treated PVC V1 twelve weeks after flame treatment washed with hexane, it resulted in an increase in contact angle for the treated PVC V1 from  $59^{\circ} \pm 3$  to  $74^{\circ} \pm 2$ . The contact angle between the untreated PVC V2 and water was  $90^{\circ} \pm 4$ , this was a decrease in contact angle of the treated PVC V2 in comparison to untreated PVC V2 sample from

90°± 4 to 59° ± 3. After washing the surface of the treated PVC V2 with hexane, it resulted in an increase of contact angle in the treated PVC V2 from 59° ± 3 to 74° ± 4.

The contact angle between the untreated PVC V2 plain and water was 98° ± 2, after flame treatment the contact angle of treated PVC V2 plain decreased to 63° ±3. Once the surface of treated PVC V2 plain washed with hexane, it resulted in an increase in contact angle of the treated PVC V2 plain from 63° ±3 to 78° ±3. Although after the surface of the treated PVC V samples was washed with hexane solvent it increased the contact angle of the PVC V as much as 10°, the contact angle of the treated sample after washing by hexane is about 20° lower than untreated sample.

Table 4.13 Result of sessile contact angle measurements of PVC Veka before and after flame treatments

Samples No	Elapse time /day	Angle/degree	Standard Deviation	Release agent	Plain	Hexane
PVC V 1		91	±3	✓		
PVC V 1		90	±1			✓
PVC V 2		90	±4	✓		
PVC V 2		93	±4			✓
PVC V 2		98	±2		✓	
PVC V 1	4	59	±3	✓		
PVC V 2	4	59	±3	✓		
PVC V 2	4	63	±3		✓	
PVC V 1	90	74	±3	✓		✓
PVC V 2	90	74	±3	✓		✓
PVC V 2	90	78	±3		✓	✓

Table 4.14 shows the result of the contact angle of untreated and treated PVC R samples. The effect of the flame treatment on PVC R samples were similar to PVC V samples, the decrease in contact angle of all PVC R samples after flame treatment was as much as 28°. These results remained constant, same as PVC V samples afterwards.

The row 1 and 2 also 3 and 4 of table 4.14 are the result of the contact angle for untreated PVC R1 and R2 with and without release agent 86° ±2 ,87° ±2 and 85° ±2 ,86° ±1 respectively. The row 5 of the table 4.14 shows the result of the contact angle for untreated PVC R2 plain 93° ±2. The contact angle of treated PVC R1, R2 and R2 plain

decreased in comparison to untreated PVC R1, R2 and R2 plain to  $59^{\circ} \pm 4$ ,  $57^{\circ} \pm 4$  and  $70^{\circ} \pm 3$  respectively. The surface of the treated PVC R washed with hexane twelve weeks after flame treatment resulted in an increase in contact angle of PVC R1,R2 and R2 plain from  $65$  to  $68^{\circ}$ ,  $64$  to  $71^{\circ}$  and  $65$  to  $84^{\circ}$  respectively. Despite the fact that applying the hexane on surface of the PVC R samples could increase the contact angle of the samples, the contact angle of treated sample after washing with hexane still show as much as  $10^{\circ}$  lower contact angle to untreated PVC R samples.

The contact angle for treated PVC R2 plain had greatest contact angle amongst all the treated PVC samples. These results match the result of the XPS and the ToF-SIMS analysis. So, the surface concentration of the oxygen in survey spectrum of the PVC R2 plain was 17 at% Table 4.12, this was lowest surface concentration of the oxygen in the survey spectra of all the treated PVC samples. Also it shows an increase in relative intensity of the Irgafos 168 and Irganox 1010 ions of treated PVC R2 plain in comparison with untreated PVC R2 plain figure 4.40. When the Irgafos and Irganox segregate to the surface of the PVC R2 plain, they work as boundary layer between the surface of the PVC and liquid which can be water, adhesive or coating does not let the liquid to run easily on the surface of the sample.

Table 4.14 Result of sessile contact angle measurements of PVC Rehau before and after flame treatments

Samples No	Elapse time /day	Angle/ degree	Standard Deviation	Release agent	Plain	Hexane
PVC R 1		86	$\pm 2$	✓		
PVC R 1		87	$\pm 3$			✓
PVC R 2		85	$\pm 2$	✓		
PVC R 2		86	$\pm 1$			✓
PVC R 2		93	$\pm 2$		✓	
PVC R 1	4	59	$\pm 4$	✓		
PVC R 2	4	57	$\pm 4$	✓		
PVC R 2	4	70	$\pm 3$		✓	
PVC R 1	90	68	$\pm 4$	✓		✓
PVC R 2	90	71	$\pm 2$	✓		✓
PVC R 2	90	84	$\pm 4$		✓	✓

## 4.11 ToF-SIMS analyses

The ToF-SIMS mass spectra obtained from PVC window profile V and R samples before and after flame treatment were calibrated and by Ionspec software. Then the Bach static application of the software used to normalise the intensity of the peaks by total ion intensity and convert them to excel data. The same sample that were analysed by XPS in this investigation were also analysed by ToF-SIMS.

The Figure 4.42 indicates that the relative intensity of the hydrocarbon ions  $C_3H_7^+$ ,  $C_4H_7^+$  and  $C_4H_9^+$  reduces the flame treated sample in comparison with to untreated samples. The flame treated samples shows higher relative intensities for  $C_2H_3O^+$ ,  $C_3H_3O^+$  and  $C_3H_5O^+$  molecular ions in comparison with untreated samples. The increase in relative intensity of the  $C_2H_3O^+$ ,  $C_3H_3O^+$  and  $C_3H_5O^+$  ions is influenced by flame treatment and increasing the oxygen functional group on surface of the samples.

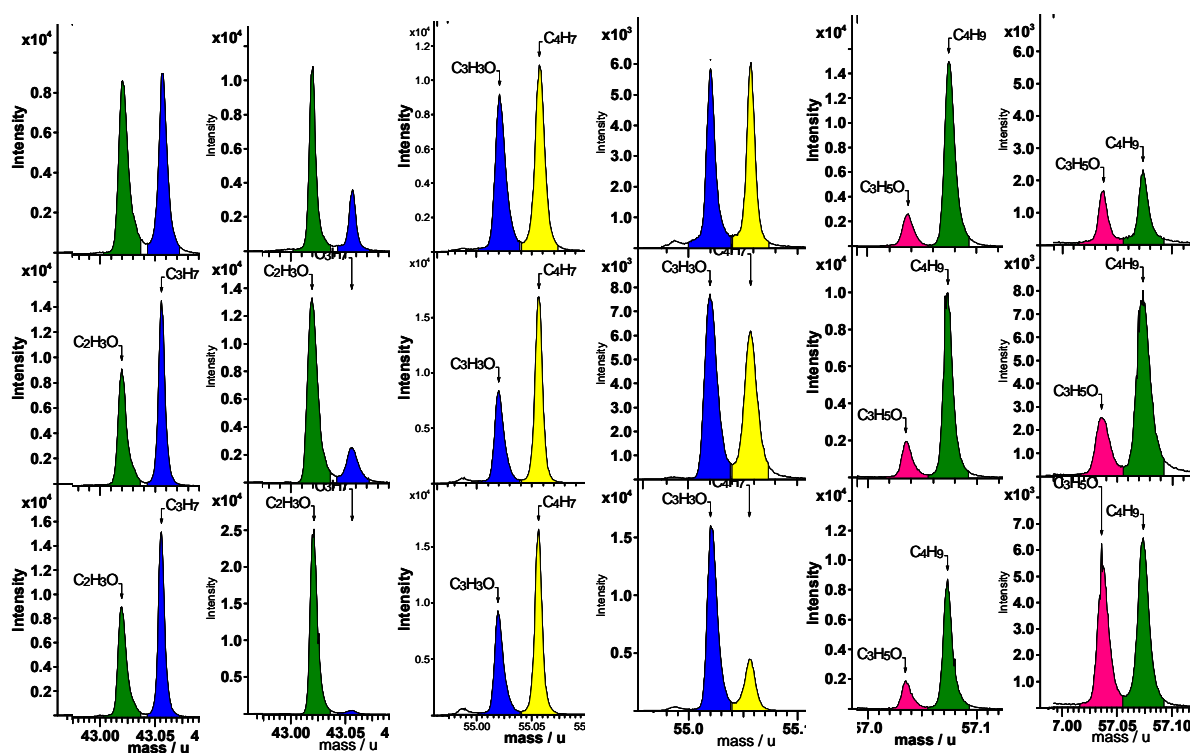


Figure 4-42 Positive ToF-SIMS spectra of PVC V1 in top row, V2 middle row and V2 plain in bottom row at masses 43, 55, 57 before and after flame treatment.

The Figure 4.43 is information from loading graph of normalising the intensity by total ion of the acrylic co-polymers ions  $C_2H_3O_2^+$ ,  $C_4H_7O_2^+$ ,  $C_5H_9O_2^+$  and  $C_7H_7O_3^+$  at the PVC V surface, the acrylic copolymer distributed throughout the PVC V bulk, which is a

component of impact modifier in PVC profile formulation. Figure 4.35 shows a reduction in relative intensity of acrylic fragments at 59 m/z, 87 m/z, 101 m/z and 139 m/z in PVC V1 spectrum after flame treatments in comparison with untreated PVC V1 sample. The relative intensity  $C_2H_3O_2^+$ ,  $C_5H_9O_2^+$  and  $C_7H_7O_3^+$  ions shows the similar trend of PVC V1 for PVC V2 but with lesser relative intensity reduction in  $C_4H_7O_2^+$  ion.

The relative intensity of the  $C_2H_3O_2^+$ ,  $C_4H_7O_2^+$ ,  $C_5H_9O_2^+$  and  $C_7H_7O_3^+$  ions increased dramatically in surface treated sample of PVC 2 plain comparison with untreated PVC 2 plain. This result indicates a greater concentration of the acrylic co-polymers at the surface of the PVC V2 plain (without release agents) after flame treatment. Hence PVC profile samples with release agent and flame treatment were less likely to show additives and other components to segregate to the surface of the samples. However, the contact angle of the PVC V2 plain samples after flame treatment was greater than contact angle of PVC V1 and V2 with release agent on the surface. This associated by segregating of other components such as acrylic copolymer from bulk of the PVC to it surface of PVC and performs such as boundary layer.

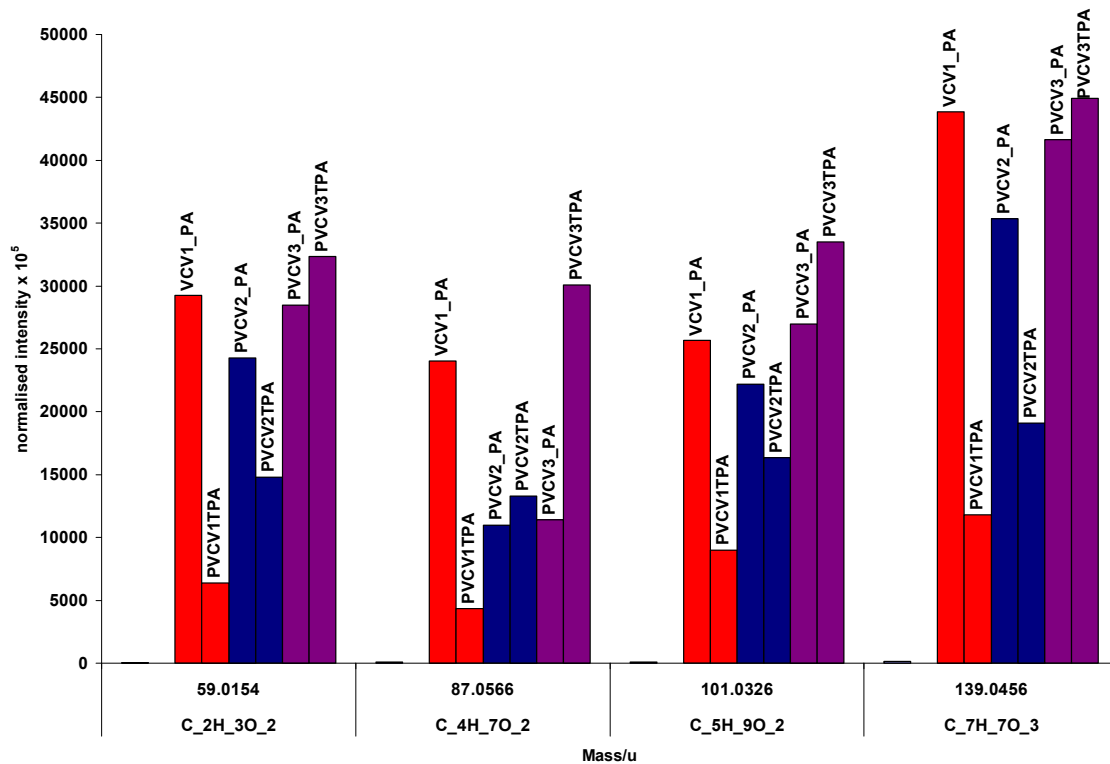


Figure 4-43 Result of the positive ToF-SIMS analysis of PVC V1 in red, V2 in blue and V2 plain in purple related to acrylic peaks normalised by total ion at Masses 59, 87, 101 and 139 before and after flame treatment

The Figure 4.44 exhibits the information from loading graph of normalising the intensity of positive ToF-SIMS spectra of PVC V samples by total ion of Irganox 1010 at masses 203m/z and 259m/z and Irgafos 168 at mass 441m/z. The relative intensity of the  $C_{14}H_{19}O^+$ ,  $C_{17}H_{23}O_2^+$  (Irganox 1010) and  $C_{28}H_{42}PO_2^+$  (Irgafos 168) ions decreased in ToF-SIMS spectrum obtained from treated PVC V1 sample in comparison with untreated PVC V1 sample. The formulation of PVC V1 was different from PVC V2 and PVC V2 plain. The relative intensity of the  $C_{14}H_{19}O^+$ ,  $C_{17}H_{23}O_2^+$  (Irganox 1010) and  $C_{28}H_{42}PO_2^+$  (Irgafos 168) ions increased in ToF-SIMS spectra obtained from treated PVC V2 and V2 plain in comparison with the untreated PVC V2 and V2 plain samples. These results indicate 1- greater concentration of Irganox 1010 in PVC V formulation than the Irgafos 168, 2- the Irgafos and Irganox contributed from the bulk of the PVC as well as the release agent. However, Irganox and Irgafos are two antioxidant agents that blend with many polymers. On the surface of PVC V2 plain profile there was no release agent, this meant that if Irgafos and Irganox contributed to the release agent it would not have been seen on ToF-SIMS spectra of the samples without protective film, hence the Irganox

and Irganox are part of the PVC R samples formulation that segregate to the surface of the samples.

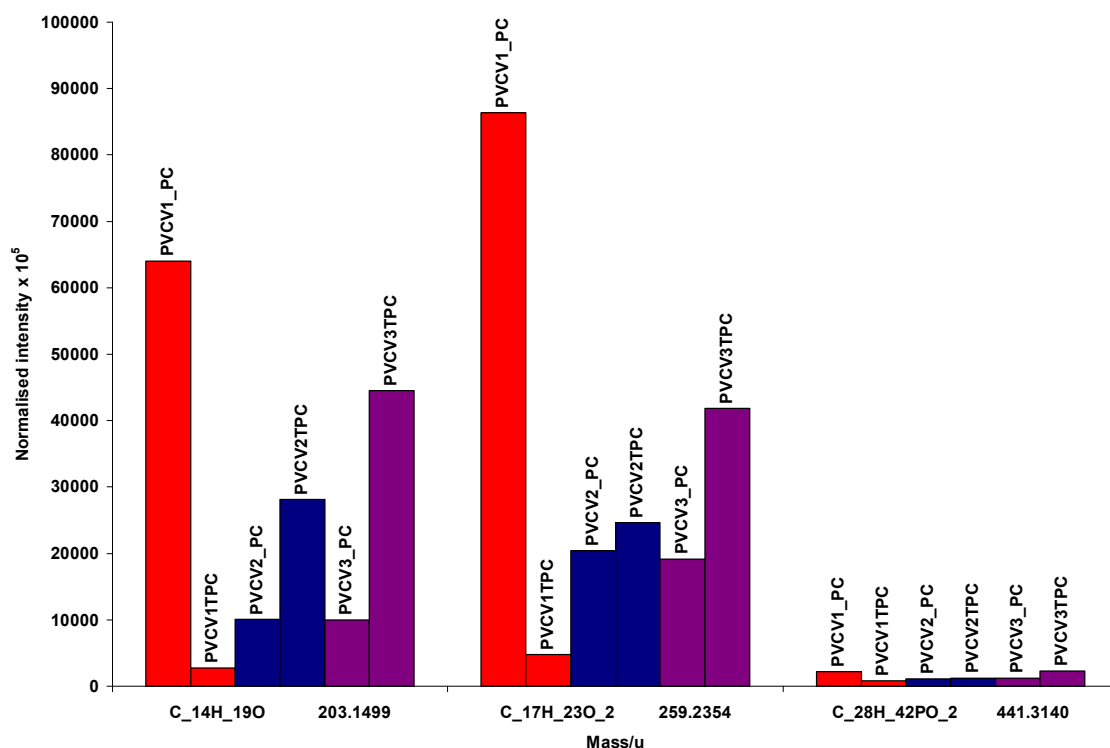


Figure 4-44 Result of the positive ToF-SIMS analysis of PVC V1 in red ,V2 blue and V2 plain in purple related to Irganox 1010 at masses 203 and 259 also Irgafos 168 at mass 441 peaks normalised by total ion before and after flame treatment

Figure 4.45 exhibited positive ToF-SIMS spectra of PVC R1, R2 and R2 plain before and after flame treatment. Although the PVC window profile V and R had different formulation the effect of the of the flame treatment on the surface of them were quite similar. All the ToF-SIMS spectra of PVC R samples indicate the relative intensity of the hydrocarbon ions  $C_3H_7^+$ ,  $C_4H_7^+$  and  $C_4H_9^+$  were reduced in the flame treated samples in comparison to the untreated samples. The flame treated PVC R samples show higher relative intensities for  $C_2H_3O^+$ ,  $C_3H_3O^+$  and  $C_3H_5O^+$  molecular ions in comparison with untreated samples. The reduction in relative intensity of hydrocarbon ions and an increase in relative intensity of oxygen functional group by the flame treatment, shows that in the entire treated sample there is an increase in oxygen concentration. These results differentiate between treated and untreated samples. In the case of the hydrocarbon

ions by flame treatment, the reaction of the broken chains results in the generation of oxygen containing functional groups on the surface.

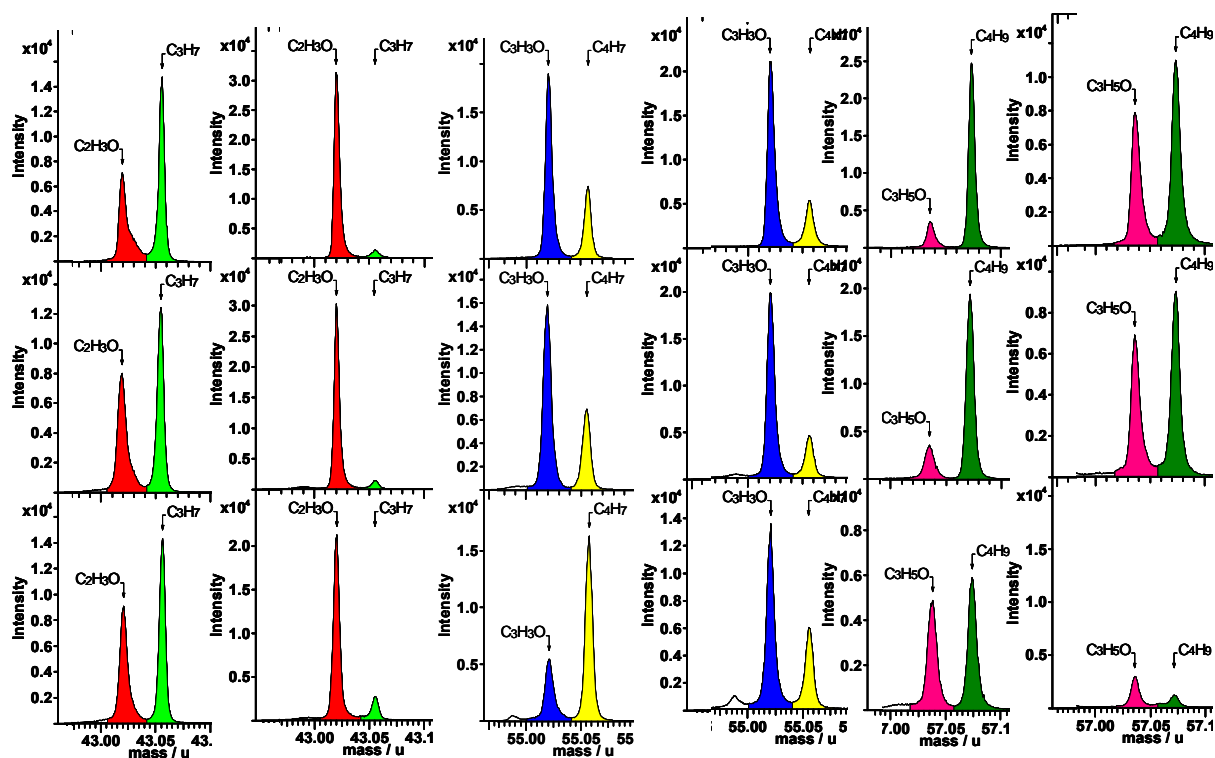


Figure 4-45 Positive ToF-SIMS spectra of PVC R1 in top row, R2 middle row and R2 plain in bottom row at masses 43, 55, 57 before and after flame treatment.

Figure 4.46 presents the results of normalised intensity by total ion of ToF-SIMS positive spectra of PVC R1, R2 and R2 plain. It is exhibited reduction in relative intensity of the  $C_3H_7^+$ ,  $C_4H_7^+$  and  $C_4H_9^+$  hydrocarbons ions treated sample in comparison with the untreated samples of PVC window profile R1,r2 and R2 plain samples.

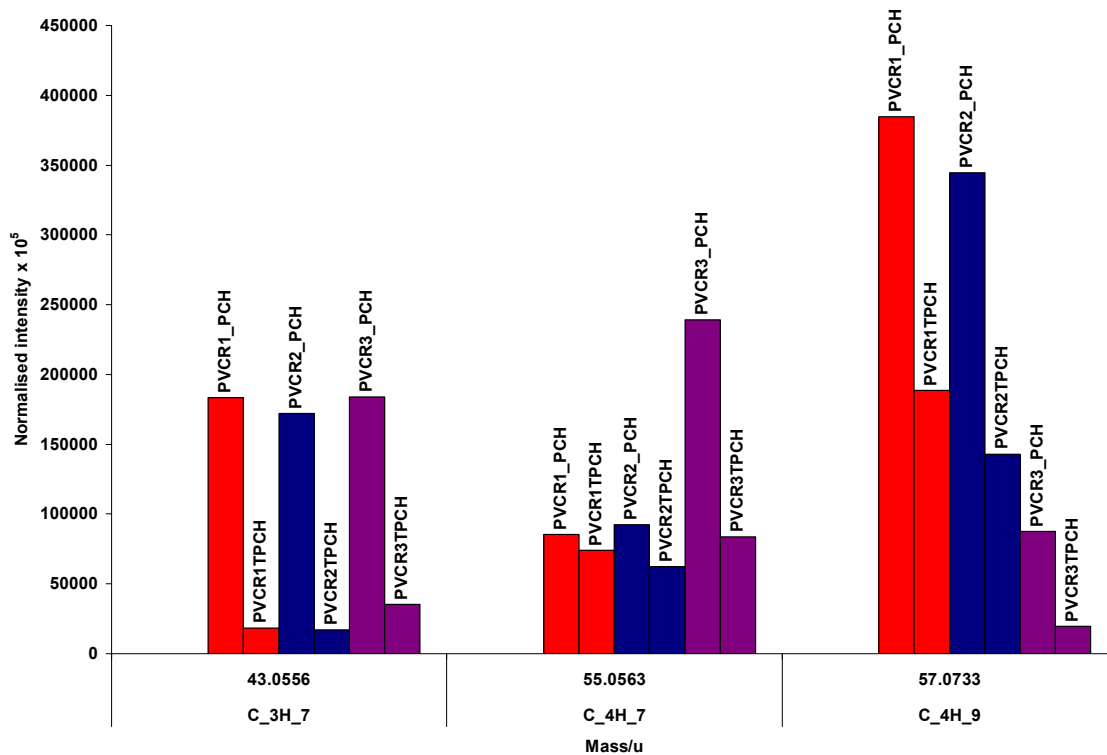


Figure 4-46 Result of the positive ToF-SIMS analysis of PVC R1 in red , R2 blue and R2 plain in purple related to hydrocarbons peaks normalised by total ion at Masses 43,55, and 57 before and after flame treatment

Figure 4.47 shows information from loading graph of normalising the intensity by total ion of the acrylic co-polymers ions  $C_2H_3O_2^+$ ,  $C_4H_7O_2^+$ ,  $C_5H_9O_2^+$  and  $C_7H_7O_3^+$  at the PVC R samples surface. Similar to the PVC V samples the acrylic copolymer distributed throughout the PVC R bulk, that is component of impact modifier in PVC profile formulation. The figure 4.39 indicates different result from PVC V samples. This was an increase in relative intensity of acrylic fragments at 59 m/z, 87 m/z and 101 m/z but slightly different in fragment 139 m/z in PVC R1 spectrum after flame treatments in comparison with untreated PVC V1 sample. The relative intensity  $C_2H_3O_2^+$ ,  $C_4H_7O_2^+$ ,  $C_5H_9O_2^+$  and  $C_7H_7O_3^+$  ions increase in treated PVC R2 samples in comparison with untreated PVC R2 sample. The PVC window profile R2 plain did not have protection film on the surface of the profile. Effect of the flame treatment gave different results between the PVC V2 plain and PVC R2plain. It was an increase in all the relative intensity of acrylic fragments in treated PVC V2, but in case of the PVC R2plain it showed dramatic reduction in relative intensity of the  $C_2H_3O_2^+$ ,  $C_4H_7O_2^+$ ,  $C_5H_9O_2^+$  and  $C_7H_7O_3^+$  ions in comparison to untreated PVC R2 plain.

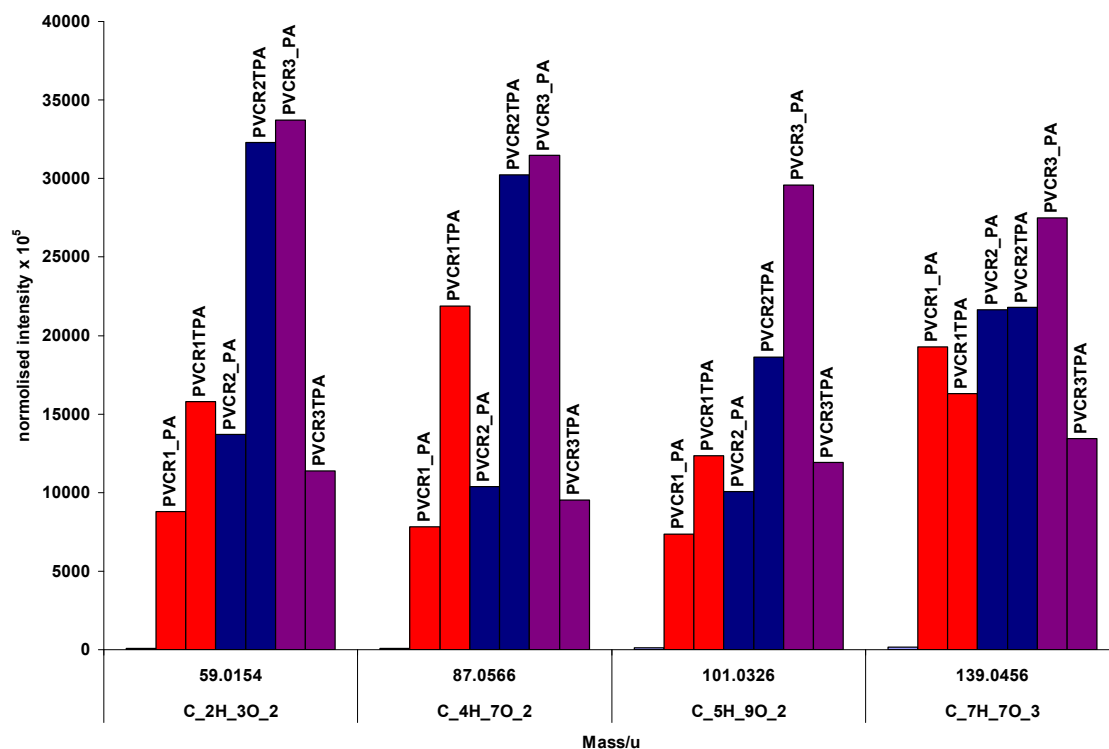


Figure 4-47 Results of the positive ToF-SIMS analysis of PVC R1 in red, R2 in blue and R2 plain in purple related to acrylic peaks normalised by total ion at Masses 59, 87, 101 and 139 before and after flame treatment

Figure 4.48 exhibits the information from loading graph of normalising the intensity of positive ToF-SIMS spectra of PVC V samples by total ion of Irganox 1010 at masses 203m/z and 259m/z and Irgafos 168 at mass 441m/z. The effect of the flame treatment on surface of the PVC R1 and R2 was similar, but it was different to PVC 2plain. The relative intensity of the  $C_{14}H_{19}O^+$  (Irganox 1010) ion was increased in ToF-SIMS spectra obtained from treated PVC R1 and R2 samples in comparison to untreated PVC R1 and R2. A decrease in relative intensity of  $C_{17}H_{23}O_2^+$  (Irganox 1010) and  $C_{28}H_{42}PO_2^+$  (Irgafos 168) ions in ToF-SIMS spectrum obtained from treated PVC R1 and R2 samples in comparison with untreated PVC R1 and R2 samples were observed. The relative intensity of the  $C_{14}H_{19}O^+$  (Irganox 1010) ions decrease in ToF-SIMS spectra obtained from PVC R2 plain in comparison with untreated PVC R2plain. There were an increase in relative intensity of  $C_{17}H_{23}O_2^+$  (Irganox 1010) ion and  $C_{28}H_{42}PO_2^+$  (Irgafos 168) ion in ToF-SIMS spectra obtained from treated PVC R2 plain in comparison with the untreated PVC R2plain samples. These results indicate 1- that greater concentration of Irgafos 168 exists in the formulation of PVC R samples in comparison with PVC V samples. 2- In

both PVC V and PVC R samples the Irgafos and Irganox contributed from the bulk of the PVC as well as the release agent. On the surface of PVC R2 plain there were no release agent on the surface of the profile, this suggests that the Irgafos and Irganox from the release agent would not have been seen on ToF-SIMS spectra of the samples without protective film.

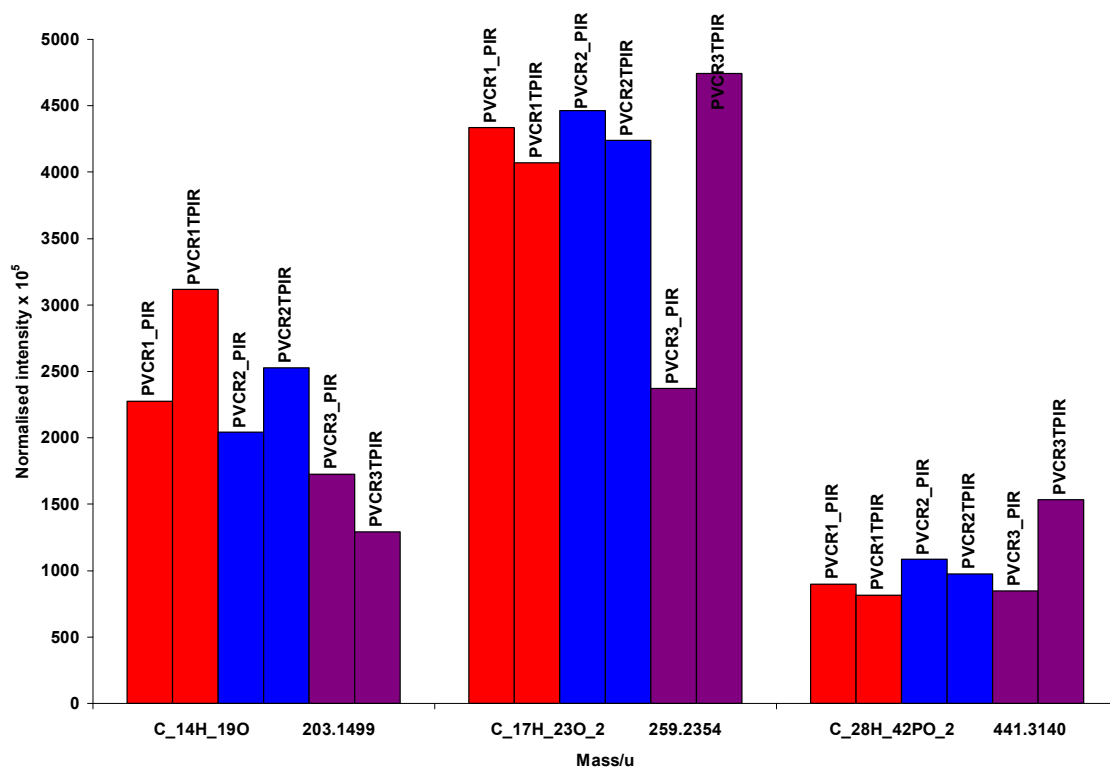


Figure 4-48 Result of the positive ToF-SIMS analysis of PVC R1 in red, R2 blue and R2 plain in purple related to Irganox 1010 at masses 203 and 259 also Irgafos 168 at mass 441 peaks normalised by total ion before and after flame treatment

#### 4.12 AFM analysis

The surface properties (topography and morphology) of all PVC V and R sample before and after surface modification were characterised by AFM. Topographic and phase images were obtained for all samples at few different scan area with size of  $10 \mu\text{m}^2$ . The existence of a thin layer on the surface of the samples with release agent on the surface (PVC V1, V2, R 1 and R2 before flame treatment) is observed, when characteristic smoothing of the surface relief was observed at low tapping amplitude. In order to For characterising the surface of the PVC buried under the release agent layer, the tapping

amplitude increased 2 to 3 times to allow penetration of the SPM tip through the release agent layer.

Figure 4.49 shows a series of 3D topography of the surface and section analysis spectrum for all PVC V samples before and after flame treatment. Figure 4.49 a, is a 3D topography image obtained from PVC V1, this smooth surface is the microstructure of the surface of the release agent. By increasing the tapping amplitude image b of Figure 4.49, it was possible for the tip to penetrate through release agent layer and characterise the surface of the PVC V1 sample before flame treatment. The image c of Figure 4.49 is the 3 D topography image of the treated PVC V1

The section analysis spectrum of each sample is show under the 3 D topographic of the sample. The maximum height of the features (distance between highest and lowest point of the surface) in image a and b of Figure 4.49 was 113.93 and 103.24nm respectively. After flame treatment of the PVC V1 the release agent and the surface of the sample fused together and produced new polymeric surface. The height of surface feature in the 3 D topography obtained from treated PVC V1 image c of Figure 4.49 reduced to 33.239nm.

Image d of Figure 4.49 is a topographic image obtained from the surface of PVC V2 before flame treatment; this is topographic image of the release agent on the surface of the untreated PVC V2. The height of the surface features in image d of Figure 96 was 55.460nm. The height of surface features at image e of Figure 4.49 obtained from the surface of the untreated PVC V2 underneath of release agent was 433.83 nm. After flame treatment of PVC V2 image f of Figure 4.49 similar to PVC V1 sample, the release agent fused to the surface of the PVC V2 sample and the height of the surface features reduced to 20.205nm.

Image g of Figure 4.49 exhibits a 3D topographic image obtained from PVC V2 plain before flame treatment, the height of surface features in this image was 377.58nm, this result reduce after flame treatment image h of Figure 4.49 to 124.88nm.

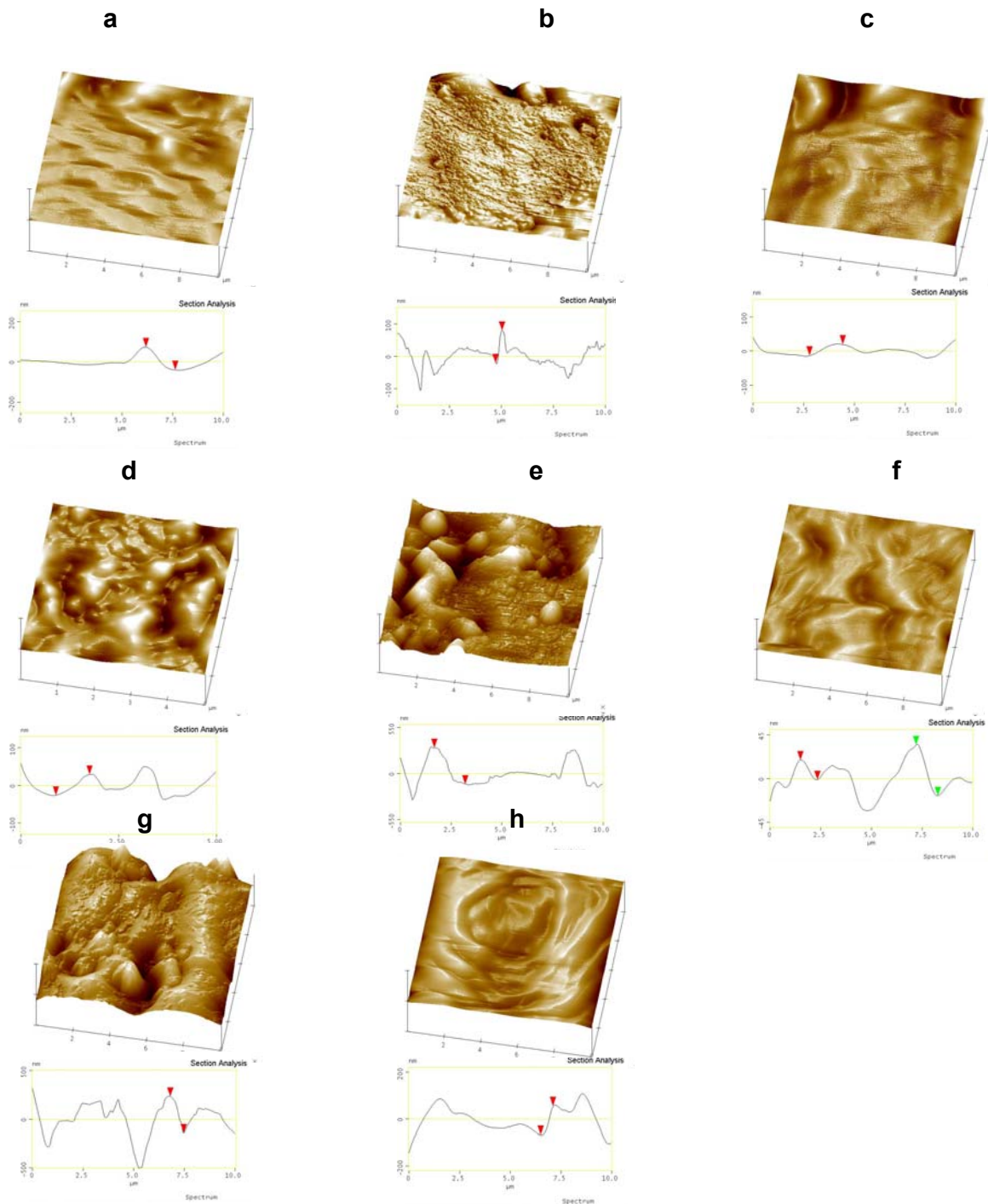


Figure 4-49 AFM height images and AFM spectrum of PVC V samples before and after FT

Figure 4.50 shows a series of 3D topographic images obtained from the PVC R samples before and after flame treatment. Image a of Figure 4.50 is 3 D topographic image obtained from untreated PVC R1, the height of surface feature in this topographic image was 152.19nm. While the surface of the PVC R1 modified by flame shows the height of

surface feature of the image b of figure 4.50 obtained from treated PVC R1 increased to 242.03nm

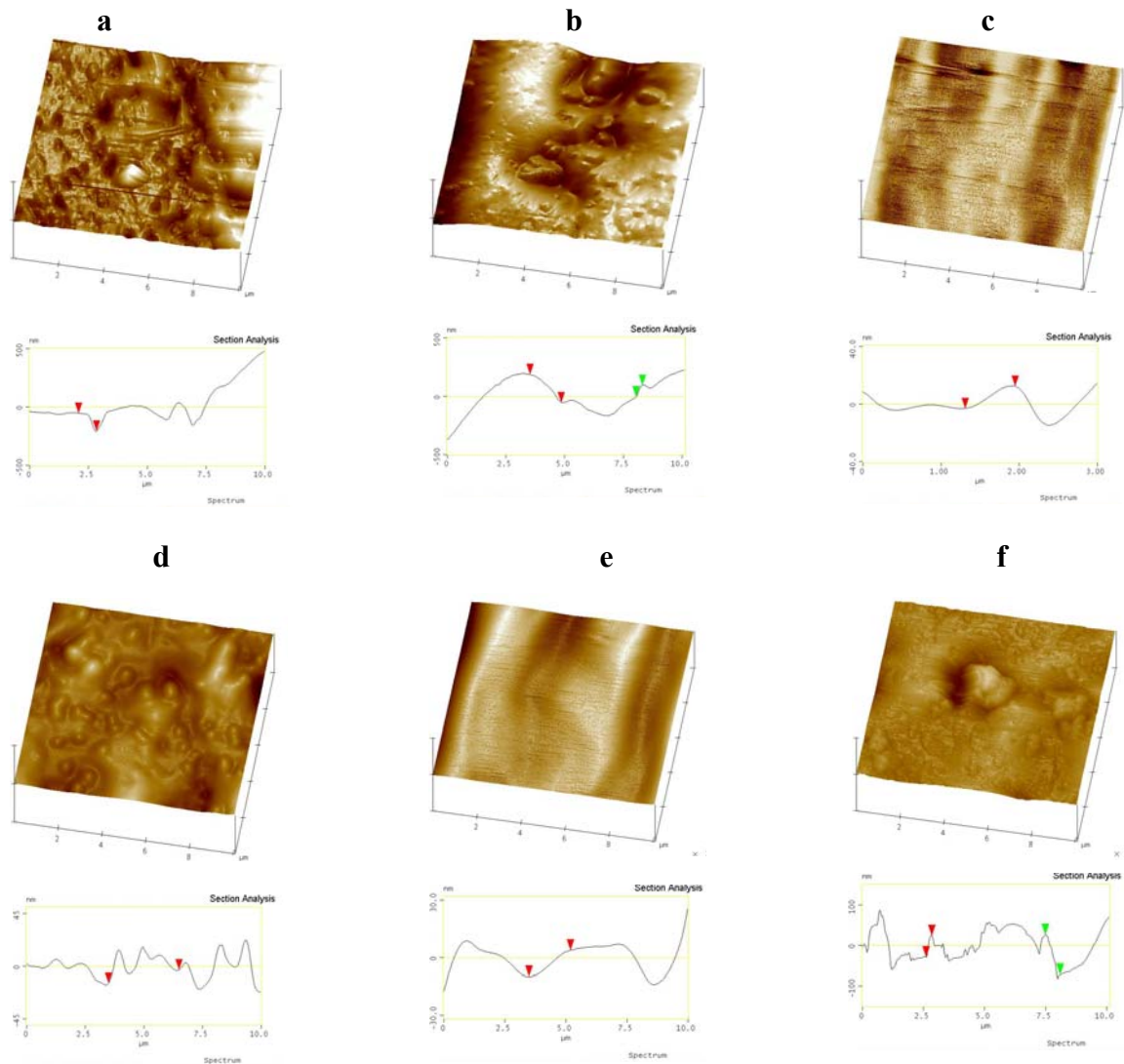


Figure 4-50 AFM height images and AFM spectrum of PVC R samples before and after FT

The image c of Figure 4.50 is 3 D topographic image obtained from untreated PVC R2, the height surface features of the image was 2.558 nm. By modifying the surface of the PVC R2 the height of surface feature in image d of Figure 4.42 obtained from treated increased to 11.750nm.

The image e of Figure 4.50 is 3 D is topographic image obtained from untreated PVC R2 plain; the height of surface feature of the image was 9.160nm. After flame treatment of PVC V2 plain the height of surface feature of 3 D topographic image f of Figure 4.50 increased to 97.732nm.

The AFM result obtained from PVC V samples was different from that obtained from PVC R samples. In the case of the PVC V 1 and 2 samples, after flame treatment the release agent was fused to the surface of the PVC samples. The surface of the treated PVC V1 and V2 was smoother than surface of the untreated PVC V1 and V2 (reduce in surface roughness). While the surface of the PVC V2 plain was treated by flame, it resulted in an increase in surface roughness.

When the surface of PVC R samples, were modified by flame, there were an increase in the surface roughness of all the treated PVC R samples, with and without release agent.

#### ***4.13 Dynamic mechanical analysis***

The DMA results of untreated and treated PVC samples were characterised in 19 months after flame treatment. The results show the remarkable effect of flame treatment on viscoelastic properties of the PVC samples. Although the measurement was carried out several months after surface modification of the sample, the effect of the treatment was seen to be stable.

Figure 4.51 shows the storage Modulus of the PVC V with release agent before and 19 months after flame treatment. The red curve exhibits the untreated PVC sample and the green curve presents treated PVC sample. The storage modulus of the PVC V with release agent has changed from 9269 MPa before surface treatment to 11136MPa after surface treatment. This indicates that the material has a higher stiffness and strength after the process of flame treatment. This was an increase of 20% in storage modulus which is directly due to penetration of the release agent onto the PVC surface.

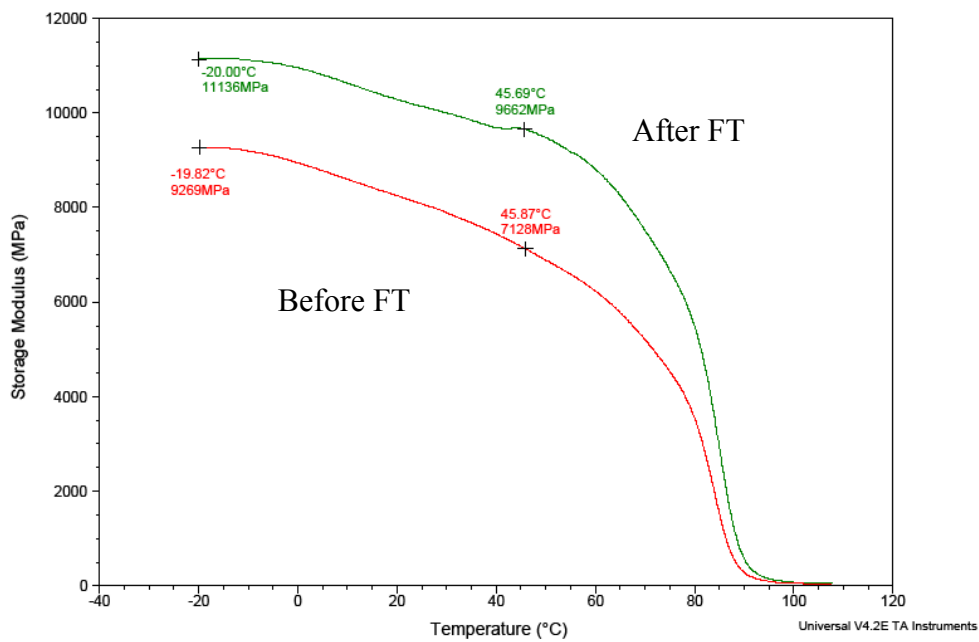


Figure 4.52 Comparison of the Tan delta profiles for PVC V with release agent before and 19 months after flame treatment. The red curve is represents the tan delta of PVC V with release agent before flame treatment and the green curve indicates the plot for after flame treatment.

By comparing the result of the tan delta of PVC-V with release agent before and after flame treatment, it can be seen that the effect of flame treatment on tan delta profile is not significant. Also the temperature value at tan delta peak indicates the value of glass transition temperature. The fact that this has not significantly changed indicates that the nature of the material has not changed after the flame treatment.

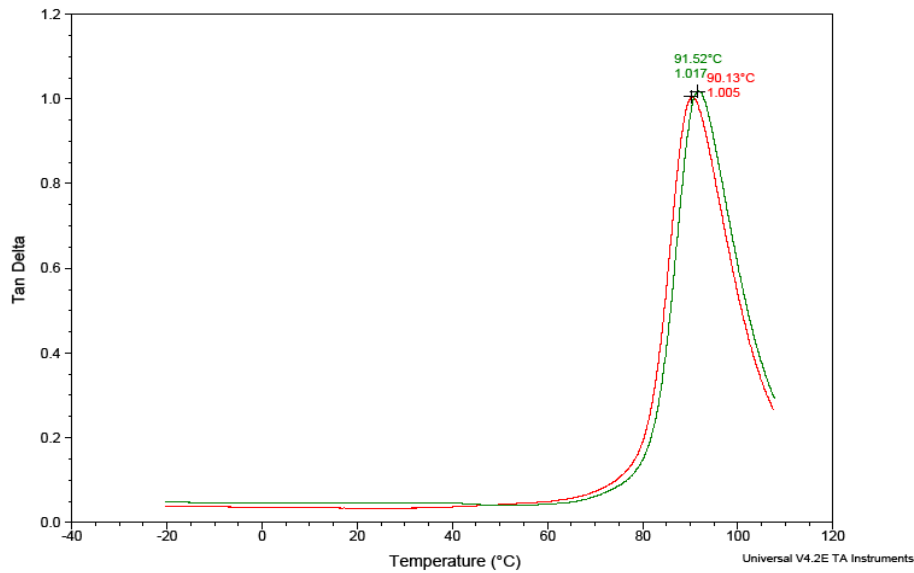


Figure 4-52 Tan Delta of PVC V with RA before and after FT

The Figure 4.53 shows the results of the loss modulus of PVC-V with release agent before and 19 months after flame treatment. By comparing the results it can be observed that significant change on loss modulus of the sample after flame treatment.

The loss modulus of the sample was changed from 1206 MPa before surface treatment to 880.5 MPa after surface treatment. This was a decrease of 36% in loss modulus, which indicates that flame treatment results in a more rigid material, because the trend in loss modulus is usually in opposite direction to storage modulus. This is thought to be due to maintaining an interlocking mechanism when the release agent is applied, which in turn helps to improve PVC performance.

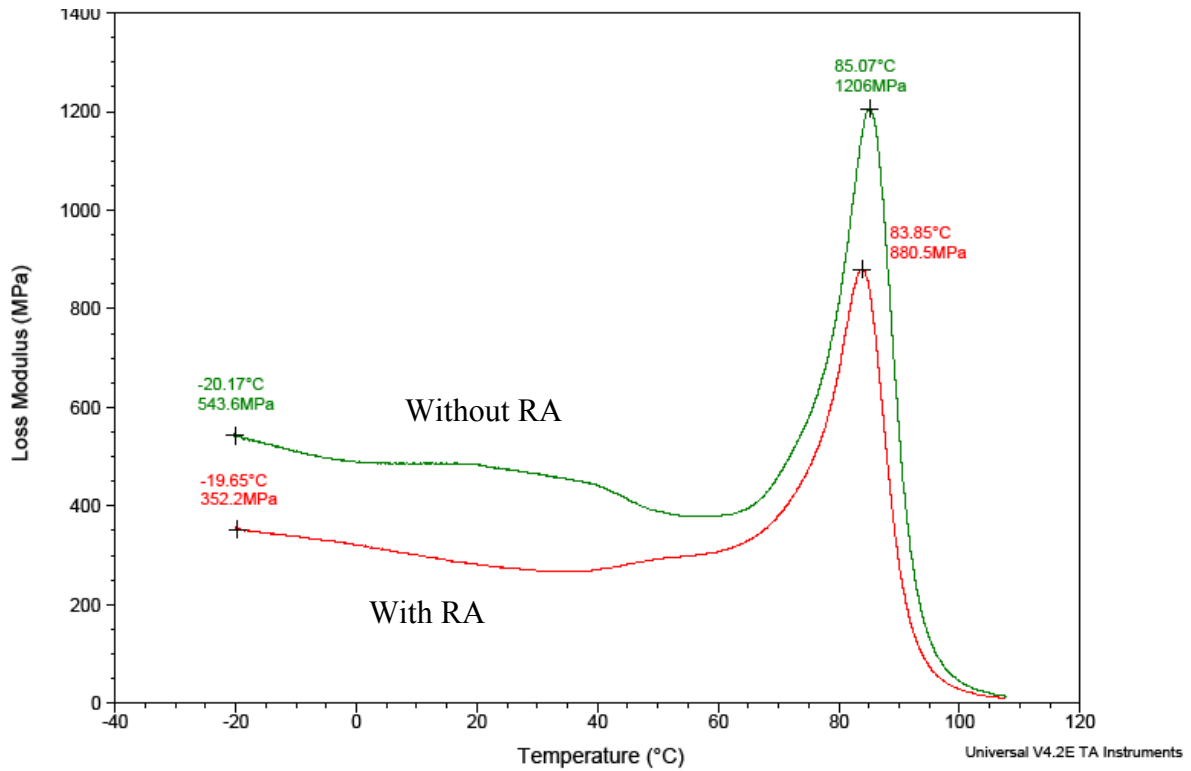


Figure 4-53 comparing the Loss modulus of PVC V with RA before and after FT

In order to study the effect of the release agent on the mechanical property of the PVC samples after flame treatment, two PVC V samples from the same batch, with and without release agent that they have been treated by flame treatment under the same conditions have been characterised by DMA.

Figures 4.52 and 4.53 show the results of storage modulus and loss modulus of PVC V with release agent (red), and PVC V without release agent (green) respectively, it should be noted that the surface of both of them was treated by flame treatment at the same time, under the same condition.

The DMA plots show the surface modification of the PVC samples after flame treatment. The results indicate that the PVC sample treated by flame treatment with the release agent shows that the release agent and PVC promote a strong bond and therefore become one solid sample. An increase of 10% in storage modulus from 8083 MPa, for samples without RA, to 8822 MPa for samples with RA. These results are in agreement with the results from AFM analysis, as described in Section 4.12. The AFM 3D topographic images obtained from the PVC samples with release agent before and after flame treatment shows that the surface of the PVC samples after flame treatment is much

smoother than before flame treatments which seems to be more uneven and bumpy (Figures 4.49-4.50 ). However the loss modulus plots in Figure 4.55 do not seem to be significantly affected by the differences in the presence of RA (see section 4.12).

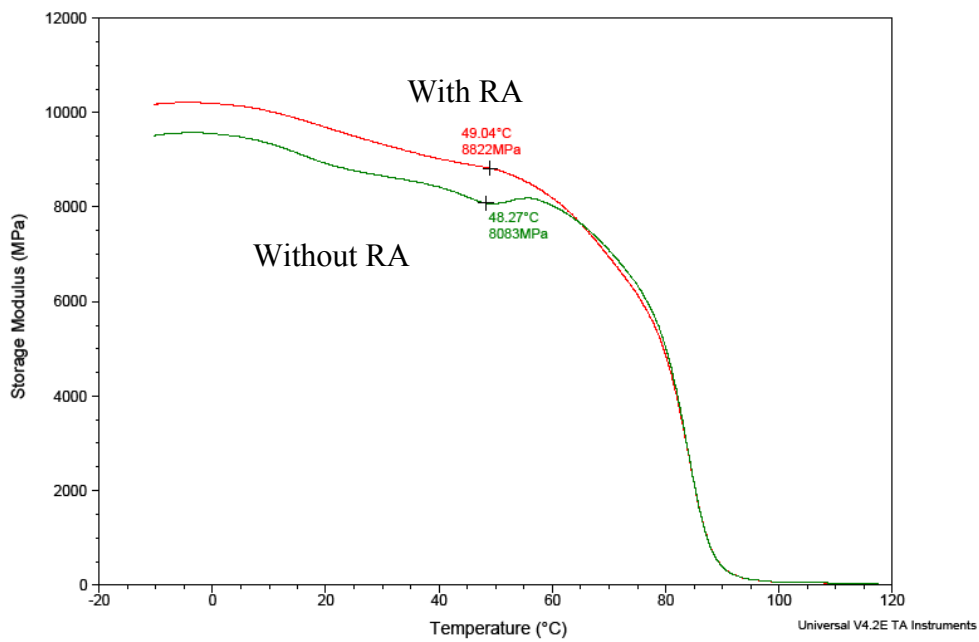


Figure 4-54 comparing the Storage Modulus of PVC V 2 with and without RA after FT

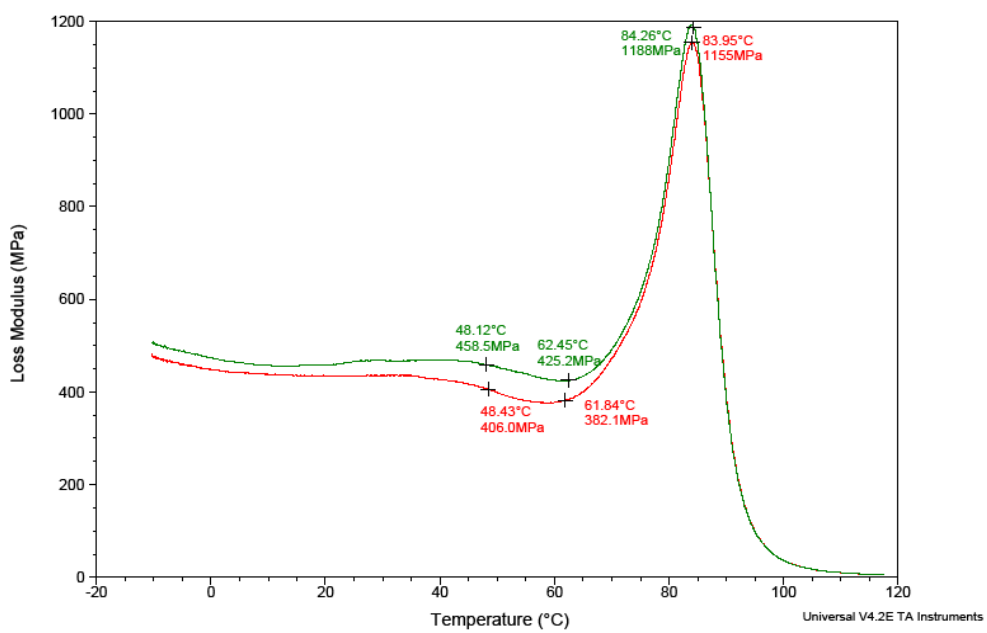


Figure 4-55 comparing the Loss modulus of PVC V2 with and without RA after FT

#### 4.14 XPS analysis of PU hot melt adhesives

The XPS analysis was carried out to find out the stability of the PU hot melt adhesives. After two months of study on the stability of the PUs, the PU 740-29-4 had the best stability amongst the four adhesives. The PU 740-29-4 was the commercial name of the reactive hot melt adhesive. The PU 740-29-4 was made of a combination of Dynacoll 7231, Dynacoll 7360 and MDI. Both Dynacolls are crystalline polyester/ polyol copolymer.

Although one of the main elements in polyurethane is nitrogen, surface concentration of the N on all the PUs were less than one per cent. The four PU hot melt adhesives (FRD-740-29-1,2,3 and 4) were characterised by XPS as a function of variation surface composition with time. Survey spectra from all four PU adhesives produced three characteristic peaks, C1s, O1s and N1s. The surface chemistry characterisation by XPS of the PU samples were carried out for two months in order to investigate the stability and durability of the adhesive as a function of variation of surface composition with time. Table 4.10 and Figure 103 show results of PU hot melt adhesive after two months of study, FRD 740-29-4 had the best stability and durability amongst all of the PU samples.

Table 4.10- Quantitative surface analyses of PU hot melt adhesives as function of time

Sample	Elapse time /day	Surface compositions/atomic %		
		C	O	N
FRD 740-29-1	1	72	26	3
FRD 740-29-1	60	70	27	2
FRD 740-29-2	1	71	27	2
FRD 740-29-2	60	70	28	2
FRD 740-29-3	1	68	30	1
FRD 740-29-3	60	68	31	0.9
FRD 740-29-4	1	70	29	0.9
FRD 740-29-4	60	70	29	0.9

Figure 4.56 shows the result of variation in surface composition of C, O and N as a function of time for two months. Surface concentration of all three characteristic elements did not change in this period; conclusion of this study was that PU 740-29-4 was more stable than other PU hot melt adhesives. Therefore bonding of PVC V to plasticised PVC was performed using PU 740-29-4.

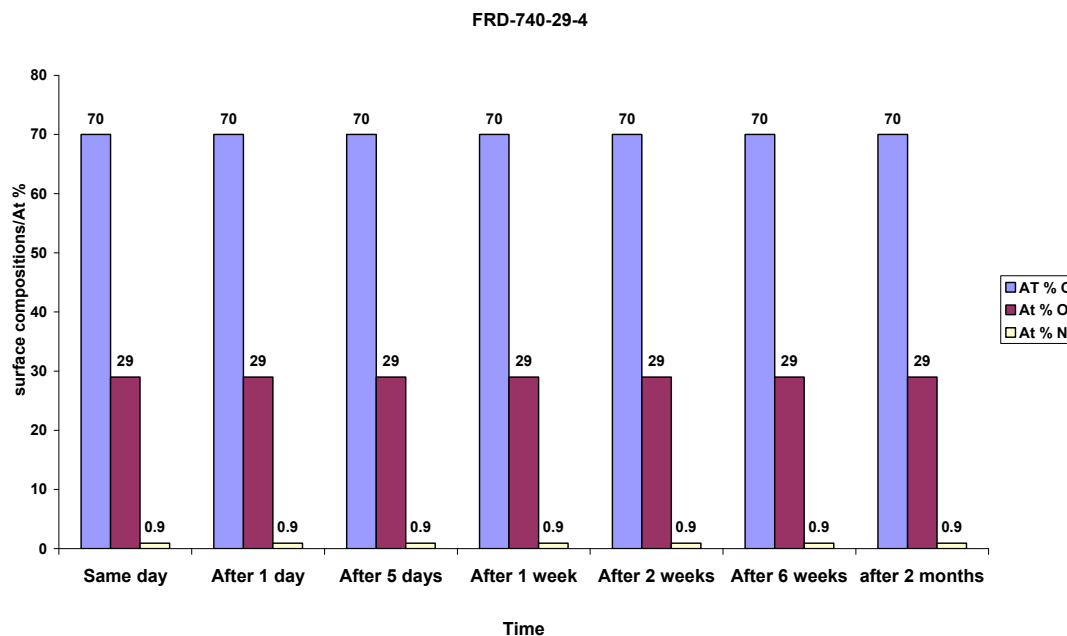


Figure 4-56 shows the change on of surface concentration (at %) of C, O and N in PU 740-29-4 as function of time (two months)

Figure 4.57 shows the XPS survey spectrum of PU FRD-740-29-4 hot melt adhesive acquired on the same day as the adhesive was coated on to the aluminium foil. The survey spectrum of PU FRD 740-29-4 hot melt adhesive has three characteristic peaks, C1s, O1s, and N1s. the surface concentration of C was 72 at%, O 26 at% and N 3 at%. The atomic percentage of these three characteristic elements was stable for up to two months when the XPS analysis was terminated.

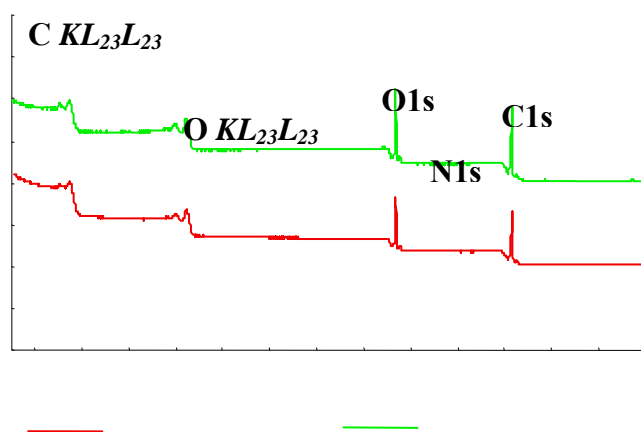


Figure 4-57 Survey spectrum of PU 740-29-4 acquired at the same day was coated on to aluminium foil and after 3 months

Figure 4.58 shows the XPS peak fitting of the high-resolution spectrum of C1s for PU FRD-740-29- The curve at 284.94 can represent three chemical groups, C-C, C-H and C=C group in of Benzene ring which the main chemical shift of that is -0.34 eV. Table 4.11 shows the chemical shift of the different chemical group.

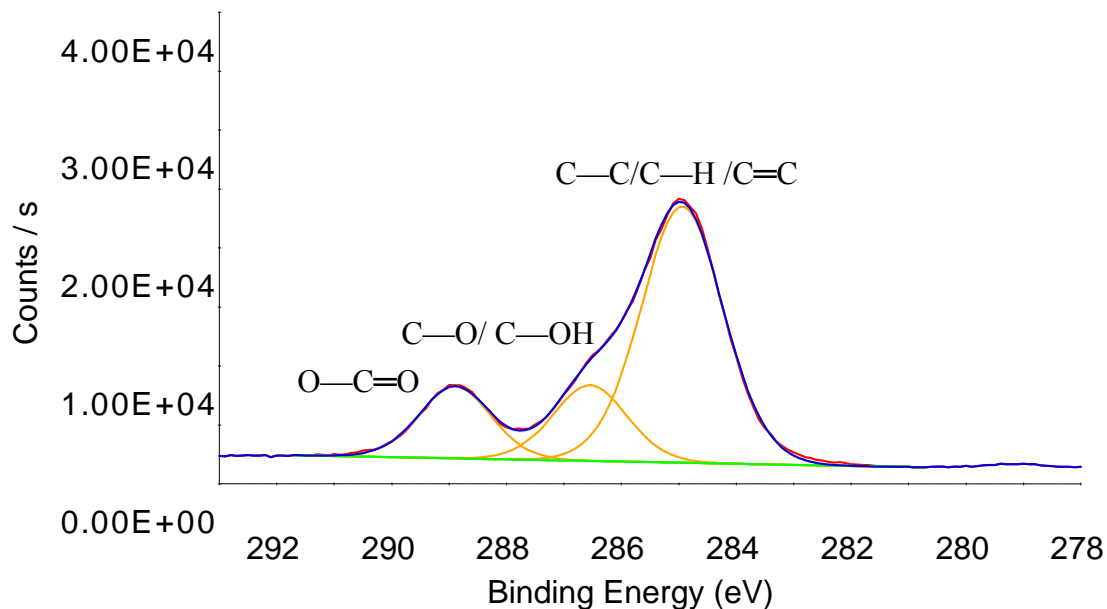


Figure 4-58 the high-resolution signal of C1s has been fitted with three curves. The CH/C-C/ C=C group at 284.94 eV as reference, C-O/C-OH group at 286.55 eV and O-C=O group at 289.14 eV.

Table 4.11- Chemical bonds in the PU 740-29-4 same day it was coated on aluminium foil

Functionality	Peak	Peak BE (eV)	Shift (ev)	Concentration (At %)
C—C/C—H/ C=C	A (reference)	284.94	0	49.5
C—O/ C—OH	B	286.55	1.61	12
O—C=O	C	289.14	3.96	13
	N1s	400		0.4
	O1s	532		25

Figure 4.59 shows the result of curve fitting of the high-resolution C1s two months after the adhesive was coated on to the aluminium foil. Indeed the result of this peak fitting is the same as the result of the curve fitting on the day the adhesive was coated on aluminium foil. Table 411 shows the result of the curve fitting of the high-resolution C1s spectrum of PU 740-29-4, which was analysed by XPS two months after the adhesive was coated on to aluminium foil.

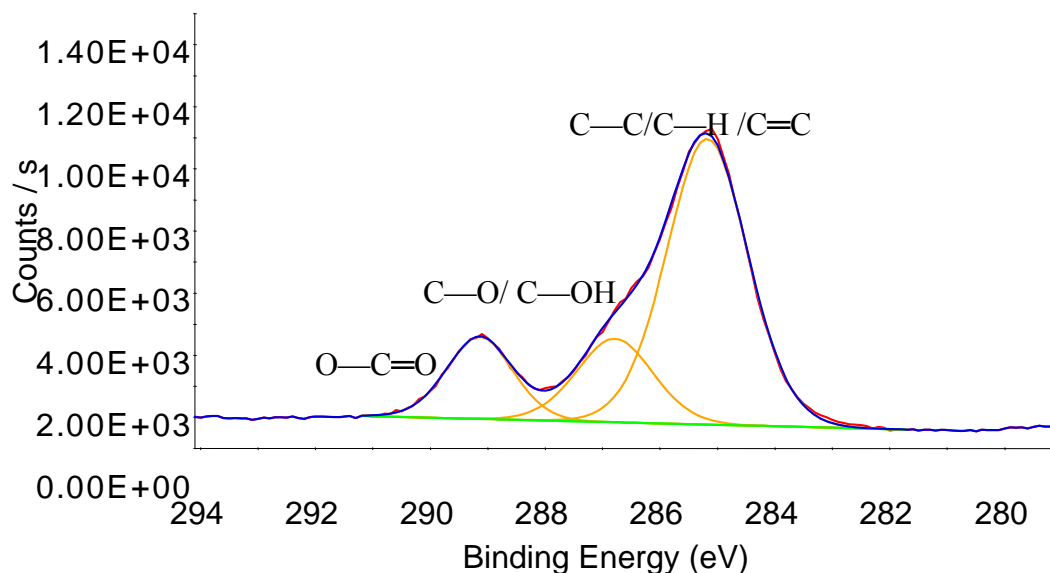


Figure 4-59 High-resolution spectra of C1s from PU 740-29-4 two months after it was coated on to aluminium foil

Table 4.12 shows the peak fitting result of high-resolution C1s spectra of PU 740-29-4 that was characterised by XPS two months after it was coated on to aluminium foil. By comparing the peak fitting result of PU740-29-4 that was characterised by XPS at the same day it was coated on to aluminium foil Table 4.2 with table 4.3, indeed the result of peak fitting was same. Due to stability of the PU 740-29-4 hot melt adhesive two months after it was coated on to aluminium foil.

Table 4.12- Chemical bonds found in the PU 740-29-4, two months after it was coated on to aluminium

Functionality	Peak	Peak BE (eV)	Shift (ev)	Concentration (At %)
C—C/C—H/ C=C	A (reference)	285.18	0.	49.3
C—O/C—OH	B	286.55	1.61	12
O—C=O	C	288.90	3.96	13.5
	N1s	400		0.3
	O1s	532		25.2

#### 4.15 Microtomy of buried interface

In the field of adhesion, for the study of the interaction between a molecule and a solid substrate there are two parameters of significance; first is the capacity of the solid surface to adsorb the molecule, second is bonding between adhesive and substrate (penetration of adhesive into the substrate). As was discussed in Chapter 4 a number of spectroscopic

techniques have been used to investigate buried interfaces. All the spectroscopic techniques are restricted to the examination of interfaces at the most a few hundred nanometres below the sample surface. The tapering of the specimens (PVC coated by hot melting PU adhesive) was performed on the same instrument as chapter 4. Tapering and sectioning of the polymeric adhesives, coating and polymeric substrate were very soft and therefore it was impossible to cut them at room temperature. During sectioning the PU coating peeled off from the substrate instead of being sectioned. As it is explained in chapter 4, here the ULAM technique has been enhanced by in situ cooling of the samples using a cryo-stage (C-ULAM). When the PE block was replaced by the copper block the temperature of the samples could be reduced to  $-2^{\circ}\text{C} \pm 2$ . Therefore, specimens of the PVC Veka coated with the PU 740-29-4, PVC 4 with release agent coated with PU740-29-4 and PVC 4 with release agent bonded to a plasticised PVC film by PU 740-29-4 were sectioned at  $-2^{\circ}\text{C} \pm 2$ .

#### **4.16 XPS analysis of buried interface**

Figure 4.60 shows result of variations in Cl and Si concentration along a C- ULAM ( $-2^{\circ}\text{C} \pm 2$ ) produced taper across a buried PVC/UV primer interface region. The reason why Cl and Si were chosen amongst all elements of UV primer and PVC was because silicon was present only in UV primer and chlorine was only in PVC. Hence, by studying the Cl and Si variation and concentration across a C-ULAM produced taper through a buried PVC/UV primer interface region will show the penetration and cross linking between UV primer and PVC. However, with knowledge of the C-ULAM angle and the XPS linescan step size employed, the application of simple geometry readily enables the horizontal distance to be transformed into an analysis depth interval.

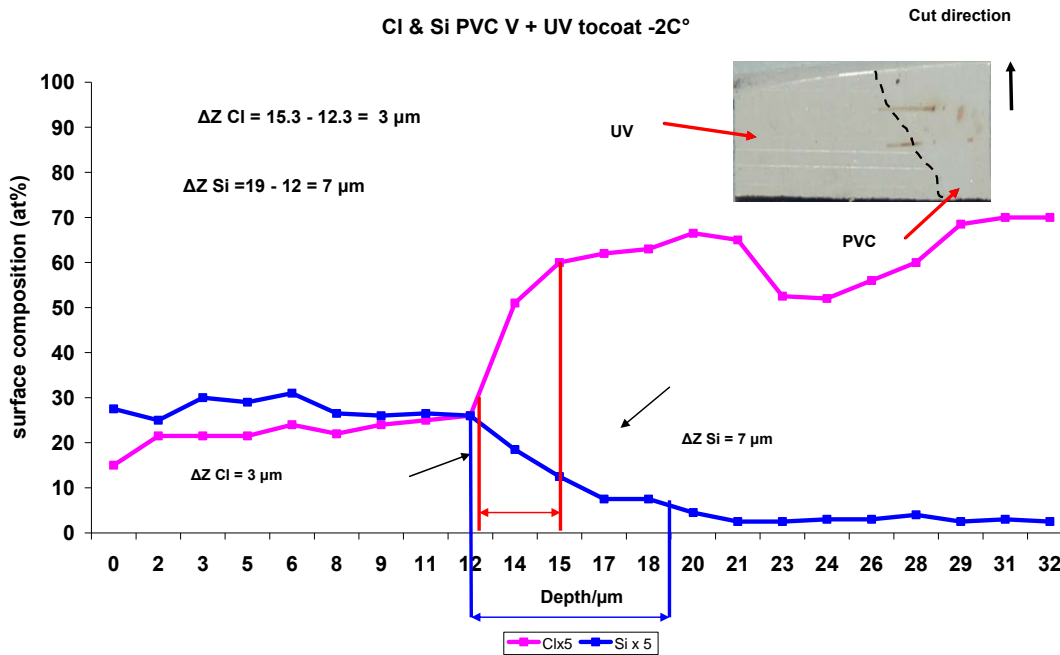


Figure 4-60 Variations in Cl and Si across a C-ULAM ( $-2^{\circ}\text{C} \pm 2$ ) produced taper across a buried PVC/UV primer interface region. Each successive analysis point increases the analysed depth by  $1.53\mu\text{m}$ . Inset is a digital image of the sample after C-ULAM sectioning

The taper angle ( $\theta$ ) was  $0.4^{\circ}$ , the area of analysis (X-ray spot size) was approximately  $100\mu\text{m}$  diameter, there were twenty two points of analysis and the step size was  $219\mu\text{m}$ . Each successive analysis point increases the analysed depth by  $1.53\mu\text{m}$ . Because the concentration of Si and Cl were low in Figures 107 and 108, their intensity has been multiplied by five to be more visible on the graph. One of the data obtained from a linescan along a C-ULAM taper across a UV/PVC interface is that of changes in elemental composition (at %) with depth. The width of the interface ( $\Delta Z$ ) of each taper was calculated using the standard 84-16% technique. The  $\Delta Z$  of Cl was calculated from depth of  $15.3 - 12.3 = 3\mu\text{m}$  and Si  $\Delta Z$  was calculated from depth of  $19 - 12 = 7\mu\text{m}$ . Indeed PU primer penetrated  $7\mu\text{m}$  into PVC substrate. In both Figures 4.12 and 4.13 the analysis starts in the UV primer top coat while the final point of analysis (depth 32.2 figure 4.61 and 37.96 Figure 108) is in the PVC bulk region of the samples.

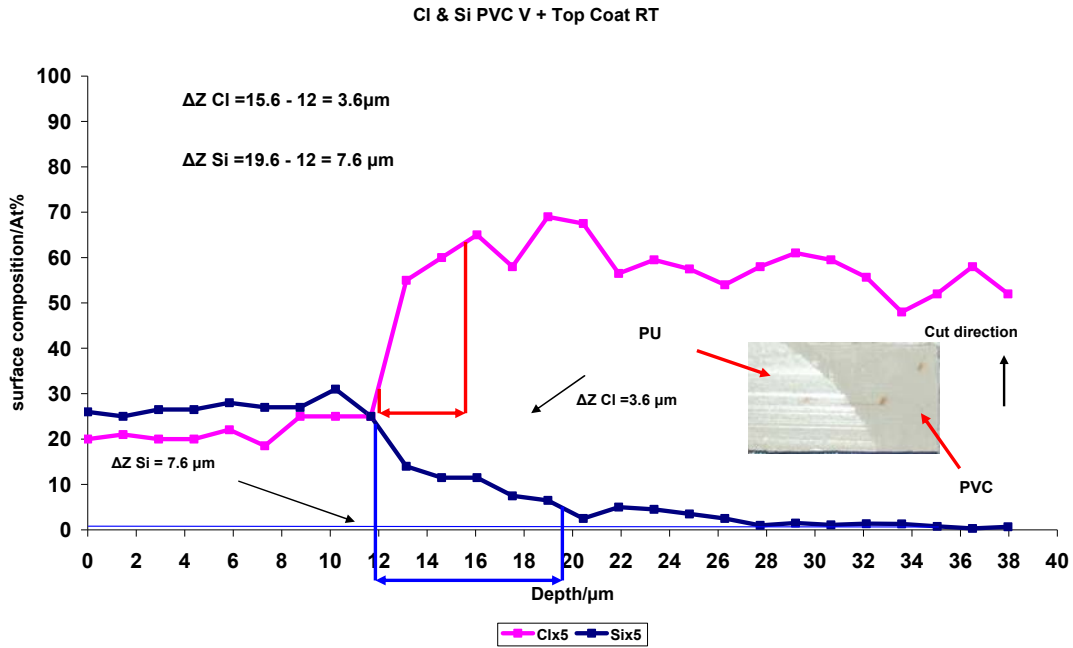


Figure 4-61 Variations in Cl and Si concentration across a ULAM produced taper through a buried PVC/UV primer interface region at room temperature. Each successive analysis point increases the analysed depth by 1.53 μm. Inset is a digital image of the UV/PVC-V interface exposed by C-ULAM.

Figure 4.61 shows the variations in Cl and Si concentration along a C-ULAM produced taper through a buried PVC/UV. The area of analysis (X-ray spot size) was approximately 100 μm diameter, there were 27 points of analysis and the step size was 209 μm. Each successive analysis point increased the analysed depth by 1.5 μm. Both samples, whether tapered at room temperature or  $-2^{\circ}\text{C} \pm 2$ , showed similar results. The  $\Delta Z$  of the buried PVC/UV primer interface at room temperature was calculated in the same way that  $\Delta Z$  was calculated in Figure 4.12. In Figure 4.13 the  $\Delta Z$  of chlorine was  $\Delta Z = 15.6 - 12 = 3.6 \mu\text{m}$  while the silicon  $\Delta Z = 19.6 - 12 = 7.6 \mu\text{m}$ . Hence, the PU primer penetrated approximately 8 μm into the PVC substrate. The result of XPS linescan obtained from both samples in Figures 107 and 108 are similar to each other, in both cases there was evidence of penetration of UV primer into the PVC.

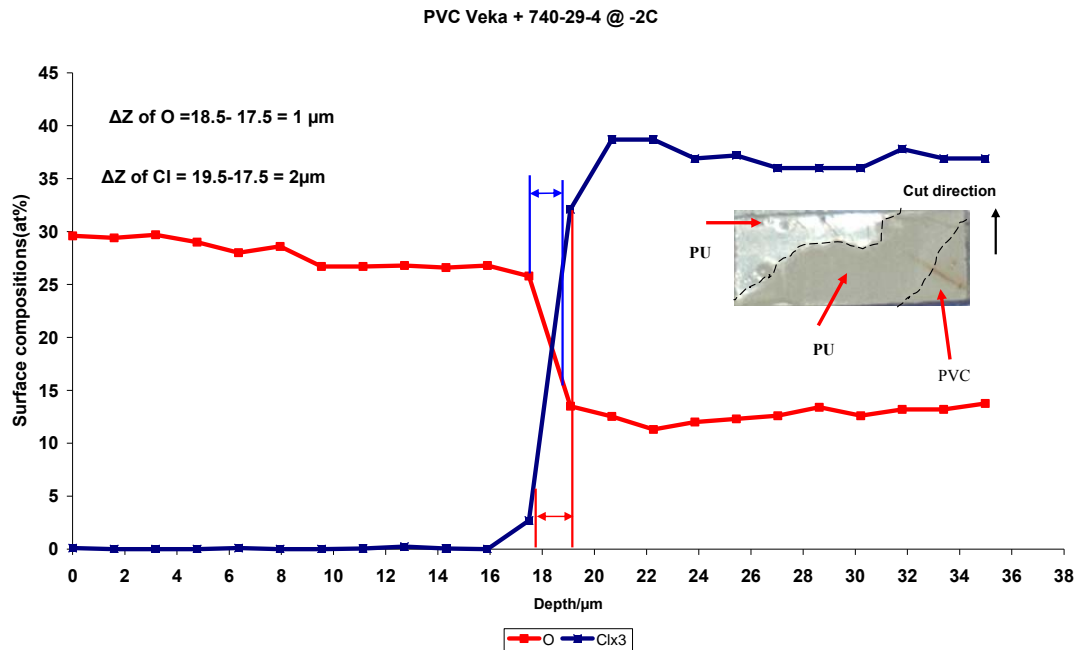


Figure 4-62 Variation in Cl and O concentrations across a C-ULAM- $-2^{\circ}\text{C} \pm 2$  produced taper through a buried PU 740-29-4/PVC interface region. Each successive analysis point increased the analysed depth by 1.6 $\mu\text{m}$ . Inset is a digital image of C- ULAM produced taper of PU 740-29-4/PVC.

Figure 4.61 shows the variation in Cl and O concentration along a C-ULAM ( $-2^{\circ}\text{C} \pm 2$ ) produced taper across a buried PU 740-29-4/PVC -V interface region. The reason why Cl and O were chosen amongst all elements of PU 740-29-4 and PVC was that, the oxygen was present only in PU 740-29-4 and chlorine was only in PVC. The surface of the PVC-V was untreated; National Starch coated the PU 740-29-4 onto the PVC-V surface. There were 23 points of analysis on C- ULAM produced taper of PU 740-29-4/PVC and the analysed depth of each successive analysis point increased by 1.6  $\mu\text{m}$ . The initial analysis point (depth = 0  $\mu\text{m}$ ) was within the PU 740-29-4 region, whilst the final point of analysis (depth = 35  $\mu\text{m}$ ) was in the PVC bulk. In the inset in Figure 109 is a digital image of the sample. Because the concentration of Cl was low in Figure 109 its intensity has been multiplied by three to be more visible on the graph. The width of the interfaces in Figure 4.14 were obtained using the following calculations,  $\Delta Z$  of Cl = 19.5 - 17.5 = 2  $\mu\text{m}$ ,  $\Delta Z$  of O = 18.5 - 17.5 = 1  $\mu\text{m}$ . The PU FRD-74-29-4 hot melt adhesive penetrated 1 $\mu\text{m}$  into the PVC-V substrate. The PU FRD 740-29-4 hot melt adhesive had less penetration into the PVC than UV primer. It is associated with the way the UV primer was applied to the PVC substrate in the liquid phase.

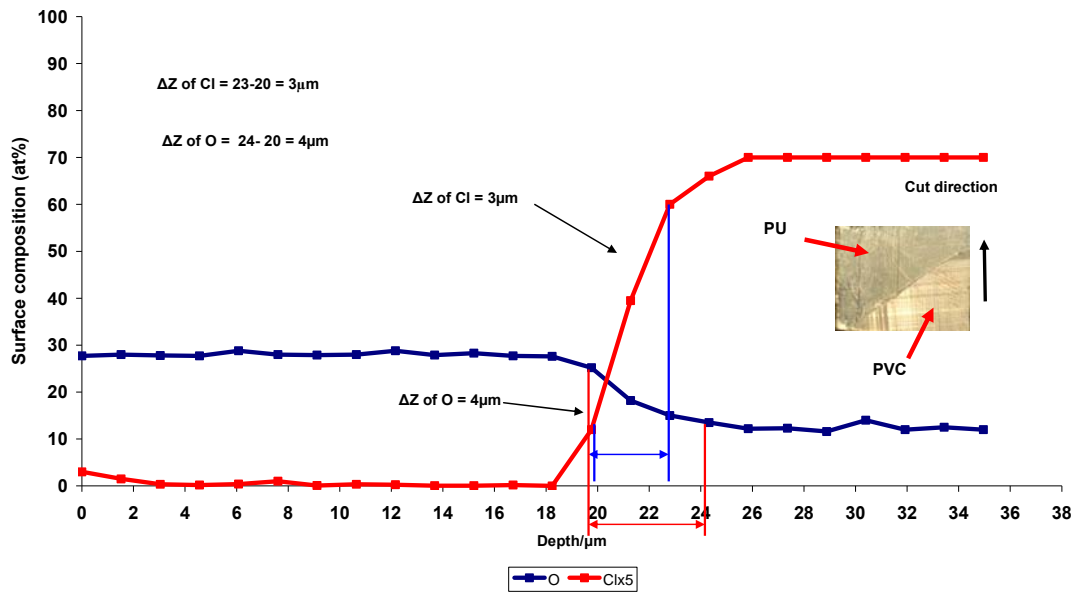


Figure 4-63 variation in Cl and O concentration along a C-ULAM produced taper across a buried PU 740-29-4/PVC 4 + release agent interface region. Each successive analysis point increased the analysed depth by 1.5μm. Inset is a digital image of a PVC-V sample.

Figure 4.63 show the variation in Cl and O concentration traversing a C-ULAM produced taper across a buried PU FRD-740-29-4/PVC 4 with release agent interface region. The surface of the PVC was modified by flame treatment technique more than one hundred days before the PU FRD-740-29-4 was coated onto the PVC. An XPS linescan analysis using a X-ray spot size of 100μm was employed to characterise C-ULAM produced taper through a buried PU FRD-740-29-4/PVC 4 + release agent interface. There were twenty-four points of analysis and the distance between successive analysis points (step size) was 218 μm. Each successive analysis point increased the analysed depth by 1.5 μm. The inset in Figure 110 is a digital image of the sample, in which are observed two regions. The PVC -V with release agent region is in the lower right hand corner of the inset in Figure 110, and the PU 740-29-4 is in the upper left hand corner of the figure. In Figure 110, the ΔZ of Cl and O was obtained from the following calculations: ΔZ for O = 24 - 20 = 4 μm and ΔZ of Cl = 23 - 20 = 3 μm. By comparing, Figure 4.14 with Figure 110, the results show that the ΔZ of O increased after flame treatment of PVC from 1μm to 4μm. Hence, flame treatment had an effect on penetration of the PU hot melt adhesive into PVC. The PU 740-29-4 had greater penetration when applied to modified PVC than unmodified PVC.

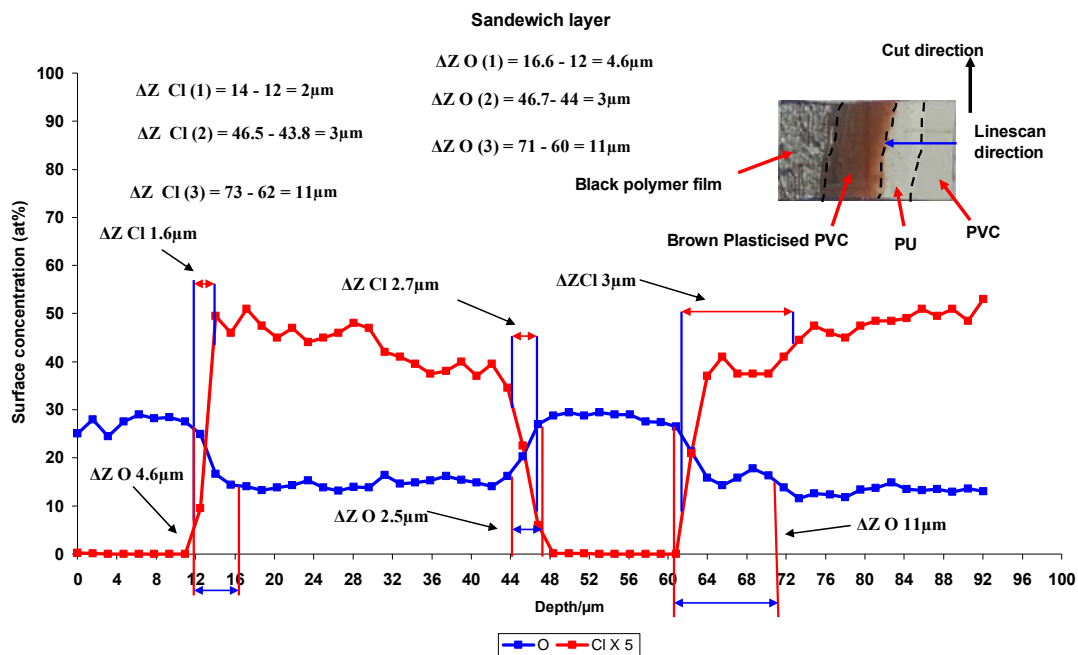


Figure 4-64 Variation in Cl and O concentration change a C-ULAM ( $-2^{\circ}\text{C} \pm 2$ ) produced taper across a buried plasticised PVC /PU 740-29-4/PVC 4 + RA interface region. Each successive analysis point increased the analysed depth by  $1.5\mu\text{m}$ . Inset is a digital image of the PVC-V sample

Figure 4.64 shows the variation in Cl and O concentration along a C-ULAM ( $-2^{\circ}\text{C} \pm 2$ ) produced taper across a buried PU 740-29-4/PVC 4 with release agent/ brown plasticised PVC/top polymer film (black) interface region. The surface of the PVC was flame treated more than one hundred days before it was bonded to the plasticised PVC using the PU 740-29-4 hot melt adhesive. As it is discussed in chapter 3 Figures 60, the PVC plasticised film was twin extruded and it was made of more than two different thin polymer films extruded together.

XPS linescan analysis with a spot size of  $100\mu\text{m}$  and a step size of  $222\mu\text{m}$  was employed to analyse the C-ULAM produced taper across a buried plasticised film/PU/PVC. There were sixty points of analysis and the analysis depth between each successive point was increased by  $1.5\mu\text{m}$ . In Figure 4.16 the analysis point for depth =  $0\mu\text{m}$  is within the black polymer film region and the final point is in PVC 4 with release agent region at  $92\mu\text{m}$ . Inset in Figure 4.65 is a digital picture of the sample in which four regions are observed which are from the right to left PVC/ PU 740-29-4/brown plasticised/black polymer film. In Figure 4.65 because the concentration of Cl was low, it was multiplied by five to be more visible. The sample in Figure 4.65 was sandwich layers; therefore it has three interfaces and four surfaces. Figure 4.65 is a digital image of the sandwich layer,

the first region on the left hand side of inset is top polymer film (black). Three other regions are brown plasticised PVC, PU 740-29-4 and PVC V 4 with release agent.

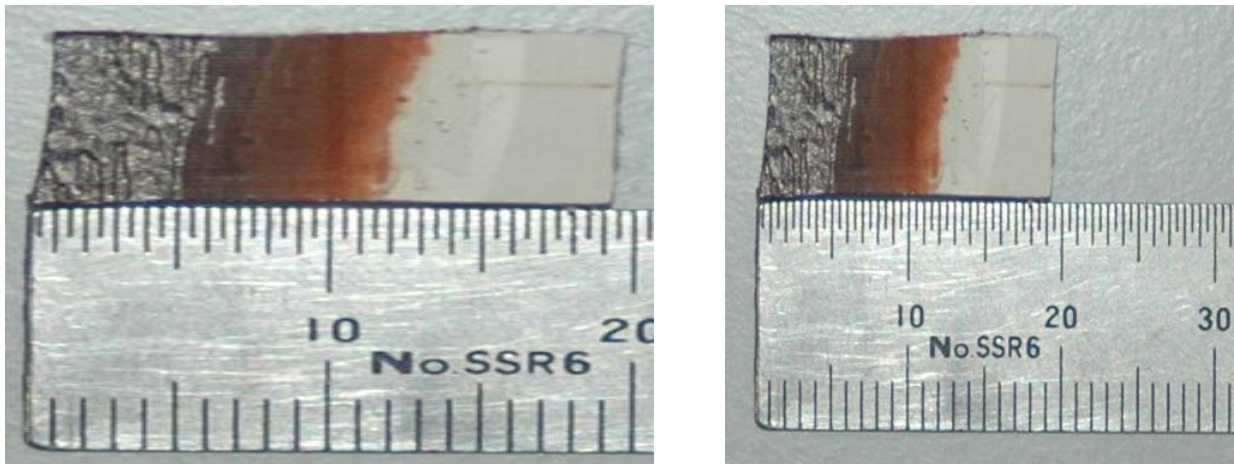


Figure 4-65 Picture of two different sample that have Microtomeed than analysed by XPS line scan analysis

The  $\Delta Z$  of the interfaces were obtained using the follow calculations:  $\Delta Z$  of Cl 1 ( Top polymer film (black)/ brown plasticized) =  $14 - 12 = 2$  ( $\mu\text{m}$ ), the  $\Delta Z$  of O 1 =  $16.6 - 12 = 4.6$  ( $\mu\text{m}$ ). The  $\Delta Z$  of Cl 2 (brown Plasticised/ PU) =  $46.5 - 43.8 = 3$  ( $\mu\text{m}$ ), the  $\Delta Z$  of oxygen 2 =  $46.7 - 44 = 3$  ( $\mu\text{m}$ ). The  $\Delta Z$  of CL 3 (PU/PV) =  $73 - 62 = 11$  ( $\mu\text{m}$ ), and the  $\Delta Z$  of O 3 =  $71 - 60 = 11$  ( $\mu\text{m}$ ). Variation in O concentration change a C-ULAM ( $-2^\circ\text{C} \pm 2$ ) produced taper across a buried plasticised PVC /PU 740-29-4/PVC 4 + RA interface regions shows, penetrations of the PU into PVC as well as plasticised film. Also the  $\Delta Z$  of oxygen in all the buried interfaces was greater than chlorine  $\Delta Z$ .

Figures 4.66, 4.67 and 4.68 exhibits the results of line scan analysis on samples 3729, 3729 70D and 3728 70D. The differences between these three sandwich layer samples are:

- The sandwich layer samples 3729 and 3729 70D produced by bonding the same material and same adhesive Hot melt PU, but the sample 3729 70D was kept in storage at  $70^\circ\text{C}$  steam environment after bonding.
- Primer 6B-23 was applied on the surface of the Rigid PVC V before Hot melt PU adhesive was applied.

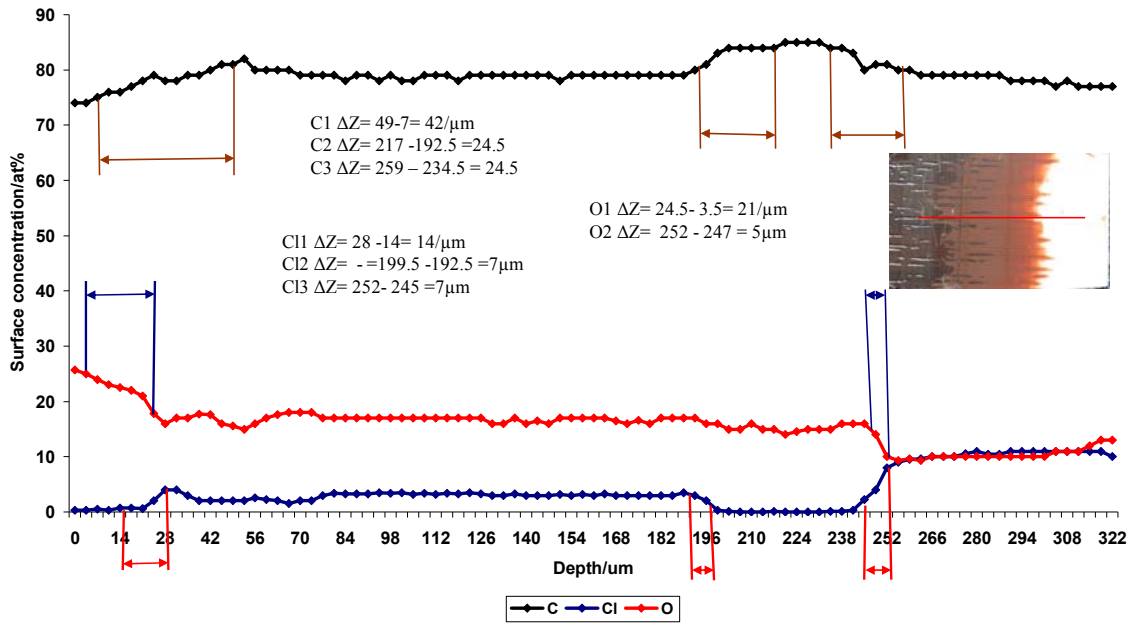


Figure 4-66 Variation in Cl and O concentration change a C-ULAM (-2°C ± 2) produced taper across a buried plasticised 3729 interface region. Each successive analysis point increased the analysed depth by 1.5μm. Inset is a digital image of the PVC-V sample.

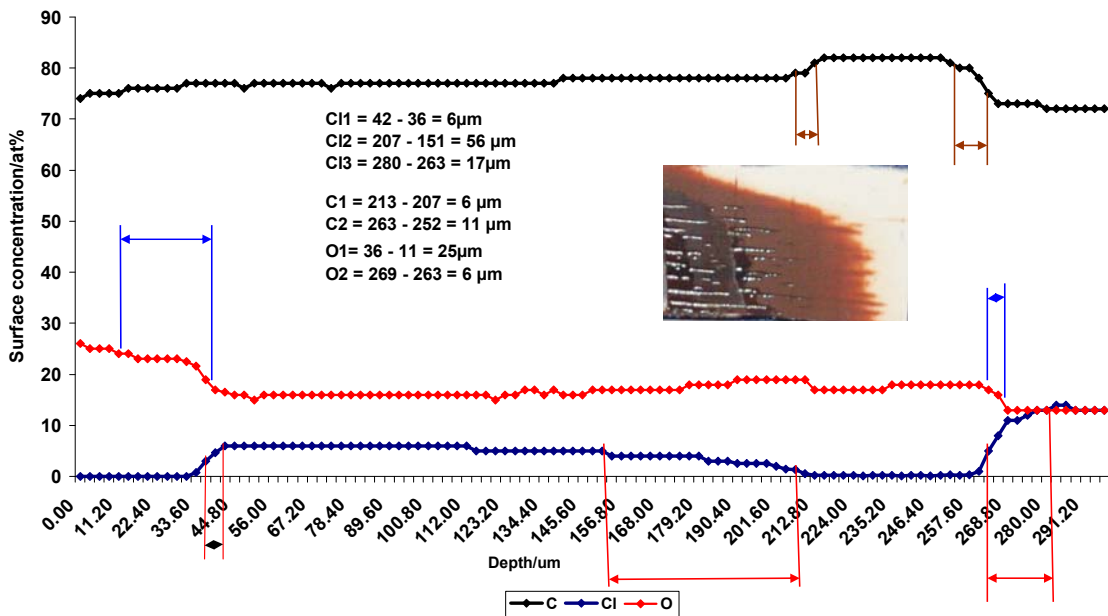


Figure 4-67 Variation in Cl and O concentration change a C-ULAM (-2°C ± 2) produced taper across a buried plasticised PVC 372970D4 + RA

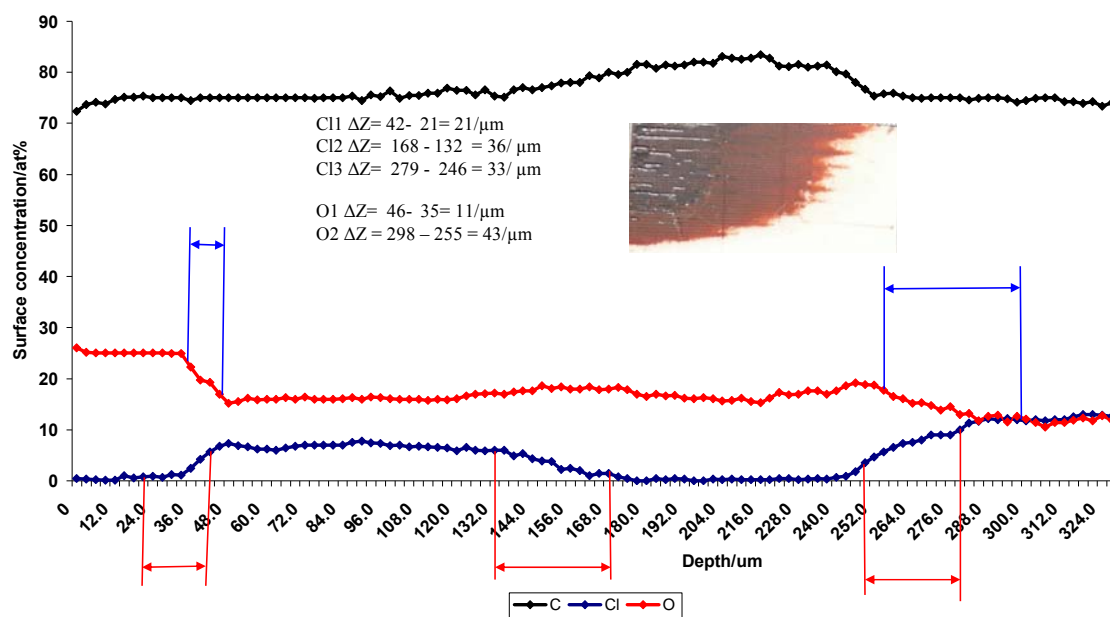


Figure 4-68 Variation in Cl and O concentration change a C-ULAM ( $-2^{\circ}\text{C} \pm 2$ ) produced taper across a buried plasticised 3728 70 D

#### 4.17 DMA of sandwich layer

The sandwich layers 3728 and 3729 were assembled at Henkel in Germany and then supplied for examination. The difference between the two samples was that on the sandwich layer 3728, hot melt adhesive was applied on to the surface of the PVC profile and then Primer 6B-23 was applied.

The sandwich layer 3729 did not have any primer on the surface of the PVC, and just hot melt adhesive was applied on the surface of PVC and bonded to plasticised PVC folder.

Both of the samples were stored in warm air storage with temperature of 120 for 30 minutes then kept at  $70^{\circ}\text{C}$  for aging for 7 days.

The figure 4.69 shows the comparison of the loss modulus results of 3728 and 3729. The graphs indicate that the loss modulus of the (sandwich layer 3728) were greater than the Sandwich layer 3729. This change was an effect of the primer 6B-23, which was applied on the surface of the PVC before PU adhesive applied on the surface of PVC. So using the Primer has increased the adhesive property for better bonding.

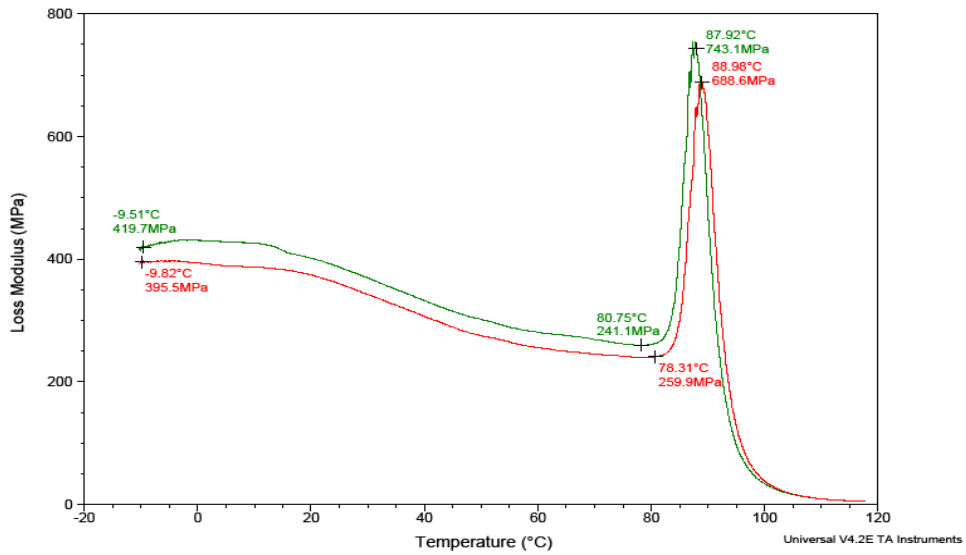


Figure 4-69 comparing loss Modulus of 3728 and 3729

The Figure 4.70 shows the result compression of the Storage modulus of sandwich layer 328 wit sandwich layers 329. The graphs indicate the change of storage modules of samples 328, after applying the primer was not significant.

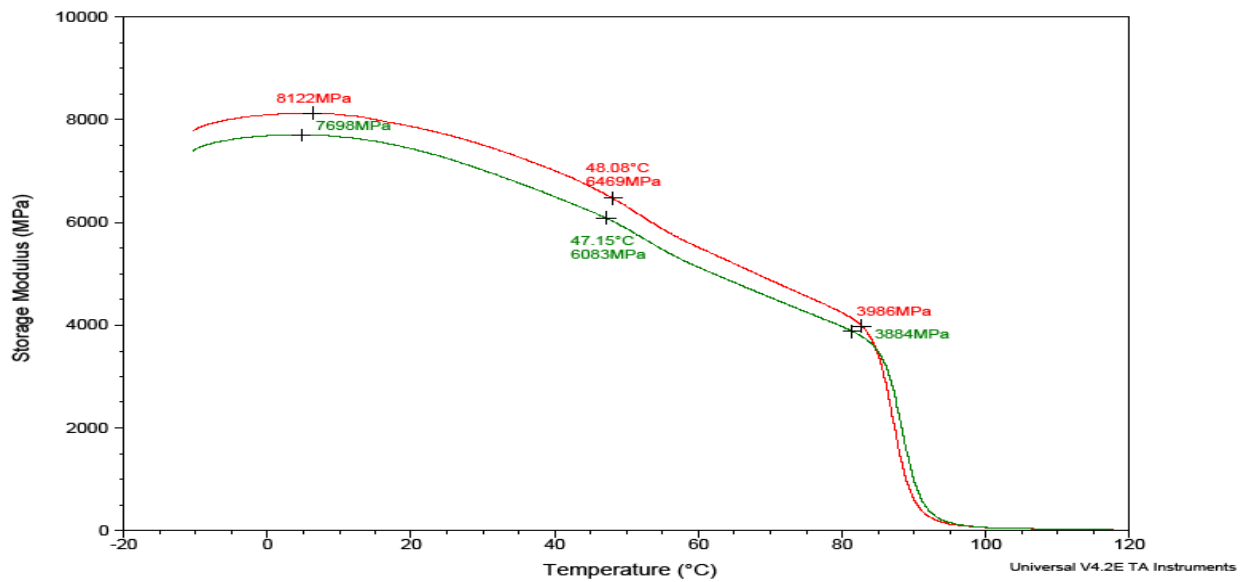


Figure 4-70 Storage Modulus of 3728 and 3729

# Chapter 5

## 5 Conclusions

### 5.1 *Review of literature*

The review of the literature presented on the surface modification of the PVC by flame treatment technique showed significant limitations. There are published work on the surface treatment of PVC with other surface modification techniques such as, Zhao et al (1998) ultrasonic etching, Dumitrascu et al corona discharge (2001), Godbey, D.J et al, (1997) and Vladkova et al Ion-plasma treatment (Cohen, 1989). However, there is very few published work on the surface treatment of PVC by flame treatment technique. One of the few works in this area was published in US Patent 5879495; in this patent Evans (1999) mentions flame treatment as one of his claims in his patent list, but he did not perform any experiments. The patent is titled 'PVC pallets and the like', but there is no evidence of any experimental work in this patent. Also there is no evidence of any published data on flame treatment of commercial PVC (PVC window profile). This suggests that the surface modification of the commercial PVC has not been studied before.

### 5.2 *Degradation of PVC*

Investigation of the X-ray degradation of Pure PVC and commercial PVCs were carried out to determine the maximum time a PVC samples can be exposed to an X-ray source, where X-ray has minimum effect on the surface of PVC.

A degradation study on pure PVC was successfully carried out employing XPS, ToF-SIMS, XPS line scan and EDX analyses. The results suggested that a XPS analysis of pure PVC should not be carried out for more than 10 minutes using a twin anode X-ray source because after 10-minute of X-ray exposure the PVC samples starts to degrade rapidly. The distance between the sample and X-ray source has an influence on the rate of degradation; therefore, in order to compare the degradation index of different samples this distance, during the analysis of samples should be kept constant.

In most published data the damage has been assessed by measuring the reduction in Cl relating to the intensity of Cl/C by assessing the Cl/C ratio. This does not distinguish by carbon of C 1 from reduction in Cl signal, because of C disposition in the form of contamination this is always positive though it's out gassing of solvent of other impurities in the PVC. A unique method was used in this work to approve the decreasing of Cl in PVC by coating 1mm diameter of gold on top of the specimens.

In this work the ULAM technique has been enhanced by in situ cooling of the samples using a cryo-stage (C-ULAM). During the sectioning, the PVC peeled off from the sample. A number of techniques were tried to develop a new way of transferring the cold from the cooling stage to the specimens. Finally, the PE block was replaced by a copper block. A spirit level was used to level the copper block in the vertical and horizontal direction (as reference points), then as a substitute for the ULAM angled section block, the specimen clamp with copper block was adjusted to set the block of copper to the desired angle. A clock gage with a magnetic base was used to set up the desired angle for the copper block, in this case the copper block was tilted, so that the outer edge of the copper block was increased by a height of 250 $\mu$ m compared to the opposite edge. Hence, the difference in height between the two edges of the copper block was 250  $\mu$ m; therefore, the angle of the slope between the two edges of the copper was calculated angle ( $\theta$ ) between 0.4° - 0.8°.

After the PE block was replaced by a copper block the temperature of the samples could be reduced to -2°C  $\pm$  2°C, therefore, specimens of pure PVC were sectioned at -2°C  $\pm$  2°C, with a taper angle ( $\theta$ ) between 0.4° - 0.8°. The Cryo-Ultra low angle microtomy (C-ULAM) processing of the samples was carried out

Initially (C-ULAM), XPS linescan analysis, ToF-SIMS analysis were employed to find depth of the degradation as function of time and X-ray exposition.

The result of degradation index of pure PVC obtained from the EDX and XPS analysis after 10 minutes X-ray exposure was similar (5%). After 70 minutes of X-ray exposure the degradation index obtained from XPS for pure PVC was 53%, while that from EDX was 30%. This was due of different depth of analysis between two techniques. The depth of analysis of XPS is about 5nm, but depth of analysis in EDX is about 2 $\mu$ m.

The XPS - line scan analysis compositional depth profile obtained along a C-ULAM produced taper, through pure PVC which had been exposed to X-ray radiation, showed that after 70 minutes the depth of degradation of the pure PVC sample was approximately 17.6 $\mu$ m.

The degradation studies of the PVC V and R profile with release agent showed that the release agent had an effect on the degradation of the PVC samples because the PVC was under the release agent. The surface concentration of Cl in PVC V and R increased when the release agent was removed from the surface of the samples. By comparing the first and last XPS survey spectra acquired for pure PVC, PVC-V and PVC-R samples, in the degradation experiment, after 93 X-ray exposure there was evidence of decreasing in surface concentration of chlorine and increasing in surface concentration of carbon on the surfaces of pure PVC, PVC-V and PVC- R samples. By sputter coating a 1mm diameter gold disc on to the all PVC V, R and PVC plasticised samples surfaces, it was shown that the Cl/C ratio decreased due to X-ray degradation, however, the Au/C ratio remained constant suggesting there was no redeposition of C on to the surface of the PVC V, R and plasticised PVC samples.

The degradation of the plasticised PVC foil was investigated. Hence, as the sample was exposed to the X-ray source, heat from the X-ray source would cause thermal degradation on the plasticised PVC. Indeed the chlorine, which came from degradation of the PVC layer beneath the top polymer layer, was segregate on the surface of foil resulting in chlorine enrichment of the surface of sample. That's why the degradation index value of plasticised foil was negative value.

By comparing the negative ion ToF-SIMS spectra from the bulk and degraded regions of pure PVC exposed to X-rays for 70 minutes, significant intensity change in the Cl and Cl<sub>2</sub> species. The intensity of the Cl and Cl<sub>2</sub> species irrespective of mass decreased in the negative ion spectra from the degraded region. The chlorine intensity in the ToF-SIMS spectra from the bulk PVC region was much greater than the intensity of chlorine in the degraded region. These results are associated with the dehydrochlorination of the PVC after 70 minutes exposure to X-rays. This result matched the result of the XPS line scan of the pure PVC film exposed to X-ray with same conditions, thus the surface concentration of the Cl in bulk PVC region was greater than surface concentration of Cl in degraded region.

### **5.3 Surface treatment**

The surface chemistry of all of the untreated and treated PVC R and V samples were characterised by XPS. By comparing XPS of the treated PVC samples with the untreated PVC samples we observed an increase in the oxygen and a decrease in the carbon surface concentrations for all treated PVC samples. As more oxygen functional groups were introduced in to the surface of the PVC samples, the surface free energy of the surface increased. Hence the surface modification of the PVC by flame treatment increased the surface free energy, ie; more wettability and hydrophilic. By comparing the result of CAM obtained from untreated and the treated PVC samples it is clear that the contact angle of treated PVC samples can be reduced by as much as 30°. The CAM results of treated PVC samples were constant even one year after the flame treatment was carried out.

The surface chemistry of untreated and treated PVC samples were also characterised by ToF-SIMS analysis. The result of ToF-SIMS, XPS and CAM are in agreement. By comparison of the result of ToF-SIMS obtained from untreated PVC samples with treated PVC samples, it is clear that the relative intensity of hydrocarbon ions decrease for the treated PVC samples. The effect of the surface treatment at the relative intensity of acrylic ions was different from one sample to another. The relative intensity of acrylic ions decrease for treated PVC V1 and V2 and increased for PVC V2plain in comparison to the untreated samples. The Irgafos 168 and Irganox 1010 were observed in ToF-SIMS analysis, obtained from both PVC samples with different surface concentrations. The surface concentration of Irganox 1010 and irgafos 168 in PVC R samples were greater than PVC V samples. The effect of the surface modification of PVC samples on Irgafos and Irganox were different between samples. The surface concentration of Irganox and Irgafos in the treated PVC V1sample was decreased, while they increased for PVC V2 and V2 plain in comparison to the untreated PVC V2 samples. The results for PVC R samples were different; we observed an increase in surface concentration of Irganox and Irgafos in treated PVC R1 and decrease in PVC R2 and R2 plain in comparison to the untreated samples.

Washing the surface of the treated PVC with hexane twelve months after surface modification resulted in an increase in contact angle of 30 °, and an increase in the surface concentration of Cl. The effect of the flame treatment was quite robust even after

twelve months from flame treatment, when the surface of the samples were analysed by different technique resulting stability on the surface of the treated samples. The contact angle of the treated sample after washing by hexane is 20° lower than the untreated sample.

Commercially the surface of the PVC profile will be modified by the flame as the release agent remained on the surface of the profile. In this study in order to have mimicked the commercial work, PVC V profile was modified by flame treatment when the release agent was on the surface of the PVC.

The surface properties (topography and morphology) of all PVC V and R sample before and after surface modification were characterised by AFM. Topographic and phase images were obtained for all samples at few different scan area with size of 10  $\mu\text{m}^2$ . The existence of a thin layer on the surface of the samples with release agent on the surface (PVC V1, V2, R 1 and R2 before flame treatment) is observed, when characteristic smoothing of the surface relief was observed at low tapping amplitude. In order to characterise the surface of the PVC buried under the release agent layer, the tapping amplitude increased 2 to 3 times to allow penetration of the SPM tip through the release agent layer.

The 3D topography of the surface and section analysis spectrum of all PVC V samples before and after flame treatment has been taken by AFM. The result indicates that, on 3 D topography image obtained from PVC V1, there is evidence of smooth surface in microstructure, which is the surface of the release agent. By increasing the tapping amplitude image, it was possible for the tip to penetrate through release agent layer and characterise the surface of the PVC V1 sample before flame treatment.

The 3 D topography image of the treated PVC V1 shows the distance between highest and lowest point of the surface. This distance was 113.93nm before flame treatment. After flame treatment of the PVC V1 the release agent and the surface of the sample fused together and produced new polymeric surface. The height of surface feature in the 3 D topography obtained from treated PVC V1 image reduced to 33.239nm. The AFM result obtained from PVC V2 was similar to the AFM result obtained from PVC V1 which showed the surface features reduced from 433.83 nm to 20.205nm

But 3 D topographic image obtained from PVC V2 plain before flame treatment showed the height of surface features was 377.58nm, this result reduce after flame treatment image 124.88nm.

The AFM result obtained from PVC V samples was different from the result obtained from PVC R samples. In the case of the PVC V 1 and 2 samples, after flame treatment the release agent was fused to the surface of the PVC samples. The surface of the treated PVC V1 and V2 was smoother than surface of the untreated PVC V1 and V2 (reduce in surface roughness). While the surface of the PVC V2 plain was treated by flame, it resulted in an increase in surface roughness.

When the surface of PVCs R samples was modified by flame, there were increases in the surface roughness of the all treated PVC R samples with and without release agent.

The DMA results of untreated and treated PVC samples were characterised 19 months after flame treatment. The results show the remarkable effect of flame treatment on viscoelastic properties of the PVC samples. Although the measurement was carried out several months after surface modification of the sample but it has been shown that the effect of the treatment was stable.

We compared the results of the storage Modulus obtained from the PVC V with release agent before and 19 months after flame treatment. The storage modulus of the PVC V with release agent has changed from 9269 MPa before surface treatment to 11136MPa after surface treatment. This indicates that the material has a higher stiffness and strength after the process of flame treatment. This is an increase of 20% in storage modulus which is directly due to penetration of the release agent onto the PVC surface.

The results of Tan delta as well as glass transition temperature (Tg), which was obtained from the PVC V with release agent before and 19 months after the flame treatment. The results indicate that, the effect of flame treatment on tan delta profile is not significant. Also the Tg results shows, no significant change indicating the in the nature of the material after the flame treatment has not changed.

In order to study the effect of the release agent on the mechanical property of the PVC samples after flame treatment, two PVC V samples from the same batch, with and without release agent, under the same conditions have been characterised by DMA.

Result of storage modulus and loss modulus were obtained from PVC V with release agent , and PVC V without release agent, which both of surfaces, were treated by flame treatment at the same time under the same conditions.

The DMA plots indicate that, when the PVC sample treated by flame while the release agent is on the surface of the PVC, the release agent and PVC promote a strong bond and therefore become one solid sample together. These resulted in an increase of 10% in storage modulus from 8083 MPa for samples without RA to 8822 MPa for samples with RA. These results are in agreement with the results from AFM analysis, as described in previous page, that the AFM 3D topographic images obtained from the PVC samples with release agent before and after flame treatment shows that the surface of the PVC samples after flame treatment is much smoother than before flame treatments, which was more uneven and bumpy. However the loss modulus plots do not seem to be significantly affected by the differences in the presence of RA

#### **5.4 Analysis of PU**

XPS was employed to study the change in surface composition of elements as a function of life time of the PU (FRD-740-29-1, 2, 3 and 4) adhesives. In order to prepare sample for XPS analysis, a thin layer of the adhesive deposited on the aluminium foil substrate with the help of a calibrated cube. A 25mm Cube Applicator manufactured by Sheen Instruments Ltd with film width of 16mm and two standard gaps of 37 and 75 $\mu$ m was employed to deposit a thin film of adhesive on to aluminium foil while the adhesives were still liquid. A thin film of each adhesives was deposited on sample stub for XPS analysis as a reference (time zero) sample.

Changes in surface composition as a function of time of PU reactive hot melt adhesive was investigated for three months using XPS analysis. The outcome of this study was that the PU 740-29-4 had the best stability amongst all four reactive hot melt PU adhesives investigated. Therefore, this PU adhesive was chosen to use as best bonding agent amongst all the four PU adhesives, to use for bonding of rigid commercial PVC to plasticised PVC film.

In order to produce a specimens made of PVC 4 with release agent (three months after surface treatment) , the FRD 740-29-4 PU was heated in an oven and coated on to the surface of PVC 4.

But in the case of the sandwich layer, made of PVC 4 with RA/ PU 740-29-4/ plasticised PVC film, the PU adhesive was deposited on to the PVC 4 with release agent substrate, then the plasticised film was bonded to the adhesive.

## **5.5 Line scan analysis**

In the field of adhesion, for the study of the interaction between a molecule and a solid substrate there are two parameters of significance; first is the capacity of the solid surface to adsorb the molecule, second is bonding between adhesive and substrate (penetration of adhesive into the substrate)

It was possible to section the specimen of PVC Veka coated with UV primer using microtomy at room temperature as well as  $-2^{\circ}\text{C} \pm 2$ .

The tapering of the specimens (PVC coated by hot melting PU adhesive) was performed on same instrument as degradation chapter. In terms of tapering and sectioning of the polymeric adhesives, coating and polymeric substrate were very soft and therefore it was impossible to cut them at room temperature. During sectioning the PU coating was peeled off from the substrate instead of being sectioned. The ULAM technique has been enhanced by in situ cooling of the samples using a cryo-stage (C-ULAM). By employing the C-ULAM employed, the temperature of the samples could be reduced to  $-2^{\circ}\text{C} \pm 2$ . Therefore, specimens made of PVC 4 with RA/ PU 740-29-4/ plasticised PVC film, were sectioned at  $-2^{\circ}\text{C} \pm 2$ .

A schematic of the ULAM set up as employed in production of the ultra-low angle tapers a variation on the ultra-low-angle microtomy technique (C-ULAM) has been developed to impart an ultra-low angle taper through a polymer multilayer at  $-2^{\circ}\text{C} \pm 2$ . XPS linescan analysis of the buried interface of the samples shows the penetration of the PU topcoat into the PVC from 2-4  $\mu\text{m}$ .

The UV primer shows greater penetration into the PVC than the reactive hot melt PU adhesive due to its application in the liquid phase at ambient temperature. The reactive hot melt PU adhesive was coated onto the PVC at 120-130 $^{\circ}\text{C}$ . This was an effect of the temperature and the method used to deposited UV primer on PVC. But the  $\Delta Z$  of the oxygen increased when the PU hot melt adhesive was coated onto flame treated PVC surface, and it had greater penetration.

An XPS linescan analysis using an X-ray spot size of 100 $\mu$ m was employed to characterise C-ULAM produced taper through a buried PU FRD-740-29-4/PVC 4 + release agent interface. There were twenty-four points of analysis and the distance between successive analysis points (step size) was 218  $\mu$ m. Each successive analysis point increased the analysed depth by 1.5  $\mu$ m. The inset in Figure 110 is a digital image of the sample, in which we observed two regions. The PVC -V with release agent region is in the lower right hand corner of the inset in Figure 110, and the PU 740-29-4 is in the upper left hand corner of the figure. In Figure 110, the  $\Delta Z$  of Cl and O was obtained from the following calculations:  $\Delta Z$  for O = 24 - 20 = 4  $\mu$ m and  $\Delta Z$  of Cl = 23 - 20 = 3  $\mu$ m. By comparing, Figure 4.14 with Figure 110, the results show that the  $\Delta Z$  of O increased after flame treatment of PVC from 1 $\mu$ m to 4 $\mu$ m. Hence, flame treatment had an effect on penetration of the PU hot melt adhesive into PVC. The PU 740-29-4 had greater penetration when applied to modify PVC than unmodified PVC.

Variation in O concentration along the C-ULAM (-2°C  $\pm$  2) produced taper across sandwich layer, and the difference between  $\Delta Z$  of O and Cl show, penetration of the PU into PVC and plasticised PVC film. The  $\Delta Z$  of O in all interfaces was greater than Cl  $\Delta Z$ .

Line scan analysis of sectioned sandwich layer of samples 3729, 3729 70D and 3728 70D was carried out.

The difference between the two samples were, that although both of them were produced by the same PVC and same hot melt polyurethane adhesives, in the case of sandwich layer 3728, the primer 6B-23 was applied on the surface of PVC before PU was deposited to PVC as surface modification agent.

The sandwich layer 3729 did not have any primer on the surface of the PVC, and just hot melt adhesive applied on the surface of PVC and bonded to plasticised PVC folder.

Both of the samples were stored in warm air storage with temperature of 120°C for 30 minutes than kept at 70°C for aging for 7 days.

The effect of the Primer 6B-23 showed an increase in the penetration of the PU adhesive into the PVC as well as plasticised PVC.

DMA Analysis

In order to study the mechanical property of sandwich layer samples, made of (Rigid PVC/PU adhesive/ Plasticised PVC), with different curing system the Dynamic mechanical analysis (Three point bending/ DMA) of all sandwich layer and samples were carried out 19 months after they have bonded together.

The MDA result indicated that using Primer 6B-23 increases the loss modules and decrease the storage modules of the sandewich layer.

## **5.6 Future work**

The future work of this project should continue with considering followings points:

At the production line of the PVC profile replace water cooling by air cooling. This technique stops the contamination of the water transfer to the surface of the PVC. the contamination causes boundary layer that stops the adhesive from penetrating to the PVC bulk.

Surface modification (Flame treatment) should take place immediately after cooling the PVC profile down by the air cooling system, than bonding to the plasticsised PVC using PU hot melt adhesive at the same time. This technique first of all stops any contamination on the surface of PVC. And also, the PVC profiles do not need the protection film.

The above suggestions save energy, speed up the work and increase the quality, stability and durability of the bonding.

For any future XPS analysis with twin anode, they have to follow the manner that has been used in this work to minimize the degradation of the PVC.

In the formulation of the PVC profile there are some additives and fillers such as acrylate material and PE resin, which segregate to the surface of the PVC and work as boundary layer. The percentages of these additives in bulk of PVC should reduce, than the mechanical test, surface analysis including CAM of PVC with new formulation should carried out to find optimum formulation with good adhesive and mechanical property of PVC profile.

We found that the flame treatment is the most effective surface modification technique of PVC profile to date. In order to save energy and time the surface treatment of a few profiles under the same burner at the same time can be carried out.

## References

- Arias, G et al, 2006. Crosslinking of PVC formulation treated with UV light. *Jornal of vinyl & additives technology*, 12(2), pp.49-54.
- Arki, E & Balkos,D, 2002. Tin soap in emulsion PVC heat stablization. *Advance in polymer technology*, 21(1), pp.65-73.
- Arki, E and Balkose, D, 2002. Tin soap in emulsion PVC heat stablilization. *Advance in polymer technology*, 21(1), pp.65-73.
- Artyushkova, K & Fulghum, J.E, 2001. Quantification of PVC-PMMA polymer blend compositions by XPS in peresent of x-ray degradation effects. *Surface and interface Anal*, 31, pp.352-61.
- Atzei,D et al, 2003. Radiation-induced migration of additives in PVC-based biomedical disposable device part 2. *surface analysis by XPS*, 35, pp.673-81.
- Barnes,H.A et al, 1996. *An Introduction tp rheology*. Amesterdam: Elsevier.
- Bassali, W.A., 1957. The transvers flexure of thin elastic disc supported at several point. *Proc Cambridge phil.Soc*, 53, pp.728-48.
- Beamson, G & Briggs,D, 1992. *High resolution of organic polymers*. Chichester: John Wiley & sons.
- Beamson,G & Briggs,D, 1992. *High Resolution XPS of organic polymer*.
- Beamson,G & Briggs,D, 1992. *High Resolution XPX of organic polymer*. Chichester: John Wiley & sons.
- Bert, F., 2004. The use of saytex RB-1930/9170 low viscosity Brominated flame retardant polyols in HFC-245fa and High water formulation. Las Vegas,NV, 2004. Alliance for the Polyurethane Industry Technical Conference.
- Biriggs,D & Seah, M.P, 1987. *Practical surface analysis by Auger and X-ray Phoelectron Spectroscopy*. Chichester: John Wiley & sons.

- Borcia,D & Popa, 2001. Corona Discharge treatment of plastified PVC sample used in Biological enviroment. *Jurnal of applied polymer science*, 81, pp.2419-25.
- BPF, 1995. *PVC Window*. British plastic.
- Bragg, W.H., 2004. *Concerning the natural of thing*.
- Bruyne,N.A & Houwink, R, 1962. *Hand book of Adhesion*.
- Calif, P., 1991. *Source Reduction and recycling of halogenated solvents in adhesive industriy*. Jacobs Engineering Group, Inc.
- Cartz, L., 1995. Nondestructive testing,ASM. *international, Materials Park*, pp.135-36.
- Castel,J et al, 2003. *IEEE Electrical insulation magazine*, 19, pp.25-29.
- Chan, C.M., 1993. *Polymer surface modification and Characterazation*. Munich: CarlHanser,GmbH & Co.
- Cehimi,M.M & Watts,J.F, 1992. *Adhesive-Sci. Technol*, 6, pp.377-93.
- Cehimi,M.M & Watts,J.F, 1992. *Journal of Adhesive Science and technology*, 6, pp.377-93.
- Chen, C et al, 2002. *Macromolecules*, 35(21).
- Clif, P., 1991. *source reduction for chlorinated Solvents*. Adhesive manufacture.
- Cohen,J.M & Castel,J.E, 1988. Scanning auger microscopy of ball-cratered polymer coated steel. In *Inst. Physic conference.*, 1988. Inst,physic conference.
- Cohen, J.M., 1989. *Simultaneous Bulk and surface analysis by X-ray analysis and Auger Electron spectroscopy*. Chichester: Wiley & sons.
- Comyn, J., 1997. *Adhesion Scence*. Cambridge: The Royal Society of Chemistry.
- Comyn, J., 1997. *Adhesion Science*. Cambridge: Royal Society of Chemistry.
- Comyn, J., 1997. *Adhesion Science*. Cambridge: Royal Society of Chemistry.

- Daning, D., 2001. *Polymer technology*. Polymer center of North london University.
- David,D.J & Staly, H.B, 1969. *Analyticalchemistry of Polyurethane*. New York: John Wiley & Sons.
- Daviesand,F.S & Fletcher,I.W, 2005. *Surface analysis of PVC flexible and rigid PVC samples*. ICI measurment scince group.
- DeArmitt, C., 2004. Rasing the softing point of PVC. *plastics additives & compounding*.
- Delassus,P.T & Whitman,N.F, 1999. Physical and mechanical property of some important polymer. *Polymer hand book*, 159-169.
- Dennis, G., 1997. product assemblly with PUR adhesive. *Adhesive age*, p.22.
- Dillingham,R.G & Moriarty,C, 2003. *Journal of adhesive*, 79, pp.269-85.
- Dillingham,R.G & Moriarty,C, 2003. *J. Adhesive* , 79, pp.269-85.
- Eling, B & Phanopolous, C, n.d. *Huntsman -Polyurethane*. Kortenberg: Everslaan.
- Evans, W., 1999. *PVC pallets and the like*.  
<http://www.patentstorm.us/patents/5879495.html>.
- Farben, G., 1937. *See German Patent*. Patent 728.981.
- Forest, 2006. Hot melt adhesive use in kitchen cabinate. *Forest Products jornal Publication*, 1.
- Frisch,K.C & Reegen,S.L, 1971-1979. *Advance in Urethane Scince and technology*. USA: Technomic Pub.Co., Westport,Conn.,USA.
- Godbey,D.J et al, 1997. Thin solid films. 308-309, pp. 470-474.
- Gonzalez, A et al, 1989. Monitoring the UV degredation of PVC window frame by microhardness analysis. *jornal od applied polymer Scince*, 38(10), pp.1879-88.
- Gonzalez, A et al, 1989. Monitoring the UV degredation of PVC window frame by microhardness analysis. *Jornal of applied polymer scince*, 38(10), pp.1879-82.

- Griffin, E.R., 2001. *Analysis of thermoplastics use in fold-and form pipe liners, special focuse PVC modification*. Dupont company.
- Hanton,S.D & Clark,P.A.C, 2000. *Encyclopedia of analytical chemistry*. Chichester: John Wily & sons.
- Hinder et al, 2004. A ToF-SIMS investigation of buried polymer/polymer interface exposed by ultra-low-angle microtomy. *surface and interface analysis*, 36.
- Hinder,S.J et al, 2004. Interface analysis and compositional depth profiling By XPS of polymer coatings prepared using Ultra low -angle microtome. *Surface and interface analysis*, 36, pp.1032-36.
- Hinder,S.J Et al, 2005. The Morphology and topography of polymer surface and interface exposed by ultra low angle microtomy. *Journal of Material science*, 40, pp.285-93.
- Huang,Y et al, 2004. Material properties-characterisation of LLDPE/nano-SiO<sub>2</sub> composite by solid-state dynamic mechanical spectroscopy. *Polymer testing*, 23, pp.9-17.
- Hughes et al, 1997. New polymerreactive hot melt applications Growing the hot melt marketplace. *Hot melt symposium*.
- Kinloch, A.J., 1987. Adhesion and adhesives. *Adhesion and adhesives*, 2(2), pp.1966-67.
- Kinloch, A.J., 1995. *Adhesion and adhesive science and technology*. Cambridge: Chapman and hall.
- Kinloch, A.J., 1995. *Adhesion and adhesive science and technology*. Cambridge: Chapman and hall Cambridge.
- Kugler, T et al, 1999. *Synthetic material*, 100(1).
- Leadley,S.R & Watts, J.F, 1997. *Journal of adhesive*, 60(175).
- Lee, L.H., 1991. *Adhesive bonding*. New York: Plenum press.
- Lee, L.H., 1991. *Adhesive Bonding*. New York: Plenum Press.

- Manfredini, M et al, 2003. Degredation of plasticized PVC for biomedical disposable device under soft x-ray irradiation. *surface and interface Anal*, 35, pp.294-300.
- Mang, J & Wang T, 2000. *Material Science engineering*, 72(2).
- Menrad, K.P., 1999. Dynamic Mechanical Analysis, a practical introduction. *CRC press Ltd*, pp.1-193.
- Michel, E.W., 1978. *Chem biotechnology*, 23, p.765.
- Miki, N et al, 2000. *J. Vac. Sci. Technol*, 1, pp.313-16.
- Pascoe, R.D & Connell, B.O, 2003. Development of method for separation of PVC and PET Using flame treatment flotation. *Minerals engineering*, pp.1205-12.
- peter, 2003. PVC profile. *Technicky Tydenik*, 51(30), p.12.
- Petrie, E.M., 2002. *Hand book of adhesive and sealants*. New York: McGraw-Hill.
- Purdy, A.P.e.a., 1997. pp.308-309 & 486-489.
- Randall, D & Lee, S, 2002. *The Polyurethane Book*. John Wiley & sons.
- Randall, D & Lee, S, 2002. *The polyurethane book*. Jhn Wiley.
- Rosberg, M et al, 2006. *Chlorinated Hydrocarbones in Ullmann's Encyclopedia of industrial chemistry*. Weinheim: Wiley-VCH.
- Rosberg, M et al, 2006. Chloronated Hydrocarbons. *Ullmann's Encyclopedia of industrial chemistry*.
- Ru & Rong, J, 2006. Studies on wettability of medical polyvinyl chloride by remote argon plasma. *applied surface science*, 252, pp.5076-82.
- Saarela, O, 1992. *LAMAD-Laminate design and analysis*,. Otanimi, Faland: Helsinki University of technology.
- Seah, M.P & SPENCER, S.J, 2003. Degredation of Polyvinyl chloride and nitrocellulose in XPS. *Surface and interface analysis*, 35, pp.906-13.

- Shingley, J.E., 2003. *Mechanical engineering design 7th ed.* London: McGraw-Hill.
- Tasi, S.W., 1987. *Composit design, think composite.* USA.
- Test Dyne. [http://www.accudynetest.com/surface\\_energy\\_material.html](http://www.accudynetest.com/surface_energy_material.html). [Online].
- Thiele, L., 2007. *Polyurethane adhesive for industrial applications.* Henkel AG & Co KGaA Germany.
- Thiele, L., 2007. *Polyurethane Adhesives for industrial applications.* Progress Report. KGaA Germany: Henkel AG & Co.
- Tseng, A.A et al, 1990. Polymer testing. *Adv. polymer technology*, 10(3), pp.205-18.
- Tydenik, T., 2003. PVC profile. *Czech*, 51(30), p.12.
- Vickerman, J.C., 1998. *Surface Analysis- The principal techniques.* Chichester: John Wiley & sons.
- Wall, J.M et al, 1979. Composition -depth profiling and interface Analysis and interfac coaying using ball cratering and the scanning auger microprob. *surface and interface analysis*, 1.
- Walls, J.M., 1990. *Method of surface analysis - Technique and applications.* Cambridge university press.
- Wang, J & Wang, T, 2000. *Material science and engineering*, 72(2).
- Wang, Q and B.K, 2005. Polymer testing. *polymer testing*, 24(3), pp.290-300.
- Watts & Wolstenholm, 2003. *An introduction to surface analysiys by EXS and AES.* Chichester: John Wiley & Sons.
- Watts, J.F & Castle, J.E, 1999. *Int. J Adhesive*, 19, pp.435-43.
- Woodman, R.T et al, 1984. Wood fiber as reinforcing fillers for polymer. *polymer engineering and science*, 24(15), pp.1166-71.
- Woods, G., 1990. *The ICI Polyuretaines book.* 2nd ed. New Yourk: John Wiley & Sons.

Woods, G., 1990. *The ICI Polyurethain book*. 2nd ed. New york: Johan Wiley & sons.

Wypych, G., 1977. *Properties of PVC Plastisols*. Wroclaw polymeric press.

Wypych, G., 2008. *PVC Degradation & stablization*. Toronto: Chemtec publisher.

Wypych, G., 2008. *PVC Degradation and stabilization*. Toronto: Chemtec publisher.

Yoshiharal,K & Tanaka,A, 2002. Interlaboratory study on degredation of Poly(Vinyl Chloride),Nitrocellulose and poly(terafluoroethylene) by x-rays in XPS. *Surface and interface analysis Anal*, 33, pp.252-58.

Zenkiewicz, M., 2000. *Adhesion and modification of polymer surface*. WNT, Warszawa.

Zhao et al, 1998. New Etching method of PVC plastic for plating by Ultrasound. *Jornal of applied polymer science*, 68, pp.1411-16.

# Chapter 6 Appendix

## 6 Appendix

### 6.1 Appendix 1

Published Paper

### 6.2 Appendix 2

Table 3: Quantitative surface analyses of flame treated PVC samples

Sample No.	Elapsed Time/day	Surface compositions/atomic %										Release agent
		C	O	N	Cl	Ca	Si	Zn	Na	Pb	F	
PVC Veka	0	83	13	0.3	4	0.4	0.0	0.0	0.0	0.1		✓
PVC Veka	0	73	13	0.0	13	1.0	0.0	0.0	0.0	0.1		
1	1	71	21	1.0	5	0.2	0.8	0.2	0.4	0.3	1	
1	7	67	15	0.0	12	0.0	0.1	0.0	0.0	0.1	5	
1	14	75	17	1.0	4	1.0	2.0	0.0	0.4	0.3		
1	21	66	26	1.0	5	1.0	1.0	0.0	1.0	1.0		
1	28	66	24	1.0	5	1.0	1.0	0.1	1.0	1.0		
2	1	70	23	0.2	5	1.0	0.0	0.1	0.3	1.0		
2	7	68	24	1.0	5	1.0	0.0	0.1	0.9	1.0		
2	14	72	22	1.0	3	0.2	0.2	0.1	0.2	0.1	2	
2	21	68	24	1.0	4	1.0	0.4	0.1	0.6	1.0		
2	28	64	28	1.0	5	1.0	0.4	0.2	0.8	0.4		
2	49	68	24	0.0	4	1.0	0.86	0.05	0.8	0.5		
3	1	73	18	0.3	5	1.0	1.0	0.1	0.8	1.0		
3	7	77	18	0.1	3	1.0	1.0	0.0	0.3	0.4		
3	14	75	18	1.0	4	1.0	0.3	0.0	0.3	0.3		
3	21	75	19	1.0	4	1.0	0.4	0.0	0.1	0.3		
3	28	74	19	1.0	4	1.0	1.0	0.0	0.4	1.0		
3	49	74	20	1.0	4	0.7	0.0	0.0	0.4	0.5		
4	1	71	22	1.0	4	1.0	1.0	0.1	1.0	0.3		
4	7	77	18	0.2	3	0.1	1.0	0.0	0.2	0.4		
4	14	74	18	1.0	3	1.0	2.0	0.1	1.0	0.4		
4	21	65	25	1.0	3	0.2	5.0	0.0	1.0	0.3		
4	28	73	20	1.0	3	1.0	2.0	0.0	0.4	0.3		
4	1	78	12	0.0	8	1.0	0.0	0.0	0.0	1.0		✓
4	7	72	22	1.0	5	0.4	0.0	0.0	0.0	0.1		✓
4	14	71	22	1.0	5	0.2	0.0	0.0	0.0	0.1		✓

4	21	74	21	1.0	4	0.1	0.0	0.1	0.0	0.1		✓
4	28	70	23	1.0	7	0.2	0.0	0.0	0.0	0.0		✓
4	49	69	22	0.0	7	0.3	0.0	0.0	0.0	0.0		✓
4	74	70	22	0.9	6	0.2	0.0	0.0	0.0	0.0		✓

**Table of Parameters used for flame treatment of PVC Veka**

Sam ple No	Gas flow/dm <sup>3</sup> min <sup>-1</sup>	Air flow/dm <sup>3</sup> min <sup>-1</sup>	Oxyg en/ %	Burner gap /mm	Conveyer speed /m min <sup>-1</sup>	Profile	Releas e agent
1	8.2	256	1.9	75	40	90 degree angle shape	
2	6.3	200	1.9	75	30	Thin PVC with line in the middle	
3	6.3	200	1.8	60	30	Thin PVC with line in the middle	
4	10	328	1.7	60	40	Thick narrow PVC	
4	10	328	1.7	60	40	Flat wide PVC	✓

### 6.3 Appendix 3

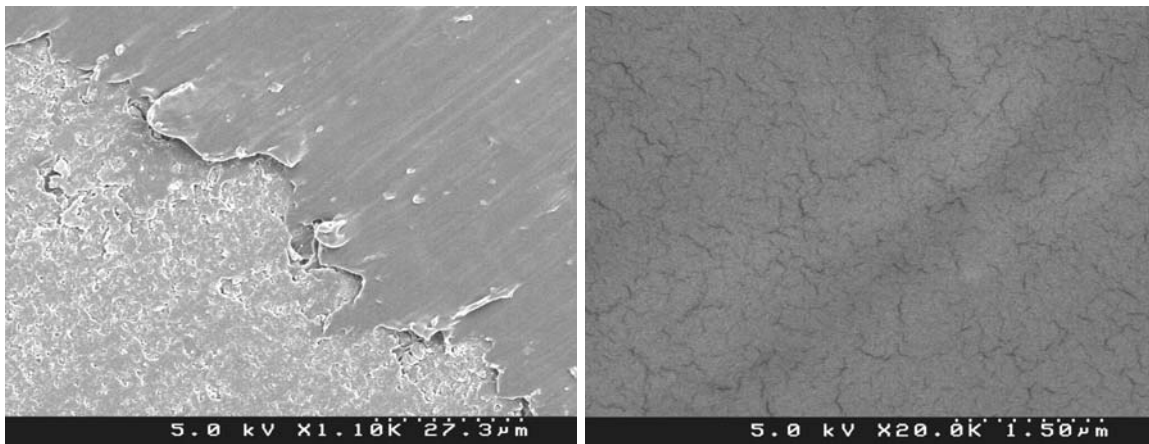
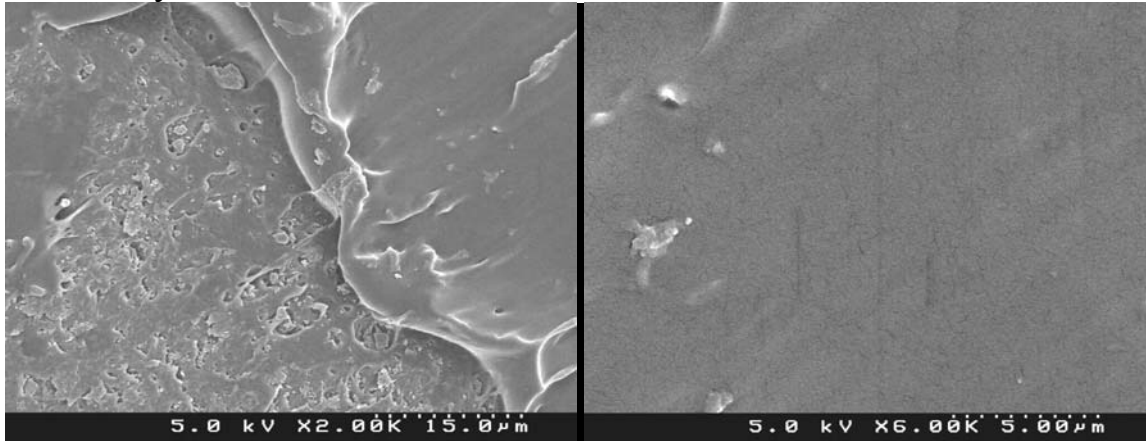
Table 2: Result of sessile contact angle measurements of PVC Veka before and after flame treatments

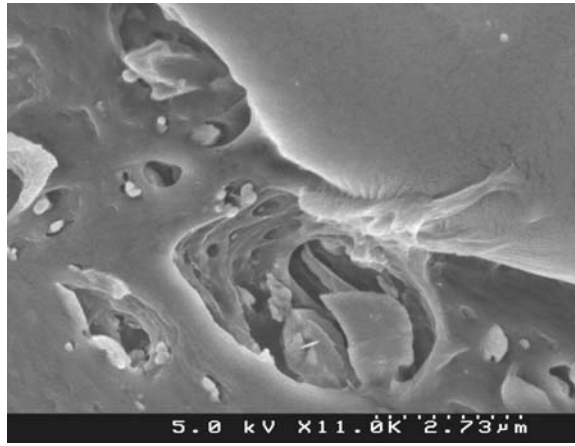
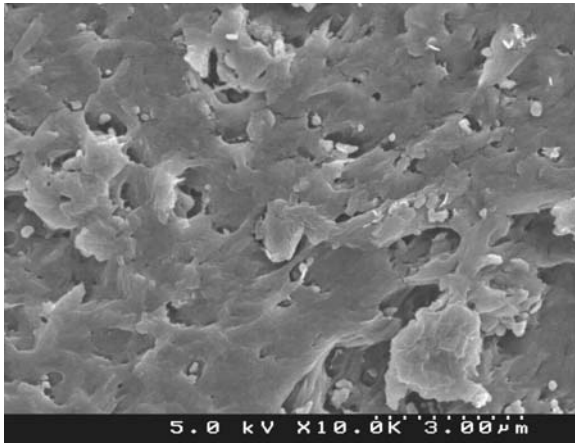
Samples No	Elapse time /day	Angle/degree	Standard Deviation	Release agent
PVC Veka	0	90	1	✓
PVC Veka	0	86	1	
1	4	73	2	
1	7	63	4	
1	18	74	3	
1	22	72	3	
1	28	74	2	
2	4	74	3	
2	7	82	3	
2	18	71	3	
2	22	69	3	
2	28	74	2	
2	53	70	2	
2	60	72	1	
3	4	82	2	
3	7	82	3	
3	18	83	4	
3	22	75	2	
3	28	79	2	
3	53	81	2	
3	60	72	2	
4	4	77	1	
4	7	85	2	
4	18	78	2	
4	22	76	2	
4	28	82	2	
4	4	69	2	✓
4	7	64	3	✓

4	18	69	2	✓
4	22	68	2	✓
4	28	64	2	✓
4	53	70	1	✓
4	60	68	2	✓

#### 6.4 Appendix 4

SEM image of surface and interface of sandwich layer that exposed by Microtomy CULAM





## 6.5 Appendix 5

AFM results obtained for PVC panels before and after flame treatment at different conditions

Pre-treatment conditions for PVC samples 1-7 are given in the Table 1:

No	Pre-treatment conditions
1	PVC without release agent and without flame treatment. Washed (cleaned) by Hexane
2	Same as No 1 but with protection film on top
3	PVC flame treated as release agent was on the top (best treatment with parameter 4)
4	PVC sample No 1 flame treated (parameter 4)
5	PVC sample No 1 flame treated (parameter 3)
6	PVC sample No 1 flame treated (parameter 2)
7	PVC sample No 1 flame treated (parameter 1)

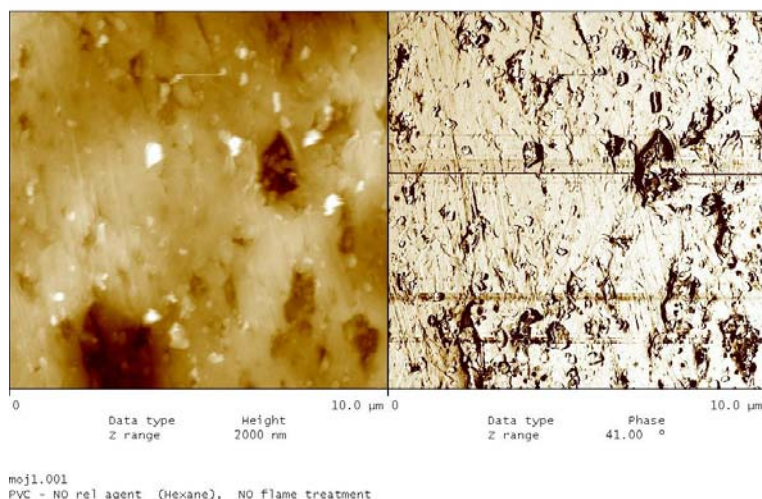
Fig. 1 shows presence of deep pits (depth 300-500nm) and deposited particles (height 200-400 nm) after PVC washing by Hexane (**sample 1**).

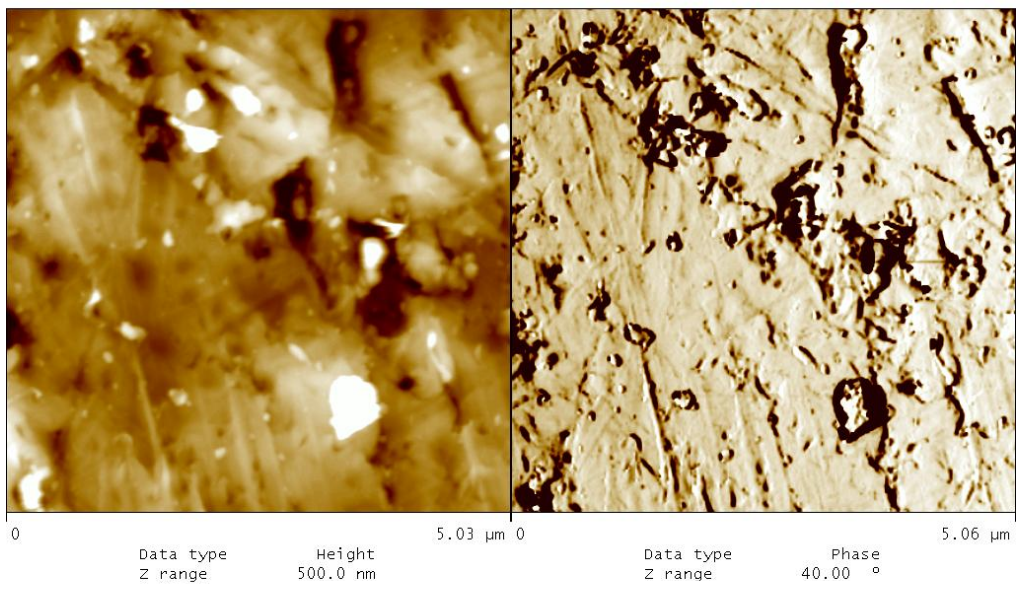
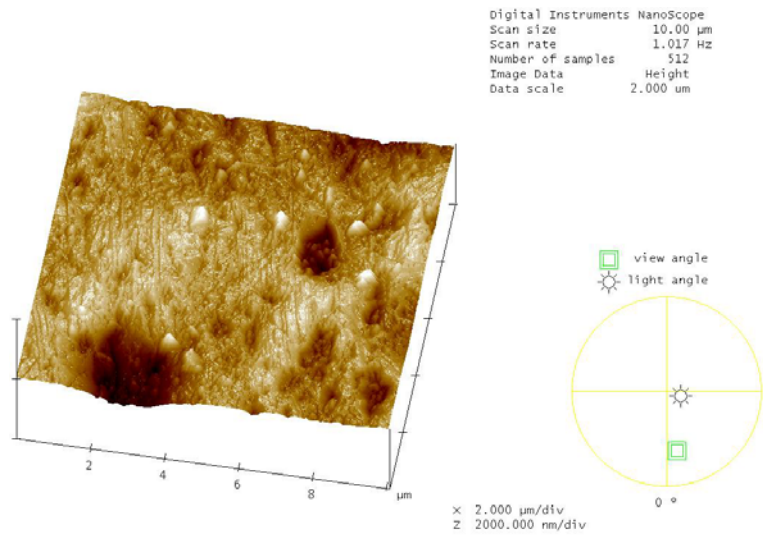
Existence of the thin sticky layer on surface of the **sample 2** is demonstrated by results presented in a Fig. 2 when characteristic smoothing of the surface relief was observed at low tapping amplitude. 2-3 times increase of the tapping amplitude allowed penetration of the SPM tip through the surface adhesive layer and it resulted in pronounced improvement of the surface resolution (Fig. 3).

Flame treatment of the PVC panel (Fig. 4) was followed by formation of extended regions characterised by different viscoelastic properties (white areas at Phase Images).

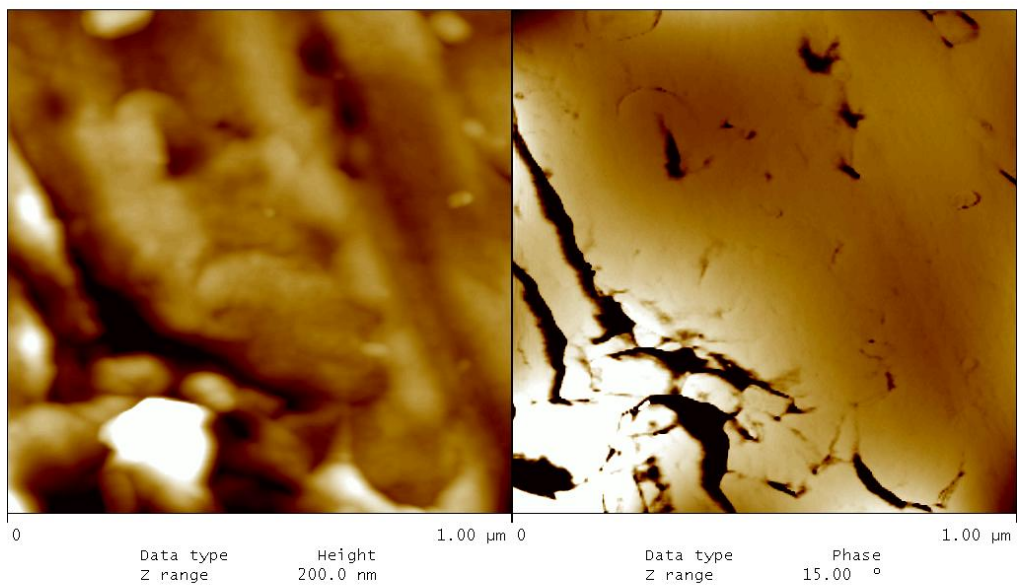
Similar results were obtained for other flame treated PVC panels (Figs. 5-8) and comparison of the Topographic and Phase Images clearly demonstrated strong dependence of surface structure on parameters of the flame treatment.

Direct comparison of the SPM data with parameters of the flame treatment (which are unknown to me) and with results of the XPS studies will make possible better understanding changes in surface chemistry and morphology, as function of parameters used during flame treatment of the PVC panels. 4/12/07



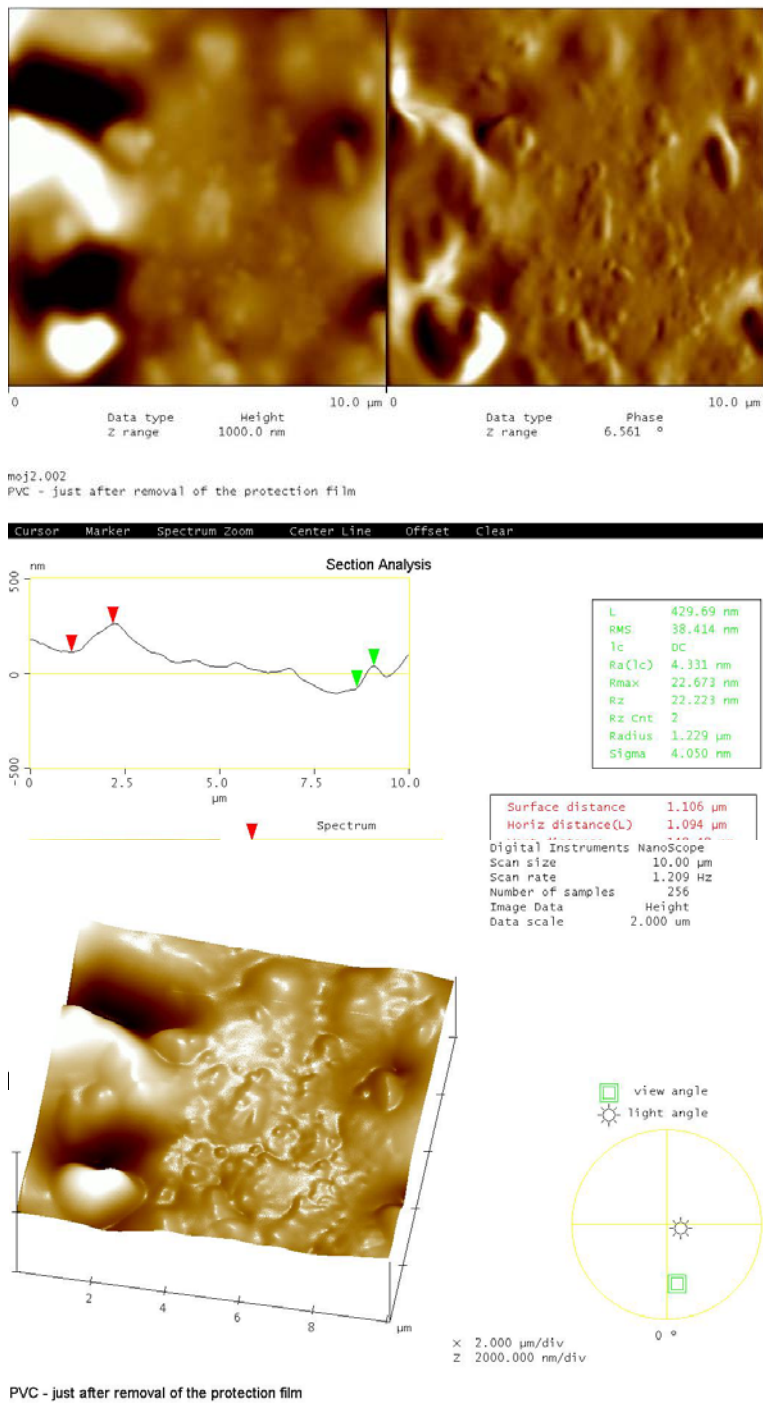


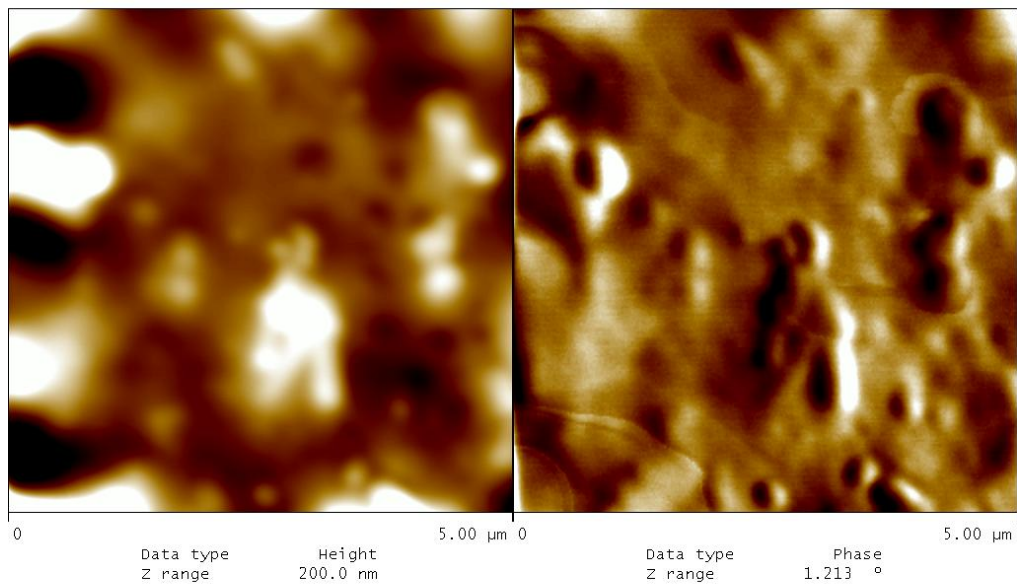
moj1.02  
 PVC - NC Fig. 1 PVC – no release agent, no flame treatment



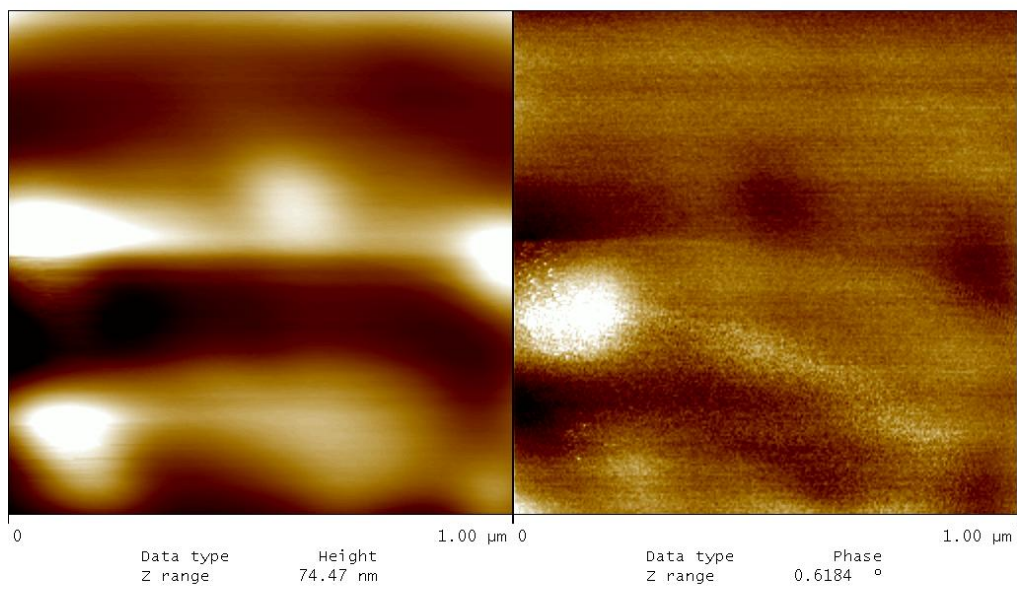
moj1.03  
 PVC - NO rel agent (Hexane), NO flame treatment

**Fig. 1 PVC – no release agent, no flame treatment**



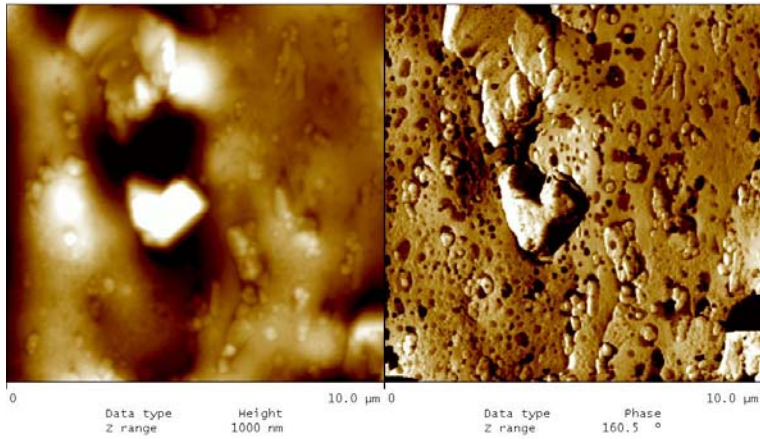


moj2.003  
PVC - just after removal of the protection film



moj2.004  
PVC - just after removal of the protection film

**Fig. 2 PVC – just after removal of the protective layer**



moj2.009  
PVC - just after removal of the protection film

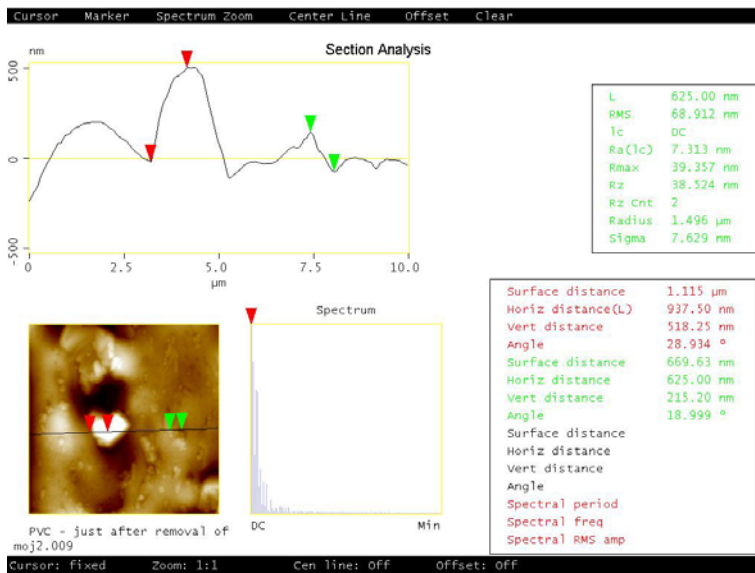
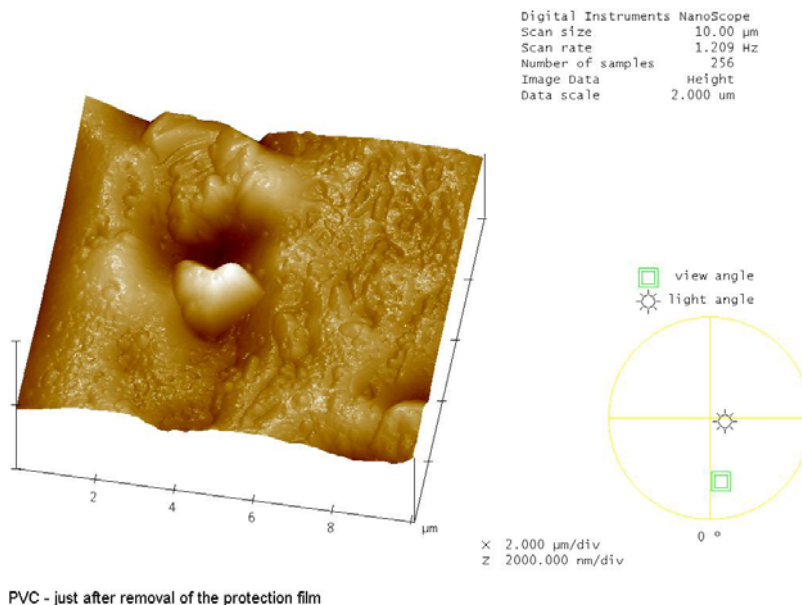
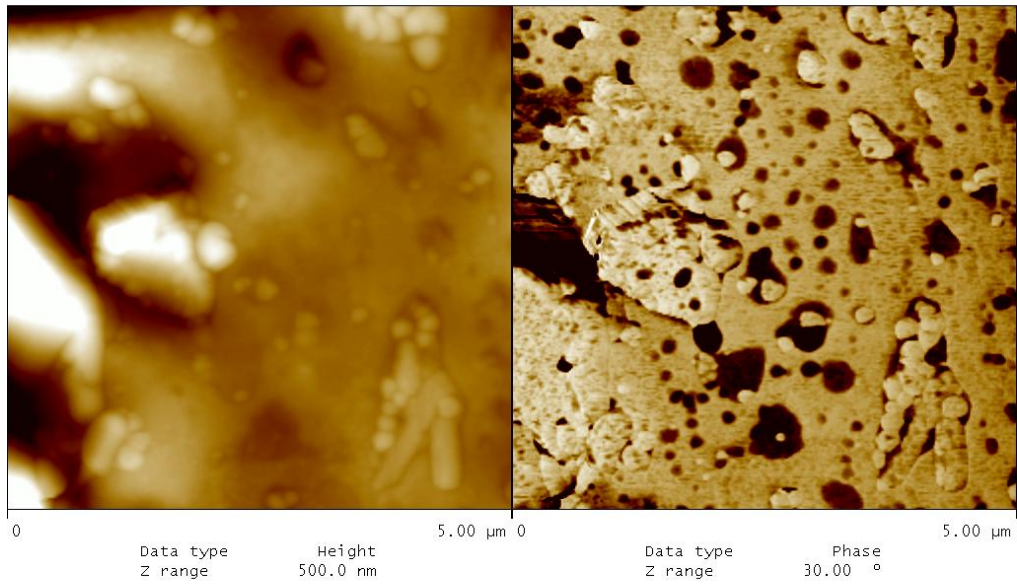
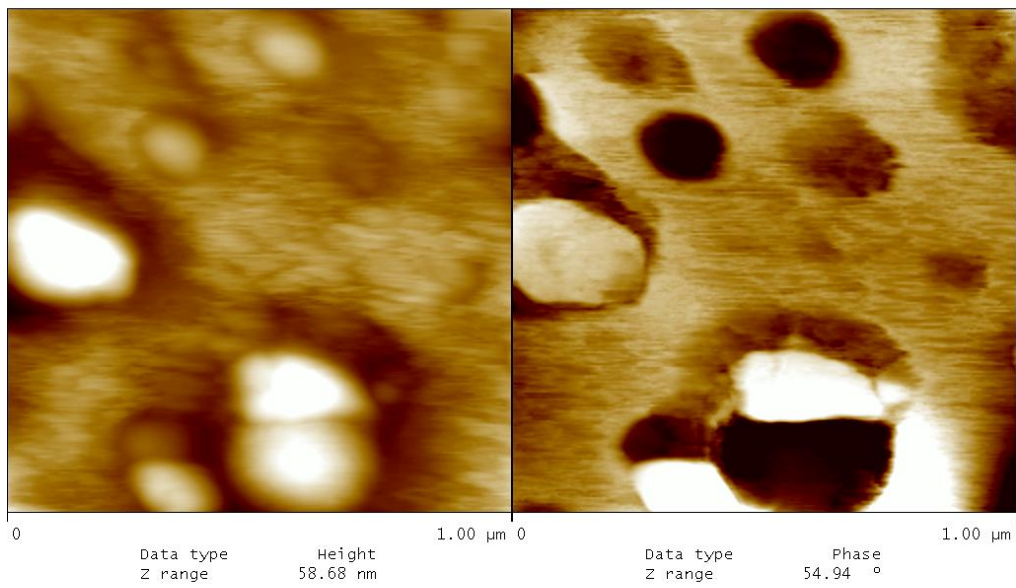


Fig. 3 PVC – after removal of the protective layer.



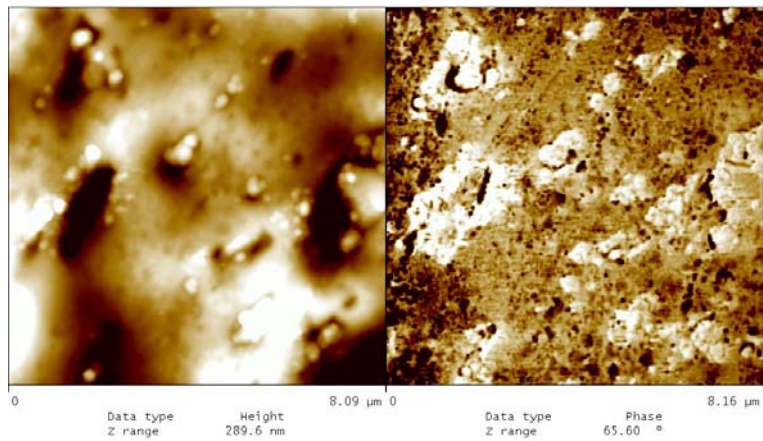


moj2.007  
PVC - just after removal of the protection film

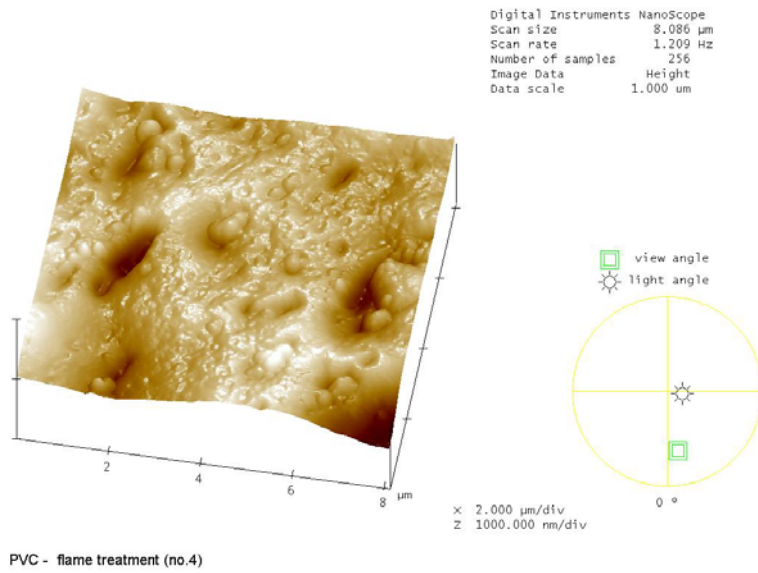
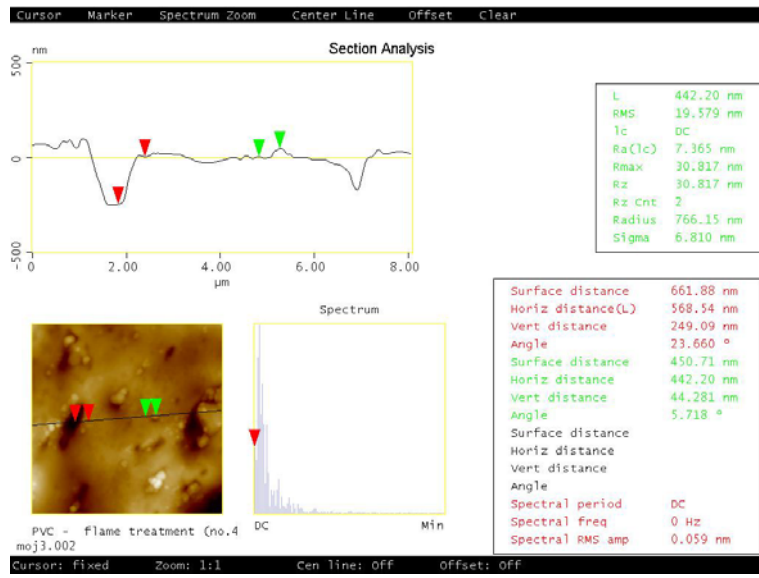


moj2.005  
PVC - just after removal of the protection film

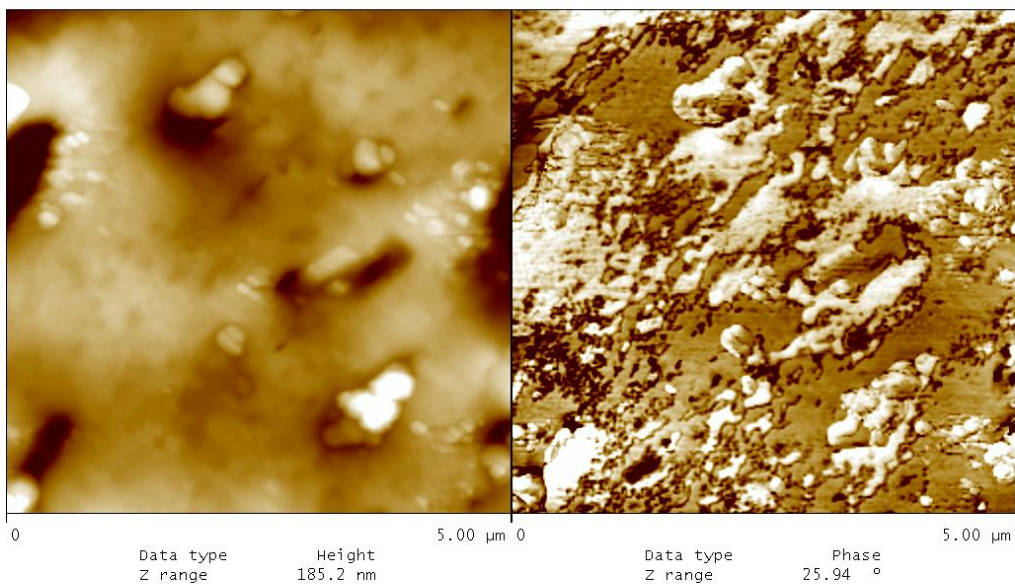
**Fig. 3 PVC – after removal of the protective layer.**

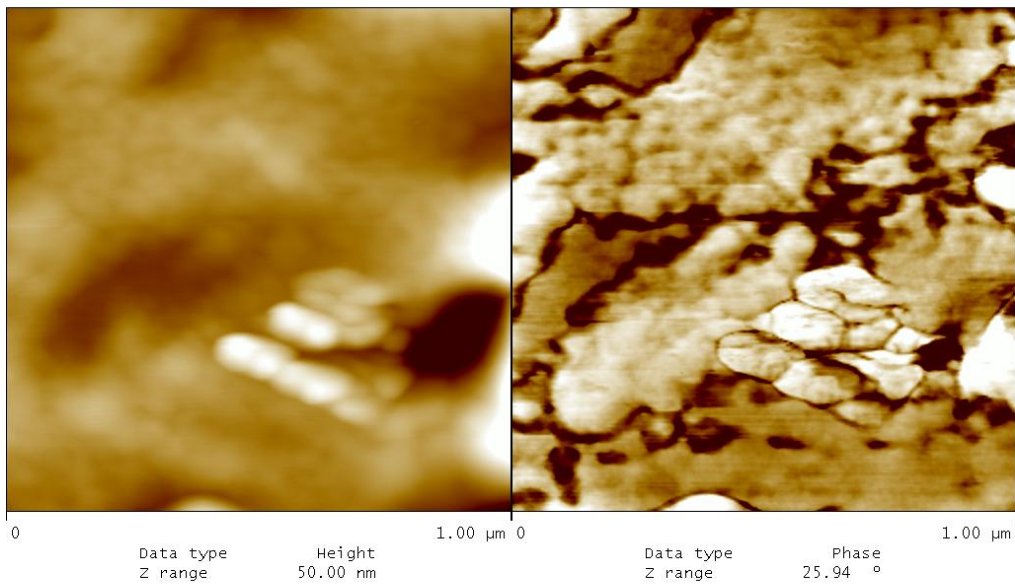


moj3.002  
PVC - flame treatment (no.4)



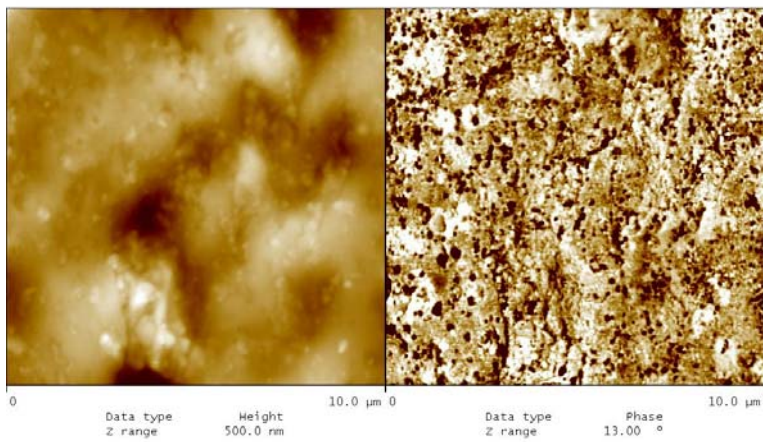
**Fig. 4 PVC – after flame treatment (param. No 4).**



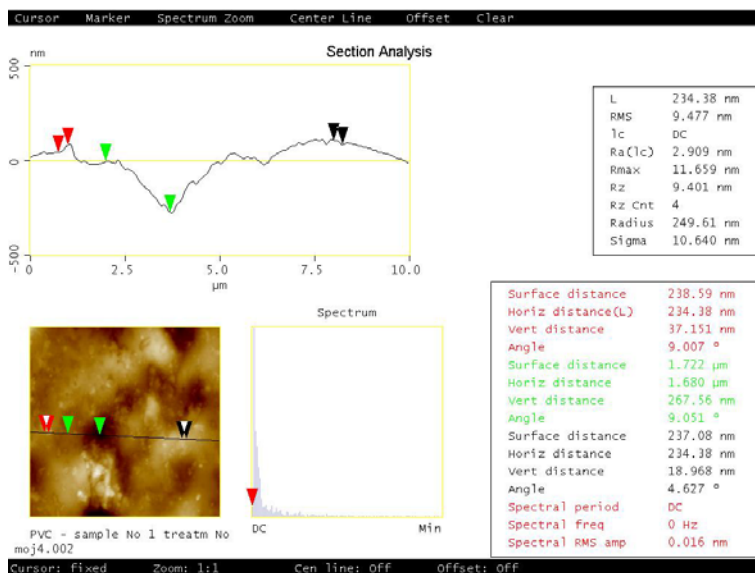


moj3.006  
PVC

**Fig. 4 PVC – after flame treatment (param. No 4).**



moj4.002  
PVC - sample No 1 treatm No 4



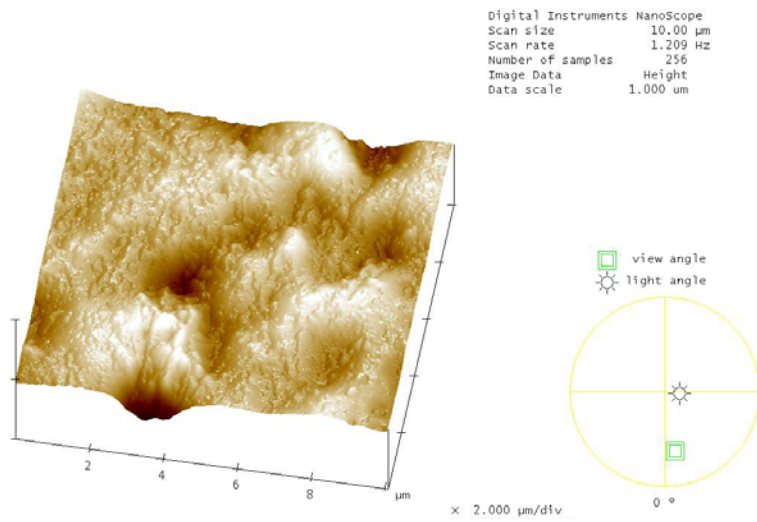
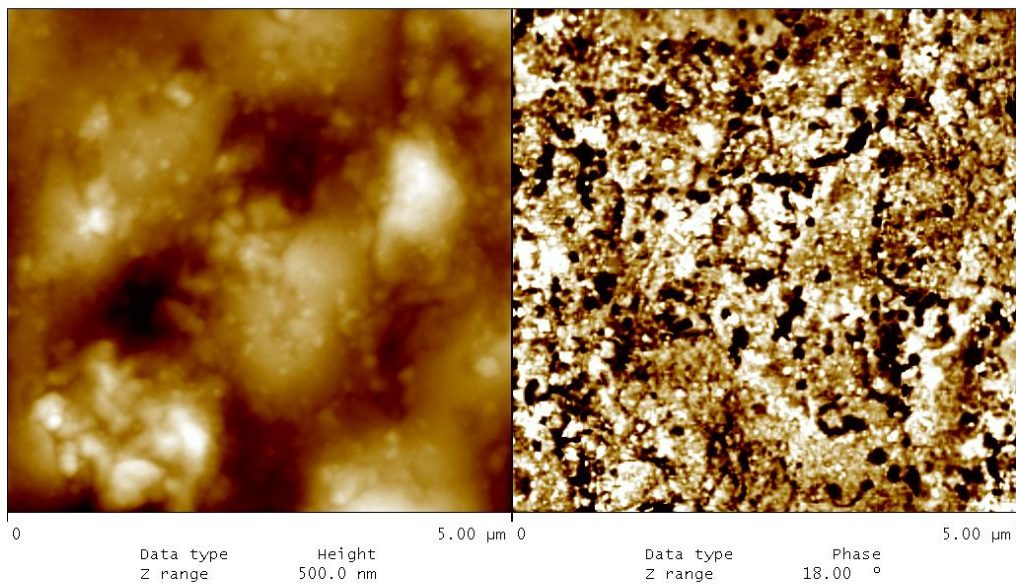
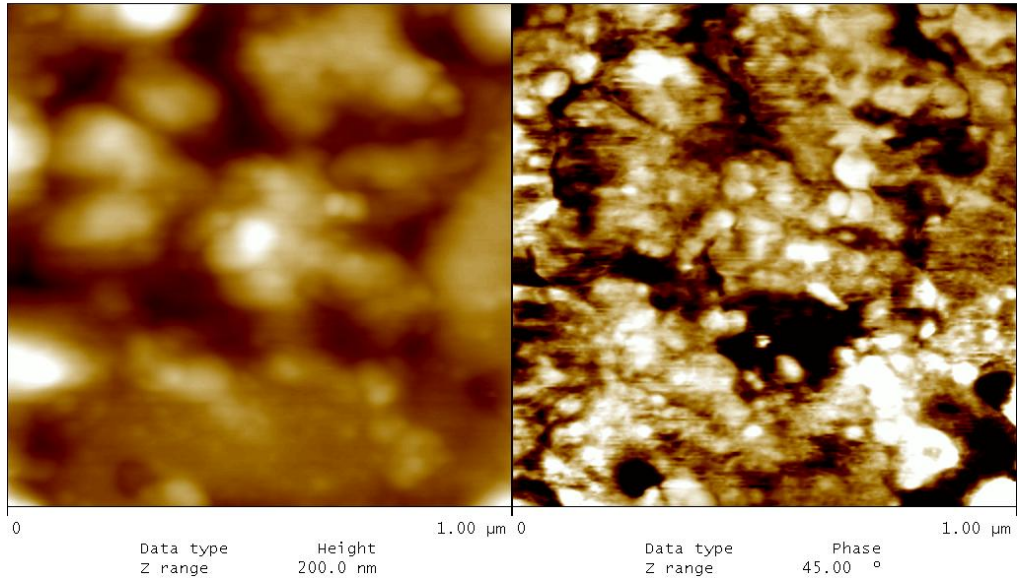


**Fig. 5 PVC – Sample No. 1 after flame treatment (param. No 4).**

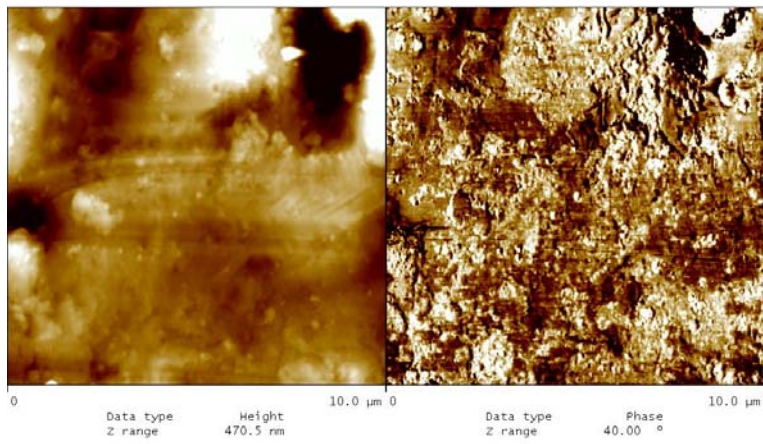


moj4.003  
 PVC - sample No 1 -treatment No 4

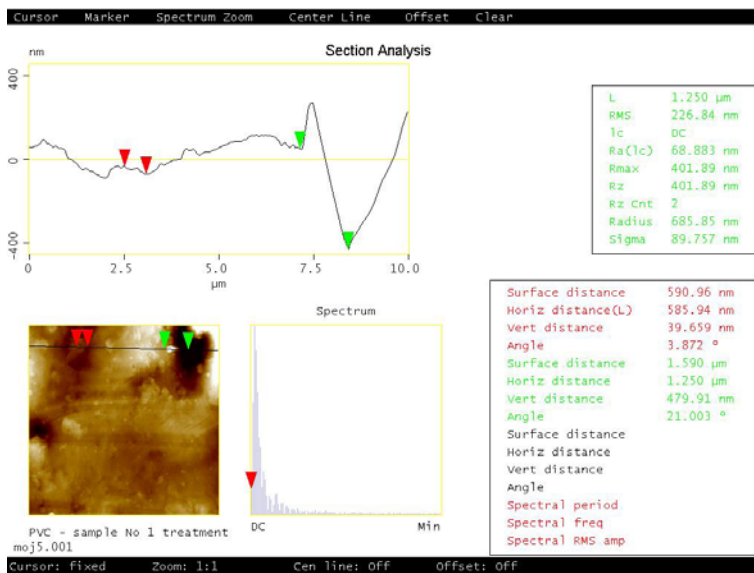


mn14\_004

**Fig. 5 PVC – Sample No. 1 after flame treatment (param. No 4).**



moj5.001  
PVC - sample No 1 treatment by par No 3



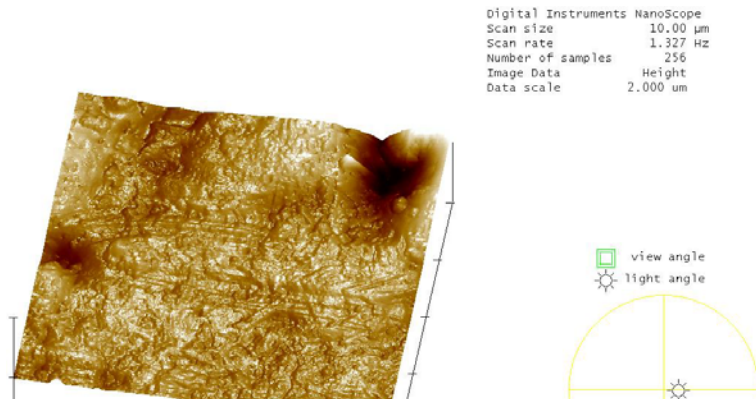
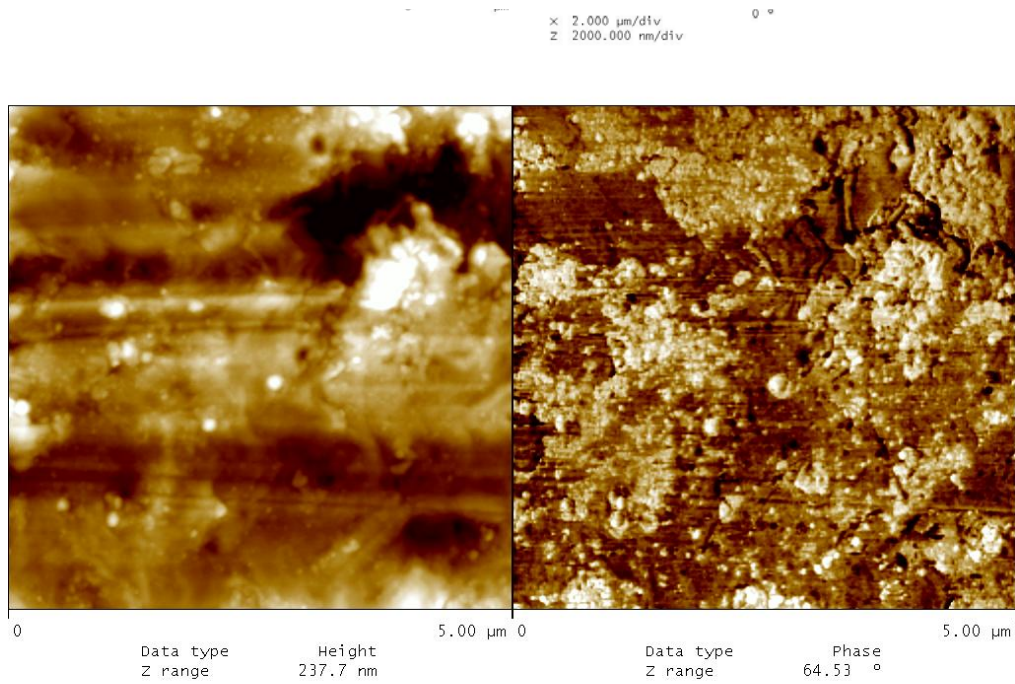


**Fig. 6 PVC – Sample No. 1 after flame treatment (param. No 3).**



moj5.002  
 PVC - sample No 1 treatment by par No 3

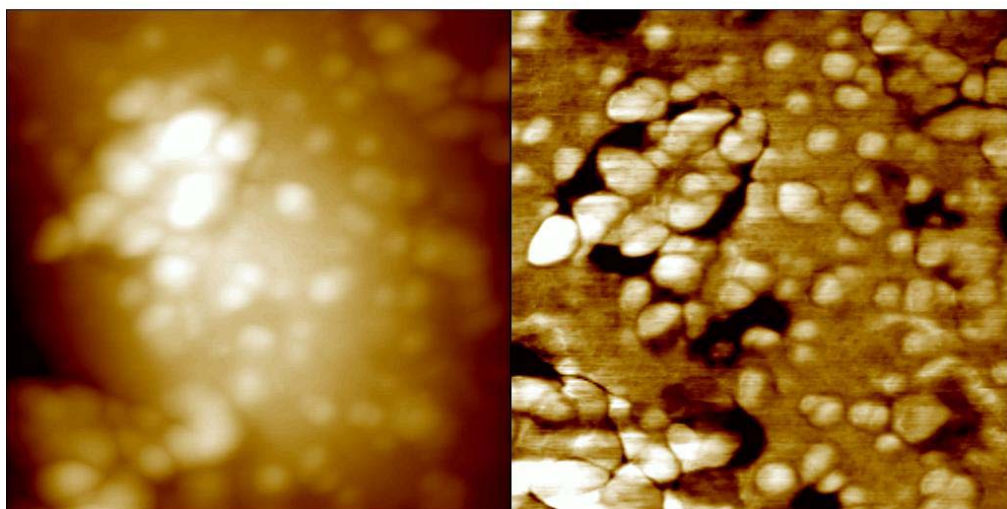
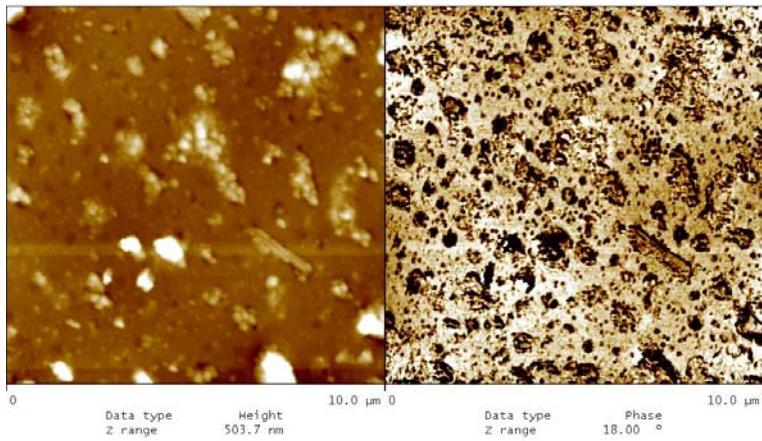
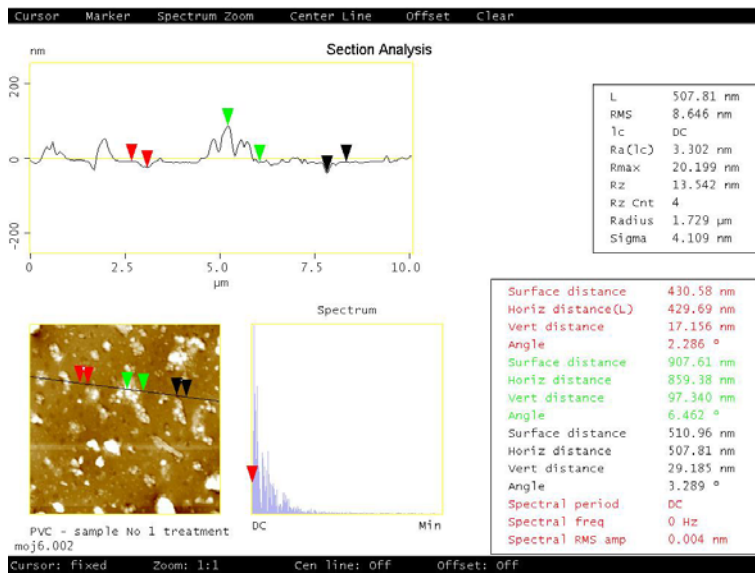


**Fig. 6 PVC – Sample No. 1 after flame treatment (param. No 3).**

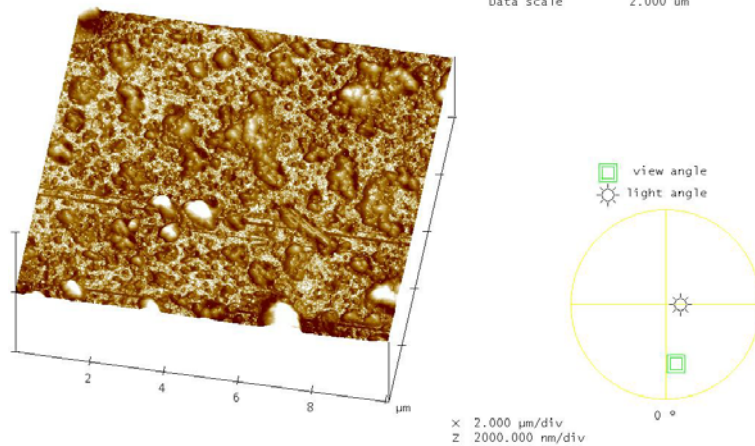


moj6.002  
PVC - sample No 1 treatment by par No 2



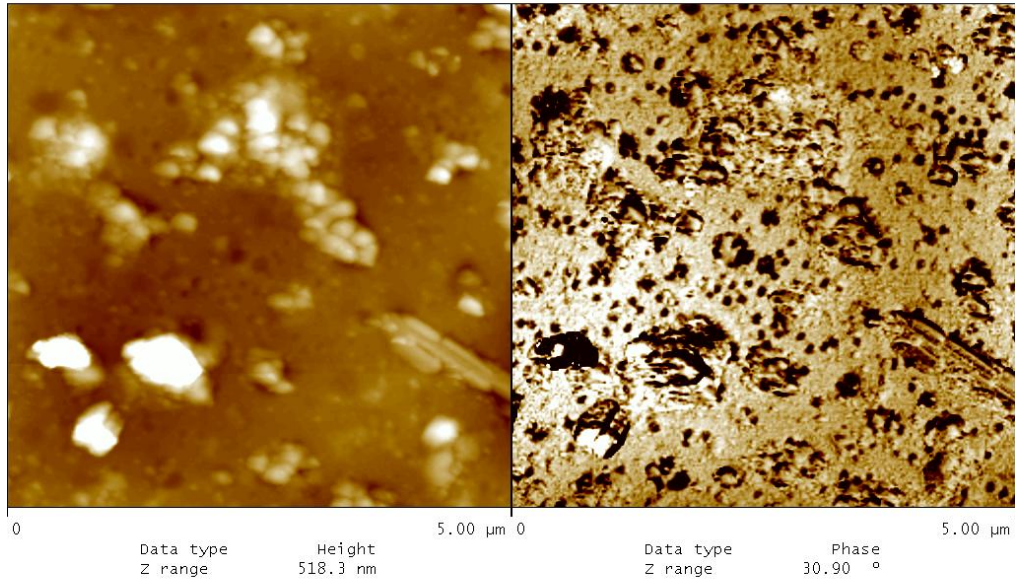
PVC - sample No 1 treatment  
moj6.002  
Cursor: Fixed Zoom: 1:1 Cen line: OFF Offset: OFF

Digital Instruments NanoScope  
Scan size 10.00 μm  
Scan rate 0.9688 Hz  
Number of samples 256  
Image Data Height  
Data scale 2.000 μm

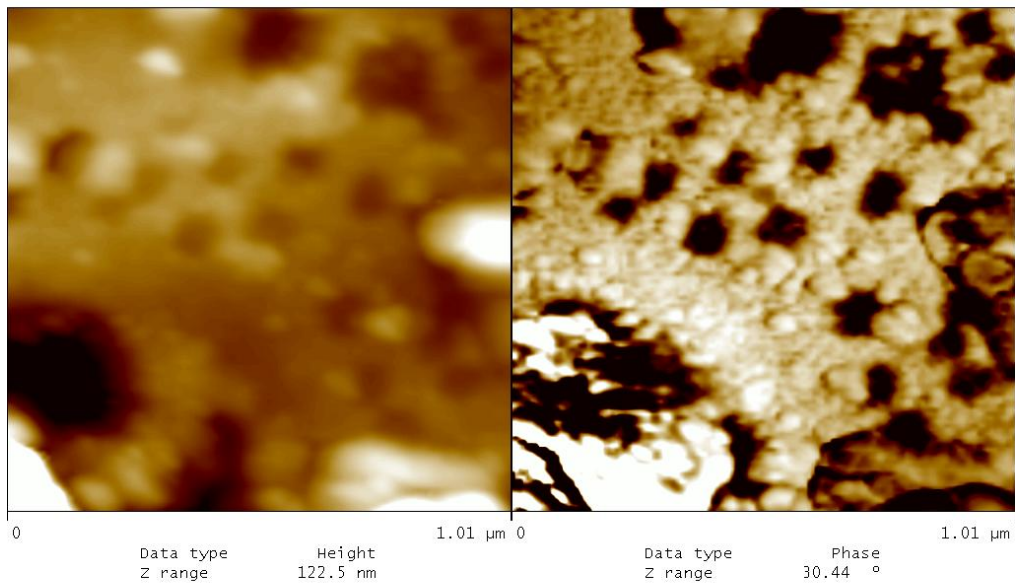


PVC - sample No 1 treatment by par No 2

**Fig. 7 PVC – Sample No. 1 after flame treatment (param. No 2).**



moj6.003  
PVC - sample No 1 treatment by par No 2



moj6.004  
PVC - sample No 1 treatment by par No 2

**Fig. 7 PVC – Sample No. 1 after flame treatment (param. No 2).**

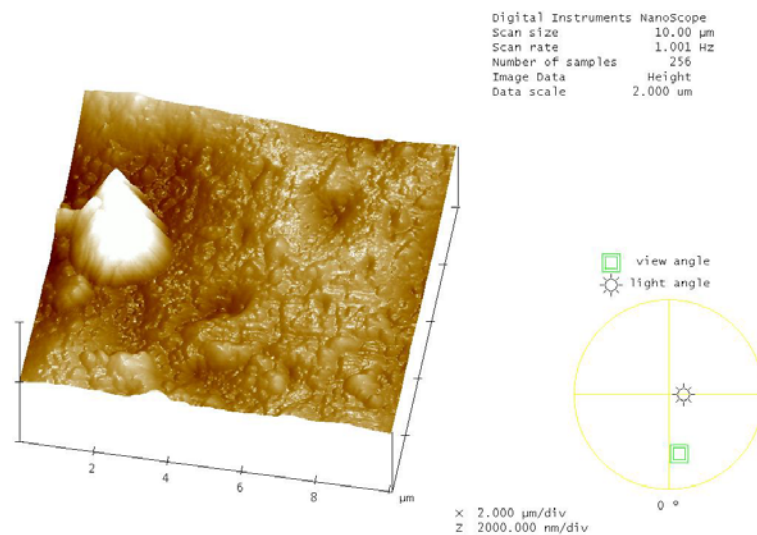
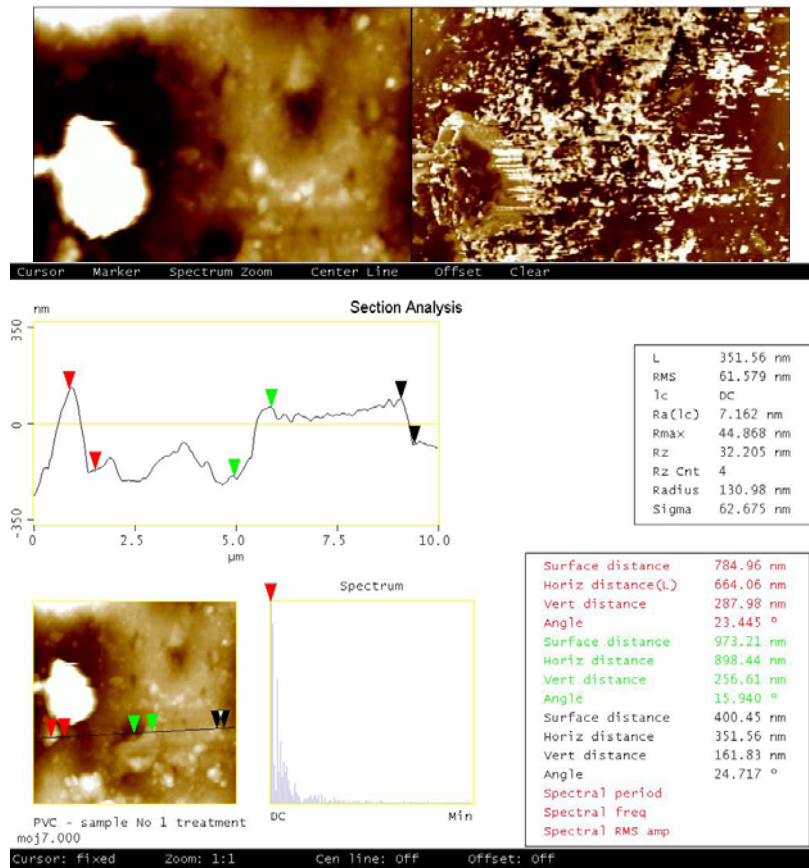
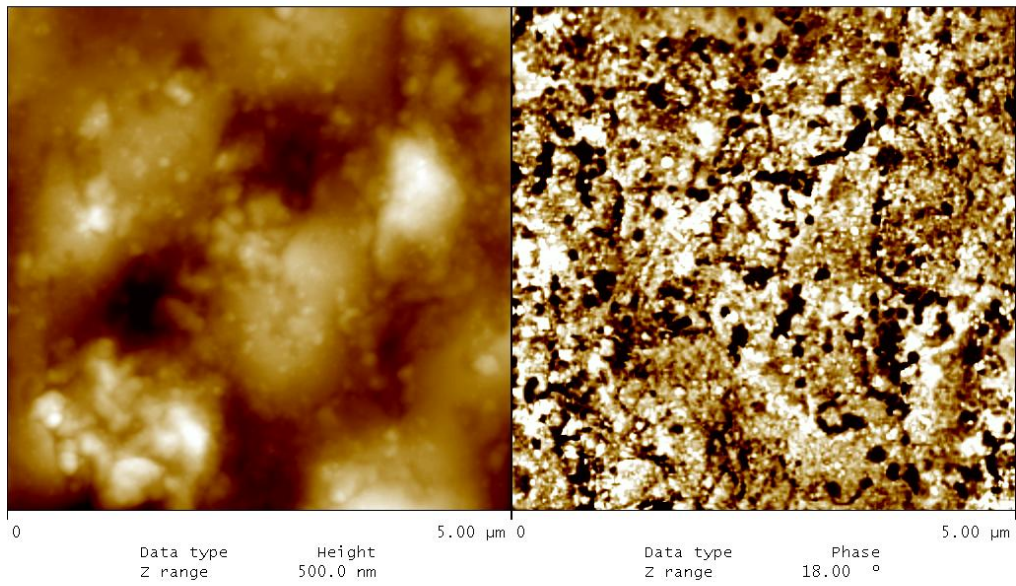
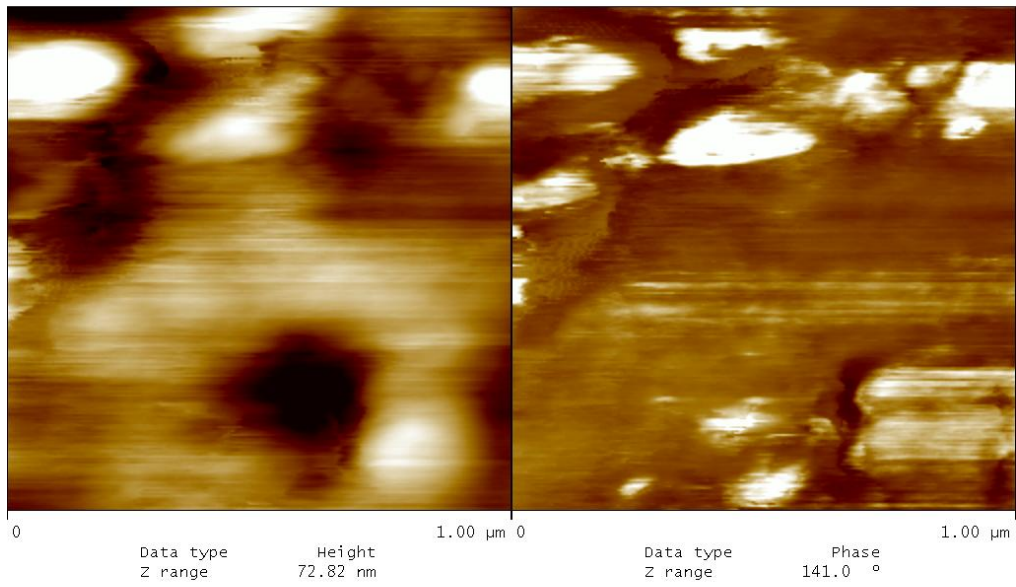


**Fig. 8 PVC – Sample No. 1 after flame treatment (param. No 1).**



moj4.003  
PVC - sample No 1 -treatment No 4



moj7.002  
PVC - sample No 1 treatment by par No 1

**Fig. 8 PVC – Sample No. 1 after flame treatment (param. No 1).**